Università degli Studi del Piemonte Orientale

"Amedeo Avogadro"

Department of Pharmaceutical Sciences

Ph.D. in Chemistry & Biology

XXXIII cycle 2017-2020

Targeting Extracellular Nicotinamide Phosphoribosyltransferase (eNAMPT) in Inflammatory Bowel Disease

Giorgia Colombo

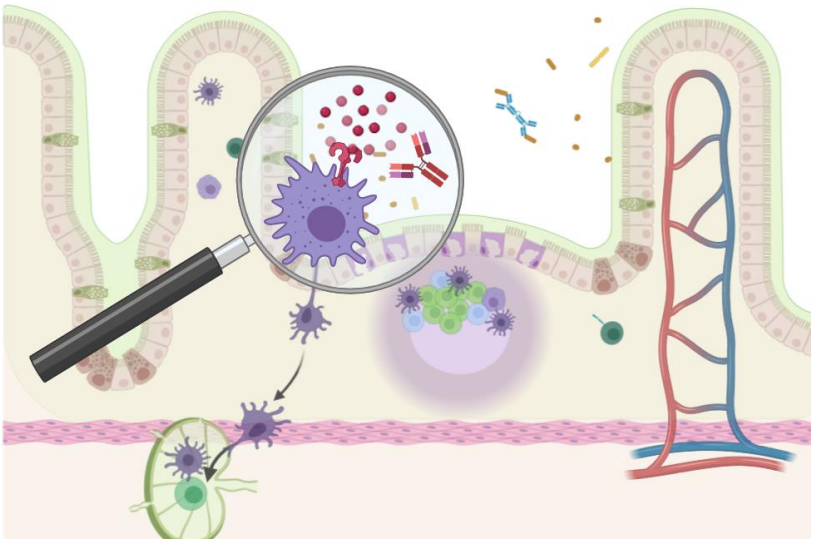

S.S.D.: BIO/14

Tutor: Prof. Armando Genazzani

PhD program co-ordinator: Prof. Gian Cesare Tron

Università degli Studi del Piemonte Orientale

"Amedeo Avogadro"

Department of Pharmaceutical Sciences

Ph.D. in Chemistry & Biology

XXXIII cycle 2017-2020

Targeting Extracellular Nicotinamide Phosphoribosyltransferase (eNAMPT) in Inflammatory Bowel Disease

Giorgia Colombo

Supervised by Prof. Armando Genazzani

PhD program co-ordinator: Prof. Gian Cesare Tron

UNIVERSITÀ DEL PIEMONTE ORIENTALE
DOTTORATO DI RICERCA
IN CHEMISTRY & BIOLOGY

Via Duomo, 6
13100 – Vercelli (ITALY)

DECLARATION AND AUTHORISATION TO ANTIPLAGIARISM DETECTION

The undersigned COLOMBO GIORGIA student of the Chemistry & Biology Ph.D course (XXXIII Cycle)

declares:

- to be aware that the University has adopted a web-based service to detect plagiarism through a software system called "Turnit.in",
- his/her Ph.D. thesis was submitted to Turnit.in scan and reasonably it resulted an original document, which correctly cites the literature;

acknowledges:

- his/her Ph.D. thesis can be verified by his/her Ph.D. tutor and/or Ph.D Coordinator in order to confirm its originality.

Date: 14/11/2020

Signature: Giorgia Colombo

XY/tcs
Percorso del file

Contents

Chapter 1

INTRODUCTION

1. INFLAMMATORY BOWEL DISEASE

The inflammatory bowel diseases (IBD) are chronic and relapsing conditions resulting from inappropriate mucosal immune activation, characterized by multifactorial etiology. IBD could be divided in two major forms: Crohn's disease (CD) and ulcerative colitis (UC). CD and UC could be distinguished by several elements, including some associated to the distribution of affected sites and the morphological expression of the disease. Ulcerative colitis is limited to left-colon (left-sided colitis), rectum (proctitis), sometimes occurs in caecum (pancolitis) or in the entire colon (extensive colitis), developing into the mucosa and submucosa. Crohn's disease, typically transmural with the development of abscesses, fistulas, and stenosis, may involve any area of gastrointestinal tract, from mouth to anus, particularly in the terminal ileum, caecum and colon. (Figure 1) [1].

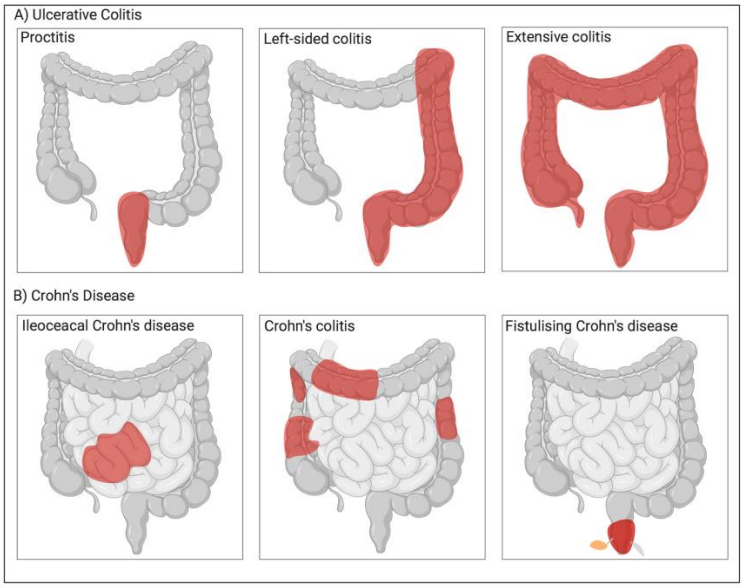

Figure 1. Lesions distribution in UC and CD [2]

IBD patients do not receive a real and resolutive cure and these pathologies are now considered one of the heaviest financial problem in the worldwide healthcare. This is a result of inefficacious or long-term treatment, without being resolutory yet. In 2017, 6.8 million IBD patients were counted all over the world. IBD is more common in the western part of the world, preferably in females, in the teens and early 20s. Moreover, it is becoming widespread in developing countries [2]. The first and most popular theory associated to the spreading of IBD is the *Hygiene Hypothesis*, which correlates the increasing incidence to better food storage and cleaner water and the consequent decrease of food infection [1]. This theory has been later reinterpreted by Rook et al. [3], who has identified IBD with idiopathic characteristics as a result of defecting combination in host interactions with intestinal microbiota, intestinal epithelial dysfunction and aberrant mucosal immune responses.

In the normal intestinal mucosa, the inflammatory state is controlled by a delicate balance between pro-inflammatory (*e.g.* TNF-α, IFN-γ, IL-1β, IL-6, IL-8, IL-17, IL-23) and anti-inflammatory (*e.g.* IL-4, IL-10, IL-11) cytokines, that are able to maintain an intact mucosal barrier from commensal microbes. The ability to maintain this barrier is driven by epithelial intestinal cells (IECs), activated by STAT3-dependent signalling, induced by natural killer T cells, intraepithelial lymphocytes, and innate lymphoid cells. A lot of cytokines help to maintain integrity, for example:

- IL-22, from T helper 17 (Th17) cells, through STAT3-mediated signalling, maintains antimicrobial defence, mucosal integrity and promotes reparation.
- IL-17A and IL-17F promote antimicrobial peptide production and IECs junction development.
- Type I interferon, from mononuclear phagocytes, through STAT1 and 2-mediated signalling, promotes the secretion of anti-inflammatory cytokines and T regulatory (Treg) response.
- IL-10 induces M2-macrophages.

- IL-2 and TGF-β maintain mucosal homeostasis and boost FoxP3$^+$ Treg cells.

Finally, the mucosa has plenty activated B cells and plasma cells that are able to produce IgA against pathogenic bacteria [4].

1.1. Etiopathogenesis

The etiology of IBD is to date unknown; what is certain is that the components of the pathogenesis are: genetic, hygienic, microbial and immune factors (Figure 2).

Genetic factors

Genetic risk factors play a fundamental role in the onset of IBD [5]. In different studies, monozygotic twins have 50% chance to manifest the disease. This evidence shows that genetic factors are not the only component of the pathogenesis of IBD, but there are other factors involved [6].

Commonly, many of these factors are characteristic of other inflammatory diseases such as rheumatoid arthritis (RA), systemic lupus erythematosus and type 1 diabetes. For this reason, genetic factors are now not considered adequate for the diagnosis and the evaluation of disease risk. DNA sequencing techniques have helped different studies on the whole human genome to be completed, with the identification of SNPs (single nucleotide polymorphisms) associated with IBD [7].

Currently, the number of gene loci related to IBDs are 163, of which 110 are associated with both CD and UC, which suggests common pathogenesis between the two pathologies, only 30 are related to CD and 23 to UC [8]. The first susceptible gene recognized for CD is *Nod2* [9], which encodes an intracellular receptor for muramyl dipeptide (MDP), usually present in bacterial peptidoglycan, of both Gram positive and Gram negative. The stimulation of this pathway is able to activate autophagy, which controls the antigen presentation and bacteria replication [10]. Autophagy plays an indispensable role in immune responses of IBD because it is directly involved in intracellular homeostasis (destruction of cytosolic organelles, resistance to infections, *etc*). It is known that gene mutations involved in autophagy,

such as ATG16L1 (variant T300A) and IRGM (mutation of the polymorphisms lead to a reduced protein expression) are related to an increased risk of developing CD. Other IBD associated genes are: IL23R, which encodes a subunit of the receptor for IL-23, cytokine involved in the maturation process of Th17 cells, IL12B, which encodes p40, IL-12 and IL-23 subunits, JAK2 and STAT3, IL-10 and other genes involved in immune function [11].

Environmental factors

Undoubtedly, environmental factors in IBD influence mostly the pathogenetic mechanism and the clinical course of these diseases.

Mainly, the knowledge of these factors is crucial because it is possible, unlike the genetic factors, to control and modify them. Some are known for their relevance in the disease: smoking, followed by diet, intake of drugs, hormone levels, psychological elements such as stress and geographic location [12].

- *Smoking*. Smoking is one of the most important etiopathogenetic factor. It is certain that it represents a negative risk factor in the CD pathogenesis and a more aggressive trend of the disease was observed (fistulising, stenosing disease) in smoking patients. Moreover, it correlates with the site of the inflammation, mainly affecting the ileus of patients. The underlying pathogenetic mechanism appears to be the systemic chronic condition of hypoxia smokers (stabilization of HIF-2α), which compromises the integrity of the intestinal barrier, improves lumen exposure to antigens, inflammatory reaction and increases severity of CD [13]. In addition, exposure to cigarette smoking predisposes to a greater onset of extraintestinal manifestations of the disease; the most common are enteropathic arthritis, erythema nodosum and uveitis. Upon termination of smoking, the prevalence of extra-intestinal manifestations is reduced until it reaches the level of non-smokers within 1-2 years. On the other hand, smoking improves clinical settings of UC, reduces surgery request and treatments. The underlying pathogenetic mechanism is

the induction of a gene (HSPA6) by smoking, which stabilizes antiapoptotic BCL-XL and provides epithelial protection, contributing to the beneficial effect of cigarette smoke [13,14].

- *Microbiome*. At birth, the human intestine is sterile; the microbiota is initially acquired during childbirth and in the first weeks of life through contact with the environment, for example during breastfeeding. The colon mucosa is protected by a layer of mucus composed in turn of two layers, one internal and one external [15]. The first is tightly adherent and sterile, the second is more mobile and excellent for bacterial growth; bacteria protect against epithelial damage and regulate many functions of the epithelium, creating a balanced environment. The human gut microbiota is consisting of approximately 1150 bacterial species [16]. Biodiversity and stability of flora are reduced in IBD patients compared to healthy ones, according to analysis conducted on the faecal microbiota. This is normally composed of *Firmicutes* and *Bacteroidetes*, which contribute to the production of substrates for intestinal metabolism; in IBD patients, however, these are reduced in favour of *E. Coli* and Enterobacteriaceae. The presence of a particular *E. Coli* phenotype, the adherent and invasive (AIEC), was observed in the CD, within epithelial cells and macrophages [17].
- *Drugs, Vitamin D and other substances*. Definitely, certain drugs play an important role in the pathogenesis of IBD. For example, non-steroidal anti-inflammatory drugs (NSAIDs) have a damaging action against the intestinal mucosa. Their mechanism of action involves inhibition of cyclooxygenases (COX), with parallel reduction of prostaglandins, fundamental for mucus production, and an increase of intestinal permeability [18]. In particular, prostaglandins have an immunomodulating effect through TNF inhibition and IL-10 induction, which is reduced. Another class of drugs that was associated with the onset of IBD are oral and hormonal contraceptives. They are suspected to be thrombogenic at the intestinal mucosa level, stimulating

proliferation of macrophages [19]. Vitamin D, in addition to its well-known beneficial effects on bone metabolism, is involved in numerous other processes. Its levels in IBD patients are often low and it is correlated with a worsening of the disease. In pre-clinical experiments, it was observed that a deficiency of 1,25-dihydroxyvitamin D3, or in knock-out mice for the vitamin D receptor gene, increases risk of UC [20]. Moreover, it has been highlighted that the administration of vitamin D in these mice ameliorates inflammation and suppresses proinflammatory genes such as TNFα [20].

- *Lifestyle*. Such as diet, stress, and depression.

Immunological factors

The mucosa of the gastrointestinal tract is continuously exposed to antigens of food origin and antigens of the resident bacterial flora. The balance between an efficient epithelial barrier and the immune system guarantees a response to harmful antigens, recognized as "non-self" and a tolerance towards harmless antigens, defined as "self". In IBD patients, there is an alteration of this balance, in which the immune system reacts against antigens normally recognized as "self" [21]. Innate immunity is firstly activated facing pathogens. Usually, it is immediate (minutes or hours) and non-specific, mediated by a broad spectrum of cells: epithelial cells, neutrophils, macrophages, natural-killer cells, dendritic cells. The recognition of a high number of antigens (PAMPs, pathogen-associated molecular patterns) occurs through toll-like receptors (TLRs) located on the cell surface and NOD-like receptors in the cytoplasm, which together constitute the category of PRRs (pattern-recognition receptors). For example, these two fundamental components were altered in IBD patients, loss of function mutations of NOD2 reduce the inhibition on TLR2, which remains continuously activated, stimulating Th1-mediated inflammatory responses in excessive way [22,23]. These mutations alter the expression of NF-κB, which is less activated in IBD, resulting in reduced antibacterial response to pathogenic stimuli such as LPS [24]. The first physical barrier that all antigens faced is the

mucous layer that covers the intestinal epithelium, composed of two layers internal and external. The importance of this barrier was observed in mice knock-out for a protein that composes these layers, MUC2. In this case, mice spontaneously develop colitis and colorectal cancer, due to the direct contact of the various antigens with the epithelium [25,26]. A recent study has observed a reduction in the expression of MUC1 mRNA in patients with CD [27].

The second physical barrier is the intestinal epithelium; it defends itself from pathogens thanks to peptides produced by enterocytes, Paneth cells and Goblet cells. A defect in the production of these antimicrobial peptides and an increased intestinal permeability have been observed in patients with IBD [28]. Among these peptides we have defensin, produced both in response to recognition of bacterial components and constitutively by Paneth cells, that are reduced in patients with CD. As it has already noted above, the genetic factors encoding innate immunity are often altered in IBD: ATG16L1 and IRGM, involved in autophagy, IL-23 and its receptor, involved in the coordination of both innate and adaptive responses. Regarding adaptive immunity, it is specific, long-term and, as the term says, it adapts to the antigen presented collaborating with innate immunity, especially with dendritic cells. The key cells of this type of immunity are T lymphocytes, which mature from Th0 to Th1, useful in the response to intracellular pathogens, Th2, protective against parasites and allergic reactions and Th17, essential in the clearance of extracellular fungi and bacteria. However, this maturation process undergoes unregulated activation and inflammation for various reasons, with variability between the two main disease phenotypes: the Th1 response prevails in CD, while an unconventional Th2 response prevails in UC [29,30].

There are differences between the two types of response based on the cytokine levels detected:

• Th1 is induced by IL-12 and IL-18 and produces high amounts of IFN-γ, high levels of which have been found in serum of CD patients in several studies [31].

• Th2 releases IL-4, IL-5, IL-13 detected respectively in UC patients, mainly by atypical natural killer cells [32].

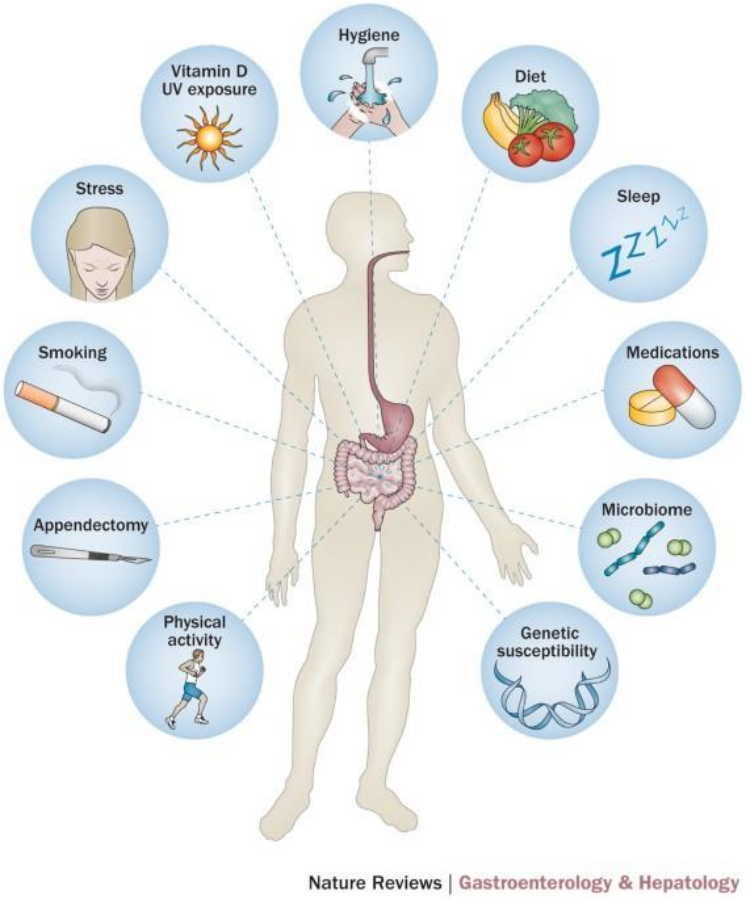

Figure 2: Etiopathogenesis of IBD [33]

However, in recent studies, this clear separation seems to be disappeared after studies carried out on *ex vivo* biopsies of the colon mucosa of CD and UC patients, finding similar levels of IFN-γ [34]. The Th17 response is characterized by the production of high levels of IL-17A, IL-21, IL-22 in response to TGF-β and IL-6, whose expression is promoted by IL-23. This cascade is critical because IL-21-mediated increase of IL-23 expression has been observed, identifying a self-sustaining positive feedback loop [35]. This finding has shifted attention to this type of response and

numerous studies have identified high levels of IL-17A in both CD and UC patients and its over-expression in the *lamina propria* of IBD patients [36].

1.2.Ulcerative colitis

Ulcerative colitis (UC) is characterized by the involvement of the rectum and colon with ulcers aligned along the long axis of the colon, creating area with regenerating mucosa, that often swells into the lumen as pseudo-polyps. There are evidences about infiltration of inflammatory cells into *lamina propria*, crypt abscesses and distortions, epithelial metaplasia, while the inflammatory process is diffused and limited to the mucosa and superficial submucosa, without granulomas.

The major symptoms are: (*i*) rectal bleeding with mucoid material, (*ii*) abdominal pain and cramps relieved by defecation, (*iii*) loss of weight and (*iv*) tenesmus.

The symptoms may persist for days, weeks or months, and sometimes patients required colectomy [2].

The chronic inflammation of UC is characterized by a massive gut infiltration of granulocytes and macrophages, especially $CD4^+$ Th lymphocytes.

Normally, naïve $CD4^+$ Th cells differentiate into (*i*) Th1, responsible of cell-mediated immunity, producing IL-2, IFN-γ and TNF-α, (*ii*) Th2, responsible of humoral immunity, producing IL-4 and IL-5, (*iii*) Th17 and (*iv*) subpopulation of regulatory T lymphocytes (Tregs).

UC is mainly a Th2-polarizated disorder, indeed these cells in UC disease produce IL-4, IL-5, IL-10 and IL-13, necessary for humoral response. IL-4 and IL-5 support immunoglobulins synthesis, while IL-10, IL-13 and IL-4 inhibit Th1-activated macrophages. Moreover, mononuclear cells from intestinal *lamina propria* show high levels of IL-13. IL-19 secreted from Th9 cells are able to reduce the protective ability of the mucus.

The role of Tregs, activated by the two anti-inflammatory cytokines IL-10 and TGF-β, produced by dendritic cells, is tissue repairing [37,38].

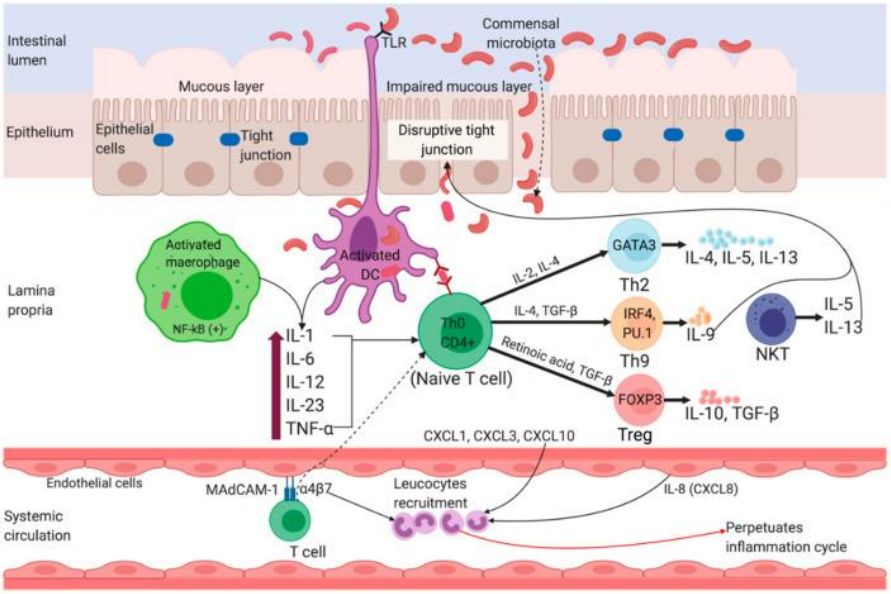

Figure 3: Pathophysiology of UC [2]

1.3. Crohn's disease

Commonly, CD involves the entire gastrointestinal tract. The number of various symptoms does not help to diagnose the pathology. Clinically, similar UC symptoms may occur as (*i*) rectal bleeding, (*ii*) diarrhea, (*iii*) tenesmus and (*iv*) anorexia. At the endoscopic level, CD is characterized by aphthous ulcers that may elongated themselves with a serpentine appearance. Moreover, the cobblestone appearing is typical, described as big holes into mucosa, and the fissures that may flow into fistulas. Therefore, microscopically, there is a strong neutrophile infiltration that create crypt abscesses and, consequently, their destruction. Several cycles of crypt destruction and consequent regeneration determine the distortion of mucosa architecture, metaplasia and non-caseating granulomas [1,2].

For CD, the chronic inflammation is Th1-dependent and is characterized by increased levels of IFN-γ and IL-17. Into patients' *lamina propria* the production of IL-6, IL-23 and TGF-β by innate immune cells and APCs determines Th17

phenotype. While IFN-γ-dependent activation of STAT4 and T-bet promotes Th1-dependent response [2].

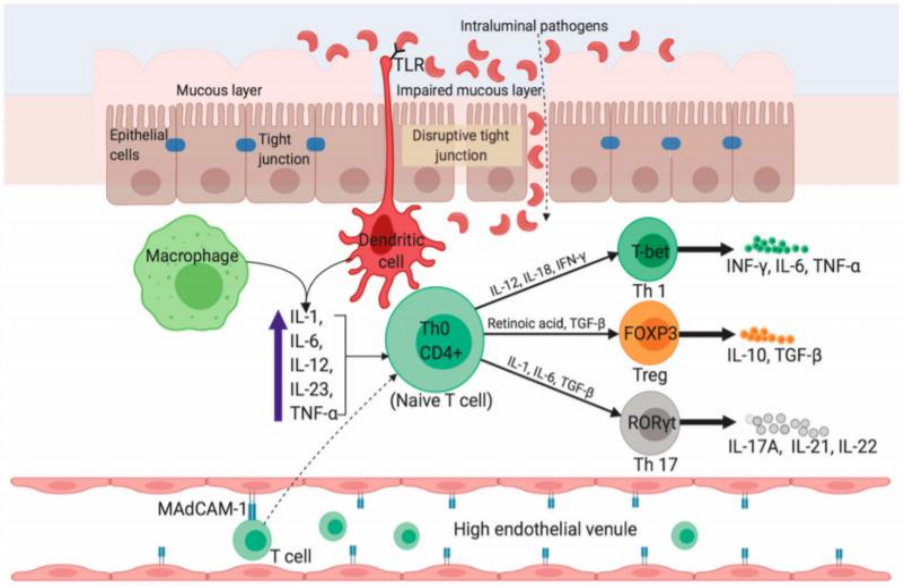

Figure 4: Pathophysiology of CD [2]

1.4. Diagnosis

The diagnosis of IBD is largely based on the accurate collection of the patient anamnestic data, with particular attention to family and physiological medical history and lifestyle habits such as smoking, drug intake and diet. The pathological medical history should focus on the specific symptoms detected by the patient, the change in bowel habits and other systemic signs such as fatigue or weight loss. This must be followed by a thorough examination, which can be useful for discriminating the pain of the abdomen and can detect any palpable abdominal masses. The diagnostic process continues with the differential diagnosis with infectious gastroenteritis by performing parasitology and copro-culture on a stool sample, and continues with laboratory investigations, endoscopic investigations and diagnostic imaging [39].

1.4.1. Diagnostic tests

The laboratory investigations aim at identifying a state of inflammation, without specificity towards the diagnosis of IBD, such as erythrocyte sedimentation rate (ESR) and leucocytosis. In case of severe disease, anaemia (iron deficiency) can be observed, or megaloblastic anaemia from vitamin B12 malabsorption. Other parameters that can be inspected are those concerning the nutritional status: hypoalbuminemia, hypercholesterolemia, hypotriglyceridaemia, electrolyte alterations. The bio-humoral markers used in the first instance are: C-reactive protein C (CRP) on blood samples and faecal calprotectin on stool samples. CRP is an acute phase protein synthesized in the liver under a cytokine stimulus from macrophages. It is the most sensitive marker of inflammation and also the one that rises earlier. It is a high predictive negative value: it has been shown that with values below 5 mg/dl the probability of having active IBD is less than 1% of cases [40]. However, it was found to be unable to distinguish between CD and UC.

Faecal Calprotectin is a direct marker of intestinal inflammation, produced by the degranulation of neutrophils; it remains elevated in the faeces for about 7 days after degranulation. It is also non-specific, since high levels have been found in other intestinal diseases, such as diverticulitis. It is considered an excellent marker of disease activity if the diagnosis is confirmed by other methods. Concentration ranges have also been established by which disease activity can be defined:

• Values below 50-100 μg/g represent quiescent disease.

• Values between 100 and 250μg/g are indeterminate.

• Values above 250 μg/g represent inflammation [41].

As second level, other non-specific markers that can be used are anti-cytoplasmic antibodies of perinuclear neutrophils (p-ANCA), whose positivity was obtained in 6-39% of CD patients and 41-73% of UC patients; this indicates a low specificity in the diagnosis of CD, but a sensitivity of 52% and a specificity of 91% in distinguishing the two disease patterns [42]. Antibodies against Saccharomyces

cerevisiae (ASCA), present in 60% of CD and in 13% of UC, can be useful in diagnosing CD, with sensitivity of 72% and specificity of 82% [43].

1.4.2. Endoscopic techniques and medical imaging

The gold standard examination for IBD diagnosis is colonoscopy with visualization of the terminal segment of the ileum, associated, according to the guidelines, with at least two biopsies in at least five areas of the intestine, including the rectum and the ileum. For a complete histological diagnosis, macroscopically disease-free areas of the gut should also be sampled to ensure adequate disease staging [44].

1.5. Disease index evaluation

Based on the parameters detected in the diagnostic process, it is possible to classify the disease and correctly address the therapeutic approach. There are scores in the literature that consider exclusively clinical parameters and others integrated with endoscopic parameters, all different for each pathology.

Particular attention should be paid to the clinical scores for each pathology.

In clinical practise, we have:

- the Crohn's Disease Activity Index (CDAI) and the Harvey-Bradshaw Index (HBI) for patients with CD;
- the Mayo Score for UC;
- CDEIS (Crohn's Disease Endoscopic Index of Severity) index as endoscopic score for CD;
- Montreal classification for endoscopic score for UC [45,46].

1.6. Treatment guidelines for ulcerative colitis [47]

The heterogenic clinical course of these diseases makes the therapeutic management of IBD a constantly evolving challenge. Patients are used to receive increasingly personalized treatments in order to obtain a complete response: clinical, laboratory

and histological. The choice of treatments is wide and is based on the characteristics of the pathology (affected site, severity, duration, any extra-intestinal manifestations), those of the patient (age, sex, etc.), any drug intolerances and the doctor's experience. There are two treatment phases, the first defined as the "induction phase", in which the goal is the remission, the second called "maintenance phase", which ensures that the remission takes place over a long period. The approach to these diseases can take place in two ways: "step-up" or "step-down". The first involves a gradual approach, with the use of less aggressive drugs first and then more aggressive drugs; the second strategy, on the other hand, involves an initially aggressive treatment which can, once remission is reached, become milder, with dose reduction or suspension of some drugs.

Ulcerative colitis treatments

The elective treatments are:

1. **Aminosalicylates** (5-ASA, aminosalicylic acid, orally or intra-rectally), as mesalazine and sulphasalazine are the election treatment to treat mild to moderate UC. 5-ASA interacts with gut epithelial cells to mediate the release of lipid factors, cytokines and oxygen reactive species, with a local anti-inflammatory response. They are usually well-tolerated, but nephrotoxicity may occur.
2. **Corticosteroids**, with a superior ability to induce remission compared to 5-ASA, but usually related with important side effects. They are used in 5-ASA intolerant patients with mild to moderate UC.
    a. Prednisolone
    b. Budesonide MMX, launched in 2015, the first corticosteroid modified-release dosage formulation for UC, with a lower incidence of common corticosteroid side effects as adrenal suppression and reduction of bone mineral density
    c. Beclomethasone dipropionate.

Some patients fail to maintain remission in front of these treatments:

- Options for 5-ASA failure in UC patients:
    - Thiopurines, as azathioprine and mercaptopurine, immunomodulators that promote T and B cells apoptosis. They are indicated for subjects who have required more of two corticosteroid treatments within a year in combination with 5-ASA.
    - Anti-TNFs, as infliximab, adalimumab, certolizumab and golimumab. They are able to interfere with TNFα.
    - Anti-integrins, as vedolizumab, specifically targeting integrin-$\alpha_4\beta_7$ and counteracting the bind with mucosal vascular addressin cell adhesion molecule 1 (MAdCAM-1) on colonic epithelial cells, blocking T cell migration.
    - Janus Kinase (JAK) inhibitor, as tofacitinib
    - Anti-IL12/IL23, as ustekinumab
    - Methotrexate. inhibitor of dihydrofolate reductase, commonly used as an antineoplastic agent, but also as an immunosuppressive drug at lower doses. It is not useful in the maintenance of remission.

The choice of immunosuppressive drug or biological treatment in front of 5-ASA failure are influenced by several factors. In the past, the elective choices were immunosuppressant for a reason of costs and with less toxicity. The plenty studies comparing immunosuppressants and biologicals are now considered decisional factors for the route of administration according to patient preference, potential immunogenicity of different biologicals, cancer risk, possible relapse after a period of remission.

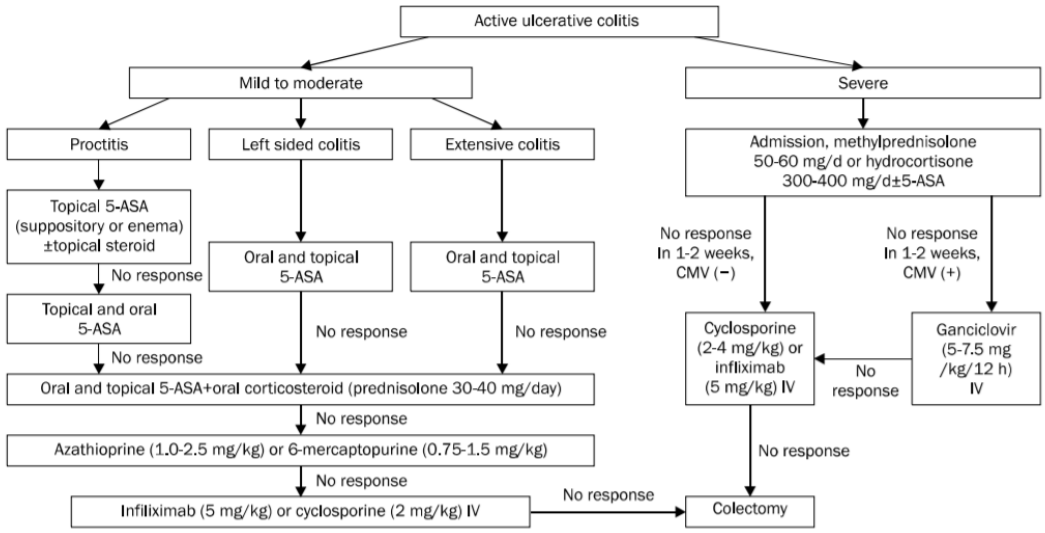

Figure 5: Algorithm treatment for UC [48]

Moreover, clinicians may face also anti-TNF failure. In this case, the preferred choices are vedolizumab and JAK inhibitors. Of note, vedolizumab efficacy is better characterized in anti-TNF naïve patients.

Importantly, also ciclosporin or tacrolimus, inhibitors of calcineurin, may be used, with the intent to prevent clonal expansion of T cells, working as immunosuppressive drugs. They are primary applied for acute severe colitis and in colectomized patients.

Chron's disease treatments

Initial treatment for mild to moderate CD:

1. **Corticosteroids**, as budesonide (not MMX formulation, that is exclusively for UC) or prednisolone.
2. **Antibiotic therapy**, with rifaximin or azithromycin in patients with complicated infection or perianal fistulas.

For moderate to severe CD treatments, where corticosteroids should be avoided because they are inefficacious and with plenty side effects, it is usual considered an

early use of biologics, considering the age of the patients (*e.g.* < 40 years at the diagnosis), the complexity of the disease, perianal fistulas and subjective lifestyle. For maintenance CD treatment:

- Immunomodulators, as thiopurines or methotrexate
- Anti-TNFs, in combination or not with immunomodulators
- Vedolizumab or ustekinumab, preferably on anti-TNF naïve patients
- Hematopoietic stem cell transplantation, in patients in which surgical resection is still not recommended.

The pathogenesis of IBD is complex and different inflammatory pathways are activated in the chronic condition. Nowadays, the treatments in clinical are sometimes still unable to achieve remission. The aim to solve this unmet clinical need is to find new targets to improve patients' life.

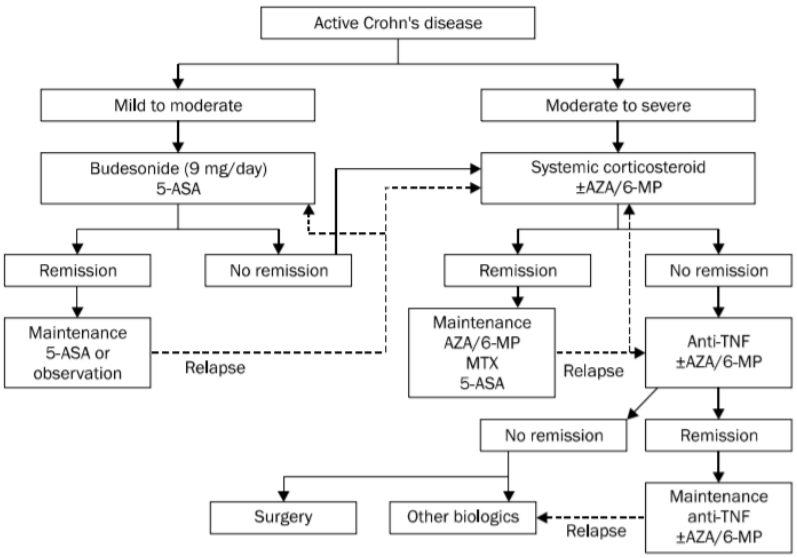

Figure 6: Algorithm treatment for CD [49]

Until now, we have plenty possible therapies under phase 2 and 3 clinical trials, including new antibodies such as anti-IL12/IL23, anti-IL17A/IL17F (vidofludimus), anti-IL13, anti-CXCL10 (eldelumab), anti-β7 integrin (etrolizumab), new JAK inhibitors (filgotinib), S1P1 modulator as etrazimod, Smad7 anti-sense oligonucleotide (mongersen) and others [50].

1.7. Prediction of primary response to biologic treatments

The use of biologics has revolutionized the treatment for IBD. Their ability to disadvantage corticosteroids treatment, to boost mucosal healing, to reduce hospitalizations and surgeries has improve patients' quality of life.

Hitherto, only two thirds of anti-TNF-treated patients are responsive to treatment. Finding a way to stratify the patients before the biologic infusion and waying them to a selective treatment may be beneficial both in term of costs and quality of life.

Several manuscripts have highlighted that mechanisms undergoing non-response are multifactorial. But until now, as revised by Gisbert [51], there is no single marker able to be a prognostic marker for all biologics in clinics. Several markers have been proposed for the single biologic class (for anti-TNF, vedolizumab and ustekinumab).

Anti-TNF predictive markers

The literature characterizing anti-TNFs is plentiful and several predictive markers have been proposed through the years. Gisbert's elegant revision [51] has orderly grouped these markers into three class: (i) patient-related factors, (ii) disease-related factors and (iii) immune-epithelial factors.

In the first class, markers thar are considered significantly favourable are: age, furthermore younger patients better response to anti-TNFs in some studies, and higher weight that is associated to negative response in AR patients rather than IBD.

Through disease-related, some of them factors are considered favourable: disease duration, patients with a short disease duration response better to anti-TNFs; disease location, ileal structuring CD is associated to lack of response; C-reactive protein,

elevated values are associated to positive outcome; pANCA and ASCA, which positivity is related to non-responsiveness or calprotectin and lactoferrin, which higher levels are associated to a better response.

In the immune-epithelial factor group, different markers have been proposed such as a group of proteins including apolipoproteins, plasminogen, complement factors that are up-regulated in no-responsive patients.

Among the plenty studies conducted, they are still too small and with insufficient statistical power, so no specific marker can be used in clinics at the moment [51].

2. NICOTINAMIDE PHOSPHORIBOSYLTRANSFERASE (NAMPT): A PROTEIN WITH A PLEIOTROPIC BEHAVIOUR

NAD is the most important coenzyme required in mammalian metabolic pathways, involved in redox biochemistry and energetic metabolism, as an oxidised agent, important for cellular homeostasis. Nicotinamide adenine dinucleotide (NAD^+) is finely regulated by intracellular nicotinamide phosphoribosyltransferase (iNAMPT). Plenty metabolic disorders and the physiological ageing are related with the decrease NAD levels, due to cytosolic NAMPT influence on NAD-dependent enzymes [52]. NAMPT is also characterized by an extracellular form, named eNAMPT, which has a cytokine-like activity. Increased eNAMPT levels are associated with a number of metabolic and inflammatory disorders.

2.1. The NAD salvage pathway

NAD is produced as a result of three different pathways:

a) From quinolinic acid (QA) in the *de novo* pathway. QA is derived from tryptophan, L-aspartate and dihydroxyacetone phosphate,
b) From nicotinamide riboside,
c) From nicotinic acid (NA) or nicotinamide (NAM or vitamin B3 or PP) in the salvage pathway.

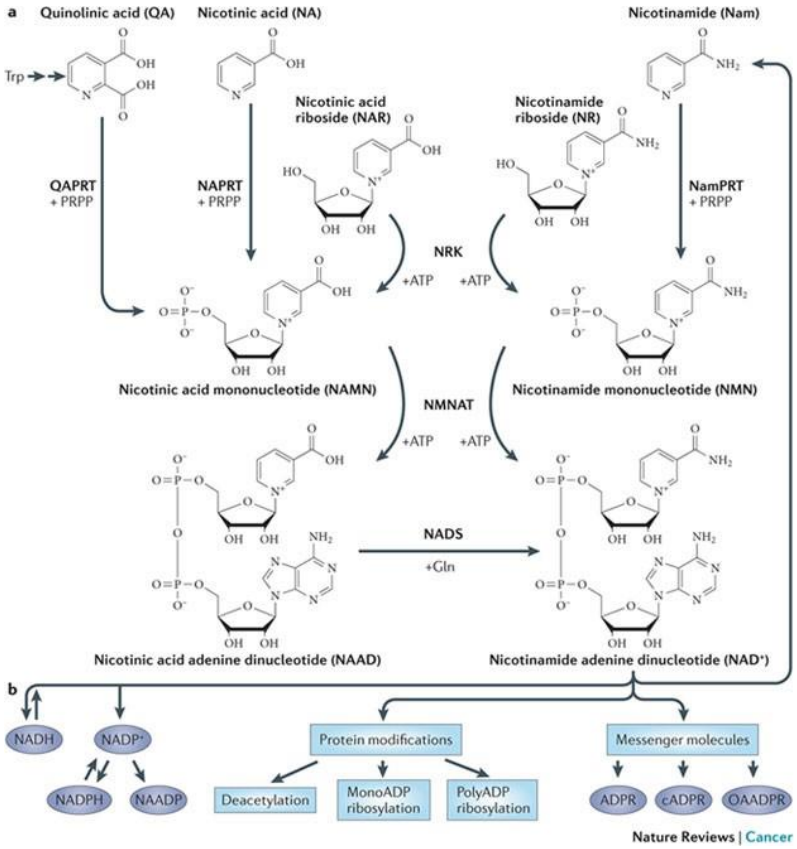

Figure 4. The NAD metabolome in humans [52]

All of these three nucleotides are converted in nicotinic acid mononucleotide (NaMN) and nicotinamide mononucleotide (NMN) by phosphoribosyltransferases, while the obtainment of the dinucleotidic form is operated by nicotinamide mononucleotide adenylyltransferase (NMNAT) [53] (Figure 4).

2.2. The NAD salvage pathway: role of NAMPT

NAMPT is a homodimer class type II phosphoribosyltransferase, a key enzyme of NAD biosynthesis, starting from nicotinamide (NAM) and phosphoribosyl pyrophosphate (PRPP) generates NMN. The second passage of this pathway involves adenosine triphosphate (ATP), that helps NMN to be converted in NAD^+

by NMNAT [54]. The reaction conducted by NAMPT is the rate-determining step of NAD production in the salvage pathway.

In 1994, a 52 kDa-cytokine, imputable to the extracellular form of NAMPT, was discovered. This cytokine, discovered from a human peripheral blood lymphocyte cDNA library, expressed in bone marrow stromal cells, was called PBEF (pre-B-cell colony-enhancing factor), according to its ability to develop pre-B-cell colonies in combination with IL-7 and stem-cell factor (SCF) [55].

In 2005 [56,57], also visfatin has been identified, described as an adipokine or adipocytokine, due to its presence in the adipose tissue.

Currently, according to HUGO Gene Nomenclature Committee, we should gather these two cytokines under a common name: eNAMPT. Indeed, PBEF and visfatin have the same structure of NAMPT, although its enzymatic activity in the extracellular space remains unclear [58].

2.3. iNAMPT regulates ATP levels and NAD-dependent enzymes

iNAMPT activity is crucial for several metabolic processes such as glycolysis, nucleotide biosynthesis and ATP generation. NAD^+, and its reduced counterpart NADH, are rapidly reduced or oxidised to generate ATP. As it has been highlighted in Figure 4, iNAMPT is able to couple ATP hydrolysis and NMN synthesis. The ATP hydrolysis reflects a more efficient catalysis driven by iNAMPT. One or more molecules of ATP are formed for one molecule of NMN synthesised [52]. Moreover, NAMPT is also able to catalyse the synthesis and degradation of adenosine 5'-tetraphosphate (Ap4) through its facultative ATPase activity, recognized as a potent signalling molecule. This molecule is both present in the intracellular and extracellular space, with a vasoconstricting activity through P2X1 receptor-activation [59].

NAD-related functions include transcriptional regulation, cell cycle progression, apoptosis, DNA repair, circadian rhythms, telomerase activity and its demand is crucial for cell survival [60]. Since iNAMPT controls NAD levels in cells, its activity

and expression modulate several NAD-dependent enzymes such as sirtuins (1-7), mono- and poly-ADP-ribose polymerases (ARTs; PARPs) and CD38/CD157, involved in transcription, apoptosis, aging, inflammation and other several processes in cells.

Of note, iNAMPT has been found abundantly in cytosol, secondly in the nucleus, but it is still not univocally demonstrated its presence in the mitochondria [61,62]

Recently, two important manuscripts have focused their attention on iNAMPT role in the nucleus. The first one has shown that no-dividing cells maintain iNAMPT into the nucleus, while dividing cells distribute the enzyme both in cytoplasm and nucleus, considering that iNAMPT is transported into cytoplasm in cell cycle-dependent way [63]. Moreover, Grolla et al. have highlighted that this transport may be promoted by the interaction of iNAMPT with glyceraldehyde 3-phosphate dehydrogenase (GADPH), in presence of stressful stimuli [64]. To note, iNAMPT is freely moving between the cellular compartments in support of the different NAD-dependent enzymes present in both nucleus and cytoplasm.

iNAMPT indirectly regulates the activity of the main NAD-dependent enzymes. **Sirtuins** use NAD^+ as cofactor. This class of enzymes is composed of seven members, distributed in the nuclear space (SIRT1; SIRT6-7), in the cytoplasm (SIRT1-2) and in mitochondria (SIRT3-4-5). These enzymes consume NAD^+ to generate nicotinamide, removing an acetyl group. Their activities are involved in genes expression (including genes which promote innate immunity), cell cycle regulation, apoptosis, and metabolism.

PARPs are divided in 18 classes that catalyse the polymerization of ADP-ribose and subsequently, the binding to glutamic or aspartic acid residues. These enzymes are present in the nucleus, responsible of DNA repairing. In front of minimal DNA damage, they activate repairing pathways, while, when the damage is extended or irreversible, they promote apoptosis or necrosis [65].

CD38 is a plasma membrane-associated glycoprotein, able to convert NAD to cADP-ribose, a second messenger involved in intracellular calcium release. CD38 is

expressed on the surface of different immune cells, including B cells, T cells, NK cells, and myeloid cells [66]. As an ectozyme, CD38 catalyses synthesis and hydrolysis of cyclic ADP-ribose (cADPR), converting NAD to ADP-ribose (ADPR), as well as cADPR into ADPR. Furthermore, in a condition of acid pH, CD38 catalyses synthesis and hydrolysis of nicotinic acid adenine dinucleotide phosphate (NAADP). Both reactions are essential for calcium signalling, specifically for mobilization of intracellular calcium, therefore essential for regulating immune response, metabolic reactions and cell adhesion [65].

2.4. The metabokine eNAMPT

From the discovery of extracellular NAMPT in 1994, several studies have been conducted and currently a series of scientific evidences highlighted its presence in the supernatant of numerous cell types, including differentiated adipocytes, hepatocytes, leucocytes, cardiomyocytes, neurons, amniotic epithelial cells, pancreatic β cells and inflammatory cells from innate and adaptive immunity [67] (Table 1).

	Cell type
Adipocytes	• 3T3-L1 adipocytes
	• SGBS adipocytes
	• Adipocytes derived from healthy donors
	• HIB-1B adipocytes
Immune cells	• LPS-activated monocytes
	• Macrophages in visceral adipose tissue
	• Leucocytes
	• Peripheral blood lymphocytes
Brain cells	• PC12 cells
	• Primary neurons
	• Primary glial cells
Cancer cells	• Hepatoma cells (HepG2, Huh-7)
	• Colorectal cancer cells (HCT-116, LS180)
	• Breast cancer cells (MCF10A, MCF7, T47D, MDA-MB-2 BT549, MDA-MB-468)
	• Melanoma cells (B16, MeWo, HMCB, SkMel28, LB24)
	• Neuroblastoma and glioma cells (SH-SY5Y, SK-N-Be, U87)
	• Mesothelioma (MSTO)
	• Prostate cancer cells (DU-145)
	• Cervical cancer cells (HeLa)
	• Chronic lymphocytic leukemia lymphocytes
Other cells	• Fibroblast (COS-7, PA317, CHO)
	• Amniotic epithelial cells
	• Inflamed HUVECs
	• Neonatal rat cardiomyocytes
	• Pancreatic beta cells
	• Isolated human islets
	• Sebocytes
	• Melanocytes

Table 1. Cell types which secrete eNAMPT [64]

There are limited informations about the relative amounts of eNAMPT found in the extracellular space, compared with the amount of iNAMPT found intracellularly. It is clear that eNAMPT release occurs in lack of cell death and therefore appears to be a true and specific phenomenon. Overall, a wide range of stimuli have been used to modulate eNAMPT release both *in vitro* and *in vivo*. These can be classified into three categories: (i) cellular stress; (ii) nutritional signals and (iii) inflammatory signals. This may indicate that eNAMPT secretion is recruited under specific conditions, but physiological role of this, in addition of those associated with cancer

pathology and inflammatory disorders, has not been clarified yet.

2.4.1. eNAMPT secretion mechanism

Since an active secretion has been proven, several authors tried to investigate in detail the mechanism of eNAMPT secretion, but, until now, this is still a matter of debate.

Unlike many secreted proteins, eNAMPT lacks a signal peptide. This suggests that it is not released through a classical pathway, which involves ER-Golgi compartments. Indeed, most reports suggest that its release is insensitive to brefeldin-A and monensin, inhibitors of the classical ER-Golgi-dependent pathway [68,69]. Further evidence has been proved by using chloroquine, an inhibitor of the classical lysosomal releasing pathway, that doesn't modify eNAMPT secretion in the extracellular space [58]. Firstly, eNAMPT is present in 100-300 nm microvesicles, but is absent in exosomes [70]. In 2019, Imai's group have highlighted the presence of eNAMPT in extracellular vesicles in systemic circulation of both humans and mice, which decreases with age [71].

Taken together, the current data shows that eNAMPT is released mainly by unconventional secretion pathways.

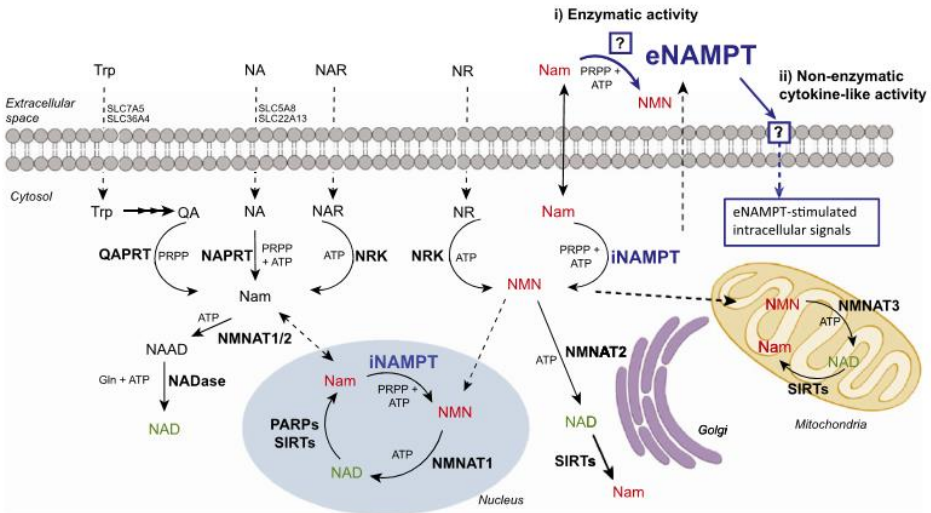

Figure 5. The localization of NAMPT in the cell [72]

2.4.2. NAMPT post-translational modifications: which is their role?

To note, post-translational modifications (PTMs) represent another important property of eNAMPT release and iNAMPT function and localization (nuclear or cytoplasmic). The most important PTM on iNAMPT, is the autophosphorylation on His247, which significantly increases its efficiency. The activation of the enzyme, thanks to this PTM, reinforces the interactions between the two monomers that form the catalytic site, allowing an efficient bond with Nam and PRPP, thus obtaining the synthesis of NMN. The iNAMPT regulation is a process that is precisely modulated by a series of curbs, furthermore, the regulation of NAMPT also depends on some acetylation sites of the protein.

In a paper(s) published by Imai's group are analysed some post-translational modifications of NAMPT, including acetylation and ribosylation of ADP, and they observed that iNAMPT is acetylated in brown and white adipose tissue. Relatively low levels of acetylated iNAMPT were detected in cell extracts while its acetylation significantly increases when cells are treated with deacetylase inhibitors. There are five acetylation residues identified on iNAMPT (K53, K79, K107, K331, K369) and they are all present on iNAMPT, surprisingly only the K369 residue is acetylated on eNAMPT [73].

Moreover, it has been reported that some modifications of the intracellular form could affect its secretion. The NAMPT peptide sequence encodes two putative sites for asparagine glycosylation (a characteristic modification that occurs in many secreted proteins) and at least 24 phosphorylation sites (14 serines, 3 threonines and 7 tyrosine), but, whether they seem to affect its secretion, it has to be experimentally demonstrated. Pillai et al. [74] treated cardiomyocytes with trichostatin A (a histone deacetylase inhibitor) or with high concentrations of nicotinamide (a non-specific SIRT inhibitor) and found that both treatments reduce the intracellular levels of iNAMPT and completely block eNAMPT release after stress, suggesting that an acetylation-dependent mechanism is likely to participate in protein release.

More recently, Sayers et al. have studied the structural and functional modifications

of eNAMPT in beta cells dysfunctions of type 2 diabetes (T2D). In healthy subjects, eNAMPT is at lower concentrations (around 1 ng/ml) in a dimeric form, while in T2D patients this concentration rises to 5 ng/ml and eNAMPT appears to be release in a monomeric way, inducing beta cell apoptosis, *via* NAD-dependent inflammatory pathways. They have also highlighted that a specific mutation of $Ser^{199/200}$ to aspartic acid impairs eNAMPT ability to create the dimeric form. The treatment of beta cells with this mutated form determine beta cells seizure [75].

Hitherto, all these mechanisms continue to be very vague and further experimental analysis need to be performed to highlight the key steps of these mechanisms.

2.4.3. eNAMPT: incontrovertible evidence and gigantic doubts

Many evidences confirm the eNAMPT cytokine-like activity and its association with the activation of intracellular signalling pathways. It still remains unclear if this activity might be mediated by an interaction with a plasma membrane receptor. In addition, confusing studies concerning its ability to produce NMN in the extracellular space are present in literature.

Putative receptors

Several molecular screening studies (*e.g.* two-hybrid assays, affinity capture and co-fractionation) have identified eNAMPT as a putative protein-binding partner [76,77], even if most of them have not been validated yet. The first receptor postulated was the insulin receptor, but the paper which demonstrated this interaction has been retracted in a second moment [56].

Another receptor proposed was the C-C chemokine receptor type 5 (CCR5), furthermore was found that eNAMPT is able to inhibit the infection by R5 HIV strain (so the virus able to bind CCR5 receptor) in macrophages and PBMCs, on the contrary of the X4 strain (virus with CXCR4 receptor) [78].

At present, the best candidate for being eNAMPT receptor is the Toll-like receptor type 4 (TLR4), besides it has been observed a homology between eNAMPT and MD-

2, the lipopolysaccharide-binding protein to TLR4. Indeed, Garcia and collaborators demonstrated that the circulating levels of eNAMPT are associated with the physiopathology of ventilator-induced inflammatory lung injury (VILI) through the activation of NF-κB, and this activation is mediated by the TLR4 binding [79].
More recently, also Deaglio's group has highlighted TLR4 as the main receptor of eNAMPT, with the ability to activate macrophages [80].

Extracellular enzymatic activity

Another important viewpoint, associated with the biological role of eNAMPT, is the possible extracellular enzymatic activity. iNAMPT, as an enzyme, works as a dimer. It has been demonstrated that dimeric eNAMPT is observable in conditioned media of HIB-1B adipocytes, with high level of NMN in mouse plasma [68]. As mention above, more recently it has been determined that eNAMPT seems to be present in a monomeric form in a pathological condition [75].
Several studies have suggested that the extracellular enzymatic activity is lower than the intracellular one due to the reduced availability of PRPP and NAM in the extracellular space. Although, the cellular death, like a necrosis tissue of the tumour, could enlarge the amount of PRPP and NAM available in the extracellular space and consequently sharpens the eNAMPT active state [81].
The simpler way to study the extracellular activity is its own inhibition with a common NAMPT inhibitor, FK866. In this case, since molecule cell permeability, the procedure for discriminating the two forms is unworkable. Indeed, some reports, have shown no effect of FK866 on eNAMPT function, demonstrating that at least part of its effects are independent from enzymatic activity [76,82]. Recently, some specific and polar eNAMPT inhibitors have been developed, unable to cross the plasma membrane [83].
Moreover, it has been revealed useful the studies of NAMPT mutated variants. Some of them, are characterized by loss of function (*e.g.* H247E) or loss of dimer oligomerization (S200D), preserving pathway activation, interleukins secretion and

macrophage activation, as the *wild-type* protein [82].

2.4.4. Signal transduction pathways triggered by eNAMPT

As a cytokine, eNAMPT is secreted by a number of cells, determining the activation of specific pathways on the targets.

In Figure 6, the major pathways activated by eNAMPT in each cell types are summarized, which demonstrate a physiological and pathological role of this cytokine. Despite physiological characteristics, eNAMPT has been studied and well identified in pathological conditions.

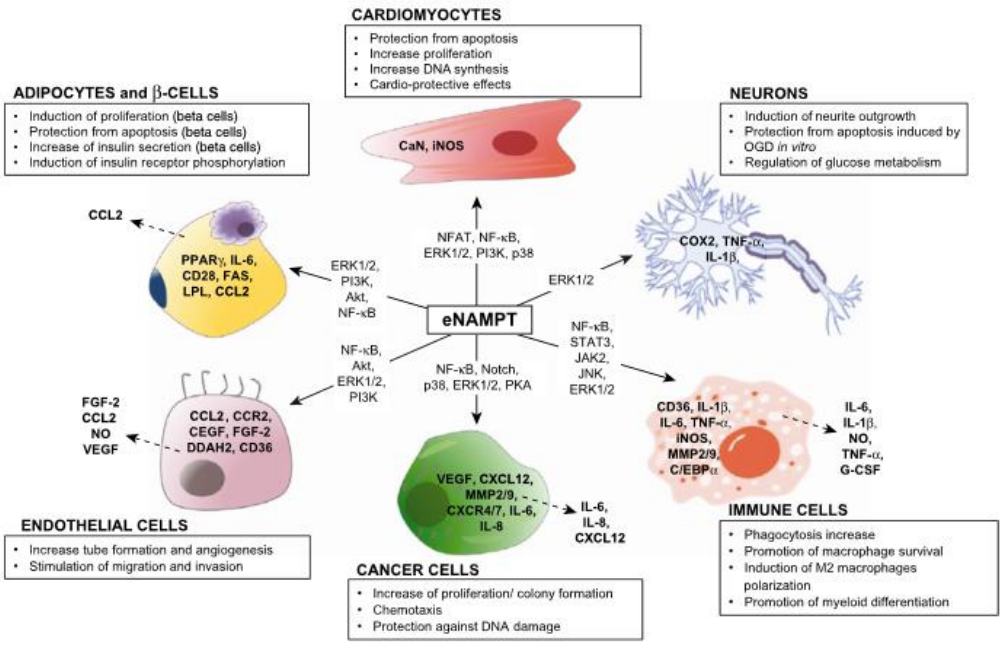

Figure 6. Pathways triggered by eNAMPT in different cell types [72]

For example, in adipocytes it has been reported the eNAMPT-mediated phosphorylation of insulin receptor and AKT induces proliferation, inhibition of apoptosis and increases of glucose uptake [68]. Moreover, p42/p44 MAPK activation determines the overexpression of monocyte chemoattractant protein (MCP-1), a

molecule which increases the risk of metabolic and vascular disorder in obese subjects, recruiting inflammatory cells [84].

2.5. Role of eNAMPT in pathology

Based on the different roles of eNAMPT in various cellular functions, it is not surprising that it could also be involved in the pathogenesis of different diseases linked to metabolic syndromes, inflammatory diseases and cancer.

Several pathologies have shown increased eNAMPT levels in serum but also, a direct involvement of this cytokine in the recruitment of immune cells as a direct link of the recrudescence of inflammation.

Inflammation

The first evidence of eNAMPT role in immunity has been demonstrated with its capacity to synergize with IL-7 and SCF to stimulate early stage B cell formation [55]. Abundant inflammatory stimuli are able to cause eNAMPT over-secretion, especially from innate immune cells such as neutrophils, monocytes and macrophages [65]. eNAMPT release is mediated by proinflammatory cytokines as tumour necrosis factor (TNF), interleukin 1β (IL-1β), and IL-6, but it also promotes chemotaxis and production of this cytokines [85].

In this regard, peripheral blood monocyte cells (PBMCs), incubated with eNAMPT, induce a dose-dependent induction of IL-1β, IL-1 receptor, IL-6 and TNF-α, through the activation of $CD14^+$ monocytes, but also macrophages and dendritic cells.

eNAMPT is also involved in the upregulation of several monocyte surface molecules, such as:

- CD54 (or iCAM1), promoting T cells activation and leucocytes infiltration,
- CD40, a costimulatory protein in antigen presenting cells (APCs), inducing their persistence and the activation of B cells by T helper cells,

- CD80 (or B7-1) and CD86, determining costimulatory signals which sustains T cells activation and response.

This activation is sustained by p38 MAPK signalling pathway and PI3K, producing TNF-α [86].

NAMPT and macrophages

Macrophages are professional phagocytic cells derived from bone marrow precursors or from monocytes in the peripheral blood. They are able to maintain and safeguard host tissues and in front of a "non-self" stimulus, they propagate a pro-inflammatory response. They play plenty roles in both healthy and pathological conditions and the activation is largely dependent on the surrounding microenvironment [87].

Macrophages plasticity is the key role of their activation: they are able to polarize themselves through a M1 pro-inflammatory and a M2 anti-inflammatory modulation. In macrophages, eNAMPT potently blocks apoptosis induced by a number of ER stressors. The mechanism involves a two-step sequential process: rapid induction of IL-6 secretion, followed by IL-6-mediated autocrine/paracrine activation of the pro-survival signal transducer STAT3. These data suggest eNAMPT role in balancing macrophage survival and death [76]. More important, Audrito and collaborators have described for the first time a role of eNAMPT as a critical element in the induction of an immunosuppressive and tumour-promoting microenvironment of chronic lymphocytic leukaemia (CLL). eNAMPT is important for differentiation of resting monocytes, polarizing them toward tumour supporting M2-macrophages. These cells express high levels of CD206, CD163, and IDO and secrete immunosuppressive (IL-10, CCL18) and tumour-promoting (IL-6, IL-8) cytokines. NAMPT-primed M2 macrophages activates extracellular-regulated kinase and NF-κB signalling, promoting leukemic cell survival and reduces T-cell responses [82]. Overall, eNAMPT is a critical element in both induction of an immunosuppressive and tumour-promoting microenvironment.

eNAMPT promotes also the survival of macrophages, monocytes and neutrophils, especially in obesity-related inflammatory diseases, which promotes atherosclerosis [76]. Indeed, eNAMPT is also secreted in the extracellular space by several types of cells and it could promote inflammation-related diseases. It has been reported that eNAMPT is present in vascular smooth muscle cells within atherosclerotic plaque. In this place eNAMPT promotes the overexpression of iNOS, NF-κB and ERK-signalling, which determines the releasing of inflammatory cytokines and endothelial damage [88].

Moreover, eNAMPT also upregulates TGF-β, a cytokine that controls several functions concerning cell growth, differentiation and apoptosis in immune cells [89]. The effect of eNAMPT is also significant for the granulocyte colony-stimulating factor (G-CSF)-induced myeloid differentiation. In this case, it has been postulated that eNAMPT triggers G-CSF in both healthy and severe congenital neutropenic subjects, verifying an increase of iNAMPT and NAD^+ in myeloid cells. Consequently, the amount of iNAMPT and NAD^+ levels cause the differentiation of $CD34^+$ hematopoietic progenitor cells in *vitro* [90].

Bermudez et al. demonstrated that iNAMPT, overexpressed in macrophages derived from bone marrow, can reduces M1 pool, and that the signal mediated by this protein is not enough by itself to drive polarization. Otherwise, he also proved that eNAMPT increases the expression of IL-6, TNF-α and CCL2 and it controls M1 polarization [91].

eNAMPT effects could be summarized in Figure 7, as an inflammation promoter in the extracellular space, increasing the common pro-inflammatory cytokines, and inducing an M1- or an M2-phenotype, as far as the inflammatory condition occurs.

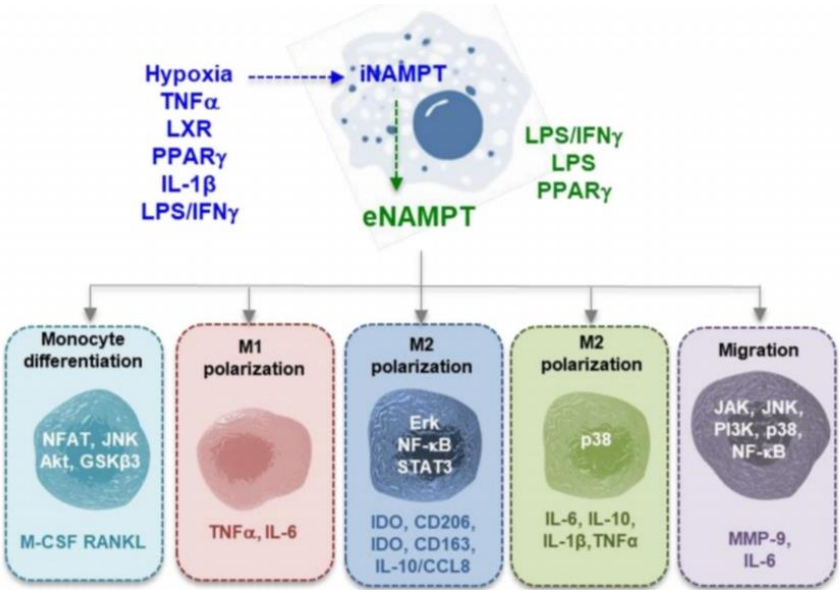

Figure 7: role of iNAMPT/eNAMPT in monocytes/macrophages [92].

eNAMPT is secreted during the inflammation process. Indeed LPS, LPS/IFN-γ and PPAR-γ are able to promote eNAMPT secretion in macrophages and myeloid cells [93–95].

2.6. Inflammatory-eNAMPT-related diseases

eNAMPT has been associated to several inflammatory diseases like tumours, a wide series of inflammatory diseases and diabetes, as described in Figure 8.

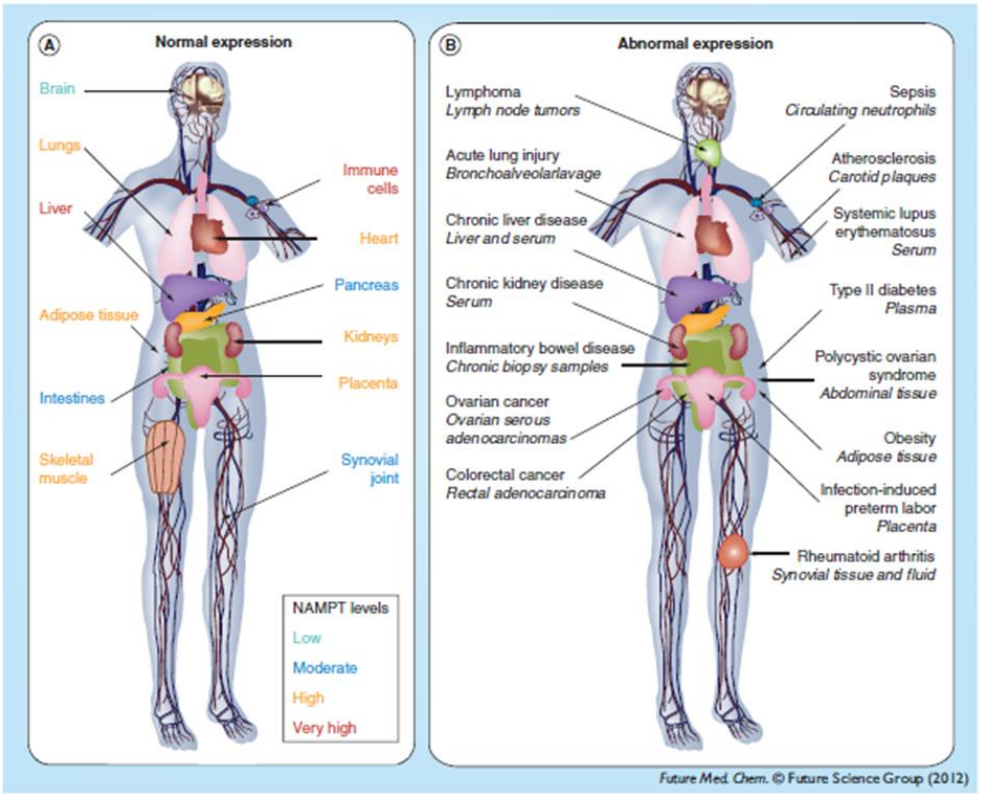

Figure 8. Normal and pathological expression of eNAMPT [96]

The major inflammatory-related diseases are:

- Diabetes-related inflammatory diseases and metabolic syndrome
- Rheumatoid arthritis (RA), osteoarthritis and lupus erythematosus
- Acute respiratory distress syndrome (ARDS) and ventilator-induced lung injury (VILI)
- Inflammatory bowel disease (IBD).

Diabetes and metabolic syndrome

Diabetes mellitus is a metabolic disease characterized by hyperglycaemia. eNAMPT role has been associated with diabetes mellitus type 2, secreted from visceral adipose tissue. Moreover, eNAMPT seems to be linked with lipid metabolism [97], due to

their adipocytokine-like activity and it is able to increase monocytes chemoattractant protein 1 (MCP-1) through p42/p44 MAPK signalling pathway [84].
Its secretion exasperates metalloproteinases 2 and 7 (MMP-2 and 7), TNFα, IL-6, IL-1, iNOS and VEGF production, determining increased proliferation, capillary-like formation and cell adhesion. In this case, eNAMPT enhances atherogenic and inflammatory niche [84,98], causing plaque destabilization.

Rheumatoid arthritis, osteoarthritis and lupus erythematosus
Several studies have demonstrated that high serum and synovial levels of eNAMPT [99] are associated with the gravity of joint damages, clinical scores, prompting cartilage erosion. In this case, eNAMPT levels are not associated with obesity and metabolic disorder, but they are related to the ability to regulate inflammatory process. Indeed, in RA patients, eNAMPT levels do not correlated with the lipid profile [100].
eNAMPT finely regulates the production of several factors that may influence RA pathogenesis:

- IL-1β, IL-6, IL-10 and TNF-α in PBMCs
- IL-1β, IL-6 and TNFα in $CD14^+$ monocytes (p38 MAPK and MEK1 dependent)
- PGE2, MMP-3,13 and ADAMTS (a disintegrin and metalloproteinase with thrombospondin motifs or aggrecanases) synthesis in chondrocytes, postulated as a degradation marker in patients.

Furthermore, the production of eNAMPT is triggered by IL-6/STAT-3 signaling, due to its positive feedback in inflammatory niche. eNAMPT promotes a significant change in RA synovial fibroblasts (RASFs) gene expression, up-regulating genes associated to aggressive erosive activity and to fibroblasts and leucocytes motility within synovial tissue. The establishment of inflammatory niche in rheumatoid arthritis synovium is enhanced by the increased influx of inflammatory cells into the

synovial tissue. The leucocytes extravasation is promoted by eNAMPT, inducing the production of IL-8, VEGF and EGF, with a strong proangiogenic effect [101].
Moreover, RA patients treated with biologicals (bDMARD) as anti-TNFs or tocilizumab (anti-IL6) decreased serum eNAMPT levels but did not correlate with disease activity. Contrary, the treatment of RA naïve patients with conventional (csDMARDs as methotrexate, sulfasalazine or leflunomide) diminished eNAMPT levels and they are associated with disease activity and progression [102].
Another disease linked to high serum level of eNAMPT is systemic lupus erythematosus (SLE). In this case, eNAMPT is not associated with metabolic disorder, as the other adipocytokines measured, but with the recrudescence of the inflammatory state with an unknown process [103].

Acute respiratory distress syndrome and ventilator-induced lung injury
Acute respiratory distress syndrome (ARDS) is one of the severe forms of acute lung injury (ALI), described with different symptoms as hypoxemia with pulmonary cell infiltrates, lung inflammation, non-cardiogenic oedema. The disease is characterized with increased vascular permeability, damaging both endothelial and epithelial cell barriers [104]. Although ventilation seems to be a life-saving intervention, it contributes to aggravate lung injury and the inflammatory niche. ARDS flows into ventilator-induced lung injury (VILI) [37].
ALI and ARDS are associated with the production of different cytokines as IL-1β, TNF-α and IL-8, resulting in barrier dysfunction.
It has been reported that eNAMPT is one of the proteins overexpressed in ALI and ARDS, determining increased levels of the cytokines mentioned before. As consequence, eNAMPT promotes endothelial cell permeability, polymorphonuclear leukocytes (PMLs) recruitments and mechanic stress.
The role of eNAMPT in the exasperation of the physiopathology of ALI/ARDS, the link between its levels and the response to mechanical stress are still unclear, but it has been shown that there is a modest protection from VILI in heterozygous

NAMPT$^{+/-}$ mice, operating with a deletion of a single allele of NAMPT itself [79,105].

Inflammatory bowel disease

Several studies have reported the correlation between high serum level of eNAMPT with the IBD [106–108]. Due to the anatomic proximity of bowel and visceral fat, the inflamed bowel wall could activate adipocytes. Visceral adipose tissue releases several cytokines and adipokines, such as leptin, adiponectin, resistin, chemerin and, of course, eNAMPT. Most of them are harmful to gastrointestinal tract, increasing the damage mediated by immunological system through the consequent secretion of pro-inflammatory factors (interleukins and adhesion factors).

eNAMPT increased levels have been observed during active UC symptoms and have been correlated with the stage of the disease. Moreover, after three months of treatment, eNAMPT levels seem to be lowered [86,106,109,110].

eNAMPT, through the promotion of IL-6 signaling, activates STAT3, BCL-2, BCL-XL and mediates resistance of T cells to apoptosis [109]. eNAMPT seems to play a fundamental role in flaring up IBD, due to activated NF-κB, p38 and MEK1 pathways [106].

Recently, Neubauer and collaborators have analyzed serum eNAMPT as a potential biomarker of mucosal healing (MH). In addition, they tested the goodness of eNAMPT in the differential diagnosis between the two types of IBD, highlighting an accurate overall precision, with poor specificity. In addition to the serum form, this study evaluated the expressed iNAMPT form in leukocytes and the tissues. The first was strongly related to serum, demonstrating its direct involvement in immune cells; the second, observed on biopsy specimens from IBD patients, was 2-4 times higher than the normal mucosal control. Moreover, in this recent study, it has been shown that the physiological effect of eNAMPT in the intestine appears to be a cellular protection from oxidative stress and hypoxia and that eNAMPT and TNFα, the effector of fibrosis in the intestine, are independently related. The oversecretion

of eNAMPT, therefore, could promote fibrosis, and confers pro-tumor mechanisms: the epithelium-mesenchymal transition (EMT), in fact, is promoted by hypoxia, which in turn stimulates the synthesis of eNAMPT *via* HIF-1α, a factor that could be fundamental in the pathogenesis of IBD or cancer associated-colitis [110].

Moreover, it has been observed high levels of eNAMPT in $TLR9^{-/-}$ mice, compared to $TLR9^{wt/wt}$, induced with DSS, as a model of chronic colitis. It has been evaluated that the lack of TLR9 in KO mice treated with DSS increases eNAMPT levels. Even though the TLR9-silencing immune response, eNAMPT continues to contribute to enhancement of colitis damage [111].

2.7. Targeting NAMPT as a therapeutic strategy

Several NAMPT inhibitors have been projected, such as FK866 (or APO866 or (E)-N-(4-(1-benzoylpiperidin-4-yl)butyl)3-(pyridine-3-yl)acrylamide) and CHS828 ((E)-1-[6-(4-chlorophenoxy)hexyl]-2-cyano-3-(pyridin-4-yl)guanidine). There are evidences supporting their potential in the therapeutic field, primary as anticancer agents, but there are also few information highlighting them as anti-inflammatory drugs [96,112]. In the anti-inflammatory field, there are evidences about the therapeutic ability of FK866 to reduce IL-1β and IL-6 secretion in collagen-inducted arthritis (CIA), model of rheumatoid arthritis, through the consequent reduction of intracellular NAD^+ stock in inflammatory cells. Gerner et al. have investigated iNAMPT expression in *lamina propria* of colon in steady-state and after 7 days of DSS colitis mice. iNAMPT in healthy colon is expressed at higher levels in epithelial cells compared to the total $CD45^+$ cells, comprehensive of $CD11b/F4/80^+$ macrophages and Ly6G neutrophils granulocytes, that is reverted in the inflamed condition [113]. iNAMPT inhibition with FK866 or compound 30c in DSS murine models ameliorates symptoms reducing NAD^+ levels and NAD^+ correlated enzymes [113,114]. In human tissue, FK866 reduces cytokine secretion in a comparable manner to dexamethasone in extracted *lamina propria* mononuclear cells of IBD [113].

These studies [96,115] have assessed the potentiality of FK866 to interfere with the inflammatory diseases caused and maintained by TNF-α, IL-6 and IL-1β. The main drawback of using NAMPT inhibitors is the uncertain ability to differentiate between the intracellular and the extracellular form.

Due to the cell permeability of these inhibitors and the undefined enzymatic activity in the extracellular space, FK866 is unable to reduce the signaling pathways activation correlated to eNAMPT [72]. Indeed, possible therapeutic strategy could be: (i) to create polar eNAMPT inhibitors (it is still unknown if the extracellular enzymatic activity could influence inflammation) or (ii) neutralizing antibodies.

eNAMPT neutralizing antibodies

A very promising method to counteract eNAMPT activity is using neutralizing antibodies. Several studies have demonstrated the ability to reverse its extracellular activity. Garcia et al. have created a neutralizing polyclonal eNAMPT antibody as a target therapy in VILI, showing a reduction of PMNs recruitment and have determined a protection against the disease [116].

Moreover, a humanization of the anti-NAMPT antibody is in production and validation phase for ARDS, VILI, and trauma- and radiation-induced lung injury and prostate cancer [117] (www.aqualungtherapeutics.com). Aqualung Therapeutics Corporation has developed this monoclonal antibody named eNamptor™ or ALT-100 designed to address and prevent the development of unchecked inflammation. eNamptor™ is an innovative monoclonal antibody therapy, that is created to be prophylactically administered at the time of patient intubation for respiratory failure and initiation of mechanical ventilation.

References

1 Kumar V, Abbas AK, Fausto N, *et al. Robbins and Cotran Pathologic Basis of Disease, Professional Edition E-Book*. Elsevier Health Sciences 2014.

2 Yeshi K, Ruscher R, Hunter L, *et al.* Revisiting Inflammatory Bowel Disease: Pathology, Treatments, Challenges and Emerging Therapeutics Including Drug Leads from Natural Products. *Journal of Clinical Medicine* 2020;**9**:1273. doi:10.3390/jcm9051273

3 Rook GAW. Hygiene hypothesis and autoimmune diseases. *Clin Rev Allergy Immunol* 2012;**42**:5–15. doi:10.1007/s12016-011-8285-8

4 Friedrich M, Pohin M, Powrie F. Cytokine Networks in the Pathophysiology of Inflammatory Bowel Disease. *Immunity* 2019;**50**:992–1006. doi:10.1016/j.immuni.2019.03.017

5 Rogler G, Biedermann L, Scharl M. New insights into the pathophysiology of inflammatory bowel disease: microbiota, epigenetics and common signalling pathways. *Swiss Med Wkly* 2018;**148**:w14599. doi:10.4414/smw.2018.14599

6 Vind I, Jespersgaard C, Hougs L, *et al.* Genetic and environmental factors in monozygotic twins with Crohn's disease and their first-degree relatives: a case report. *Digestion* 2005;**71**:262–5. doi:10.1159/000087053

7 Duerr RH. Genome-wide association studies herald a new era of rapid discoveries in inflammatory bowel disease research. *Gastroenterology* 2007;**132**:2045–9. doi:10.1053/j.gastro.2007.03.082

8 Jostins L, Ripke S, Weersma RK, *et al.* Host-microbe interactions have shaped the genetic architecture of inflammatory bowel disease. *Nature* 2012;**491**:119–24. doi:10.1038/nature11582

9 Ogura Y, Bonen DK, Inohara N, *et al.* A frameshift mutation in NOD2 associated with susceptibility to Crohn's disease. *Nature* 2001;**411**:603–6. doi:10.1038/35079114

10 Cooney R, Baker J, Brain O, *et al.* NOD2 stimulation induces autophagy in dendritic cells influencing bacterial handling and antigen presentation. *Nat Med* 2010;**16**:90–7. doi:10.1038/nm.2069

11 Zhang Y-Z, Li Y-Y. Inflammatory bowel disease: pathogenesis. *World J Gastroenterol* 2014;**20**:91–9. doi:10.3748/wjg.v20.i1.91

12 Ng SC, Shi HY, Hamidi N, *et al.* Worldwide incidence and prevalence of inflammatory bowel disease in the 21st century: a systematic review of population-based studies. *Lancet* 2018;**390**:2769–78. doi:10.1016/S0140-6736(17)32448-0

13 Fricker M, Goggins BJ, Mateer S, *et al.* Chronic cigarette smoke exposure induces systemic hypoxia that drives intestinal dysfunction. *JCI Insight* 2018;**3**. doi:10.1172/jci.insight.94040

14 Mokbel M, Carbonnel F, Beaugerie L, *et al.* [Effect of smoking on the long-term course of ulcerative colitis]. *Gastroenterol Clin Biol* 1998;**22**:858–62.

15 Johansson MEV, Phillipson M, Petersson J, *et al.* The inner of the two Muc2 mucin-dependent mucus layers in colon is devoid of bacteria. *Proc Natl Acad Sci U S A* 2008;**105**:15064–9. doi:10.1073/pnas.0803124105

16 Qin J, Li R, Raes J, *et al.* A human gut microbial gene catalogue established by metagenomic sequencing. *Nature* 2010;**464**:59–65. doi:10.1038/nature08821

17 Meconi S, Vercellone A, Levillain F, *et al.* Adherent-invasive Escherichia coli isolated from Crohn's disease patients induce granulomas in vitro. *Cell Microbiol* 2007;**9**:1252–61. doi:10.1111/j.1462-5822.2006.00868.x

18 Cipolla G, Crema F, Sacco S, *et al.* Nonsteroidal anti-inflammatory drugs and inflammatory bowel disease: current perspectives. *Pharmacol Res* 2002;**46**:1–6. doi:10.1016/s1043-6618(02)00033-6

19 Cornish JA, Tan E, Simillis C, *et al.* The risk of oral contraceptives in the etiology of inflammatory bowel disease: a meta-analysis. *Am J Gastroenterol* 2008;**103**:2394–400. doi:10.1111/j.1572-0241.2008.02064.x

20 Froicu M, Zhu Y, Cantorna MT. Vitamin D receptor is required to control gastrointestinal immunity in IL-10 knockout mice. *Immunology* 2006;**117**:310–8. doi:10.1111/j.1365-2567.2005.02290.x

21 Xavier RJ, Podolsky DK. Unravelling the pathogenesis of inflammatory bowel disease. *Nature* 2007;**448**:427–34. doi:10.1038/nature06005

22 Fukata M, Abreu MT. TLR4 signalling in the intestine in health and disease. *Biochem Soc Trans* 2007;**35**:1473–8. doi:10.1042/BST0351473

23 Watanabe T, Kitani A, Murray PJ, *et al.* NOD2 is a negative regulator of Toll-like receptor 2-mediated T helper type 1 responses. *Nat Immunol* 2004;**5**:800–8. doi:10.1038/ni1092

24 Bonen DK, Ogura Y, Nicolae DL, *et al.* Crohn's disease-associated NOD2 variants share a signaling defect in response to lipopolysaccharide and peptidoglycan. *Gastroenterology* 2003;**124**:140–6. doi:10.1053/gast.2003.50019

25 Van der Sluis M, De Koning BAE, De Bruijn ACJM, *et al.* Muc2-deficient mice spontaneously develop colitis, indicating that MUC2 is critical for colonic protection. *Gastroenterology* 2006;**131**:117–29. doi:10.1053/j.gastro.2006.04.020

26 Velcich A, Yang W, Heyer J, *et al.* Colorectal cancer in mice genetically deficient in the mucin Muc2. *Science* 2002;**295**:1726–9. doi:10.1126/science.1069094

27 Buisine MP, Desreumaux P, Debailleul V, *et al.* Abnormalities in mucin gene expression in Crohn's disease. *Inflamm Bowel Dis* 1999;**5**:24–32. doi:10.1097/00054725-199902000-00004

28 Wehkamp J, Harder J, Weichenthal M, *et al.* Inducible and constitutive beta-defensins are differentially expressed in Crohn's disease and ulcerative colitis. *Inflamm Bowel Dis* 2003;**9**:215–23. doi:10.1097/00054725-200307000-00001

29 Cobrin GM, Abreu MT. Defects in mucosal immunity leading to Crohn's disease. *Immunol Rev* 2005;**206**:277–95. doi:10.1111/j.0105-2896.2005.00293.x

30 Targan SR, Karp LC. Defects in mucosal immunity leading to ulcerative colitis. *Immunol Rev* 2005;**206**:296–305. doi:10.1111/j.0105-2896.2005.00286.x

31 Podolsky DK. Inflammatory bowel disease. *N Engl J Med* 2002;**347**:417–29. doi:10.1056/NEJMra020831

32 Heller F, Florian P, Bojarski C, *et al.* Interleukin-13 is the key effector Th2 cytokine in ulcerative colitis that affects epithelial tight junctions, apoptosis, and

cell restitution. *Gastroenterology* 2005;**129**:550–64. doi:10.1016/j.gastro.2005.05.002

33 Ananthakrishnan AN. Epidemiology and risk factors for IBD. *Nat Rev Gastroenterol Hepatol* 2015;**12**:205–17. doi:10.1038/nrgastro.2015.34

34 Rovedatti L, Kudo T, Biancheri P, *et al.* Differential regulation of interleukin 17 and interferon gamma production in inflammatory bowel disease. *Gut* 2009;**58**:1629–36. doi:10.1136/gut.2009.182170

35 Sarra M, Pallone F, Macdonald TT, *et al.* IL-23/IL-17 axis in IBD. *Inflamm Bowel Dis* 2010;**16**:1808–13. doi:10.1002/ibd.21248

36 Fujino S, Andoh A, Bamba S, *et al.* Increased expression of interleukin 17 in inflammatory bowel disease. *Gut* 2003;**52**:65–70. doi:10.1136/gut.52.1.65

37 Biasi F, Leonarduzzi G, Oteiza PI, *et al.* Inflammatory bowel disease: mechanisms, redox considerations, and therapeutic targets. *Antioxid Redox Signal* 2013;**19**:1711–47. doi:10.1089/ars.2012.4530

38 Silva FAR, Rodrigues BL, Ayrizono M de LS, *et al.* The Immunological Basis of Inflammatory Bowel Disease. *Gastroenterol Res Pract* 2016;**2016**:2097274. doi:10.1155/2016/2097274

39 Flynn S, Eisenstein S. Inflammatory Bowel Disease Presentation and Diagnosis. *Surg Clin North Am* 2019;**99**:1051–62. doi:10.1016/j.suc.2019.08.001

40 Menees SB, Powell C, Kurlander J, *et al.* A meta-analysis of the utility of C-reactive protein, erythrocyte sedimentation rate, fecal calprotectin, and fecal lactoferrin to exclude inflammatory bowel disease in adults with IBS. *Am J Gastroenterol* 2015;**110**:444–54. doi:10.1038/ajg.2015.6

41 Bressler B, Panaccione R, Fedorak RN, *et al.* Clinicians' guide to the use of fecal calprotectin to identify and monitor disease activity in inflammatory bowel disease. *Can J Gastroenterol Hepatol* 2015;**29**:369–72. doi:10.1155/2015/852723

42 Prideaux L, De Cruz P, Ng SC, *et al.* Serological antibodies in inflammatory bowel disease: a systematic review. *Inflamm Bowel Dis* 2012;**18**:1340–55. doi:10.1002/ibd.21903

43 Annese V, Andreoli A, Andriulli A, *et al.* Familial expression of anti-Saccharomyces cerevisiae Mannan antibodies in Crohn's disease and ulcerative colitis: a GISC study. *Am J Gastroenterol* 2001;**96**:2407–12. doi:10.1111/j.1572-0241.2001.04043.x

44 Mowat C, Cole A, Windsor A, *et al.* Guidelines for the management of inflammatory bowel disease in adults. *Gut* 2011;**60**:571–607. doi:10.1136/gut.2010.224154

45 Rf H, Jm B. A simple index of Crohn's-disease activity. Lancet (London, England). 1980;**1**. doi:10.1016/s0140-6736(80)92767-1

46 Mary JY, Modigliani R. Development and validation of an endoscopic index of the severity for Crohn's disease: a prospective multicentre study. Groupe d'Etudes Thérapeutiques des Affections Inflammatoires du Tube Digestif (GETAID). *Gut* 1989;**30**:983–9. doi:10.1136/gut.30.7.983

47 Lamb CA, Kennedy NA, Raine T, *et al.* British Society of Gastroenterology consensus guidelines on the management of inflammatory bowel disease in adults. *Gut* 2019;**68**:s1–106. doi:10.1136/gutjnl-2019-318484

48 Choi CH, Moon W, Kim YS, *et al.* Second Korean guidelines for the management of ulcerative colitis. *Intest Res* 2017;**15**:7–37. doi:10.5217/ir.2017.15.1.7

49 Ye B, Yang S-K, Shin S, *et al.* Guidelines for the Management of Crohn's Disease. *The Korean journal of gastroenterology = Taehan Sohwagi Hakhoe chi* 2012;**59**:141–79. doi:10.4166/kjg.2012.59.2.141

50 Argollo M, Fiorino G, Hindryckx P, *et al.* Novel therapeutic targets for inflammatory bowel disease. *J Autoimmun* 2017;**85**:103–16. doi:10.1016/j.jaut.2017.07.004

51 Gisbert JP, Chaparro M. Predictors of Primary Response to Biologic Treatment [Anti-TNF, Vedolizumab, and Ustekinumab] in Patients With Inflammatory Bowel Disease: From Basic Science to Clinical Practice. *J Crohns Colitis* 2020;**14**:694–709. doi:10.1093/ecco-jcc/jjz195

52 Chiarugi A, Dölle C, Felici R, *et al.* The NAD metabolome--a key determinant of cancer cell biology. *Nat Rev Cancer* 2012;**12**:741–52. doi:10.1038/nrc3340

53 Mattevi A. A close look at NAD biosynthesis. *Nat Struct Mol Biol* 2006;**13**:563–4. doi:10.1038/nsmb0706-563

54 Wang T, Zhang X, Bheda P, *et al.* Structure of Nampt/PBEF/visfatin, a mammalian NAD+ biosynthetic enzyme. *Nat Struct Mol Biol* 2006;**13**:661–2. doi:10.1038/nsmb1114

55 Samal B, Sun Y, Stearns G, *et al.* Cloning and characterization of the cDNA encoding a novel human pre-B-cell colony-enhancing factor. *Mol Cell Biol* 1994;**14**:1431–7. doi:10.1128/mcb.14.2.1431

56 Fukuhara A, Matsuda M, Nishizawa M, *et al.* Retraction. *Science* 2007;**318**:565. doi:10.1126/science.318.5850.565b

57 Sethi JK, Vidal-Puig A. Visfatin: the missing link between intra-abdominal obesity and diabetes? *Trends Mol Med* 2005;**11**:344–7. doi:10.1016/j.molmed.2005.06.010

58 Grolla AA, Torretta S, Gnemmi I, *et al.* Nicotinamide phosphoribosyltransferase (NAMPT/PBEF/visfatin) is a tumoural cytokine released from melanoma. *Pigment Cell Melanoma Res* 2015;**28**:718–29. doi:10.1111/pcmr.12420

59 Amici A, Grolla AA, Del Grosso E, *et al.* Synthesis and Degradation of Adenosine 5'-Tetraphosphate by Nicotinamide and Nicotinate Phosphoribosyltransferases. *Cell Chem Biol* 2017;**24**:553-564.e4. doi:10.1016/j.chembiol.2017.03.010

60 Shackelford RE, Mayhall K, Maxwell NM, *et al.* Nicotinamide phosphoribosyltransferase in malignancy: a review. *Genes Cancer* 2013;**4**:447–56. doi:10.1177/1947601913507576

61 Pittelli M, Formentini L, Faraco G, *et al.* Inhibition of nicotinamide phosphoribosyltransferase: cellular bioenergetics reveals a mitochondrial

insensitive NAD pool. *J Biol Chem* 2010;**285**:34106–14. doi:10.1074/jbc.M110.136739

62 Cantó C, Menzies KJ, Auwerx J. NAD+ Metabolism and the Control of Energy Homeostasis: A Balancing Act between Mitochondria and the Nucleus. *Cell Metabolism* 2015;**22**:31–53. doi:10.1016/j.cmet.2015.05.023

63 Svoboda P, Krizova E, Sestakova S, *et al.* Nuclear transport of nicotinamide phosphoribosyltransferase is cell cycle-dependent in mammalian cells, and its inhibition slows cell growth. *J Biol Chem* 2019;**294**:8676–89. doi:10.1074/jbc.RA118.003505

64 Grolla AA, Miggiano R, Di Marino D, *et al.* A nicotinamide phosphoribosyltransferase-GAPDH interaction sustains the stress-induced NMN/NAD+ salvage pathway in the nucleus. *J Biol Chem* Published Online First: 27 January 2020. doi:10.1074/jbc.RA119.010571

65 Luk T, Malam Z, Marshall JC. Pre-B cell colony-enhancing factor (PBEF)/visfatin: a novel mediator of innate immunity. *J Leukoc Biol* 2008;**83**:804–16. doi:10.1189/jlb.0807581

66 Deaglio S, Mehta K, Malavasi F. Human CD38: a (r)evolutionary story of enzymes and receptors. *Leuk Res* 2001;**25**:1–12. doi:10.1016/s0145-2126(00)00093-x

67 Garten A, Schuster S, Penke M, *et al.* Physiological and pathophysiological roles of NAMPT and NAD metabolism. *Nat Rev Endocrinol* 2015;**11**:535–46. doi:10.1038/nrendo.2015.117

68 Revollo JR, Körner A, Mills KF, *et al.* Nampt/PBEF/Visfatin regulates insulin secretion in beta cells as a systemic NAD biosynthetic enzyme. *Cell Metab* 2007;**6**:363–75. doi:10.1016/j.cmet.2007.09.003

69 Garten A, Petzold S, Barnikol-Oettler A, *et al.* Nicotinamide phosphoribosyltransferase (NAMPT/PBEF/visfatin) is constitutively released from human hepatocytes. *Biochem Biophys Res Commun* 2010;**391**:376–81. doi:10.1016/j.bbrc.2009.11.066

70 Tanaka M, Nozaki M, Fukuhara A, *et al.* Visfatin is released from 3T3-L1 adipocytes via a non-classical pathway. *Biochem Biophys Res Commun* 2007;**359**:194–201. doi:10.1016/j.bbrc.2007.05.096

71 Yoshida M, Satoh A, Lin JB, *et al.* Extracellular Vesicle-Contained eNAMPT Delays Aging and Extends Lifespan in Mice. *Cell Metab* 2019;**30**:329-342.e5. doi:10.1016/j.cmet.2019.05.015

72 Grolla AA, Travelli C, Genazzani AA, *et al.* Extracellular nicotinamide phosphoribosyltransferase, a new cancer metabokine. *Br J Pharmacol* 2016;**173**:2182–94. doi:10.1111/bph.13505

73 Yoon MJ, Yoshida M, Johnson S, *et al.* SIRT1-Mediated eNAMPT Secretion from Adipose Tissue Regulates Hypothalamic NAD+ and Function in Mice. *Cell Metab* 2015;**21**:706–17. doi:10.1016/j.cmet.2015.04.002

74 Pillai VB, Sundaresan NR, Kim G, *et al.* Nampt secreted from cardiomyocytes promotes development of cardiac hypertrophy and adverse ventricular remodeling. *Am J Physiol Heart Circ Physiol* 2013;**304**:H415-426. doi:10.1152/ajpheart.00468.2012

75 Sayers SR, Beavil RL, Fine NHF, *et al.* Structure-functional changes in eNAMPT at high concentrations mediate mouse and human beta cell dysfunction in type 2 diabetes. *Diabetologia* 2020;**63**:313–23. doi:10.1007/s00125-019-05029-y

76 Li Y, Zhang Y, Dorweiler B, *et al.* Extracellular Nampt promotes macrophage survival via a nonenzymatic interleukin-6/STAT3 signaling mechanism. *J Biol Chem* 2008;**283**:34833–43. doi:10.1074/jbc.M805866200

77 Wan C, Borgeson B, Phanse S, *et al.* Panorama of ancient metazoan macromolecular complexes. *Nature* 2015;**525**:339–44. doi:10.1038/nature14877

78 Van den Bergh R, Morin S, Sass HJ, *et al.* Monocytes Contribute to Differential Immune Pressure on R5 versus X4 HIV through the Adipocytokine Visfatin/NAMPT. *PLoS One* 2012;**7**. doi:10.1371/journal.pone.0035074

79 Camp SM, Ceco E, Evenoski CL, *et al.* Unique Toll-Like Receptor 4 Activation by NAMPT/PBEF Induces NFκB Signaling and Inflammatory Lung Injury. *Sci Rep* 2015;**5**. doi:10.1038/srep13135

80 Managò A, Audrito V, Mazzola F, *et al.* Extracellular nicotinate phosphoribosyltransferase binds Toll like receptor 4 and mediates inflammation. *Nat Commun* 2019;**10**:4116. doi:10.1038/s41467-019-12055-2

81 Hara N, Yamada K, Shibata T, *et al.* Nicotinamide Phosphoribosyltransferase/Visfatin Does Not Catalyze Nicotinamide Mononucleotide Formation in Blood Plasma. *PLOS ONE* 2011;**6**:e22781. doi:10.1371/journal.pone.0022781

82 Audrito V, Serra S, Brusa D, *et al.* Extracellular nicotinamide phosphoribosyltransferase (NAMPT) promotes M2 macrophage polarization in chronic lymphocytic leukemia. *Blood* 2015;**125**:111–23. doi:10.1182/blood-2014-07-589069

83 Travelli C, Aprile S, Mattoteia D, *et al.* Identification of potent triazolylpyridine nicotinamide phosphoribosyltransferase (NAMPT) inhibitors bearing a 1,2,3-triazole tail group. *Eur J Med Chem* 2019;**181**:111576. doi:10.1016/j.ejmech.2019.111576

84 Sommer G, Kralisch S, Kloting N, *et al.* Visfatin is a positive regulator of MCP-1 in human adipocytes in vitro and in mice in vivo. *Obesity (Silver Spring)* 2010;**18**:1486–92. doi:10.1038/oby.2009.462

85 Jacques C, Holzenberger M, Mladenovic Z, *et al.* Proinflammatory actions of visfatin/nicotinamide phosphoribosyltransferase (Nampt) involve regulation of insulin signaling pathway and Nampt enzymatic activity. *J Biol Chem* 2012;**287**:15100–8. doi:10.1074/jbc.M112.350215

86 Moschen AR, Kaser A, Enrich B, *et al.* Visfatin, an Adipocytokine with Proinflammatory and Immunomodulating Properties. *The Journal of Immunology* 2007;**178**:1748–58. doi:10.4049/jimmunol.178.3.1748

87 Amit I, Winter DR, Jung S. The role of the local environment and epigenetics in shaping macrophage identity and their effect on tissue homeostasis. *Nat Immunol* 2016;**17**:18–25. doi:10.1038/ni.3325

88 Yun MR, Seo JM, Park HY. Visfatin contributes to the differentiation of monocytes into macrophages through the differential regulation of inflammatory cytokines in THP-1 cells. *Cell Signal* 2014;**26**:705–15. doi:10.1016/j.cellsig.2013.12.010

89 Sun Z, Lei H, Zhang Z. Pre-B cell colony enhancing factor (PBEF), a cytokine with multiple physiological functions. *Cytokine Growth Factor Rev* 2013;**24**:433–42. doi:10.1016/j.cytogfr.2013.05.006

90 Skokowa J, Lan D, Thakur BK, *et al.* NAMPT is essential for the G-CSF-induced myeloid differentiation via a NAD(+)-sirtuin-1-dependent pathway. *Nat Med* 2009;**15**:151–8. doi:10.1038/nm.1913

91 Bermudez B, Dahl TB, Medina I, *et al.* Leukocyte Overexpression of Intracellular NAMPT Attenuates Atherosclerosis by Regulating PPARγ-Dependent Monocyte Differentiation and Function. *Arterioscler Thromb Vasc Biol* 2017;**37**:1157–67. doi:10.1161/ATVBAHA.116.308187

92 Travelli C, Colombo G, Mola S, *et al.* NAMPT: A pleiotropic modulator of monocytes and macrophages. *Pharmacological Research* 2018;**135**:25–36. doi:10.1016/j.phrs.2018.06.022

93 Halvorsen B, Espeland MZ, Andersen GØ, *et al.* Increased expression of NAMPT in PBMC from patients with acute coronary syndrome and in inflammatory M1 macrophages. *Atherosclerosis* 2015;**243**:204–10. doi:10.1016/j.atherosclerosis.2015.09.010

94 Svoboda P, KříŽová E, Čeňková K, *et al.* Visfatin is actively secreted in vitro from U-937 macrophages, but only passively released from 3T3-L1 adipocytes and HepG2 hepatocytes. *Physiol Res* 2017;**66**:709–14. doi:10.33549/physiolres.933370

95 Mayi TH, Rigamonti E, Pattou F, *et al.* Liver X Receptor (LXR) activation negatively regulates visfatin expression in macrophages. *Biochem Biophys Res Commun* 2011;**404**:458–62. doi:10.1016/j.bbrc.2010.12.002

96 Nowell M, Evans L, Williams A. PBEF/NAMPT/visfatin: a promising drug target for treating rheumatoid arthritis? *Future Med Chem* 2012;**4**:751–69. doi:10.4155/fmc.12.34

97 Zhang LQ, Heruth DP, Ye SQ. Nicotinamide Phosphoribosyltransferase in Human Diseases. *J Bioanal Biomed* 2011;**3**:013–25. doi:10.4172/1948-593X.1000038

98 Hognogi LDM, Simiti LV. The cardiovascular impact of visfatin - an inflammation predictor biomarker in metabolic syndrome. *Clujul Med* 2016;**89**:322–6. doi:10.15386/cjmed-591

99 Otero M, Lago R, Gomez R, *et al.* Changes in plasma levels of fat-derived hormones adiponectin, leptin, resistin and visfatin in patients with rheumatoid arthritis. *Ann Rheum Dis* 2006;**65**:1198–201. doi:10.1136/ard.2005.046540

100 Sglunda O, Mann H, Hulejová H, *et al.* Decreased Circulating Visfatin Is Associated with Improved Disease Activity in Early Rheumatoid Arthritis: Data from the PERAC Cohort. *PLOS ONE* 2014;**9**:e103495. doi:10.1371/journal.pone.0103495

101 Meier FMP, Frommer KW, Peters MA, *et al.* Visfatin/pre-B-cell colony-enhancing factor (PBEF), a proinflammatory and cell motility-changing factor in rheumatoid arthritis. *J Biol Chem* 2012;**287**:28378–85. doi:10.1074/jbc.M111.312884

102 Franco-Trepat E, Guillán-Fresco M, Alonso-Pérez A, *et al.* Visfatin Connection: Present and Future in Osteoarthritis and Osteoporosis. *J Clin Med* 2019;**8**. doi:10.3390/jcm8081178

103 Chung CP, Long AG, Solus JF, *et al.* Adipocytokines in systemic lupus erythematosus: relationship to inflammation, insulin resistance and coronary atherosclerosis. *Lupus* 2009;**18**:799–806. doi:10.1177/0961203309103582

104 Wheeler AP, Bernard GR. Acute lung injury and the acute respiratory distress syndrome: a clinical review. *Lancet* 2007;**369**:1553–64. doi:10.1016/S0140-6736(07)60604-7

105 Garcia JGN. Methods and compositions involving PBEF inhibitors for lung inflammation conditions and diseases. 2016.https://patents.google.com/patent/US9409983B2/en (accessed 19 Jun 2020).

106 Dogan S, Guven K, Celikbilek M, *et al.* Serum Visfatin Levels in Ulcerative Colitis. *Journal of Clinical Laboratory Analysis* 2016;**30**:552–6. doi:10.1002/jcla.21901

107 Waluga M, Hartleb M, Boryczka G, *et al.* Serum adipokines in inflammatory bowel disease. *World J Gastroenterol* 2014;**20**:6912–7. doi:10.3748/wjg.v20.i22.6912

108 Starr AE, Deeke SA, Ning Z, *et al.* Proteomic analysis of ascending colon biopsies from a paediatric inflammatory bowel disease inception cohort identifies protein biomarkers that differentiate Crohn's disease from UC. *Gut* 2017;**66**:1573–83. doi:10.1136/gutjnl-2015-310705

109 Karrasch T, Schaeffler A. Adipokines and the role of visceral adipose tissue in inflammatory bowel disease. *Ann Gastroenterol* 2016;**29**:424–38. doi:10.20524/aog.2016.0077

110 Neubauer K, Bednarz-Misa I, Walecka-Zacharska E, *et al.* Oversecretion and Overexpression of Nicotinamide Phosphoribosyltransferase/Pre-B Colony-Enhancing Factor/Visfatin in Inflammatory Bowel Disease Reflects the Disease Activity, Severity of Inflammatory Response and Hypoxia. *Int J Mol Sci* 2019;**20**. doi:10.3390/ijms20010166

111 Karrasch T, Schmid A, Kopp A, *et al.* Impact of toll-like-receptor-9 (TLR9) deficiency on visceral adipose tissue adipokine expression during chronic DSS-induced colitis in mice. *Exp Clin Endocrinol Diabetes* 2015;**123**:80–7. doi:10.1055/s-0034-1398502

112 Galli U, Travelli C, Massarotti A, *et al.* Medicinal chemistry of nicotinamide phosphoribosyltransferase (NAMPT) inhibitors. *J Med Chem* 2013;**56**:6279–96. doi:10.1021/jm4001049

113 Gerner RR, Klepsch V, Macheiner S, *et al.* NAD metabolism fuels human and mouse intestinal inflammation. *Gut* 2018;**67**:1813–23. doi:10.1136/gutjnl-2017-314241

114 Travelli C, Aprile S, Rahimian R, *et al.* Identification of Novel Triazole-Based Nicotinamide Phosphoribosyltransferase (NAMPT) Inhibitors Endowed with Antiproliferative and Antiinflammatory Activity. *J Med Chem* 2017;**60**:1768–92. doi:10.1021/acs.jmedchem.6b01392

115 Busso N, Karababa M, Nobile M, *et al.* Pharmacological Inhibition of Nicotinamide Phosphoribosyltransferase/Visfatin Enzymatic Activity Identifies a New Inflammatory Pathway Linked to NAD. *PLoS ONE* 2008;**3**:e2267. doi:10.1371/journal.pone.0002267

116 Hong S-B, Huang Y, Moreno-Vinasco L, *et al.* Essential role of pre-B-cell colony enhancing factor in ventilator-induced lung injury. *Am J Respir Crit Care Med* 2008;**178**:605–17. doi:10.1164/rccm.200712-1822OC

117 Sun BL, Sun X, Casanova N, *et al.* Role of secreted extracellular nicotinamide phosphoribosyltransferase (eNAMPT) in prostate cancer progression: Novel biomarker and therapeutic target. *EBioMedicine* 2020;**61**:103059. doi:10.1016/j.ebiom.2020.103059

Chapter 2

OUTLINE OF THE THESIS

Nicotinamide phosphoribosyltransferase (NAMPT), the rate-limiting enzyme in NAD^+ biosynthesis, is upregulated in activated immune cells, such as monocytes, macrophages, dendritic, T and B cells, as well as in hematopoietic precursors. Interestingly, a soluble form, called eNAMPT, has been found in the extracellular space, with cytokine-like properties. How eNAMPT exerts its extracellular functions has not been fully elucidated. Van der Bergh et al. proposed a direct binding to CCR5 through which eNAMPT prevents HIV R5 strain infection in macrophages and PBMCs *in vitro* and we have confirmed that it may have an antagonistic role on this receptor, but data that shows TLR4 activation as the primary mechanism of action at present appears to be the more consistent. On the contrary, a second line of thought hypothesizes that the enzymatic activity is important, and it has been recently shown that a significant amount of eNAMPT is found in microvesicles. Moreover, few post-translational modifications (PTMs) on NAMPT have been described. While it is well known that PTMs control the activity of several enzymes and their localization, no NAMPT PTMs have highlighted to do so.

eNAMPT in the immune system is linked to lymphocytes survival, it increases the production of pro-inflammatory cytokines, enhances monocyte activation, included inhibition of macrophages apoptosis and induces granulocytic and monocytic differentiation. All these eNAMPT functions sustain a possible role of this cytokine triggering inflammatory niche in inflammatory-related diseases.

High serum eNAMPT levels in patients affected by inflammatory diseases, in particular in IBD, led us to determine its possible implication in the pathogenesis of these pathologies. Noteworthy, several studies demonstrated an increased expression and secretion of NAMPT in IBD patients and a correlation between enhanced levels of NAMPT and worse prognosis. In this setting, the expression of NAMPT is increased in biopsies of IBD patients and positive correlates with Disease Activity

Index. In a recent phase 2 open-label study of 103 golimumab-treated UC patients, NAMPT emerged as one of the 13 genes predictive of poor response. Moreover, Moschen's group have demonstrated that selective inhibitors of iNAMPT reduced inflammation in murine models of IBD. Unfortunately, such enzymatic inhibitors have been associated with severe on-target side effects.

These beliefs and the generation of monoclonal anti-NAMPT antibodies in our laboratory brought my work to investigate them on the IBD field.

My Ph.D. thesis is mainly focused on (as presented in the following chapters):

1. The determination of the potential anti-inflammatory activity of anti-NAMPT antibody (called C269) in preclinical murine models of IBD and the possible outcome of eNAMPT levels in IBD patients treated with biologics.
2. The biological effect of eNAMPT on one of its putative receptors, CCR5.
3. Identification of (PTMs) on nicotinamide phosphoribosyltransferase (NAMPT) in murine melanoma B16 cells and its possible role
4. The role of eNAMPT on macrophages and the possible priming effect with other inflammatory cytokines.

Chapter 3

Journal of Molecular Medicine (2020) 98:595–612
https://doi.org/10.1007/s00109-020-01892-0

JMolMed

ORIGINAL ARTICLE

Neutralization of extracellular NAMPT (nicotinamide phosphoribosyltransferase) ameliorates experimental murine colitis

Giorgia Colombo[1] · Nausicaa Clemente[2] · Andrea Zito[3] · Cristiano Bracci[3] · Federico Simone Colombo[4] · Sabina Sangaletti[5] · Elena Jachetti[5] · Davide Giuseppe Ribaldone[6] · Gian Paolo Caviglia[7] · Luca Pastorelli[8,9] · Marco De Andrea[2,10] · Samuele Naviglio[11] · Marianna Lucafò[12] · Gabriele Stocco[13] · Ambra A. Grolla[1] · Michela Campolo[14] · Giovanna Casili[14] · Salvatore Cuzzocrea[14] · Emanuela Esposito[14] · Fabio Malavasi[3] · Armando A. Genazzani[1] · Chiara Porta[1,2] · Cristina Travelli[15]

Received: 3 August 2019 / Revised: 25 February 2020 / Accepted: 28 February 2020 / Published online: 27 April 2020

Abstract

Extracellular nicotinamide phosphoribosyltransferase (eNAMPT) is increased in inflammatory bowel disease (IBD) patients, and its serum levels correlate with a worse prognosis. In the present manuscript, we show that eNAMPT serum levels are increased in IBD patients that fail to respond to anti-TNFα therapy (infliximab or adalimumab) and that its levels drop in patients that are responsive to these therapies, with values comparable with healthy subjects. Furthermore, eNAMPT administration in dinitrobenzene sulfonic acid (DNBS)-treated mice exacerbates the symptoms of colitis, suggesting a causative role of this protein in IBD. To determine the druggability of this cytokine, we developed a novel monoclonal antibody (C269) that neutralizes in vitro the cytokine-like action of eNAMPT and that reduces its serum levels in rodents. Of note, this newly generated antibody is able to significantly reduce acute and chronic colitis in both DNBS- and dextran sulfate sodium (DSS)-induced colitis. Importantly, C269 ameliorates the symptoms by reducing pro-inflammatory cytokines. Specifically, in the *lamina propria*, a reduced number of inflammatory monocytes, neutrophils, Th1, and cytotoxic T lymphocytes are found upon C269 treatment. Our data demonstrate that eNAMPT participates in IBD and, more importantly, that eNAMPT-neutralizing antibodies are endowed with a therapeutic potential in IBD.

Key messages

- **What are the new findings?**
- Higher serum eNAMPT levels in IBD patients might decrease response to anti-TNF therapy.
- The cytokine-like activity of eNAMPT may be neutralized with a monoclonal antibody.
- Neutralization of eNAMPT ameliorates acute and chronic experimental colitis.
- Neutralization of eNAMPT limits the expression of IBD inflammatory signature.
- Neutralization of eNAMPT impairs immune cell infiltration in *lamina propria*.

Keywords NAMPT · Experimental colitis · Neutralizing antibody · Mucosal immunity

Chiara Porta and Cristina Travelli contributed equally to this work.

Electronic supplementary material The online version of this article (https://doi.org/10.1007/s00109-020-01892-0) contains supplementary material, which is available to authorized users.

✉ Chiara Porta
chiara.porta@uniupo.it

✉ Cristina Travelli
cristina.travelli@unipv.it

Extended author information available on the last page of the article

Introduction

Crohn's disease (CD) and ulcerative colitis (UC) are the two major forms of inflammatory bowel diseases (IBD). Although the pathogenesis is still poorly understood, both forms are associated with a genetic predisposition, compromised epithelial barrier permeability, an abnormal gut microbiota, and exacerbated intestinal immune responses [1]. The unbalance between the innate and adaptive immune systems is a key feature of the disease. The inflamed intestine of both mice and

humans shows a displacement of tissue resident macrophages towards inflammatory monocytes, which have ongoing responsiveness to microbe-derived factors and produce high levels of inflammatory cytokines [2]. These inflammatory molecules exacerbate intestinal inflammation by disrupting the epithelial barrier and promoting recruitment and activation of pathogenic T cell responses [3].

Accordingly, the most relevant drugs that entered in clinic over the last two decades are inhibitors of tumor necrosis factor (TNFα) that impair both macrophage activation and T cell survival [4], and ustekinumab that targets the IL-12p40 subunit shared by IL-12 and IL-23 consequently inhibits T helper (Th) 1 and 17 cell responses [5, 6]. Furthermore, beyond inhibition of T cell repertoire or trafficking [5, 7], modulation of innate immunity has recently emerged as an additional therapeutic effect of anti-integrins (i.e., vedolizumab) [8]. Biologic drugs have been found effective in many IBD patients; however, a large proportion of patients with severe disease fail to achieve remission due to lack of drug response, loss of response, drug intolerance, or severe side effects that require cessation of therapy. Therefore, there is a clinical need for predictive response biomarkers as well as for new therapeutic strategies.

Nicotinamide phosphoribosyltransferase (NAMPT) is the bottleneck enzyme of the NAD salvage pathway and thereby is a controller of cellular NAD concentrations [9]. This enzyme is also actively secreted by many cell types, including monocytes/macrophages [10, 11]. Although there are accounts on the enzymatic activity of extracellular NAMPT (eNAMPT), the low levels of the substrates in the circulation [12] suggest that a receptor binding mode may be a more plausible mechanism mediating the cytokine-like activity of eNAMPT [13]. Currently, TLR4 and CCR5 [14, 15] have been suggested as putative eNAMPT receptors, but further confirmations are needed before these can be considered bona fide receptors of eNAMPT. Several evidences indicate that NAMPT influences different aspects of myeloid cell biology, including differentiation, migration, and functional activation [11, 16]. Exposure of macrophages to pro-inflammatory stimuli triggers both iNAMPT expression and eNAMPT secretion, and it has been suggested that eNAMPT acts as a positive support to inflammation in the extracellular space [11, 17].

Importantly, different studies have shown an increased expression/secretion of NAMPT in IBD patients and a correlation between elevated NAMPT levels and an unfavorable disease outcome. Indeed, NAMPT was significantly upregulated in biopsies from a cohort of pediatric IBD patients, and NAMPT levels were associated with Crohn's Disease Activity Index [18]. Immunohistochemistry analysis of human colonic biopsies showed that NAMPT co-localizes with dendritic cells and macrophages, but not with T or B cells, suggesting that, in this pathological context, iNAMPT might be mainly upregulated in the myeloid subset [17]. Consistently, in an animal model of chemically induced colitis, flow cytometry analysis of inflamed colons showed a selective increased expression of iNAMPT in macrophages, neutrophils, and inflammatory monocytes [19]. Noteworthy, it has been recently demonstrated that selective small molecule enzymatic inhibitors of NAMPT (FK866, compound 30c) are able to reduce colitis in murine models of IBD [19, 20]. Unfortunately, pre-clinical and clinical investigations in cancer have shown that iNAMPT inhibitors can induce severe side effects [21–24] (www.clinicaltrials.gov). To overcome these limitations, the possibility to act exclusively on the extracellular form (eNAMPT) with a neutralizing antibody, sparing the intracellular metabolic activity, is a highly attractive option.

In the present contribution, we have explored the therapeutic potential of eNAMPT neutralization in IBD.

Materials and methods

Patients The study was approved by the Burlo-Garofolo Institute Ethical Committee (n. 111/2015), by AOU Città della Salute e della Scienza di Torino – A.O. Mauriziano – A.S.L. TO1 Ethical Committee (n. 0056924 of 08/06/2016), and by ASL Milano-2 (n. 2726 of 02/10/2012), and written consent was obtained from patients. Patient characteristics, schedule of drug therapy, and maintenance are published elsewhere [25, 26]. Clinical response is defined as a reduction of > 2 points in HBI (for Crohn's disease) and in pMAYO (for ulcerative colitis) from baseline.

Induction of experimental colitis Animal care was in compliance with Italian regulations on protection of animals used for experimental purposes and were authorized by the Ministry of Health (120/2018 DB064.27 of 04/10/2017). Eight- to 10-week-old male mice were used for all the experimental procedures. BALB/C mice and C57BL/6 (Charles River laboratories) were maintained under 12-h light/dark cycle at 21 ± 1 °C and 50 ± 5% humidity. Standard laboratory diet and tap water were available ad libitum.

Acute colitis was induced in 8- to 10-week-old mice by rectal administration of DNBS (2–3 mg/mouse, Sigma). For chronic colitis, mice were induced by rectal administration of DNBS (3 mg/mouse) at day 0 and at day 21 and sacrificed at day 24.

In different preliminary experiments, this dose of DNBS was found to induce reproducible colitis without mortality. Mice were anesthetized by isoflurane (3%), and DNBS (2–3 mg in 100 μl of 50% ethanol) was injected intrarectally with a 0.05-mM catheter inserted 4 cm proximally into the anus. Vehicle alone (100 μl of 50% ethanol) was administered in control experiments (Sham). Then, animals were kept for 90″

in Trendelenburg position to avoid reflux. After the induction, the animals were observed for 4 or 5 days. At the day of the sacrifice, the sera were collected from the eye by retro-orbital puncture and the abdomen opened, removing colon and stocked for histological, biochemical, and flow cytometry studies. Animals were weighted every day.

Acute colitis was also induced with the administration of 1.5% dextran sulfate sodium (DSS) salt (36,000–50,000 M wt, MP Biomedicals), in drinking water ad libitum for 6 days. The DSS-containing water was substituted on day 7. From day 1, mice were monitored daily for body weight loss and general conditions. On day 8 and 14, mice were euthanized.

Treatments Control IgG1 or C269 (50 μg per mouse in phosphate-buffered saline, PBS) and respective vehicle were injected at day 0 and 3 post-DNBS induction and on day 0–3–7 day post-DSS induction. Recombinant eNAMPT (50 μg in PBS, endotoxin levels 0.02 EU/ml) and respective vehicle were injected every day during the experiments.

FACS analysis of *lamina propria* cells *Lamina propria* cells were isolated as previously described [27]. Briefly, colons were cut into 1-cm pieces and incubated with HBSS with 50-mM EDTA, two times, for 20 min, at 37 °C, under rotation. Colons were then filtered with a strainer, for removing epithelial cells, and were added HBSS with $CaCl_2$ to neutralize EDTA. Then, colons were digested with HBSS with collagenase/dispase (1 mg/ml, Roche), DNase I (40 μg/ml, Roche), and collagenase IV (0.25 mg/ml, Serva) for 30 min, at 37 °C under rotation. After digestion, cells were collected using 100-μM and 70-μM cell strainers and centrifugated at 1200*g*. Cells were stained in 0.5% FBS, HBSS solution with antibodies reported in Supplementary Table I. Cytofix/Cytoperm and Perm/Wash staining kit (eBioscience) were used for intracellular staining (TNFα and IFNγ), according to the manufacturer's instructions. Expression levels of cytokines (TNFα, IFNγ) were evaluated after 3 h of stimulation with pherbol-12 13-acetate (PMA; 40 ng/ml) and ionomycin (1 μg/ml) in the presence of brefeldin A (5 μg/ml; Sigma). Cells were incubated with TruStain fcXTM (anti-CD16/32) antibody (Biolegend), according to the manufacturer's instructions. Afterwards, 1×10^6 cells were stained with antigen-specific antibodies in the presence of LIVE/DEAD Fixable Violet (Invitrogen) to evaluate cell viability. Cells were acquired using BD LSRFortessa™, and data were analyzed using the BD FACSDiva 8.0.1 and FlowJo (9.3.2) software.

Ex vivo colonic explant Small pieces of colon (5 mM of mid-colon) were isolated and rinsed in HBSS/BSA and weighed. Colon explants were cultured overnight in 24-well tissue culture plates in 500-μl complete RPMI 1640 at 37 °C in an atmosphere containing 5% CO_2. After centrifugation at 10000*g* to pellet debris, culture supernatants were transferred to fresh tubes and stored at − 20 °C. eNAMPT concentrations were measured using enzyme-linked immunosorbent assay (ELISA kit from AdipoGen, Inc.) and were normalized to the weight of the colon explant.

Treatments Production, purification, and characterization of control IgG1, C269, and recombinant NAMPT (rNAMPT) are described further on.

ELISA Serum eNAMPT was evaluated with a commercially available sandwich enzyme-linked immunosorbent assay for human or murine NAMPT (ELISA kit from AdipoGen, Inc.; Seoul, Korea).

Recombinant murine eNAMPT purification Wild-type murine full-length NAMPT (ORF GenBank BC018358) was cloned in pET28a (NdeI/EcoRI) and expressed in *ClearColi* BL21(D3) (induction with IPTG 0.5 mM for 3 h at 25 °C) and purified by his-tag affinity chromatography with NiNTA Superflow resin (Qiagen). Endotoxin levels were evaluated with ToxinSensor Chromogenic LAL Endotoxin Assay kit (GeneScript). Only preparations with less than 0.1 EU/ml endotoxin levels were used.

Anti-eNAMPT antibody production Twelve hybridoma cell lines producing 12 different anti-eNAMPT antibodies were obtained by AbMart service. Cell supernatants were screened for the ability to recognize NAMPT using an ELISA method and western blot. The supernatants were also subjected to ouchterlony immunodiffusion assay to determine the isotype. The antibody C269 and the control IgG1 were produced from culture supernatants of respective hybridoma cell lines.

ELISA for hybridoma clone selection Indirect ELISA tests were carried out using the following procedure: 100 μl of coating antigen eNAMPT diluted with coating buffer of 1 μg/ml was pipetted into a microtiter plate and incubated at 4 °C overnight. Plates were washed three times using 300 μl/well of washing buffer solution, and 100-μl antibody diluted with PBS was added to each well. Unbound compounds were removed by washing solution after incubation for 1 h at 37 °C. A total of 100-μl HRP-IgG was added to each well for 1 h at 37 °C then washed four to six times with washing buffer. A total of 100 μl of substrate solution was then added to each well, and the enzymatic reaction was stopped after 15 min incubation at 37 °C by addition

of 100 μl/well of stopping solution. Absorbance values were measured at 450 nm.

Isotype determination Ouchterlony test was performed according to [28].

Anti-eNAMPT antibody (C269) purification Hybridoma cell lines were propagated in cell culture flasks (Cellstir® culture flask, Wheaton) and supernatants collected weekly. Obtaining a 5-L supernatant, cell broth was filtered with 0.45 μM and concentrated with hollow fiber system, and ready to be used for purification. Purification was carried out by protein G affinity chromatography; concentrate was loaded onto the column equilibrated with 20-mmol/L phosphate buffer. After elution of the unbound material, the eluent was changed to 0.1-mol/L glycin–HCl buffer (pH 2.7) to elute the bound material. Finally, it was washed with 20% (v/v) ethanol, as a regeneration step and for preservation of chromatographic column. The bound fraction was collected, immediately neutralized with a few drops of 1-mol/L Tris (pH 9.0), desalted by dialysis, and removed by endotoxins using Detoxi-Gel Endotoxin Removing Gel (ThermoFisher). The desalted protein was characterized by SDS-PAGE system to determine IgG purity and recovery yield and by enzyme-linked immunosorbent assay (ELISA) and western blot, to evaluate the immunoreactivity. Endotoxin levels were evaluated with ToxinSensor Chromogenic LAL Endotoxin Assay kit (GeneScript). Only preparations with endotoxin levels less than 0.1EU /ml were used.

NAMPT enzymatic activity The activity of recombinant NAMPT has been evaluated in the presence of vehicle (PBS), control IgG1, or C269, as previously described [29]. Briefly, the reaction mixtures containing 1 mM ATP, 0.5 mM PRPP, 0.5 mM nicotinamide 80 mM HEPES/NaOH buffer, pH 7.5, 12 mM $MgCl_2$, 0.5 mg/ml bovine serum albumin, 75 mM ethanol, 30 mM semicarbazide, and 4.5 mM NH_4Cl were incubated at 37 °C in the presence of 0.024 U/ml PncC, 0.192 U/ml NadD, 0.081 U/ml NadE, and 12.5 U/ml ADH as the ancillary enzymes of NAD pathway. The production of NADH was continuously monitored by OD measurement (340 nm).

NMN levels 4T1 cells were treated with C269, control IgG1, or FK866 as positive control for 18 h. After nucleotide extraction [30], cell lysates were tested for NMN levels. Thirty microliters of cell lysates were incubated at 37 °C in the presence of NAM (25 μM), PRPP (50 μM), and ATP (2 mM). Sequentially, 15 μl of 20% acetophenone and 15 μl of 2 M KOH were added. The reaction were incubated on ice for 10 min. Then, 67.5 μl of 100% formic acid was added, and the presence of the fluorescent NMN product was detected at Ex/Em, 382/445 nm [31].

Platelets and red blood cell counts To determine platelet (PTLs) number, 18 μl of blood collected by retro-orbital vein was mixed with 2 μl acid citrate dextrose. Ten microliters of the mixture were then blended with 190 μl $NaNH_3$ for 5 min at RT to lysis red blood cells. Then, 10 μl of this solution was diluted in 90 μl of PBS and then counted in a Burker chamber on a microscope with a × 40 objective [32].

To determine red blood cells' (RBCs) number, 1 unit of the whole blood was diluted in 199 units of Gower's solution (an isotonic solution that prevents lysis of RBCs). Ten microliters of this mixture were counted in a Burker chamber on a microscope with a × 40 objective.

Gene expression analysis Colons were homogenized with Trizol reagent (Life-technologies) using a potter and extracted with chloroform. One microgram mRNA was reverse transcribed with SENSIFAST kit as manufacturer's protocol (Aurogene) and cDNA expression determined with qPCR using SYBR-green (BioRad) and detected by the CFX96 real-time system (BioRad). Expression data were normalized to actin expression. The sequences of gene-specific primers are reported in Supplementary Table II.

Histological analysis At the end of the experiment, mice were euthanized; colons were resected, flushed with PBS, opened longitudinally, and rolled up. For the histological analysis, colon tissues were fixed at room temperature in a buffered formaldehyde solution (10% in phosphate-buffered saline), then samples were dehydrated in graded ethanol and embedded in Paraplast (Sherwood Medical, Mahwah, NJ). Next, 7-μM sections were deparaffinized with xylene and stained with hematoxylin-eosin. The following morphologic criteria were considered: score 0, no damage; score 1, focal epithelial edema and necrosis; score 2, diffuse swelling and necrosis of the villi; score 3, presence of neutrophil infiltrate in the submucosa; score 4, necrosis with neutrophil infiltrate; score 5, massive neutrophil infiltrate and hemorrhage. Colon damage (sections $n = 6$ for each animals) was scored by two independent pathologists blinded to the experimental protocol.

Immunohistochemistry Colon samples were fixed in 10% PBS-buffered formaldehyde and subsequently embedded

in paraffin, and 7-μm sections were cut from samples. After deparaffinization, endogenous peroxidase was quenched with 0.3% (v/v) hydrogen peroxide in 60% (v/v) methanol for 30 min. Slides were permeabilized with 0.1% (w/v) Triton X-100 in PBS for 20 min. Endogenous avidin or biotin binding sites were blocked by sequential incubation for 15 min with avidin and biotin (Vector Laboratories, Burlingame, CA), respectively. Sections were incubated overnight with the specific antibodies. Specific labeling was detected with a biotin-conjugated goat anti-rabbit IgG and avidin–biotin peroxidase complex (Vector Laboratories, Burlingame, CA). Sections were incubated with the following: (1) purified goat polyclonal antibody directed towards anti-P-selectin antibody (1:250 in PBS, v/v; Santa Cruz Biotechnology sc-6941) or (2) with anti-ICAM-1 antibody (1:250 in PBS, v/v; Santa Cruz Biotechnology sc:8439) or (3) with anti-TNF-α antibody (1:250 in PBS, v/v; Santa Cruz Biotechnology sc-52746) or (4) anti-Il-1β antibody (1:250 in PBS, v/v; Santa Cruz Biotechnology sc-32294) or (5) with anti-NF-κB antibody (1:250 in PBS, v/v; Santa Cruz Biotechnology sc-8008) or (6) with anti-IκB-α antibody (1:250 in PBS, v/v; Santa Cruz Biotechnology sc-1643) or (7) anti-NAMPT (1:100 in PBS v/v).To verify antibody-binding specificity, some slides were also incubated with only primary antibody or secondary antibody; no positive staining was found. Immunohistochemistry photographs were evaluated by densitometry by using Optilab Graftek software.

Cell culture 4T1 cells (ATCC) were cultured in MEM medium (Sigma-Aldrich) supplemented with 10% fetal bovine serum (FBS), 2 mM glutamine, 10 units/ml penicillin, and 100 g/ml streptomycin. Wild-type, overexpressing NAMPT (oeNAMPT) or silencing NAMPT (SH_NAMPT) B16-F10 cells (ATCC) [33] were cultured in DMEM medium (Sigma-Aldrich) supplemented with 10% fetal bovine serum (FBS), 2 mM glutamine, 10 units/ml penicillin, and 100 g/ml streptomycin. Cells were maintained in a humidified incubator supplied with 5% CO_2/95% air at 37 °C and were subcultured as needed by detaching the cells with 0.25% trypsin and 5 mM EDTA.

For immunoblot analysis, cells were cultured onto 60-mm plates. After the indicated treatments, cell lysates were prepared, and protein concentration was determined using the Micro BCA Protein Assay Kit (Thermo Fisher Scientific, Waltham, MA). Thirty micrograms of total protein from cell lysates were analyzed by SDS-polyacrylamide gel electrophoresis and western blotting using anti-phospho-STAT3 (Cell Signaling), anti-NAMPT (Adipogen), and anti-β-actin (Sigma).

Western blot analysis B16 and 4T1 cells were lysed in a lysis buffer (20 mM HEPES, 100 mM NaCl, 5 mM EDTA, 1% Nonidet-P40$^+$ Protease & Phosphatase Inhibitor Cocktail, Sigma). Protein quantification was performed with Bradford protein assay (Sigma), and proteins were resolved on SDS-PAGE and transferred with TurboBlot system (BioRad, Hemel Hempstead, UK).

Recombinant eNAMPT immunoprecipitation Antibodies (IgG1, C269, or commercial anti-NAMPT antibody, OMNI379 Adipogen) were incubated overnight with Protein A/G PLUS Agarose (Santa Cruz Biotechnology, USA) at 4 °C. Then, beads were centrifuged to eliminate the unbound antibody, and rNAMPT (500 ng in 200 μl) were added and incubated for 3 h. After five washes, beads were eluted by glycine, and the eluate was analyzed by SDS-PAGE with rabbit anti-NAMPT antibody (Gentex).

Statistics Data are presented as mean ± SEM or median and IQR. The normality of data distributions was assessed using Shapiro–Wilk test. Parametric (unpaired *t* test and one-way analysis of variance (ANOVA) followed by Tukey's post hoc) or non-parametric (Mann–Whitney *U* test and one-way Kruskal–Wallis *H* test followed by Dunn's post hoc) statistical analysis was used for comparisons of data. All statistical assessments were two-sided, and a value of $P < 0.05$ was considered statistically significant. For histological analysis, one-way ANOVA followed by Bonferroni post hoc test was used. Statistical analysis was performed using GraphPad Prism software (GraphPad Software, Inc., USA).

Results

Serum eNAMPT levels in adult and pediatric IBD patients

Different studies have shown high serum levels of eNAMPT in IBD [17, 34, 35], although a recent analysis in a large cohort of IBD patients has highlighted a high degree of variability [36].

To contribute to the field as well as to gather a rationale to investigate neutralization of eNAMPT as a therapeutic strategy, we determined levels of this cytokine in three small cohorts of patients that were not controlled by DMARDs and were treated with infliximab (IFX, cohort 1 and 3) or adalimumab (ADA, cohort 2).

A first cohort (Trieste) included serum from 21 pediatric patients (5 with ulcerative colitis and 16 with Crohn's disease), treated with infliximab. A second cohort (Torino) included a cohort of 31 patients (2 with ulcerative colitis and 29 with Crohn's disease), treated with adalimumab. A third cohort (Milano) included 38 patients (14 with ulcerative colitis and 25 with Crohn's disease), treated with infliximab. The three cohorts were analyzed separately, given that their recruitment was done in different periods and centers.

All the three cohorts were compared with a group of healthy donors (data not shown). We found for healthy donors a median of 0.28 ng/ml, which is superimposable to what was described previously [37]. As shown in Fig. 1a, we confirmed a pronounced variability through the cohorts, identifying a group of patients with eNAMPT serum levels comparable with healthy adult populations and a group that showed elevated levels of eNAMPT. Performing a ROC curve analysis, a cutoff of 4.5 ng/ml can be extrapolated to discriminate these two populations. Using this cutoff, the low-eNAMPT group had medians of 0.39 ng/ml (cohort 1), 1.4 ng/ml (cohort 2), and 0.46 ng/ml (cohort 3), while the high eNAMPT group had a median of 6.8 ng/ml, 5.7 ng/ml, and 5.5 ng/ml, respectively.

Noteworthy, 100% patients ($n = 52$) with levels of eNAMPT below 4.5 ng/ml were responsive to infliximab or adalimumab (Fig. 1b) across the three cohorts and maintained a low amount of circulating eNAMPT after 14 (median 0.30 ng/ml, 0.90 ng/ml, 0.78 ng/ml respectively) weeks of treatment. For the pediatric cohort 1, we also had eNAMPT determinations at 22 weeks and the same trend applied (Fig. 1c). In contrast, anti-tumor necrosis factor (TNFα) therapy failed either at 14 or 22 weeks in some patients with high circulating levels of eNAMPT (19/38), indicating that high systemic eNAMPT might be associated with an increased risk of resistance to anti-TNF therapy (Fig. 1b). While differences in the percentage not responders occurred in the three cohorts (24%, 26%, 16%), the general principle was applied.

Noteworthy, ELISA results showed a decrease in circulating eNAMPT at 14 weeks of treatment in responders and the maintenance of high systemic levels of eNAMPT in non-responders (Fig. 1b). Only a single patient, in the cohort 3, maintained response while increasing its eNAMPT levels.

The cohort 1 also contained two patients that showed an initial response at week 14, but this response was lost at week 22, and regained at week 54. To our great surprise, loss of response to treatment correlated with an increase in circulating eNAMPT (Fig. 1d).

While the cohorts used were small, the result is strengthened by the fact that the three cohorts all showed superimposable results. This, together with the literature data, primed us to hypothesize that eNAMPT is not a simple bystander but a pathogenic determinant of IBD, and its neutralization might be a pharmacological strategy worth investigating.

Development of an eNAMPT-neutralizing antibody (C269)

To test our hypothesis, we generated anti-eNAMPT-neutralizing antibodies. We initially developed 12 antibodies via a commercial source (Abmart). Mice were immunized with 12 different fragments of NAMPT (Fig. S1a), and 12 hybridoma clones were obtained. The supernatants of all 12 clones were first evaluated for the ability to recognize recombinant NAMPT (rNAMPT) by ELISA and western blot (Fig. S1b-c) and for the isotype (Fig. S1d). Based on these data, we then chose 5 clones (named C24.2, C43, C269, C382, and C47). These 5 hybridoma clones were then propagated, the antibodies were purified, and the selectivity on rNAMPT was re-evaluated. The clones C269, C43, and C24.2 were able to recognize rNAMPT by ELISA and western blot, and clone C269 had a performance similar to a commercial antibody used as standard (Fig. S1e-f). Since C269 is an IgG1k, we also purified a control IgG1 to use in all the experiments as a control. As shown in Fig. 2 a and b, C269, unlike the control IgG1, was able to detect rNAMPT in ELISA and in western blot analysis. Importantly, C269 detected a band at 55 kDa corresponding to NAMPT in cellular lysates (Fig. 2c), as determined by the commercial antibody (Adipogen).

NAMPT, as mentioned in the introduction, is an enzyme involved in cellular NAD metabolism but also acts as a cytokine. We therefore evaluated the effect of C269 on these two properties. As shown in Fig. 2d, C269 (up to 50 μg/200 μl) was devoid of any enzymatic inhibitory activity. Moreover, in comparison with FK866, C269 was not able to reduce intracellular NMN levels, (Fig. S1h), while it was able to abolish the phosphorylation of STAT-3 induced by eNAMPT in 4T1 cells (Fig. 2e–f).

In summary, we have generated a murine IgG1k antibody against eNAMPT that neutralizes the cytokine activity of this protein but does not interfere with its enzymatic properties (Fig. 2h).

Targeting eNAMPT with C269 ameliorates acute DNBS- and DSS-induced colitis

To investigate whether the neutralization of eNAMPT could reduce intestinal inflammation, we evaluated the effects of C269 on acute DNBS-induced colitis. BALB/C mice received an intrarectal administration of 3 mg of DNBS followed by two intraperitoneal (i.p.) injections of vehicle, C269, or control IgG1 (2.5 mg/kg per mouse; at day 0 and 3) and were

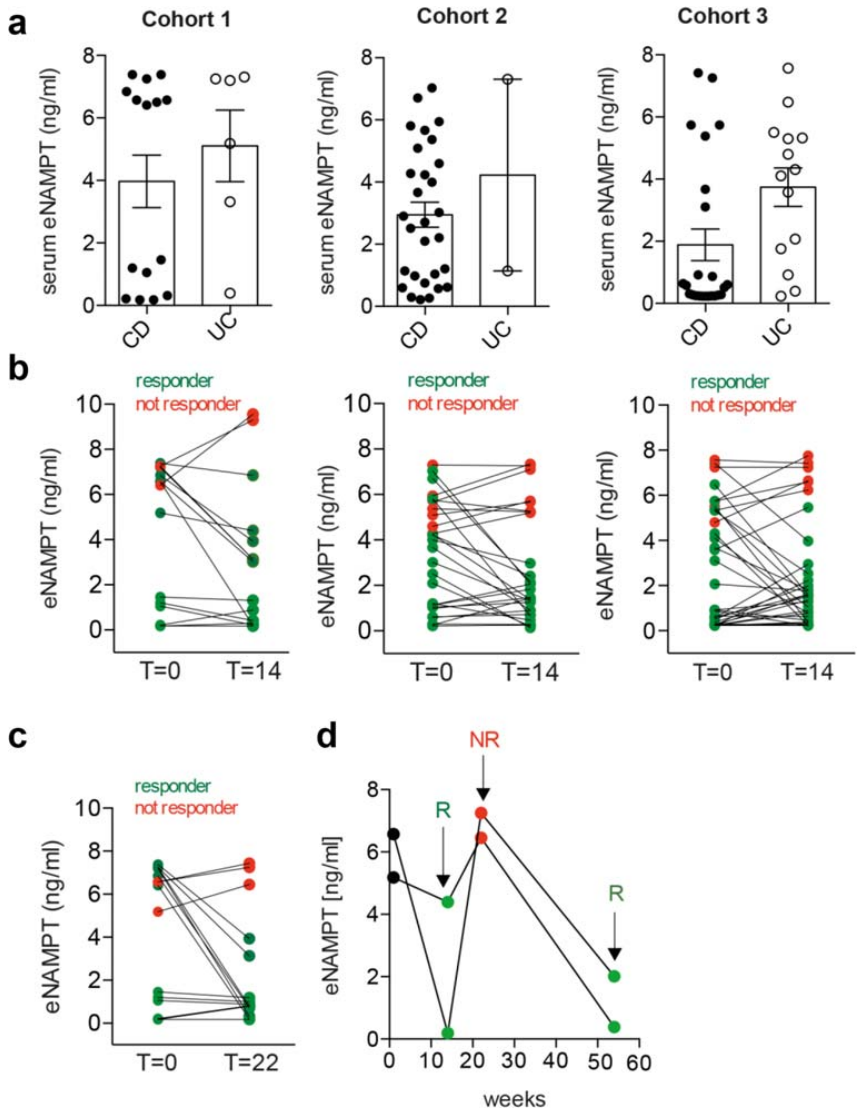

Fig. 1 Serum eNAMPT levels and anti-TNFα response in IBD patients. **a** eNAMPT levels in serum of three different cohorts before anti-TNFα treatment, $n = 91$. **b** eNAMPT levels in patients after 14 weeks of IFX and ADA treatment in three different cohorts, $n = 79$ and **c** after 22 weeks of treatment with IFX in cohort 1, $n = 21$. **d** eNAMPT serum levels of two patients that lose response at 22 weeks but regain it after 54 weeks from the first IFX infusion of cohort 1. R, responders; NR, not responders

sacrificed at day 5 (Fig. 3a). As shown in Fig. 3b, DNBS-induced body weight loss was significantly counteracted by C269 administration as compared with mice that received vehicle or control IgG1. Accordingly, colon shortening was significantly reduced by C269 treatment (Fig. 3c). Histological analysis of colonic tissue sections showed pronounced transmural necrosis and oedema in association with a consistent leukocyte infiltrate in the submucosa of DNBS-treated mice that received control IgG1, which was reverted by C269, leading to a significant lower colitis score (Fig. 3d).

Overall, these results indicate that targeting eNAMPT by C269 ameliorates acute colitis. Next, we evaluated the ex vivo production of this *metabokine* in colonic explants. To reduce the overall number of mice required for each experiment, we decided to use IgG1-treated mice as the control group. At the end of the experimental period, small pieces of colons from treated- and untreated mice were cultured in medium at 37 °C. After 24 h, cell-free tissue culture medium was collected and analyzed for eNAMPT levels. In comparison with sham mice (median 230 pg/mg), colonic explants from colitic IgG1-treated mice released a higher amount of eNAMPT (median 744 pg/mg), whereas C269 treatment was able to rescue eNAMPT levels (median 187.5 pg/mg) to the steady state level (Fig. 3e). These results confirm that eNAMPT levels are closely associated to the extent of intestinal inflammation. Given that circulating levels of eNAMPT are frequently

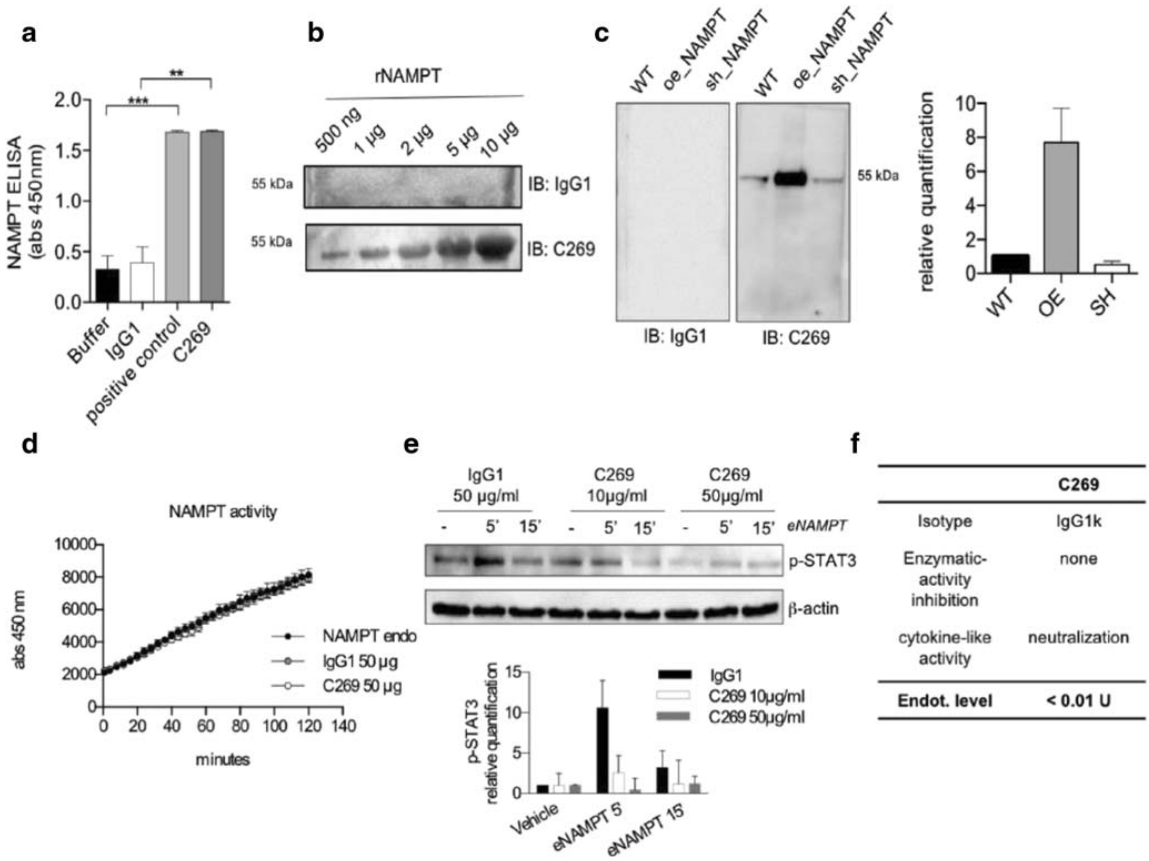

Fig. 2 Generation and validation of an eNAMPT-neutralizing antibody C269. **a** ELISA assay for NAMPT detection and **b** representative western blot of recombinant NAMPT detection using a control IgG1, a commercial anti-NAMPT antibody (positive control), and C269 (10 µg/ml), $n = 3$ independent experiments. **c** Representative western blot (left) and quantification (right) of NAMPT in wild-type B16 cells (WT), in B16 cells over-expressing NAMPT (oe_NAMPT) or in B16 cells in which NAMPT was knocked down (sh_NAMPT), using a control IgG1 or C269, $n = 2$ independent experiments. **d** In vitro NAMPT enzymatic activity determination in the presence of control IgG1 or C269 (50 µg), $n = 4$ independent experiments. **e** Representative western blot and quantification of p-STAT3 and β-actin in 4T1 cells stimulated with eNAMPT (500 ng/ml) in the presence of IgG1 or C269, $n = 3$ independent experiments. **f** Summary characteristics of C269. $^{***}p < 0.001$, $^{**}p < 0.01$ by unpaired two-tailed *t* test

increased in IBD patients, we evaluated whether the augmented local production of this inflammatory molecule in the colon of DNBS-treated mice also resulted in higher amount of systemic eNAMPT. We measured the levels of this *metabokine* in the serum of treated and sham mice, and we found that circulating eNAMPT levels were higher in colitic IgG1-treated mice (median at sacrifice 1.3 ng/ml) than in sham or DNBS-treated mice that received C269 (median at sacrifice, 0.77 ng/ml; Fig. 3f). While these latter data are obviously explained by treatment with a neutralizing antibody, the evidence as a whole point out that eNAMPT increases with increased damage.

We next evaluated the anti-inflammatory effects of C269 by using an additional widely used model of IBD that is based on the administration of the chemical irritant dextran sodium sulfate (DSS). C57BL/6 mice were treated with 1.5% of DSS in drinking water for 7 days, and starting from day 0, they were injected with C269 or control IgG1 every 4 days. Mice drinking regular tap water were used as control (sham). The results fully recapitulated the protective effect of C269 administration in terms of reduced body weight loss (median 85.1% of IgG1 vs 93.8% of C269; $p < 0.01$), colon shortening (median 7.4 cm of IgG1 vs 8.2 cm of C269; $p < 0.001$), and histological score (3 vs 2; $p < 0.05$, Fig. S2a-d). We also confirmed that ex vivo production of eNAMPT by colonic explants paralleled the amount of intestinal inflammation (median 680.1 pg/mg in IgG1 vs 351.5 pg/mg in sham mice; $p < 0.01$) and was effectively dampened by C269 treatments (median 401.5 pg/mg vs IgG1; $p < 0.01$, Fig. S2e). Despite this

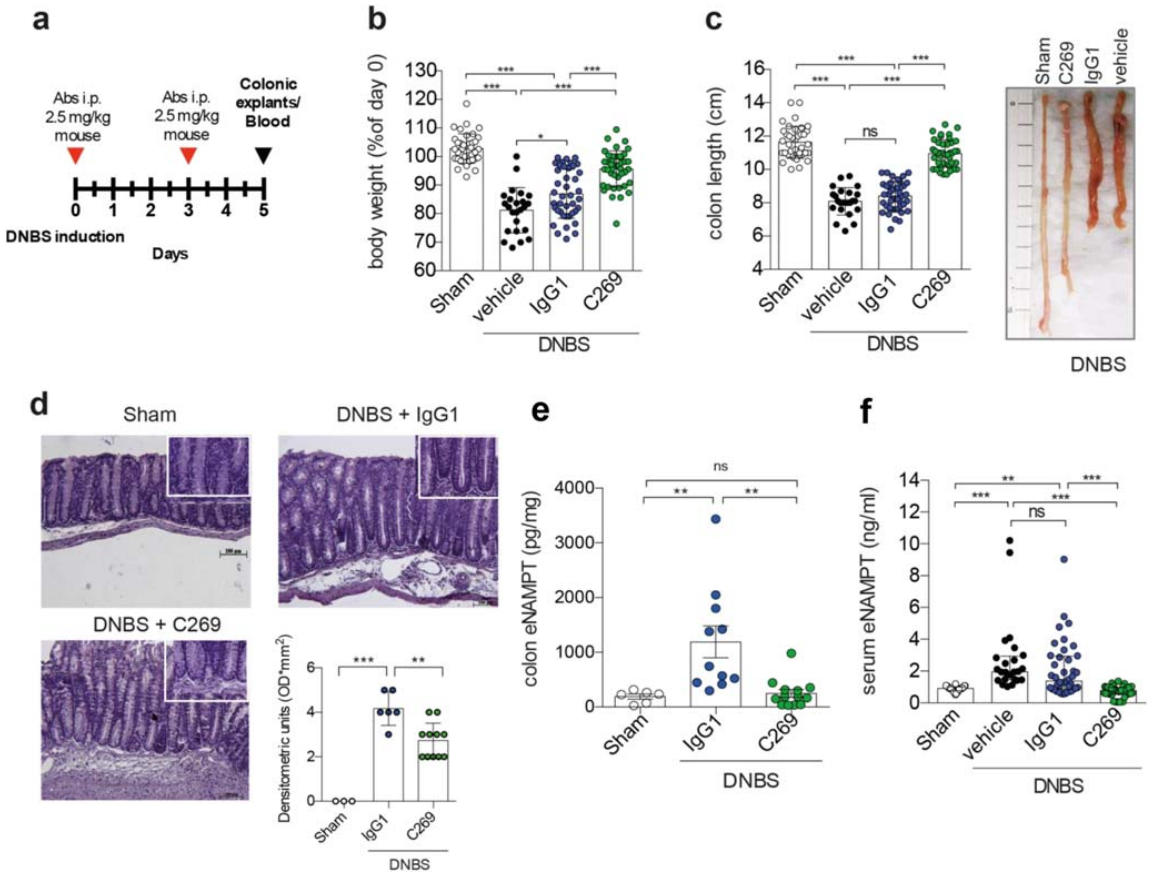

Fig. 3 C269 reduces DNBS-induced acute colitis. **a** Experimental design of the treatments in the acute DNBS model. **b** Analysis of body weight and **c** colon length in Sham- ($n = 38$), vehicle- ($n = 24$), IgG1- ($n = 41$), or C269- ($n = 42$) treated mice. Panel to the right is a representative image of colon lengths at day 5 with the different treatments. **d** Representative H&E analysis and quantification of colons at day 5 in Sham- ($n = 3$), IgG1- ($n = 6$), or C269- ($n = 11$) treated mice (***$p < 0.001$, **$p < 0.01$ by Bonferroni post hoc test). **e** eNAMPT levels in supernatants of colonic explants in Sham- ($n = 6$), IgG1- ($n = 11$), or C269- ($n = 13$) treated mice. **f** Serum eNAMPT levels in Sham- ($n = 38$), vehicle- ($n = 24$), IgG1- ($n = 40$), or C269- ($n = 42$) treated mice. Values are means ± SEM (***$p < 0.001$, **$p < 0.01$ by one-way ANOVA)

significant local variation of eNAMPT levels, we did not measure a consistent elevation of the amount of circulating eNAMPT in the different groups of mice (Fig. S2f). Potential explanations could be related to a lower severity of colitis triggered by DSS (median colitis score of control IgG1 group 3) as well as to the inherent differences in the two mouse strains. Indeed, C57BL/6 mice have basal circulating levels of eNAMPT that are almost twofold higher compared with BALB/C mice.

Taken together, the results obtained in the two models of acute colitis demonstrate that eNAMPT-targeting by C269 leads to a consistent reduction of intestinal inflammation that is paralleled by a decrease of eNAMPT present in plasma or produced by the inflamed colon.

C269 inhibits chronic DNBS- and DSS-induced colitis

To strengthen the therapeutic potential of targeting eNAMPT, we investigated the effect of C269 in a chronic model of DNBS-induced colitis based on two administrations of DNBS (3 mg/mouse) separated by a period of 21 days [38, 39] (Fig. 4a). Even in this setting, we confirmed that C269 administration ameliorated colitis in terms of reduction of body weight loss, colon shortening (Fig. 4b–d), and tissue damage (Fig. 4e). Also, C269 is able to reduce eNAMPT levels in colonic explants and serum (Fig. 4f–g). Noteworthy, mice survival was significantly improved by C269 treatment ($p = 0.003$). Indeed, 53.1% of mice injected with control IgG1 died by 8 days, and only 37.5% of these mice survived until the end of the

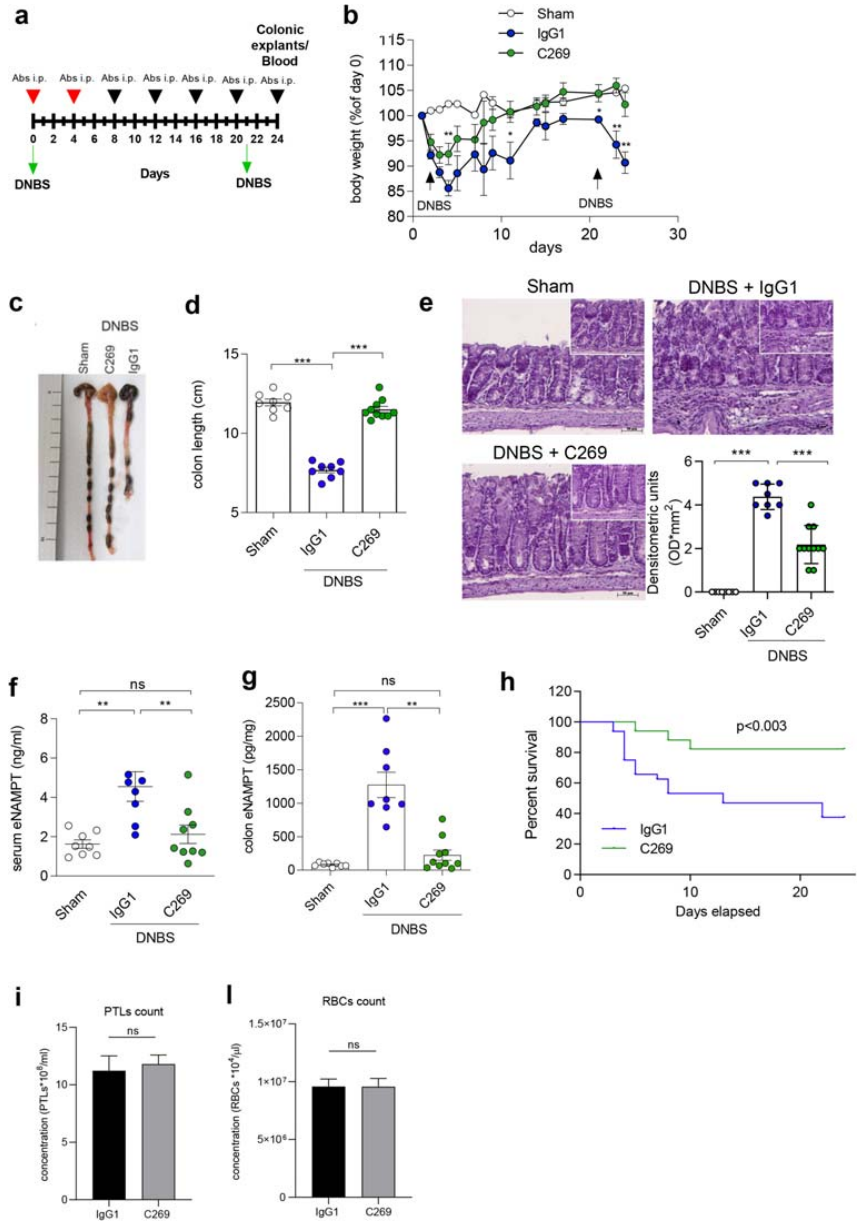

Fig. 4 C269 reduces DNBS-induced chronic colitis. **a** Experimental design of BALB/C mice injected intrarectally with 3 mg of DNBS at day 0 and day 21 and treated or not with vehicle, a control IgG1 (2.5 mg/kg, twice a week), or C269 (2.5 mg/kg, twice a week). **b** Analysis of body weight $n = 10$, 25, 23 mice, respectively. **c** Representative image of colons and **d** colon length in Sham- ($n = 10$), IgG1- ($n = 12$), or C269- ($n = 19$) treated mice. **e** Representative H&E analysis and quantification of colons at day 24 in Sham- ($n = 8$), IgG1- ($n = 8$), or C269- ($n = 11$) treated mice (***$p < 0.001$, **$p < 0.01$ by Bonferroni post hoc test). **f** Serum eNAMPT levels in Sham- ($n = 8$), IgG1- ($n = 8$), or C269- ($n = 11$) treated mice. **g** eNAMPT levels in supernatants of colonic explants of Sham- ($n = 9$), IgG1- ($n = 13$), or C269- ($n = 13$) treated mice. **h** Survival of IgG1- ($n = 22$) or C269- ($n = 20$) treated animals. **i**–**l** Platelets and red blood cell count after control IgG1 and C269 administration in mice ($n = 8$ each). Values are means ± SEM (***$p < 0.001$, **$p < 0.01$ by one-way ANOVA)

experiment, whereas the majority C269-treated mice (82.4%) overcome the second challenge of DNBS (Fig. 4h). To rule out the potential hematotoxicity of iNAMPT inhibitors, we analyzed the blood of mice at the end chronic DNBS colitis. Prolonged administration of C269 does not affect the number of platelets (PTLs) or red cells (RBCs; Fig. 4i–l), demonstrating the tested dose of C269 devoid of side effects such as thrombocytopenia.

Consistent with these findings, in a chronic model of DSS-induced colitis, we also observed that C269 administration significantly reduced body weight loss over the entire experimental period (Fig. S3g-h).

Therefore, neutralization of eNAMPT in both chronic models of colitis was able to rescue intestinal inflammation and DNBS-associated mortality indicating the importance of eNAMPT in the exacerbation of chronic pathology.

Targeting eNAMPT with C269 restrains pathogenic immune responses

We next analyzed the mRNA expression of inflammatory and immune-related genes in the colon of mice treated for 5 days with DNBS. qPCR evaluations showed an increased expression of many genes encoding for inflammatory molecules, including NAMPT, in colitic IgG1-treated mice as compared with sham mice. Noteworthy, eNAMPT neutralization by C269 was able to hamper the expression of genes encoding for both inflammatory cytokines (*Tnf*, *Il6*, *Il1b*, *Il18*) and enzymes involved in the production of crucial inflammatory molecules (*Nos2*, *Cox2*, *Nox2*, *Nampt*) (Fig. 5a). Accordingly, immunostaining of colonic tissue sections confirmed the increased expression of selective inflammatory gene products (TNFα, IL-1β, and NAMPT) in the DNBS-treated, IgG1 group as compared with Sham mice, as well as the ability of C269 to restrain the upregulation of these inflammatory molecules (Fig. 5b). We also analyzed the activation of NF-κB, the major orchestrator of inflammation, by evaluating the levels of both p65-NF-κB subunit and IκB-α in tissue samples. In line with inflammatory gene expression, immunohistochemical analysis showed that neutralization of eNAMPT hampered DNBS-induced NF-κB activation by limiting both IκB-α degradation and overall p65-NF-κB levels (Fig. 5c). Overall, these results demonstrate that eNAMPT is a promoter of crucial inflammatory circuits, which are typically expressed by innate myeloid cells. To further gain an insight on the impact of eNAMPT on the activation of mucosal immunity, we evaluated the expression of genes that are associated with pathogenic type 1 and type 17 immune responses. IL-12 is a crucial cytokine that triggers differentiation of naïve $CD4^+$ T cells into IFNγproducing Th1 cells and the effector functions of cytotoxic lymphoid cells (NK, NKT, $CD8^+$ T cells). Tbet (*Tbx21*) is the main transcription factor guiding Th1/group 1 innate lymphoid cells (ILC1) differentiation and enhancing the cytotoxic activity of $CD8^+$ T cells (CTL), and IFNγ is the major cytokine produced by activated type 1 lymphoid cells. Strikingly, the expression levels of these genes (*Il12b*, *Tbx21*, and *Ifng*) increased in colitic mice but dropped to the basal level following C269 administration, indicating that neutralization of eNAMPT dampened cytotoxic type 1 immune responses (Fig. 5d). Next, we evaluated the expression of typical type 17 genes, namely *Rorc2*, that encodes for the Th17/ILC3-driving transcription factor RORγt, *Il23* a crucial cytokine for Th17 expansion and activation and *Il17a*, *Il17f*, *Il21*, and *Il22* that are the signature cytokines produced by type 17 cells. As expected, we measured a consistent induction of *Il17a*, *IL17f*, *Rorc2*, *Il23a*, *Il21*, and *Il22* transcripts in the inflamed colon of IgG1-treated mice as compared with control (Sham) mice. Noteworthy, these upregulated-type 17-related genes were drastically inhibited by C269 administration, indicating that eNAMPT participates also in pathogenic-type 17-immune responses (Fig. 5e).

Next, we analyzed the expression of *Il4* and *Gata3*, the key transcription factor for Th2/ILC2-differentiation, but we found that both genes were similarly expressed in the colon of naïve (sham) and colitic mice (either IgG1- or C269-treated mice) indicating that type 2 immune responses were not engaged in our DNBS-treated mice (Fig. S3a). Finally, we addressed whether eNAMPT could also affect the anti-inflammatory circuits associated with the maintenance of intestinal homeostasis. The expression of the anti-inflammatory cytokines *Il10* and *Tgfb*, as well as the Treg-specific transcription factor *Foxp3*, was not altered by DNBS or C269 treatments suggesting that eNAMPT does not impair differentiation/activity of gut-associated immunoregulatory cells (Fig. S3b). Overall, this transcriptional profile was confirmed also in the model of acute colitis triggered by DSS (Fig. S4) therefore strengthening the idea that eNAMPT fuels intestinal inflammation by enhancing the classic pro-inflammatory activation of myeloid cells in association with pathogenic Th1/Th17 adaptive immunity.

We also evaluated the intestinal expression of ICAM-1 and P-selectin. As expected, DNBS treatment resulted in an increased staining for ICAM-1 and P-selectin in vessels of the *lamina propria* (LP) and submucosa as well as in epithelial cells of injured colon of IgG1-treated mice, whereas C269 administration significantly hampered the expression of both markers indicating a lower capacity to recruit inflammatory cells (Fig. 6a).

Next, to characterize the composition of the immune infiltrate, 5 days after the administration of DNBS, we analyzed LP cells from the colon of mice treated with C269 or IgG1. LP cells from Sham mice were also analyzed as control. FACS analysis showed that DNBS-induced colitis in IgG1-treated mice was associated with an increased frequency of monocytes ($CD45^+CD11b^+Ly6C^{high}Ly6G^-$) and neutrophils ($CD45^+CD11b^+Ly6C^{low/-}Ly6G^+$), which was significantly dampened by eNAMPT neutralization (Fig. 6b). According to the transcriptional profile of total colon, FACS analysis showed that LP myeloid cells expressed a higher level of TNFα in IgG1-treated colitic mice than sham mice, whereas C269 administration in DNBS-treated mice reduced TNFα expression by myeloid cells to the basal level (sham mice) (Fig. S5A, Fig. 6b–c). LP macrophages ($CD45^+CD11b^+F4/80^+Ly6C^{low/-}$cells) similarly increased in colitic mice treated with IgG1 or C269 (Fig. 6b–c). However, in line with the intestinal macrophage commitment towards a tolerant phenotype [27], LP macrophages of sham and colitic mice (either IgG1- or C269-treated mice) expressed a comparable amount of TNFα (Fig. 6b–c). Hence, these findings suggest that C269 can dampen DNBS-induced intestinal inflammation by limiting both the recruitment and the activation of monocytes and neutrophils in the colon. We then investigated the effect of

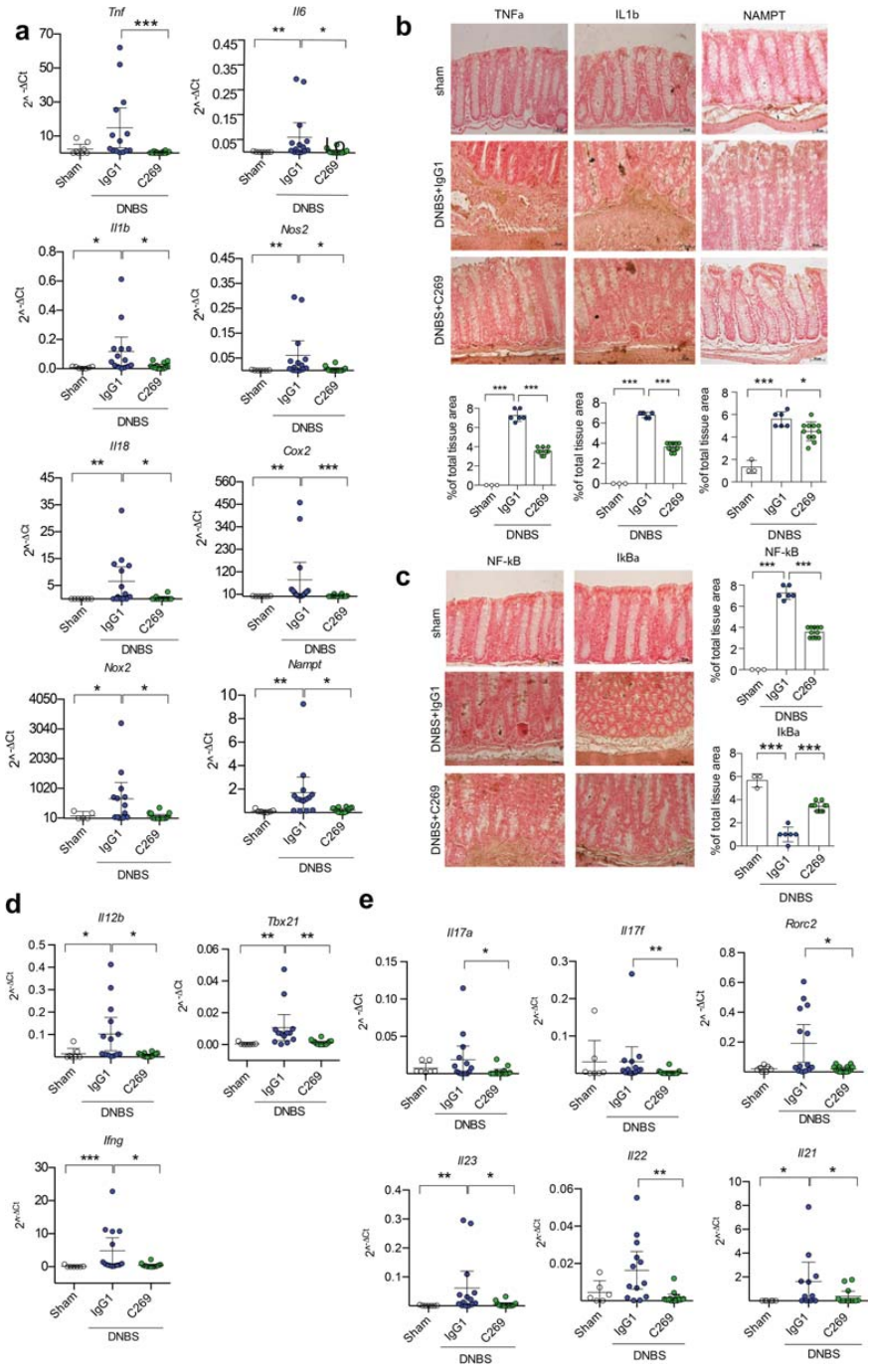

Fig. 5 C269 hampers the molecular pathways that drive intestinal inflammation. **a** Gene expression analysis quantified by qPCR in colons of Sham- ($n = 7$), IgG1- ($n = 14$), or C269- ($n = 14$) treated mice. **b** Representative images and quantification of IHC analysis of TNFα, IL-1β, NAMPT, and **c** NF-κB and IκB-α in colons of Sham- ($n = 3$), IgG1- ($n = 6$), or C269- ($n = 11$) treated mice. Values are means ± SEM (***$p < 0.001$, *$p < 0.05$, with Bonferroni post hoc test). **d**–**e** Gene expression analysis in colons of Sham- ($n = 7$), IgG1- ($n = 14$), or C269- ($n = 14$) treated mice. Values are means ± SEM (***$p < 0.001$, **$p < 0.01$, *$p < 0.05$, with non-parametric Kruskal–Wallis test followed by a Dunn's multiple comparison test)

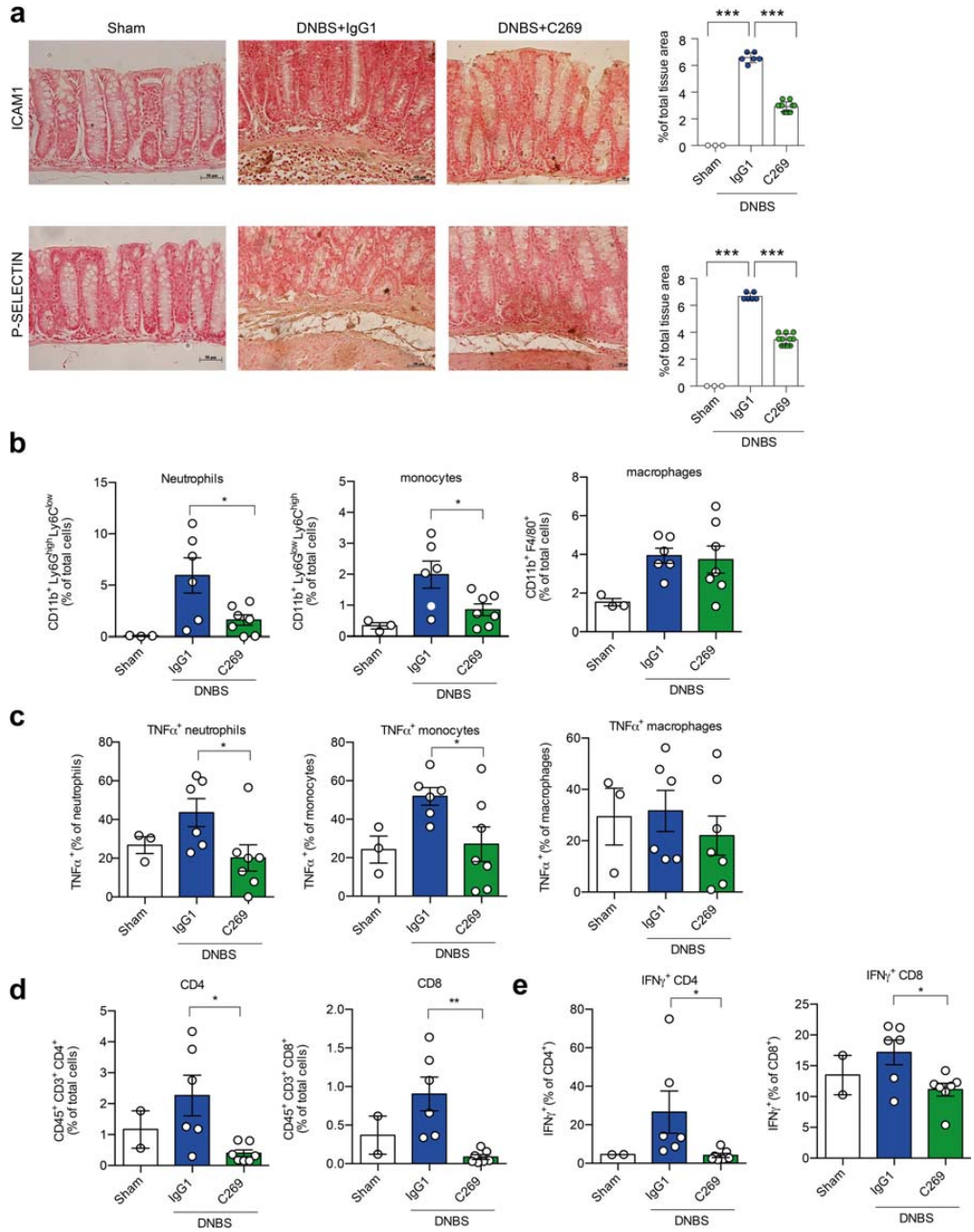

Fig. 6 C269 reduces mucosal immune cell infiltration. **a** Representative IHC images and quantification of ICAM1 or P-selectin in colons of Sham ($n = 3$), IgG1 ($n = 6$), or C269 ($n = 11$) DNBS-treated mice. Values are means ± SEM (***$p < 0.001$, with Bonferroni post hoc test). **b** Mean percentage ± SEM of *lamina propria* neutrophils ($CD45^+CD11b^+Ly6G^+Ly6C^-$), monocytes ($CD45^+CD11b^+Ly6G^-lY6C^+$), and macrophages ($CD45^+CD11b^+F4/80^+$) estimated by flow cytometry. **c** % of *lamina propria* TNFα-expressing neutrophils, monocytes, and macrophages. **d** Mean percentage ± SEM of *lamina propria* $CD4^+$ ($CD45^+CD3^+CD4^+CD8^-$) and $CD8^+$ ($CD45^+CD3^+CD4^-CD8^+$) lymphocytes estimated by flow cytometry. **e** % of IFNγ-expressing $CD4^+$ and $CD8^+$ lymphocytes. Values are means ± SEM of Sham- ($n = 3$), IgG1- ($n = 6$), and C269- ($n = 7$) treated mice, representative of 3 independent experiments with similar results (**$p < 0.01$, *$p < 0.05$, with unpaired two-tailed t test). **f** Fold changes values of M1 and M2 genes of peritoneal macrophages treated with eNAMPT (500 ng/ml) for 4/16 h. Data were compared with control (control values = 1). Mean + SEM of 7 independent experiments. **g** Gene expression analysis quantified by qPCR of PECs treated with C269 and control IgG1 (10 μg/ml) in absence or presence of eNAMPT (500 ng/ml) mean + SEM of 2 independent experiments

C269 on T cell subsets. As shown in Fig. 6d, the number of $CD4^+$ and $CD8^+$ T cells significantly increased in DNBS-treated mice (IgG1-treated mice) as compared with both sham and C269-treated mice. Next, we evaluated the activation of LP T cells, and we found a consistent reduction of IFNγ-expressing $CD4^+$ and $CD8^+$ T cells after C269 administration (Fig. S5b, Fig. 6e). Hence, neutralization of eNAMPT by C269 resulted in a clear impairment of expansion and activation of pathogenic Th1 ($CD3^+CD4^+IFN\gamma^+$ cells) and cytotoxic effector cells ($CD3^+CD8^+$ $IFN\gamma^+$ cells).

Exogenous recombinant NAMPT increases DNBS-induced colitis and C269 reverts the effect

To formally prove the pathogenic role of eNAMPT in IBD, we evaluated whether this *metabokine* could either trigger or exacerbate intestinal inflammation.

Daily injection of recombinant eNAMPT alone (rNAMPT; 50 μg/mouse, i.p. in PBS, endotoxin levels < 0.02 EU/ml) in BALB/C mice for 5 days or in C57BL/6 mice for up to 10 days did not lead to changes in body weight or colon length (Fig. 7a) indicating that eNAMPT alone is unable to break intestinal homeostasis.

To investigate whether eNAMPT may exacerbate or contribute to intestinal pathology, we evaluated the administration of rNAMPT in mice treated with low dose of DNBS (2 mg per mouse), which per se induces a mild colitis. In this instance, daily injection of rNAMPT heightened mucosal inflammation (as demonstrated by body weight loss, colon shortening, and histological colitis score) whereas C269 treatment restored a benign pathology (Fig. 7b–d).

Furthermore, administration of rNAMPT induced a significant augmentation of circulating eNAMPT (median 2.890 ng/ml vs 1.196 ng/ml of IgG1 group; $p < 0.01$), which was fully reverted by C269 (median = 0.9052 ng/ml; Fig. 7e).

Consistent with this finding, immunohistochemical analysis showed an enhanced expression of ICAM1, TNFα, IL-1β, and degradation of IκB-α in colonic tissue of mice treated with rNAMPT, whereas its neutralization by C269 resulted in a solid reduction of vascular adhesion molecules (ICAM1 and P-selectin), inflammatory cytokines (TNFα, IL-1β, and IL-6), NAMPT, and NF-κB activation (Fig. 7f–g).

Discussion

Although cytokine neutralization has provided important benefits for IBD, major challenges remain, since a consistent percentage of patients do not respond to therapies or lose responsiveness over time. Furthermore, previous treatments reduce the response rate to subsequent biologics. Therefore, the identification of both valuable biomarkers to guide the selection of patients towards a specific therapy and new therapeutic targets is urgently needed. Our results indicate that extracellular NAMPT might represent a novel biomarker of disease activity and response to anti-TNF therapies and whose neutralization might be of benefit for IBD patients.

First, we have shown that low levels of eNAMPT correlate with response to anti-TNF therapies (infliximab and adalimumab). On the contrary, high pre-treatment levels are predictive of poor response, and patients that do not respond maintain high eNAMPT levels. While our numbers were small ($n = 90$ patients), our conclusions are supported by the consistency across three separate cohorts recruited in three different clinical centers and a number of previous reports [17, 34–36]. Of note, in a recent phase 2 open-label study of 103 golimumab-treated UC patients, NAMPT was one of the 13 genes in the gene expression signature predictive of poor response in biopsies [40]. These data provide an additional confirmation of the predictive potential of eNAMPT to anti-TNF therapies. The possibility to measure eNAMPT in the serum, hence using a low invasive approach, represents an added value of our findings, further opening towards its evaluation in large prospective studies. Furthermore, the analysis of serum eNAMPT levels as predictor of response might be also easily extended to the response to other biologics, such as vedolizumab or ustekinumab.

Beyond its role as a biomarker, our results originally indicate that eNAMPT is also an important player, rather than a simple bystander, of IBD pathogenesis. Indeed, administration of rNAMPT in mice is able to exacerbate intestinal pathology indicating that eNAMPT is an important promoter of the inflammatory pathways that sustains IBD.

To ascertain the impact of eNAMPT in IBD, we generated and validated an eNAMPT monoclonal-neutralizing antibody (C269). This antibody neutralizes the eNAMPT cytokine-like activity while sparing the enzymatic activity. To our knowledge, this is the first such antibody described, although a polyclonal-neutralizing antibody has been published and shown to revert the symptoms of acute lung injury [14] and to affect macrophage polarization [28].

Importantly, we found that eNAMPT is elevated (locally and systemically) in acute and chronic models of chemically induced colitis, confirming it as a biomarker of disease activity in these murine models of IBD. Noteworthy, both models respond to drugs currently used in IBD patients and are thus considered relevant for pre-clinical testing of new potential therapeutic agents [41, 42]. C269 consistently ameliorates symptoms across models, either in acute or in chronic settings which mimic colitis flares and relapses, consequently, more closely reflect IBD symptoms and pathology. TNBS/DNBS-induced colitis shares significant properties with human Crohn's disease, including contribution of cytokines such as IL-12, TNFα, and IL-17A and of CD4+

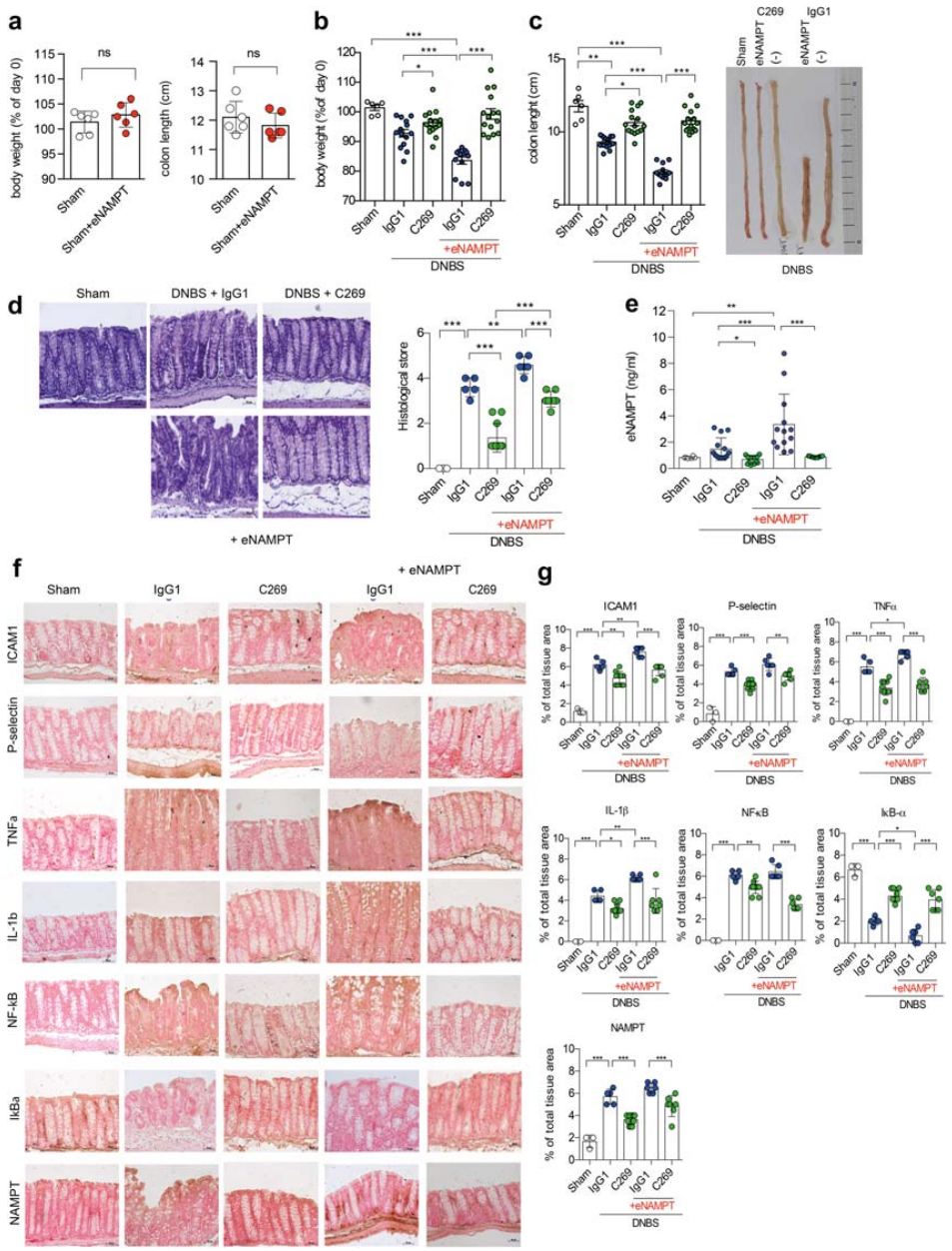

Fig. 7 Recombinant eNAMPT exacerbates DNBS-induced acute colitis. **a** Analysis of body weight (left) and colon length (right) of Sham mice injected or not with recombinant eNAMPT (50 μg/mouse, every day) for 5 days, $n = 6$ mice/group. **b** Analysis of body weight. **c** Colon length (left) and representative image of colons (right). **d** H&E analysis. **e** eNAMPT serum levels of Sham mice ($n = 6$), DNBS-induced mice treated with IgG1 (2.5 mg/kg, at day 0 and 3; $n = 14$) or with C269 alone (2.5 mg/kg, at day 0 and 3; $n = 15$) or in the presence of recombinant eNAMPT and IgG1 ($n = 13$), or in the presence of recombinant eNAMPT and C269 ($n = 15$). Values are means ± SEM (***$p < 0.001$, **$p < 0.01$, *$p < 0.05$ by one-way ANOVA and Bonferroni post hoc test for H&E analysis). **f** Representative IHC and **g** quantification of ICAM1, P-selectin, TNFα, IL-1β, NF-κB, IκB-α, and NAMPT in colons of Sham mice ($n = 3$), DNBS-induced mice treated with IgG1 (2.5 mg/kg, at day 0 and 3; $n = 5$) or with C269 alone (2.5 mg/kg, at day 0 and 3; $n = 11$) or in the presence of recombinant eNAMPT and IgG1 ($n = 6$), or in the presence of recombinant eNAMPT and C269 ($n = 7$). Values are means ± SEM (***$p < 0.001$, **$p < 0.01$, *$p < 0.05$ by Bonferroni post hoc test)

T cells [43]; albeit innate immune cells are also crucial for development of intestinal inflammation [44]. DSS acts mainly by disrupting the intestinal epithelial barrier, thereby exposing subepithelial immune cells to commensal bacteria. It causes an acute and chronic colitis in mice with some morphological changes similar to human ulcerative colitis, including an increased expression of adhesion molecules, infiltration of leukocytes, production of inflammatory mediators, and gut injury [45]. Neutrophils and macrophages are the major orchestrators of acute DSS colitis while lymphocytes are also involved in chronic DSS colitis [46, 47]. In both models, eNAMPT neutralization similarly restrains pathogenic immune responses, indicating C269 as a valuable therapeutic for the both forms of IBD. Indeed, the neutralization of eNAMPT results in a clear impairment of expansion and activation of pro-inflammatory monocytes ($CD45^+CD11b^+Ly6C^{high}Ly6G^-TNF\alpha^+$) and neutrophils ($CD45^+CD11b^+Ly6C^{low/-}Ly6G^+TNF\alpha^+$), as well as pathogenic Th1 ($CD3^+CD4^+IFN\gamma^+$) and cytotoxic effector cells ($CD3^+CD8^+$ $IFN\gamma^+$). These effects might be explained by the ability of C269 to reduce the recruitment and activation of myeloid cells with a consequent impairment of T cell activation too, or by a direct effect of eNAMPT neutralization on both innate and adaptive immune cells. The use of chronic colitis model based on T cell transfer (e.g., adoptive transfer of naïve $CD4^+CD45RB^{high}$ T cells from wild-type mice into $RAG1^{-/-}$ recipients) might be useful to better address the impact of eNAMPT on T cell-driven pathology. Albeit the molecular mechanism linking eNAMPT with these immunomodulatory activities requires further dissection, our results highlight a strong correlation between the neutralization of eNAMPT and the inhibition of a characteristic IBD inflammatory signature. Indeed, across models, C269 treatment resulted in a strong decrease of myeloid-derived inflammatory cytokines (Tnf, Il1, Il6, Il18) and molecules (*Cox2*, *Nox2*, *Nos2*, *Nampt*) as well as cytotoxic type 1 (*Il12b*, *Tbx21*, *Ifng*) and type 17 (*Il23*, *Rorc2*, *Il17a*, *Il17f*, *Il21*, *Il22*) immune effectors. Of course, these findings require additional confirmation in humans, as colitis models cannot be truly representative of human IBD in terms of disease onset, clinical manifestations, pathophysiology, and response to therapeutics.

Moreover, the effect of diet-associated changes in microbiota composition on the levels of eNAMPT and, on the other way around, the impact of eNAMPT levels on gut microbiota composition are certainty relevant aspects of IBD pathology that are totally unexplored and might be interesting to evaluate in future studies.

In conclusion, this is the first demonstration that serum eNAMPT might be a predictor of response to anti-TNF, and its neutralization, without enzymatic inhibition, is able to interrupt the cytokine and cellular circuits that fuel IBD pathology. Given the toxicity of enzymatic inhibitors of iNAMPT [48, 49], targeting eNAMPT represents therefore a promising approach to restore intestinal homeostasis, sparing the effect on NAD homeostasis.

Acknowledgments The authors thank Paolo Dante for data collection of Torino cohort and Beatrice Riva for the protocol of PTLs count.

Author contributions The study was designed by C.T., C.P., and A.A. Genazzani. G. Colombo did the major part of the experiments. N.C. helped in in vivo experiments. A.A. Grolla helped us in protein purification. A.Z., C.B., and F.M. gave us support in antibody production. F.S.C. analyzed the flow cytometry data. S.N., M.L., G.S., D.R.G., G.P.C., L.P., and M.D.A. provided us human samples and clinical data. S.S. and E.J. helped with immune cells experiments. M.C. and G. Casili performed IHC experiments, and S.C. and E.E analyzed the IHC data. G. Colombo, C.T., and C.P. discussed and interpreted findings. C.T. and C.P. directed the work, and C.T., C.P., G. Colombo, and A.A. Genazzani wrote the manuscript. All of the authors have seen and approved the final version of the manuscript.

Funding information C. Travelli was supported by a FIRC/AIRC (Associazione Italiana Ricerca sul Cancro) fellowship, Fondazione Veronesi Fellowship, Leonino Fontana e Maria Lionello Fellowship, project code 14832, and Università degli Studi del Piemonte Orientale (research funding 2016) to C. Porta.

Compliance with ethical standards

The study was approved by the Burlo-Garofolo Institute Ethical Committee (n. 111/2015), by AOU Città della Salute e della Scienza di Torino – A.O. Mauriziano – A.S.L. TO1 Ethical Committee (n. 0056924 of 08/06/2016), and by ASL Milano-2 (n. 2726 of 02/10/2012), and written consent was obtained from patients.

Animal care was in compliance with Italian regulations on protection of animals used for experimental purposes and were authorized by the Ministry of Health (120/2018 DB064.27 of 04/10/2017).

Conflict of interest The authors declare that they have no conflict of interest.

References

1. Park JH, Peyrin-Biroulet L, Eisenhut M, Shin JI (2017) IBD immunopathogenesis: a comprehensive review of inflammatory molecules. Autoimmun Rev 16:416–426
2. Kmieć Z, Cyman M, Ślebioda TJ (2017) Cells of the innate and adaptive immunity and their interactions in inflammatory bowel disease. Adv Med Sci 62:1–16
3. Nielsen OH, Ainsworth MA (2013) Tumor necrosis factor inhibitors for inflammatory bowel disease. N Engl J Med 369:754–762
4. Levin AD, Wildenberg ME, van den Brink GR (2016) Mechanism of action of anti-TNF therapy in inflammatory bowel disease. J Crohns Colitis 10:989–997
5. Feagan BG, Sandborn WJ, Gasink C, et al (2016) Ustekinumab as induction and maintenance therapy for Crohn's disease. In: https://doi.org/10.1056/NEJMoa1602773. https://www.nejm.org/doi/10.1056/NEJMoa1602773?url_ver=Z39.88-2003&rfr_id=ori%3Arid%3Acrossref.org&rfr_dat=cr_pub%3Dwww.ncbi.nlm.nih.gov. Accessed 25 Apr 2019
6. Friedrich M, Pohin M, Powrie F (2019) Cytokine networks in the pathophysiology of inflammatory bowel disease. Immunity 50:992–1006
7. Sandborn WJ, Feagan BG, Rutgeerts P, Hanauer S, Colombel JF, Sands BE, Lukas M, Fedorak RN, Lee S, Bressler B, Fox I, Rosario M, Sankoh S, Xu J, Stephens K, Milch C, Parikh A, GEMINI 2

Study Group (2013) Vedolizumab as induction and maintenance therapy for Crohn's disease. N Engl J Med 369:711–721
8. Zeissig S, Rosati E, Dowds CM, Aden K, Bethge J, Schulte B, Pan WH, Mishra N, Zuhayra M, Marx M, Paulsen M, Strigli A, Conrad C, Schuldt D, Sinha A, Ebsen H, Kornell SC, Nikolaus S, Arlt A, Kabelitz D, Ellrichmann M, Lützen U, Rosenstiel PC, Franke A, Schreiber S (2019) Vedolizumab is associated with changes in innate rather than adaptive immunity in patients with inflammatory bowel disease. Gut 68:25–39
9. Burgos ES, Vetticatt MJ, Schramm VL (2013) Recycling Nicotinamide. The transition-state structure of human nicotinamide phosphoribosyltransferase. J Am Chem Soc 135:3485–3493
10. Carbone F, Liberale L, Bonaventura A et al (2017) Regulation and function of extracellular nicotinamide phosphoribosyltransferase/visfatin. In: Comprehensive Physiology. American Cancer Society, pp 603–621
11. Travelli C, Colombo G, Mola S, Genazzani AA, Porta C (2018) NAMPT: a pleiotropic modulator of monocytes and macrophages. Pharmacol Res 135:25–36
12. Hara N, Yamada K, Shibata T, Osago H, Tsuchiya M (2011) Nicotinamide phosphoribosyltransferase/visfatin does not catalyze nicotinamide mononucleotide formation in blood plasma. PLoS One 6:e22781
13. Grolla AA, Travelli C, Genazzani AA, Sethi JK (2016) Extracellular nicotinamide phosphoribosyltransferase, a new cancer metabokine. Br J Pharmacol 173:2182–2194
14. Camp SM, Ceco E, Evenoski CL, Danilov SM, Zhou T, Chiang ET, Moreno-Vinasco L, Mapes B, Zhao J, Gursoy G, Brown ME, Adyshev DM, Siddiqui SS, Quijada H, Sammani S, Letsiou E, Saadat L, Yousef M, Wang T, Liang J, Garcia JGN (2015) Unique toll-like receptor 4 activation by NAMPT/PBEF induces NFκB signaling and inflammatory lung injury. Sci Rep 5:1–14
15. Van den Bergh R, Morin S, Sass HJ et al (2012) Monocytes contribute to differential immune pressure on R5 versus X4 HIV through the adipocytokine visfatin/NAMPT. PLoS One 7. https://doi.org/10.1371/journal.pone.0035074
16. Travelli C, Consonni FM, Sangaletti S et al (2019) Nicotinamide phosphoribosyltransferase acts as a metabolic gate for mobilization of myeloid-derived suppressor cells. Cancer Res. https://doi.org/10.1158/0008-5472.CAN-18-1544
17. Moschen AR, Kaser A, Enrich B et al (2007) Visfatin, an adipocytokine with proinflammatory and immunomodulating properties. J Immunol 178:1748–1758
18. Starr AE, Deeke SA, Ning Z, Chiang CK, Zhang X, Mottawea W, Singleton R, Benchimol EI, Wen M, Mack DR, Stintzi A, Figeys D (2017) Proteomic analysis of ascending colon biopsies from a paediatric inflammatory bowel disease inception cohort identifies protein biomarkers that differentiate Crohn's disease from UC. Gut 66:1573–1583
19. Gerner RR, Klepsch V, Macheiner S et al (2018) NAD metabolism fuels human and mouse intestinal inflammation. Gut 67:1813–1823
20. Travelli C, Aprile S, Rahimian R, Grolla AA, Rogati F, Bertolotti M, Malagnino F, di Paola R, Impellizzeri D, Fusco R, Mercalli V, Massarotti A, Stortini G, Terrazzino S, del Grosso E, Fakhfouri G, Troiani MP, Alisi MA, Grosa G, Sorba G, Canonico PL, Orsomando G, Cuzzocrea S, Genazzani AA, Galli U, Tron GC (2017) Identification of novel triazole-based nicotinamide phosphoribosyltransferase (NAMPT) inhibitors endowed with antiproliferative and antiinflammatory activity. J Med Chem 60:1768–1792
21. Hasmann M, Schemainda I (2003) FK866, a highly specific noncompetitive inhibitor of nicotinamide phosphoribosyltransferase, represents a novel mechanism for induction of tumor cell apoptosis. Cancer Res 63:7436–7442
22. Hjarnaa P-JV, Jonsson E, Latini S et al (1999) CHS 828, a novel pyridyl cyanoguanidine with potent antitumor activity in vitro and in vivo. Cancer Res 59:5751–5757
23. Zabka TS, Singh J, Dhawan P, Liederer BM, Oeh J, Kauss MA, Xiao Y, Zak M, Lin T, McCray B, la N, Nguyen T, Beyer J, Farman C, Uppal H, Dragovich PS, O'Brien T, Sampath D, Misner DL (2015) Retinal toxicity, in vivo and in vitro, associated with inhibition of nicotinamide phosphoribosyltransferase. Toxicol Sci 144:163–172
24. Misner DL, Kauss MA, Singh J, Uppal H, Bruening-Wright A, Liederer BM, Lin T, McCray B, la N, Nguyen T, Sampath D, Dragovich PS, O'Brien T, Zabka TS (2017) Cardiotoxicity associated with nicotinamide phosphoribosyltransferase inhibitors in rodents and in rat and human-derived cells lines. Cardiovasc Toxicol 17:307–318
25. Naviglio S, Lacorte D, Lucafò M, Cifù A, Favretto D, Cuzzoni E, Silvestri T, Pozzi Mucelli M, Radillo O, Decorti G, Fabris M, Bramuzzo M, Taddio A, Stocco G, Alvisi P, Ventura A, Martelossi S (2019) Causes of treatment failure in children with inflammatory bowel disease treated with infliximab. J Pediatr Gastroenterol Nutr 68:37–44
26. Caneparo V, Pastorelli L, Pisani LF, Bruni B, Prodam F, Boldorini R, Roggenbuck D, Vecchi M, Landolfo S, Gariglio M, de Andrea M (2016) Distinct anti-IFI16 and anti-GP2 antibodies in inflammatory bowel disease and their variation with infliximab therapy. Inflamm Bowel Dis 22:2977–2987
27. Porta C, Ippolito A, Consonni FM, Carraro L, Celesti G, Correale C, Grizzi F, Pasqualini F, Tartari S, Rinaldi M, Bianchi P, Balzac F, Vetrano S, Turco E, Hirsch E, Laghi L, Sica A (2018) Protumor steering of cancer inflammation by p50 NF-κB enhances colorectal cancer progression. Cancer Immunol Res 6:578–593
28. Horenstein AL, Durelli I, Malavasi F (2005) Purification of clinical-grade monoclonal antibodies by chromatographic methods. In: Smales CM, James DC (eds) Therapeutic proteins: methods and protocols. Humana Press, Totowa, pp 191–208
29. Amici A, Grolla AA, Del Grosso E et al (2017) Synthesis and degradation of adenosine 5'-tetraphosphate by nicotinamide and nicotinate phosphoribosyltransferases. Cell Chem Biol 24:553–564.e4
30. Billington Richard A, Travelli C, Ercolano E, Galli U, Roman CB, Grolla AA, Canonico PL, Condorelli F, Armando A Genazzani FK866, a highly specific noncompetitive inhibitor of nicotinamide phosphoribosyltransferase, represents a novel mechanism for induction of tumor cell apoptosis. Cancer Res http://cancerres.aacrjournals.org/content/63/21/7436.long. Accessed 25 Apr 2019
31. Gardell SJ, Hopf M, Khan A, Dispagna M, Hampton Sessions E, Falter R, Kapoor N, Brooks J, Culver J, Petucci C, Ma CT, Cohen SE, Tanaka J, Burgos ES, Hirschi JS, Smith SR, Sergienko E, Pinkerton AB (2019) Boosting NAD+ with a small molecule that activates NAMPT. Nat Commun 10:3241
32. Dhanjal TS, Pendaries C, Ross EA, Larson MK, Protty MB, Buckley CD, Watson SP (2007) A novel role for PECAM-1 in megakaryocytokinesis and recovery of platelet counts in thrombocytopenic mice. Blood 109:4237–4244
33. Grolla AA, Torretta S, Gnemmi I et al (2015) Nicotinamide phosphoribosyltransferase (NAMPT/PBEF/visfatin) is a tumoural cytokine released from melanoma. Pigment Cell Melanoma Res 28:718–729
34. Dogan S, Guven K, Celikbilek M et al (2016) Serum visfatin levels in ulcerative colitis. J Clin Lab Anal 30:552–556
35. Waluga M, Hartleb M, Boryczka G, Kukla M, Zwirska-Korczala K (2014) Serum adipokines in inflammatory bowel disease. World J Gastroenterol 20:6912–6917
36. Neubauer K, Bednarz-Misa I, Walecka-Zacharska E et al (2019) Oversecretion and overexpression of nicotinamide phosphoribosyltransferase/pre-B colony-enhancing factor/visfatin

in inflammatory bowel disease reflects the disease activity, Severity of Inflammatory Response and Hypoxia. Int J Mol Sci 20. https://doi.org/10.3390/ijms20010166
37. Rosti V, Campanelli R, Massa M, Viarengo G, Villani L, Poletto V, Bonetti E, Catarsi P, Magrini U, Grolla AA, Travelli C, Genazzani AA, Barosi G (2016) Increased plasma nicotinamide phosphoribosyltransferase is associated with a hyperproliferative phenotype and restrains disease progression in MPN-associated myelofibrosis. Am J Hematol 91:709–713
38. Barone M, Chain F, Sokol H et al (2018) A versatile new model of chemically induced chronic colitis using an outbred murine strain. Front Microbiol:9. https://doi.org/10.3389/fmicb.2018.00565
39. Martín R, Chain F, Miquel S et al (2014) The commensal bacterium Faecalibacterium prausnitzii is protective in DNBS-induced chronic moderate and severe colitis models. Inflamm Bowel Dis 20:417–430
40. Telesco SE, Brodmerkel C, Zhang H et al (2018) Gene expression signature for prediction of golimumab response in a phase 2a open-label trial of patients with ulcerative colitis. Gastroenterology 155:1008–1011.e8
41. Melgar S, Karlsson L, Rehnström E, Karlsson A, Utkovic H, Jansson L, Michaëlsson E (2008) Validation of murine dextran sulfate sodium-induced colitis using four therapeutic agents for human inflammatory bowel disease. Int Immunopharmacol 8:836–844
42. Kiesler P, Fuss IJ, Strober W (2015) Experimental models of inflammatory bowel diseases. Cell Mol Gastroenterol Hepatol 1:154–170
43. Antoniou E, Margonis GA, Angelou A, Pikouli A, Argiri P, Karavokyros I, Papalois A, Pikoulis E (2016) The TNBS-induced colitis animal model: an overview. Ann Med Surg (Lond) 11:9–15
44. Fiorucci S, Mencarelli A, Palazzetti B, Sprague AG, Distrutti E, Morelli A, Novobrantseva TI, Cirino G, Koteliansky VE, de Fougerolles AR (2002) Importance of innate immunity and collagen binding integrin alpha1beta1 in TNBS-induced colitis. Immunity 17:769–780
45. Okayasu I, Hatakeyama S, Yamada M et al (1990) A novel method in the induction of reliable experimental acute and chronic ulcerative colitis in mice. Gastroenterology 98:694–702
46. Kim TW, Seo JN, Suh YH, Park HJ, Kim JH, Kim JY, Oh KI (2006) Involvement of lymphocytes in dextran sulfate sodium-induced experimental colitis. World J Gastroenterol 12:302–305
47. Morgan ME, Zheng B, Koelink PJ et al (2013) New perspective on dextran sodium sulfate colitis: antigen-specific T cell development during intestinal inflammation. PLoS One 8:e69936
48. Cassar S, Dunn C, Olson A et al (2018) From the cover: inhibitors of nicotinamide phosphoribosyltransferase cause retinal damage in larval zebrafish. Toxicol Sci 161:300–309
49. Oyarzún AP, Westermeier F, Pennanen C, López-Crisosto C, Parra V, Sotomayor-Flores C, Sánchez G, Pedrozo Z, Troncoso R, Lavandero S (2015) FK866 compromises mitochondrial metabolism and adaptive stress responses in cultured cardiomyocytes. Biochem Pharmacol 98:92–101

Affiliations

Giorgia Colombo[1] · Nausicaa Clemente[2] · Andrea Zito[3] · Cristiano Bracci[3] · Federico Simone Colombo[4] · Sabina Sangaletti[5] · Elena Jachetti[5] · Davide Giuseppe Ribaldone[6] · Gian Paolo Caviglia[7] · Luca Pastorelli[8,9] · Marco De Andrea[2,10] · Samuele Naviglio[11] · Marianna Lucafò[12] · Gabriele Stocco[13] · Ambra A. Grolla[1] · Michela Campolo[14] · Giovanna Casili[14] · Salvatore Cuzzocrea[14] · Emanuela Esposito[14] · Fabio Malavasi[3] · Armando A. Genazzani[1] · Chiara Porta[1,2] · Cristina Travelli[15]

[1] Department of Pharmaceutical Sciences, University of Eastern Piedmont, A. Avogadro, 28100 Novara, Italy

[2] Center for Translational Research on Autoimmune & Allergic Diseases (CAAD), Università del Piemonte Orientale, 28100 Novara, Italy

[3] Lab of Immunogenetics, Department of Medical Sciences, University of Turin, 10100 Turin, Italy

[4] Flow Cytometry and Cell Sorting Unit, Humanitas Clinical and Research Center – IRCCS, 20089 Rozzano, MI, Italy

[5] Molecular Immunology Unit, Department of Research, Fondazione IRCCS Istituto Nazionale dei Tumori di Milano, Milan, Italy

[6] Department of Surgical Sciences, University of Turin, 10100 Turin, Italy

[7] Division of Gastroenterology, Department of Medical Sciences, University of Turin, 10100 Turin, Italy

[8] Department of Biomedical Sciences for Health, University of Milan, Milan, Italy

[9] Gastroenterology Unit, IRCCS Policlinico San Donato, San Donato Milanese, Italy

[10] Viral Pathogenesis Unit, Department of Public Health and Pediatric Sciences, Turin Medical School, 10126 Turin, Italy

[11] Institute for Maternal and Child Health IRCCS Burlo Garofolo, 34137 Trieste, Italy

[12] Department of Medicine, Surgery and Health Sciences, University of Trieste, 34137 Trieste, Italy

[13] Department of Life Sciences, University of Trieste, 34137 Trieste, Italy

[14] Department of Chemical, Biological, Pharmaceutical and Environmental Sciences, University of Messina (ME), Messina, ME, Italy

[15] Department of Pharmaceutical Sciences, Università degli Studi di Pavia, 27100 Pavia, Italy

SUPPLEMENTARY INFORMATION

Supplementary table I: Antibodies for FACS analysis

ANTIBODY	SOURCE	IDENTIFIER
CD45- PerCp (Clone 30-F11)	BioLegend	Cat# 103130
CD45-FITC	BioLegend	Cat# 103108
CD11b–PerCP (clone M1/70)	BioLegend	Cat# 101229
F4/80–PE-Cy7 (clone BM8)	BioLegend	Cat# 123114
Ly6C-APCCy7 (clone HK1.4)	BioLegend	Cat# 128026
Ly6G-BV711 (clone 1A8)	BioLegend	Cat# 127643
CD4–PE-Cy7 (clone GK1.5)	BioLegend	Cat# 100422
CD8-APC (clone 53-6.7)	BioLegend	Cat# 100308
CD3-PE (clone 145-2C11)	BioLegend	Cat# 100307
TNFα-APC (clone MP6-XT22)	BioLegend	Cat# 103108
IFNγ-FITC (clone XMG1.2)	BioLegend	Cat# 505806
LIVE/DEAD Fixable Violet Dead Cell Stain Kit	Life Technologies	Cat# L34963

Supplementary table II: sequences of primers used for gene expression analysis

Gene	Forward 5'->3'	Reverse 5'->3'
actin	CCAACCGTGAAAAGATGACC	ACCAGAGGCATACAGGGACA
Il12b	TCCTGAAGTGTGAAGCACCAA	TCAGGGGAACTGCTACTGCT
Il23	AGCCAGTTCTGCTTGCAAAGG	GGAGGTTGTGAAGTTGCTCCATG
Ifng	TCAAGTGGCATAGATGTGGAAGAA	TGGCTCTGCAGGATTTTCATG
Tbx21	ACCAACAACAAGGGGGCTTC	CTCTGGCTCTCCATCATTCACC
Il6	GGATACCACTCCCAACAGACCT	GCCATTGCACAACTCTTTTCTC
Il1b	AAGTTGACGGACCCCAAAAGA	TGTTGATGTGCTGCTGCGA
Nampt	GCAGAAGCCGAGTTCAACAT	TCTTCTTTTCACGGCATTCA
Il21	GCTCCACAAGATGTAAGGGC	CCACGAGGTCAATGATGCCACG

Tgfb1	ACCAACTATTGCTTCAGCTTCAGCTCCAC	GATCCACTTCCAACCCAGGTC
Gata3	ACAGAAGGCAGGGAGTGTGTGAAC	TTTTATGGTAGAGTCCGCAGGC
Rorc2	CTCATGACTGAGAACTTGGCT	ACCTCCACTGCCAGCTGTGTG
Foxp3	TCCAGGTTGCTCAAAGTCTTCTTG	AGGCTGCTGTTACGGGAATAGG
Il18	AGACAGTGAAGTAAGAGGACTGCGT	CCTTTTGGCAAGCAAGAAAGTGTC
Il22	CAGCTCCTGTCACATCAGCGGT	TCCCCAATCGCCTTGATCTCTCCAC
Nos2	GCCACCAACAATGGCAACA	CGTACCGGATGAGCTGTGAATT
Cox2	AATGAGTACCGCAAACGCTTC	CAGCCATTTCCTTCTCTCCTGTA
Nox2	CCCTTTGGTACAGCCAGTGAAGAT	CAATCCCGGCTCCCACTAACATCA
Il4	CACTTGAGAGAGATCATCGGCA	GTGTTCTTCGTTGCTGTGAGGA
Il10	GGTTGCCAAGCCTTATCGGA	ACCTGCTCCACTGCCTTGCT
Tnf	GAAAAGCAAGCAGCCAACCA	CGGATCATGCTTTCTGTGCTC
Il17a	GGACTCTCCACCGCAATGAA	TTTCCCTCCGCATTGACACA
Il17f	AACCAGGGCATTTCTGTCCC	GGGGTCTCGAGTGATGTTGT

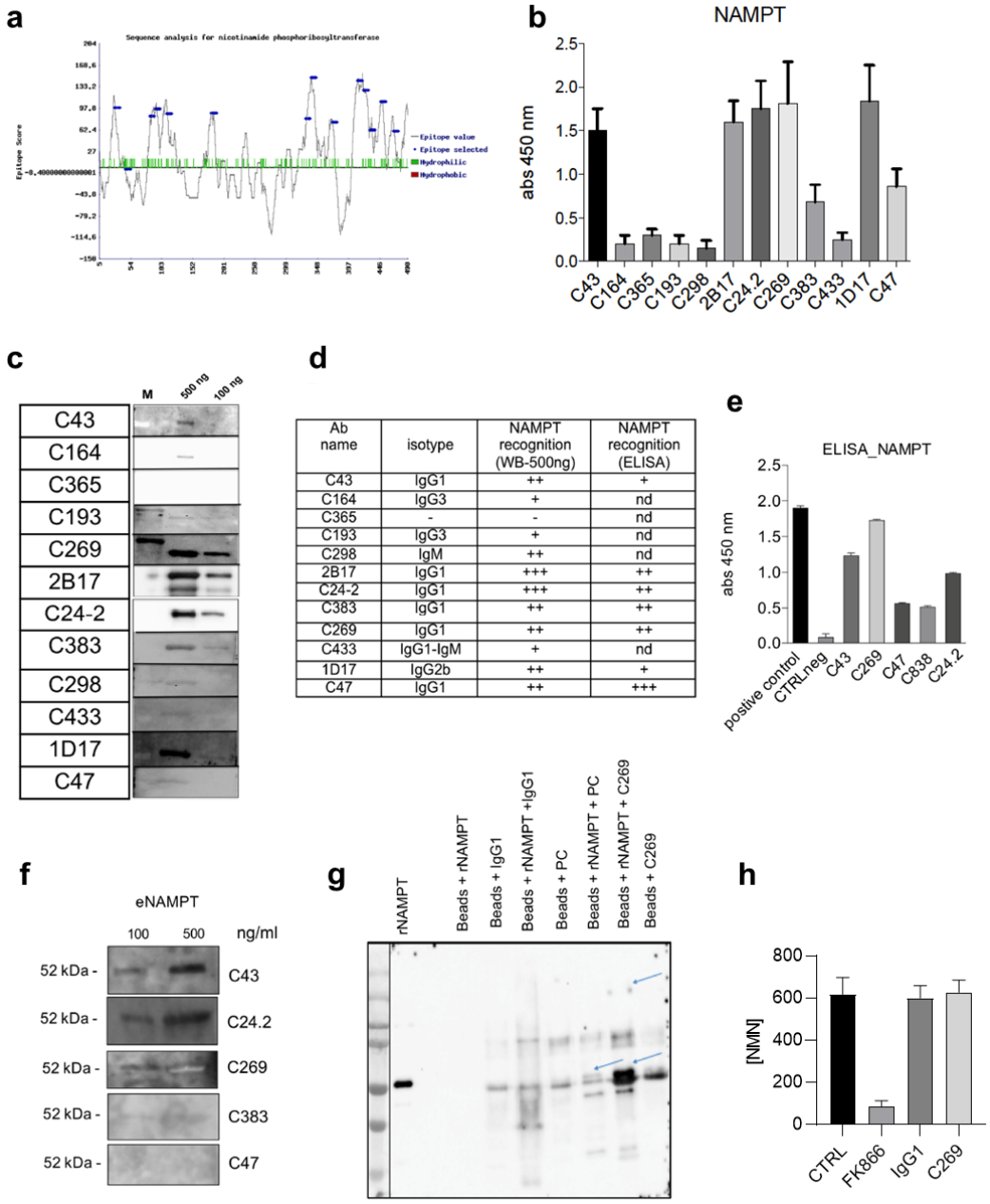

Ab name	isotype	NAMPT recognition (WB-500ng)	NAMPT recognition (ELISA)
C43	IgG1	++	+
C164	IgG3	+	nd
C365	-	-	nd
C193	IgG3	+	nd
C298	IgM	++	nd
2B17	IgG1	+++	++
C24-2	IgG1	+++	++
C383	IgG1	++	++
C269	IgG1	++	++
C433	IgG1-IgM	+	nd
1D17	IgG2b	++	+
C47	IgG1	++	+++

Supplementary Figure 1. Generation and validation of eNAMPT neutralizing antibodies. (**a**) Epitopes chosen for the generation of eNAMPT neutralizing antibodies. (**b**) ELISA assay for NAMPT using 12 different hybridoma cell supernatants, n= 3 independent experiments. (**c**) Representative Western Blot of recombinant NAMPT detection (500-100 ng) using 12 different hybridoma cell supernatants, n=3 independent experiments. (**d**) Table summarizing the results obtained by ELISA, western blot and the isotype determined by Ouchterlony assay

(n=2 independent experiments). (**e**) ELISA assay for NAMPT and (**f**) detection of recombinant eNAMPT by western blot by 5 antibodies purified, n= 4 independent experiments. (**g**) Immunoprecipitation of recombinant NAMPT using purified IgG1, PC (positive control, commercial antibody) or C269, n=2 independent experiments. (**h**) NMN production from 4T1 cells treated with FK866 (100 nM), control IgG1 and C269 (50µg/ml each) n=4 independent experiments.

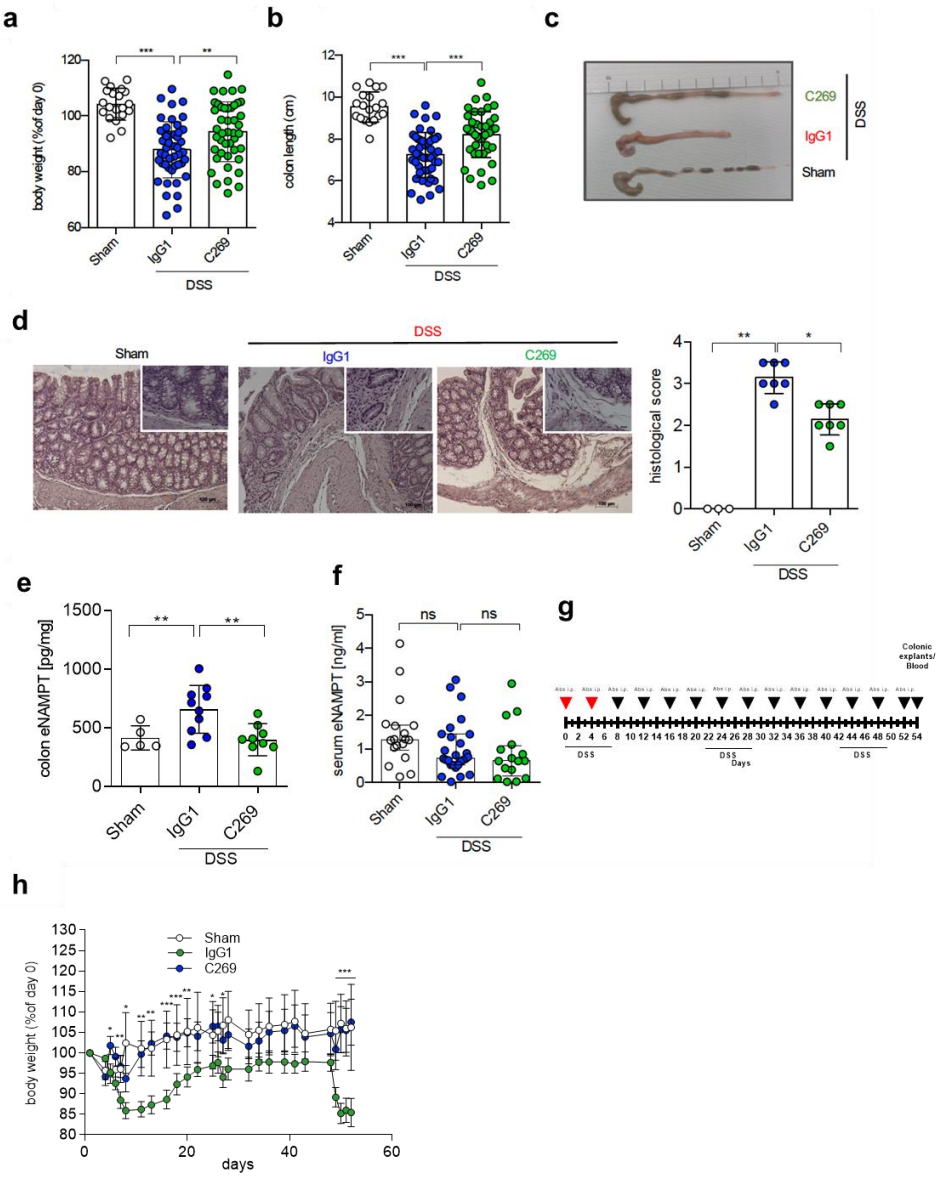

Supplementary Figure 2. C269 reduces DSS-induced acute colitis. C57BL/6 mice received 1.5% of DSS, a control IgG1 (2.5 mg/kg, at day 0-3-7) or C269 (2.5 mg/kg, at day at day 0-3-7) and sacrificed at day 11. (**a**) Analysis of body weight and (**b**) colon length in Sham (n=19), IgG1 (n=46) or C269 (n=45) treated mice. (**c**) Representative image of colon lengths at day 11 with the different treatments. (**d**) Representative H&E analysis and quantification of colons at day 11 in Sham (n=3), IgG1 (n=7) or C269 (n=7) treated mice (** p<0.01, * p<0.05 by Bonferroni post-hoc test). (**e**) eNAMPT levels in supernatants of colonic explants in Sham (n=5), IgG1 (n=10) or C269 (n=9) treated mice. (**f**) Serum eNAMPT levels in Sham (n=18), IgG1 (n=27) or C269 (n=16) treated mice. Values are means ± SEM (*** p<0.001, ** p<0.01, * p<0.05 by one-way ANOVA). (**g**) Experimental scheme of chronic DSS model. (**h**) Analysis of body weight of sham (n=6), IgG1 (n=12) and C269 (n=12) treated mice during chronic DSS model.

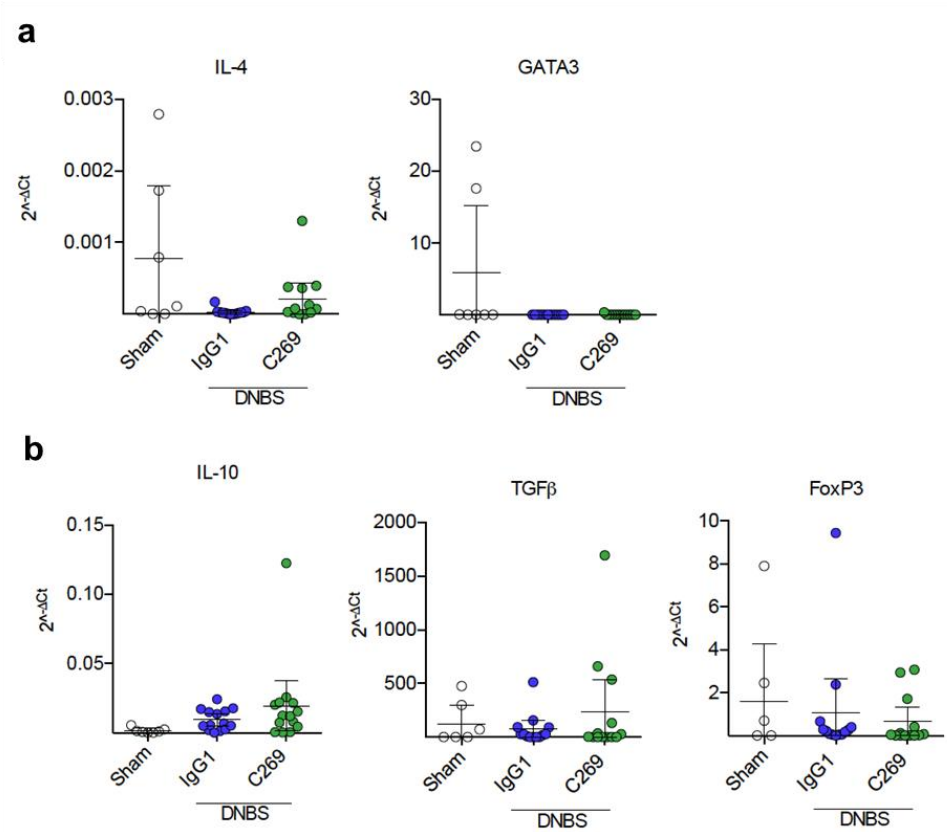

Supplementary Figure 3. C269 does not alter Th2/anti-inflammatory genes in DNBS-induced acute colitis. (**A-B**) Gene expression analysis quantified by Real-

Time PCR in colons of Sham (n=7), IgG1 (n=13) or C269 (n=13) treated mice. Values are means ± SEM (analysed with non-parametric Kruskal-Wallis test followed by a Dunn's multiple comparison test).

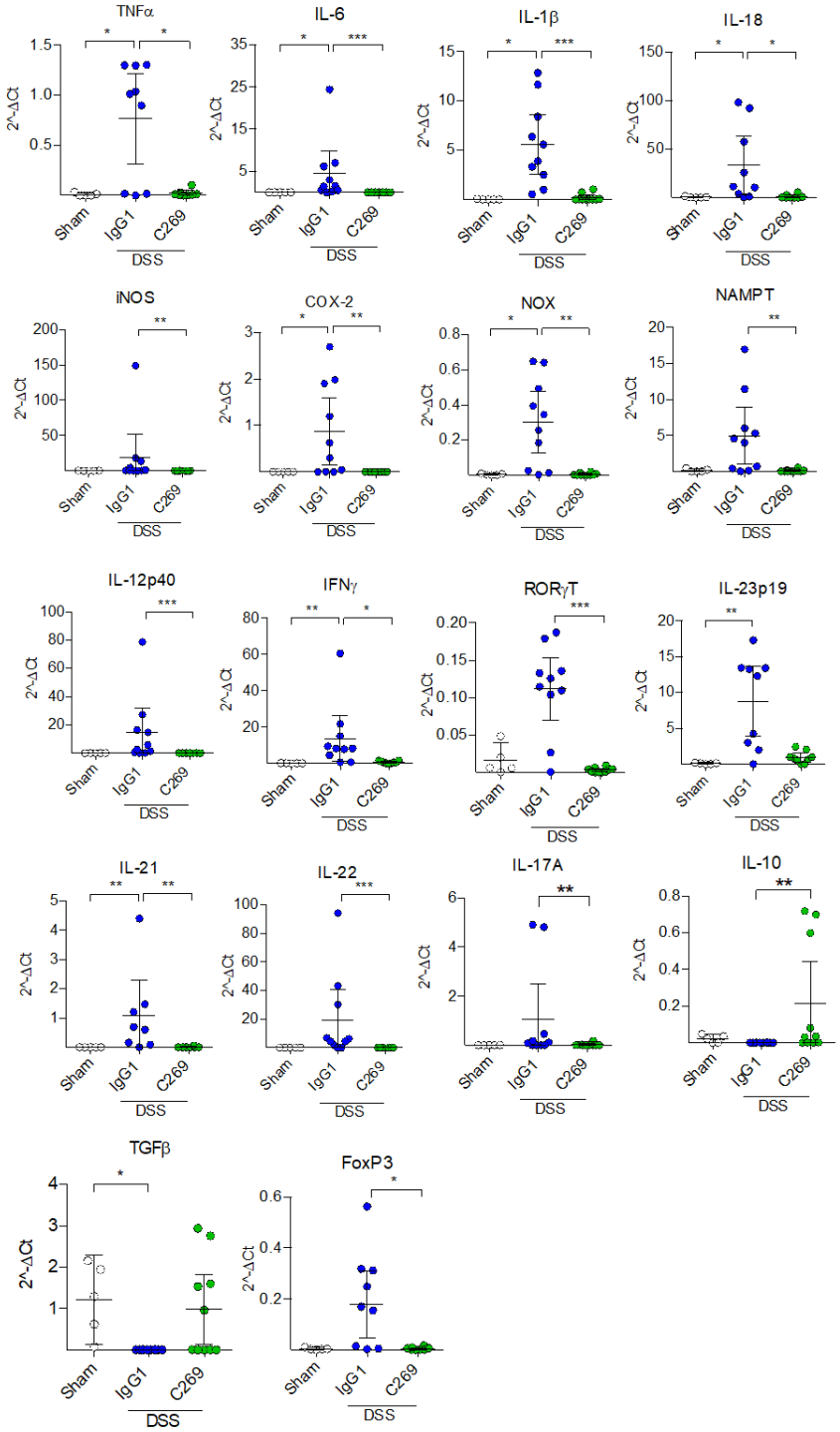

Supplementary Figure 4. C269 reduces molecular determinants of intestinal inflammation in DSS-induced acute colitis. Gene expression analysis quantified by Real-Time PCR in colons of Sham (n=5), IgG1 (n=10) or C269 (n=10) treated mice. Values are means ± SEM (*** $p<0.001$, ** $p<0.01$, * $p<0.05$ by non-parametric Kruskal-Wallis test followed by a Dunn's multiple comparison test).

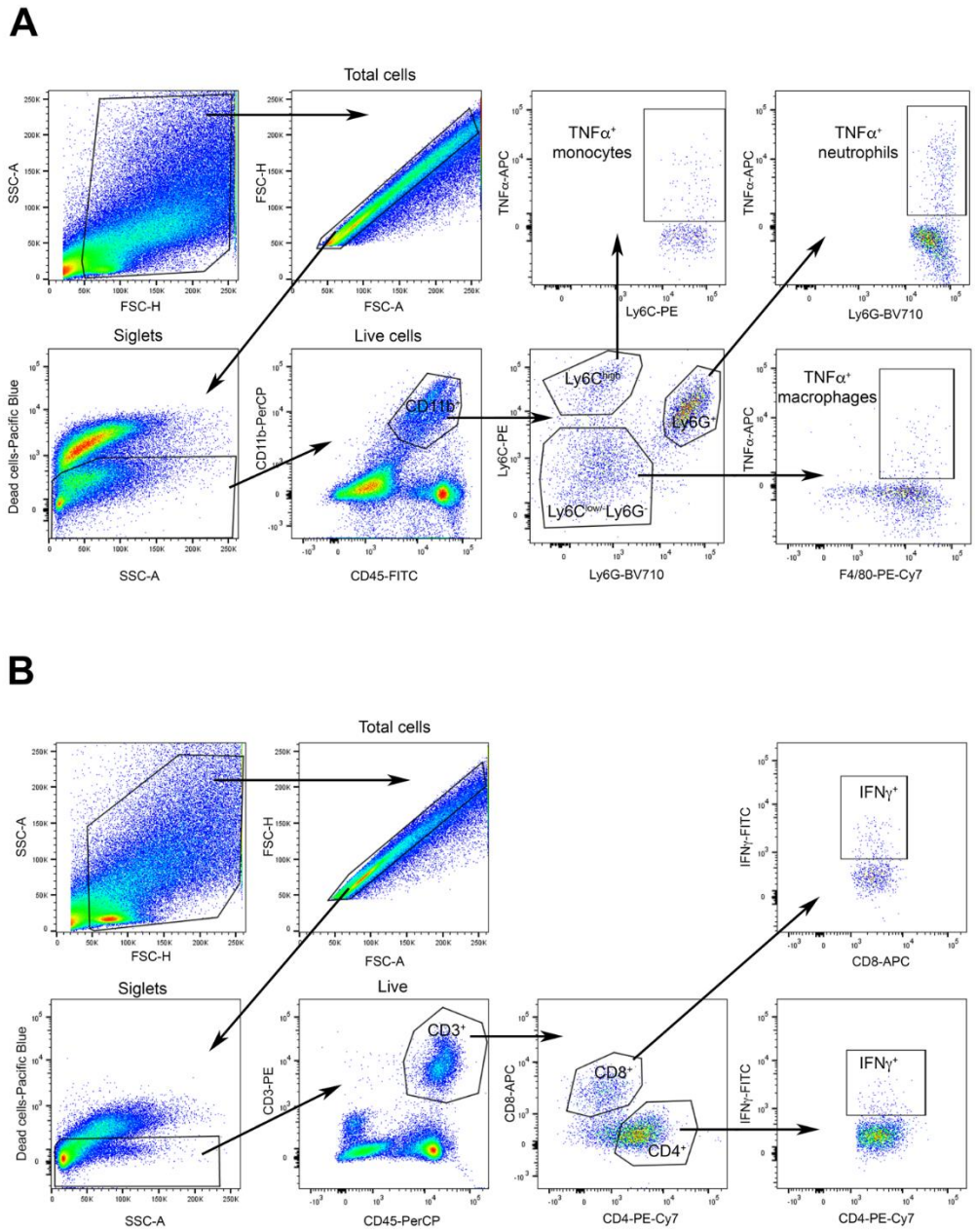

Supplementary Figure 5. Gating strategy used to analyze *lamina propria* myeloid cells (**A**) and T lymphocytes (**B**) of sham and DNBS-treated mice.

Chapter 4

cells

MDPI

Article

The Cytokine Nicotinamide Phosphoribosyltransferase (eNAMPT; PBEF; Visfatin) Acts as a Natural Antagonist of C-C Chemokine Receptor Type 5 (CCR5)

Simone Torretta [1,†], Giorgia Colombo [1,†], Cristina Travelli [2], Sara Boumya [1], Dmitry Lim [1], Armando A. Genazzani [1] and Ambra A. Grolla [1,*]

[1] Department of Pharmaceutical Sciences, Università del Piemonte Orientale, 28100 Novara, Italy; simone.torret89@gmail.com (S.T.); giorgia.colombo@uniupo.it (G.C.); sara_posta1993@yahoo.it (S.B.); dmitry.lim@uniupo.it (D.L.); armando.genazzani@uniupo.it (A.A.G.)

[2] Department of Pharmaceutical Sciences, Università di Pavia, 27100 Pavia, Italy; cristina.travelli@unipv.it

* Correspondence: ambra.grolla@uniupo.it; Tel.: +39-0321-375822; Fax: +39-0321-375821

† These authors contributed equally.

Received: 15 November 2019; Accepted: 21 February 2020; Published: 21 February 2020

Abstract: (1) Background: Extracellular nicotinamide phosphoribosyltrasferase (eNAMPT) is released by various cell types with pro-tumoral and pro-inflammatory properties. In cancer, eNAMPT regulates tumor growth through the activation of intracellular pathways, suggesting that it acts through a putative receptor, although its nature is still elusive. It has been shown, using surface plasma resonance, that eNAMPT binds to the C-C chemokine receptor type 5 (CCR5), although the physiological meaning of this finding is unknown. The aim of the present work was to characterize the pharmacodynamics of eNAMPT on CCR5. (2) Methods: HeLa CCR5-overexpressing stable cell line and B16 melanoma cells were used. We focused on some phenotypic effects of CCR5 activation, such as calcium release and migration, to evaluate eNAMPT actions on this receptor. (3) Results: eNAMPT did not induce ERK activation or cytosolic Ca^{2+}-rises alone. Furthermore, eNAMPT prevents CCR5 internalization mediated by Rantes. eNAMPT pretreatment inhibits CCR5-mediated PKC activation and Rantes-dependent calcium signaling. The effect of eNAMPT on CCR5 was specific, as the responses to ATP and carbachol were unaffected. This was strengthened by the observation that eNAMPT inhibited Rantes-induced Ca^{2+}-rises and Rantes-induced migration in a melanoma cell line. (4) Conclusions: Our work shows that eNAMPT binds to CCR5 and acts as a natural antagonist of this receptor.

Keywords: eNAMPT; visfatin; CCR5; antagonism; cancer; calcium signaling; migration

1. Introduction

Extracellular nicotinamide phosphoribosyltrasferase (eNAMPT), also known as PBEF or visfatin, is the secreted form of NAMPT (EC 2.4.2.12), a key enzyme involved in maintaining the balance of NAD and ATP levels in cells [1]. NAMPT, starting from nicotinamide (Nam), adenosine triphosphate (ATP) and phosphoribosyl pyrophosphate (PRPP), catalyzes the production of nicotinamide mononucleotide (NMN), a key precursor of NAD in mammalian cells. Importantly, different cell types secret NAMPT in the extracellular space, where it is now considered a metabokine with pro-inflammatory and pro-tumoral activity [2,3]. Of great importance, eNAMPT is overexpressed in several disorders, including cancer [4,5] where eNAMPT controls angiogenesis, tumor growth and metastasis [6,7]. The mechanism by which eNAMPT exerts its function is still an open debate. Three theories,

not necessarily mutually exclusive, are present in the literature: (i) eNAMPT binds to a yet unidentified receptor; and/or (ii) eNAMPT is enzymatically active in the extracellular milieu and this is fundamental for its actions; (iii) it is carried in the systemic circulation in extracellular vesicles (EV) and is liberated upon internalization, enhancing NAD^+ biosynthesis [8]. This latter possibility was demonstrated by Yoshida et al. both in mice and humans [8].

The possibility that eNAMPT binds to an extracellular receptor is supported by the observation that stimulation of cancer cells with exogenous eNAMPT in solutions not containing the enzymatic substrates is sufficient to activate specific intracellular signaling pathways (e.g., STAT3, NF-κB, Akt, P38) within minutes, which indicates that it is likely that eNAMPT binds to and activates a cell surface receptor. In this respect, the insulin receptor was initially proposed but the report was retracted [9]. More recently, Camp et al. demonstrated that eNAMPT induces lung inflammation via a direct interaction with Toll-like receptor 4 (TLR4). Moreover, computational analysis demonstrated that eNAMPT and MD-2, a TLR4-binding protein, share ≈30% sequence identity [10]. This interaction was recently confirmed by Managò and colleagues [11].

Less recently, it was reported that eNAMPT is able to selectively inhibit infection of monocytes by human immunodeficiency virus (HIV) and this activity was linked to a direct interaction with the C-C chemokine receptor type 5 (CCR5). The interaction was solely demonstrated by surface plasmon resonance (SPR) with a K_D of 5 μM in the 1:1 binding model [12] and no functional studies were performed.

CCR5 is a seven transmembrane, G-protein coupled receptor (GPCR), involved in inflammatory responses and it also serves as a coreceptor for the entry of R5 strains of HIV [13,14]. It recognizes Rantes (also known as CCL5) as its main ligand, although other proteins are known to affect its function including the agonists CCL3 (also known as MIP-1α), MIP1-β, CCL2, CCL8, CCL11, and CCL14 and the natural antagonist CCL7 (also known as MCP-3) [15]. Maraviroc, a competitive molecular antagonist, is currently used in HIV therapy [16]. CCR5 is overexpressed in several cancers (e.g., breast cancer, melanoma) and it has been suggested that the activation of this receptor controls tumor development [17,18]. For example, in melanoma, CCR5 expression on stromal cells is necessary for the spread of B16 melanoma cells to the lungs [19] and in CCR5-deficient mice B16 melanoma growth is delayed [20].

The present contribution aims at elucidating the correlation between CCR5 and eNAMPT in cancer cells. We now show that eNAMPT binds to CCR5 in cancer cells and acts as a natural antagonist of this receptor. Antagonism of CCR5 alone is unlikely to explain all the actions mediated by eNAMPT [3], and it therefore likely that other eNAMPT receptors exist, including the recently demonstrated TLR4.

2. Materials and Methods

2.1. Cell Culture

HeLa (human cervix carcinoma) and B16 (murine melanoma) cells were cultured in Dulbecco's modified Eagle's medium (DMEM, Sigma-Aldrich, St. Louis, MO, USA)) supplemented with 10% fetal bovine serum (FBS), 2 mg/mL glutamine, 10 U/mL penicillin, and 100 μg/mL streptomycin (Sigma-Aldrich). Cells were maintained in a humidified incubator supplied with 5% CO_2/95% air at 37 °C and detached by Trysin-EDTA.

2.2. Recombinant eNAMPT Preparation

Wild-type murine full-length and H247E NAMPT (ORF GenBank BC018358) were cloned in pET28a (NdeI/EcoRI). Recombinant eNAMPTs were expressed in *E. coli*. (ClearColi, BL21-DE3), inducted with IPTG 0.5 mM for 3 h at 20 °C, and purified by His-tag affinity chromatography with NiNTA Superflow resin (Qiagen, Hilden, Germany). Protein purity was determined by SDS-page. Only protein preparations with a purity higher than 95% and with low endotoxin levels (<0.01 U, LAL test) were used. eNAMPT in most experiments was used at a concentration of 500 ng/mL, as in most other

work on the subject (e.g., [12,21]) except for experiments in which equilibrium or semi-equilibrium conditions were reached.

2.3. Generation of Stable HeLa-CCR5 Cell Line

Murine CCR5 was cloned in the pLV lentiviral vector. Correct insertion and sequence were confirmed by DNA sequencing. The lentiviral particles were produced as described elsewhere (Grolla et al., 2015) in HEK293T cells transfected with pMDLg/pRRE, pMD2.VSVG, pRSV-Rev, and pLV-CCR5/pLV-empty plasmids. Briefly, after 48 h, cell medium was collected, filtrated, and centrifuged for 90 min at 100,000 *g*. The viral particles were resuspended and used to infect HeLa cells, after virus titration. Stable scramble (HeLa-SCR) and HeLa-CCR5 were stained with anti-CCR5 PE (Biolegend, San Diego, CA, USA) for 20 min at 4°C, then washed twice in PBS and the relative expression of CCR5 analyzed using by flow cytometry (BD Accuri C6).

2.4. Binding Assay

First, Rantes-PE was prepared by incubating avidin-PE (Invitrogen, Carlsbad, CA, USA) and biotin-Rantes (Chemotactics) for 3 min at RT. Following this, 1×10^5 cells suspension was incubated with 2U/1×10^5 cells of Heparinise I and III (2U/10^6 cells, Sigma-Aldrich) for 1 h at 4 °C. Then, cells were washed and incubated with eNAMPT (125 μg/mL; 2.25 μM) or maraviroc (10 μM, Sigma Aldrich) at 4 °C in complete medium (200 μL). After 20 min, Rantes-PE (25 ng; 16 nM) was added to the cell suspension for 2 h at 4 °C. Then, cells were washed three times in ice cold PBS, resuspended in FACS Buffer (Hanks' Balanced Salt solution HBSS + 0.5% BSA), and samples were analyzed by flow cytometry (BD Accuri C6). eNAMPT was used at this high concentration considering both the molecular weight and the oligomerization state of the proteins, to take into account the reported difference in affinity to CCR5 (0.4 nM for RANTES vs. 5 μM for eNAMPT [12,22]. In preliminary experiments, lower concentrations of eNAMPT were devoid of effect.

2.5. CCR5 Internalization

First, 2×10^5 cells were plated in 96-well plates and treated with vehicle, Rantes (100 ng/mL; 12 nM Peprotech), CCL3 (100 ng/mL; Peprotech), CCL7 (2.5 μg/mL; Peprotech), maraviroc (10 μM; Sigma-Aldrich), and/or eNAMPT (2.5 μg/mL; 45 nM) for 60 min at 37 °C or 4 °C (as a negative control). Cells were washed twice in PBS and resuspended in 100 μL of phosphate buffer saline (PBS) and stained with anti-CCR5 PE for 20 min at 4 °C. Cells were then washed twice in PBS and cell surface expression of CCR5 was determined with a BD Accuri FACS. In parallel, cells were plated on a coverslip and treated with vehicle, Rantes (100 ng/mL; 12 nM), CCL3 (100 ng/mL; 9.9 nM), and/or eNAMPT (2.5 μg/mL; 45 nM), CCL7 (250 ng/mL; 22 nM) for 60 min at 37 °C or 4 °C. Then, cells were fixed in 4% formaldehyde for 15 min at 4 °C. Subsequently, cells were stained with a primary antibody anti-mouse CCR5-PE and DRAQ5 (Invitrogen). For these experiments we used 12 nM Rantes as this concentration gave a significant level of internalization. We therefore used eNAMPT roughly at a three-fold higher concentration (45 nM). Lower concentrations of eNAMPT did not show a significant effect on preventing Rantes-mediated internalization (e.g., 500 ng/mL = 9 nM eNAMPT did not affect Rantes-mediated internalization).

2.6. Fura-2 Imaging

Cells were loaded with 2 μM Fura-2-AM (Invitrogen) in KRB solution (Krebs-Ringer modified buffer: 125 mM NaCl, 5 mM KCl, 1 mM Na_3PO_4, 1 mM $MgSO_4$, 5.5 mM glucose, 20 mM HEPES, pH 7.4) supplemented with 2 mM CaCl2, 0.01% pluronic acid and 5μM sulfinpyrazone. After washing and de-esterification (30 min), the coverslip was mounted in a chamber and placed on the stage of a Leica epifluorescent microscope equipped with a S Fluor 40×/1.3 objective. Cells were stimulated with the indicated treatments and excited at 340/380 nm by the monochromator Polichrome V (Till Photonics, Munich, Germany) and the fluorescent signal was collected by a CCD camera (Hamamatsu, Japan)

through bandpass 510 nm filter; the experiments were controlled and images analyzed with MetaFluor (Molecular Devices, Sunnyvale, CA, USA) software. To quantify the difference in the amplitude of Ca2+ transients, the ratio values were normalized according to the formula (ΔF)/F0 (referred to as normalized (norm.) ratio). NMN, ATP and carbachol were purchased from Sigma-Aldrich.

2.7. Western Blot

First, 5×10^5 cells were treated at the indicated time-points and the cells were lysed in 80 μL in lysis buffer composed of 20 mM HEPES, 100 mM NaCl, 5 mM EDTA, 1% Nonidet P-40, and Protease and Phosphatase Inhibitor Cocktail (Sigma). Proteins quantification was performed with BCA Protein Assay (Thermo Fisher Scientific, Waltham, MA, USA), and proteins were resolved on SDS–PAGE. Antibodies used: rabbit polyclonal CCR5 antibody (AB65850 Abcam); rabbit polyclonal antibody anti-p42/44 (Cell Signalling Technology); mouse anti-actin (Sigma); rabbit pPKC (pan) ZT410 Cell signaling and peroxidase-conjugated secondary antibodies (Bio-Rad, Hercules, CA, USA). Densitometry analysis was evaluated using was performed with Quantity One program (Bio-Rad).

2.8. Wound-Healing Assay

When confluent monolayers of B16 cells were established, we performed a cross-shaped scratch with tip. Then, the cells were washed twice with PBS to remove residual cell debris. Cells were then incubated with Rantes (100 ng/mL; 12 nM), eNAMPT (500 ng/mL; 9 nM), CCL7 (250 ng/mL; 22 nM), CCL3 (100 ng/mL; 9.9 nM), and maraviroc (10 μM) or the combination for 24 h and pictures of a defined wound spot were made at different time points. The area of the wound in the microscopic pictures was measured and analyzed using Image J software (National Institutes of Health, MD, USA).

2.9. Statistical Analysis

Statistics were calculated with Graphpad Prism version 6 software. A two-sided unpaired Student's *t*-test was used to compared unmatched groups and expressed as: t test * $p < 0.05$; ** $p < 0.01$; *** $p < 0.001$.

3. Results

3.1. eNAMPT Binds to CCR5, but Does Not Act as an Agonist

A previous report demonstrated that eNAMPT interacted with CCR5 with a K_D of 5 μM in a 1:1 binding model by surface plasmon resonance [21].

To understand the biological significance of this interaction, we generated HeLa cells overexpressing murine CCR5 (HeLa-CCR5) and the respective control represented by HeLa cells infected with the empty vector (HeLa-SCR). The relative overexpression of CCR5 was determined by flow cytometry analysis (Figure 1A) and Western blot analysis (Figure 1B).

As shown in Figure 1B, in HeLa-CCR5 cells the pretreatment with eNAMPT (2.25 μM) reduced the percentage of Rantes-PE (16 nM) positive cells, similarly to maraviroc (10 μM), confirming that eNAMPT binds to CCR5 [21]. Lower concentrations of eNAMPT were unable to elicit an effect, but this is likely to be due to the difference in K_D of the two ligands (K_D for Rantes approx. 0.4 nM vs. K_D for eNAMPT of approx. 5 5 μM; [12,22])

In this report, it was also shown that eNAMPT is capable of inhibiting infections by R5 HIV in monocytes [12]. Given that both CCR5 agonists and antagonists inhibit HIV infections [8], we next analyzed the consequence of such binding. For these experiments, lower doses were used as there was no competition between RANTES and eNAMPT.

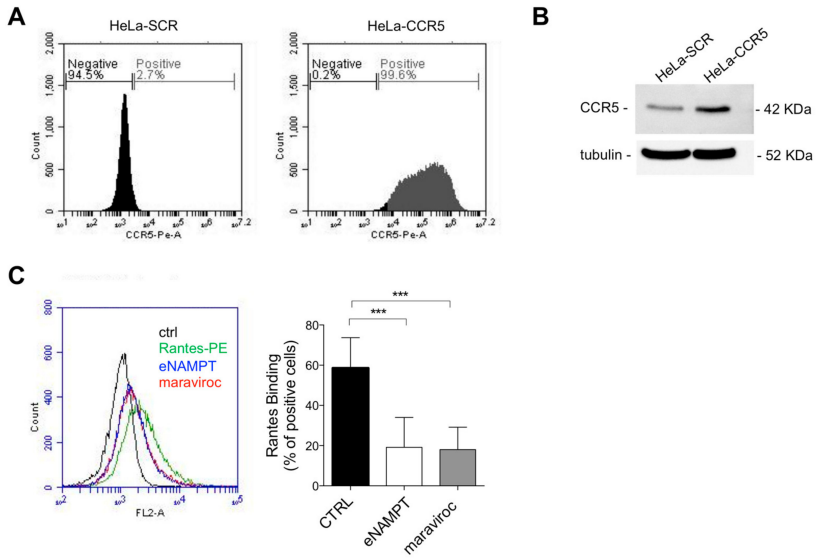

Figure 1. Extracellular nicotinamide phosphoribosyltrasferase (eNAMPT) binds to C-C chemokine receptor type 5 (CCR5) in HeLa cancer cells. (**A**) Representative flow cytometry analysis of CCR5 expression in HeLa-SCR and HeLa-CCR5 cells, using Rat anti-mouse CCR5 antibody. (**B**) Western blot analysis of CCR5 expression in HeLa-SCR and HeLa-CCR5 cells. The CCR5 antibody recognizes both human endogenous CCR5 and murine exogenous CCR5. (**C**) Representative FACS analysis and calculated percentage of positive cells of Rantes-PE (16 nM) binding on HeLa-CCR5 cells incubated in the presence or absence of eNAMPT (2.25 μM) or maraviroc (10 μM). Mean ± S.E.M. of five separate experiments; *** $p < 0.001$.

We first evaluated whether eNAMPT parallels the effects of Rantes. As it can be seen in Figure 2A, Rantes (25 ng/mL; 3 nM) was able to elicit a marked ERK phosphorylation in a time-dependent manner in HeLa-CCR5 cells, but not in HeLa-SCR cells. A trend of pERK activation was observable when cells were treated with eNAMPT (250–1000 ng/mL = 4.5 nM–8 nM), although no differences were present between HeLa SCR and CCR5 cells, meaning that it is independent of CCR5 (Figure 2A and Figure S2A). The ability of eNAMPT to induce pERK activation, independently on CCR5 pathway, has been reported previously [6,11].

Calcium signaling has also been associated with CCR5 and we therefore also evaluated this pathway. As it can be seen in Figure 2B, Rantes (3 nM) induced a cytosolic Ca^{2+} increase in HeLa-CCR5 (but not in HeLa-SCR; not shown), while eNAMPT (250–1000 ng/mL = 4.5 nM–18 nM) was again unable to do so (Figure 2B, concentrations of 250 and 1000 ng/mL not shown). In support of this data, we investigated also the ability of eNAMPT to induce CCR5 internalization, a common feature of CCR5 agonists. As shown in Figure 2C, both the agonists Rantes (100 ng/mL = 12 nM) and CCL3 (100 ng/mL = 9.9 nM) reduced the surface expression of CCR5 after 60 min. On the other hand, CCL7 (250 ng/mL = 22 nM), maraviroc (10 μM), and eNAMPT (up to 2.5 μg/mL = 45 nM) did not induce internalization of CCR5 (Figure 2C).

Considering these results, it would appear that eNAMPT is not a CCR5 agonist at nanomolar concentrations.

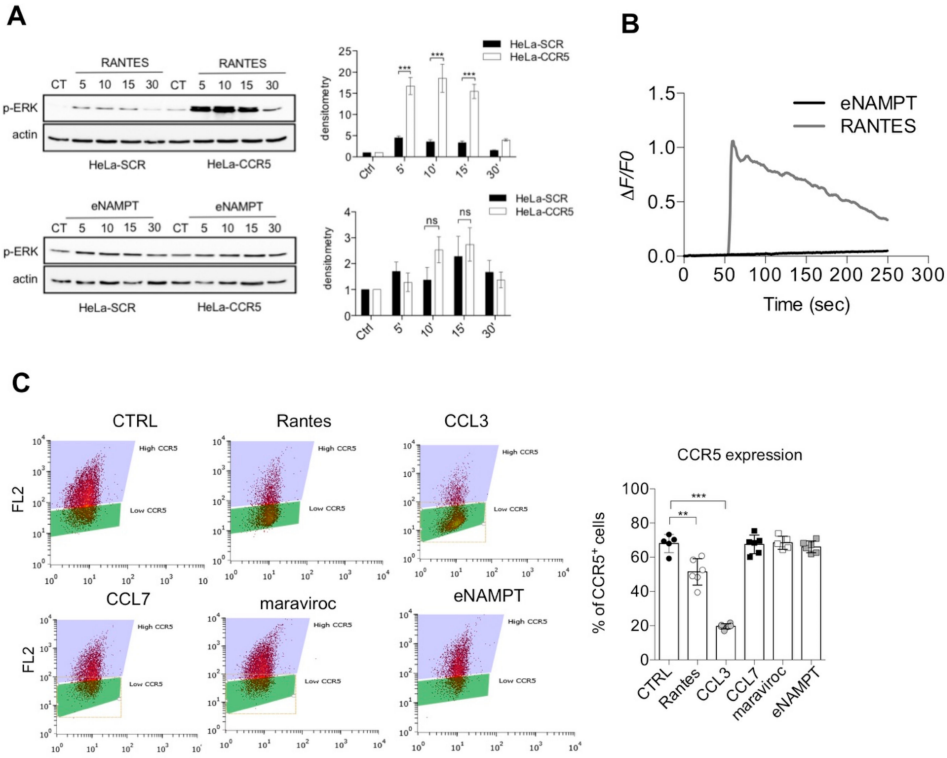

Figure 2. eNAMPT is not an agonist of CCR5. (**A**) Representative Western blot and densitometry analysis of phosphorylated ERK after 2 h of starvation followed by treatment for 5–30 min with recombinant Rantes (25 ng/mL; 3 nM) or eNAMPT (500 ng/mL; 9 nM) in serum-free conditions. Data from four separate experiments. (**B**) Representative calcium traces of HeLa-CCR5 loaded with FURA-2AM and stimulated with Rantes (25 ng/mL) or eNAMPT (500 ng/mL). Representative traces of 98–110 cells from 5–7 independent experiments. (**C**) Flow cytometry analysis of surface expression of CCR5 in HeLa-CCR5 cells treated for 1 h with Rantes (100 ng/mL = 12 nM), CCL3 (100 ng/mL = 9.9 nM), CCL7 (250 ng/mL = 22 nM), maraviroc (10 μM), and eNAMPT (2.5 μg/mL= 45 nM). The graph shows the mean ± S.E.M. of 12 determinations from four separate experiments. ** $p < 0.01$ *** $p < 0.001$; ns not statistically significant.

3.2. *eNAMPT Antagonizes CCR5 Activation in Hela-CCR5 Cells*

We next tested whether instead eNAMPT was able to modulate the responses of agonists on CCR5.

At first, we evaluated the effect of eNAMPT cotreatment with Rantes in CCR5 internalization. We observed that eNAMPT, similarly to CCL7 and maraviroc, reduced Rantes-mediated CCR5 internalization (Figure 3A,B). We corroborated this evidence by immunofluorescence, in which eNAMPT alone did not induce CCR5 internalization, while it prevented Rantes-mediated internalization (Figure S1).

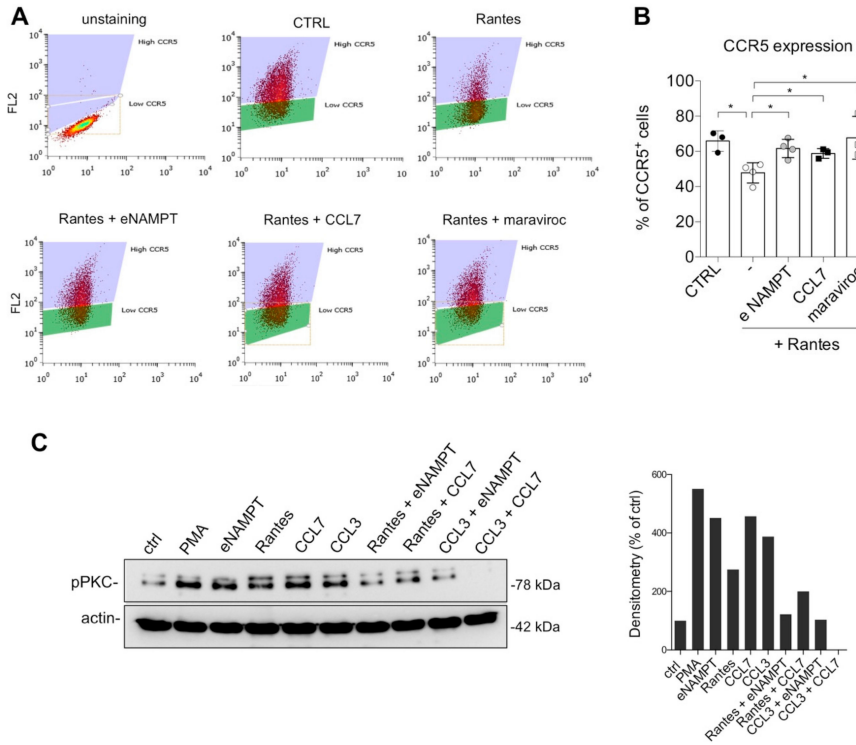

Figure 3. eNAMPT reduces CCR5 internalization and prevents pPKC activation. (**A**) Representative flow cytometry analysis of CCR5 expression in HeLa-CCR5 cells after the indicated stimuli. (**B**) Flow cytometry analysis of surface expression of CCR5 in HeLa-CCR5 cells treated for 1 h with Rantes (100 ng/mL; 12 nM) alone or pretreated for 20 min with eNAMPT (2.5 μg/mL; 45 nM) or CCL7 (250 ng/mL; 22 nM) or maraviroc (10 μM). Mean ± S.E.M. of four separate experiments. * $p < 0.05$. (**C**) Representative Western blot and densitometry of two independent experiments of phosphoPKC (pPKC) in Hela-CCR5 cells treated in serum-free for 20 min with Rantes (25 ng/mL; 3 nM), eNAMPT (500 ng/mL; 9 nM), CCL7 (250 ng/mL; 22 nM), or CCL3 (100 ng/mL; 9.9 nM) alone or combined.

We then investigated the downstream pathways of CCR5. We found that neither eNAMPT co-treatment nor pretreatment was able to interfere with Rantes-mediated ERK activation, while, as expected, this pathway was antagonized by maraviroc (Figure S2). On the contrary, eNAMPT was able to antagonize CCR5-mediated phosphorylation of PKC induced by Rantes and CCL3 in Hela-CCR5 cells. As shown in Figure 3C, the known antagonist CCL7, eNAMPT and, as expected, CCL3 and Rantes all induced PKC phosphorylation. On the other hand, pretreatment of eNAMPT prevented both PKC activation induced by Rantes and CCL3, similarly to CCL7 (Figure 3C). All this evidence suggested that eNAMPT might act as an antagonist on some of the effects mediated by CCR5, probably in a time-dependent manner.

Observing the antagonistic effect of eNAMPT on PKC activation mediated by DAG, we next tested whether eNAMPT was able to modulate CCR5-mediated calcium signaling. In accordance with our hypothesis, preincubation with eNAMPT (500 ng/mL = 9 nM) reduced significantly Rantes-induced cytosolic Ca^{2+}-rises as determined by the area under the curve (AUC) of the Ca^{2+}-rise or the percentage of responding cells (Figure 4A). The effect of eNAMPT was quantitatively similar to that of maraviroc (Figure 4A). It is important to stress that the effect of eNAMPT could not be mimicked by the buffer in which the protein was dissolved, or by proteins isolated in the same manner, such as NMNAT and ADH, at identical concentrations (Figure S3). To evaluate whether the effect of eNAMPT on calcium signaling was specific for CCR5, we evaluated its effect on Ca^{2+} signaling induced by ATP or carbachol

(CCh), whose receptors are present both in HeLa-SCR and in HeLa-CCR5 cells. As it can be observed in Figure 4B,C, eNAMPT (500 ng/mL = 9 nM) did not affect the calcium responses to ATP or CCh in either HeLa-SCR or HeLa-CCR5 cells. All this data suggests that eNAMPT selectively antagonizes Rantes-dependent calcium signaling. Very recently, Sayers et al., demonstrated a modulation of calcium release mediated by eNAMPT, which, as a dimer, increased glucose-stimulated intracellular calcium levels [23]. In this respect, in our model we were unable to appreciate any effect of eNAMPT alone at the concentrations tested (500–1000 ng/mL = 9–18 nM).

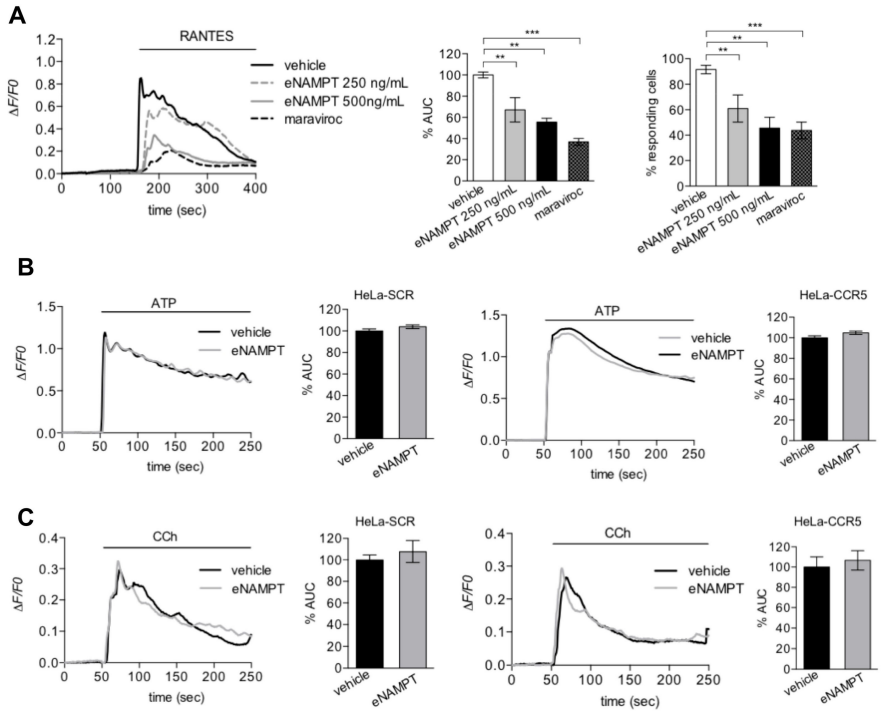

Figure 4. eNAMPT inhibits Rantes-induced cytosolic Ca2+-signals. (**A**) Representative calcium traces of HeLa-CCR5 loaded with FURA-2AM and treated with vehicle, eNAMPT (250 ng/mL; 4.5 nM or 500 ng/mL = 9 nM), or maraviroc (10 μM) 100 s before the addition of 25 ng/mL (3 nM) of Rantes. Histograms of responding cells (middle panel) and percentage of Area Under the Curve (AUC)(right panel) as mean ± S.E.M. (248–410 cells from 6–11 independent experiments). (**B**,**C**) Representative calcium traces and percentage of AUC of HeLa-SCR and HeLa-CCR5 loaded with FURA-2AM and treated with 3 μM of ATP (**B**) or 300 μM of CCh (**C**) alone or pretreated with eNAMPT (500 ng/mL = 9 nM) for 5 min. The data are summarized in histograms and expressed as mean ± S.E.M of 120–190 cells (from 5–9 independent experiments) and 105–185 cells (from 5–9 independent experiments), respectively. ** $p < 0.01$ *** $p < 0.001$.

3.3. eNAMPT Modulation of Rantes-Mediated Calcium Signaling is Independent on Its Enzymatic Activity

To test if the reduction of Rantes-dependent calcium mobilization by eNAMPT was mediated by its enzymatic activity, we investigated the effect of a mutated and enzymatically inactive form of eNAMPT (H247E; [24]). The preincubation with eNAMPT H247E (500 ng/mL; 9 nM) reduced the calcium mobilization induced by Rantes in the same manner to the WT enzyme (Figure 5A). In support of this, preincubation with nicotinamide mononucleotide (NMN), the product of eNAMPT, was devoid of any effect on calcium mobilization induced by Rantes (Figure 5B).

These data suggest that the reduction in calcium signaling by eNAMPT is mediated by the physical interaction with CCR5 and that the enzymatic activity is dispensable.

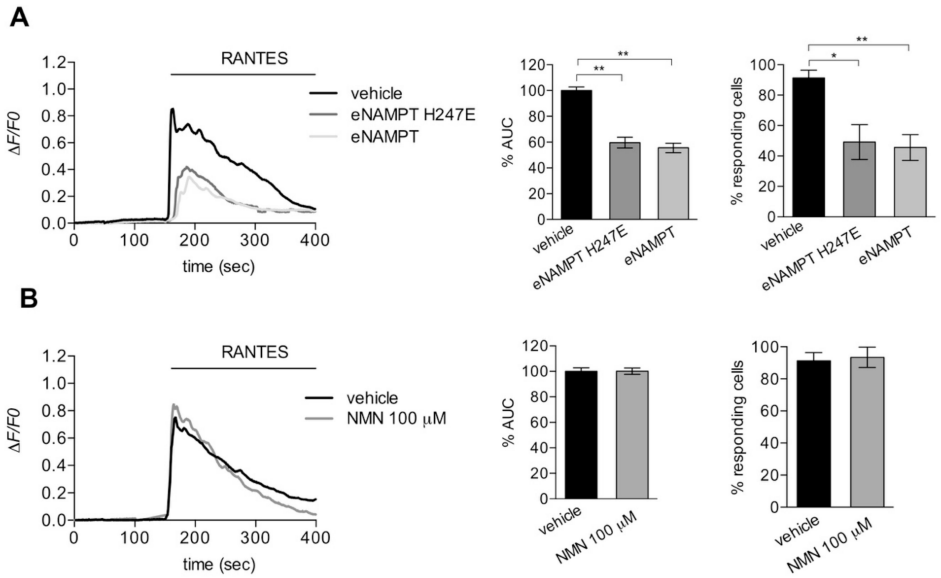

Figure 5. The catalytic activity of eNAMPT is dispensable for CCR5 antagonism. (**A**) Left, representative calcium traces of HeLa-CCR5 loaded with FURA-2AM and treated with RANTES (25 ng/mL; 3 nM) alone or pretreated with eNAMPT/eNAMPT H247E (500 ng/mL; 9 nM) for 100 s. Right, histograms of percentage of AUC (middle panel) and responding cells (right panel) as mean ± S.E.M. (180–210 cells from four independent experiments). (**B**) Left, representative calcium traces of HeLa-CCR5 loaded with FURA-2AM and pretreated for 100 s with vehicle or NMN (100 μM) before the addition of Rantes (25 ng/mL = 3 nM). Histograms of percentage of AUC (right panel) and responding cells (left panel) as mean ± S.E.M. (99–126 cells from three independent experiments). * $p < 0.05$, ** $p < 0.01$.

3.4. eNAMPT Modulates Rantes-Mediated Calcium Signaling and Migration in Melanoma Cells

We next investigated whether the interaction between CCR5 signaling and eNAMPT could be evaluated also in a system in which CCR5 was present endogenously. In this respect, we chose a murine melanoma cell line, B16, in which we have previously shown an effect of eNAMPT [6] and which expresses CCR5 (Figure 6A). In this system, Rantes was, as expected, able to induce a Ca^{2+}-response, albeit very small compared to HeLa-CCR5, that was blunted by the incubation with eNAMPT (Figure 6B,C).

Given that Rantes has been shown to promote migration, a Ca^{2+}-dependent phenomenon, in melanoma cells [25], we next decided to investigate this via the wound-healing assay. Rantes, at a concentration of 100 ng/mL (12 nM) promoted wound closure after 24 h compared to control, in analogy to CCL3 (100 ng/mL = 9.9 nM). eNAMPT (500 ng/mL = 9 nM) per se had a small not significant effect on the migration of these cells. When eNAMPT was combined with Rantes or CCL3, it antagonized their effects on migration in the same way as maraviroc or the antagonist CCL7 (Figure 6D).

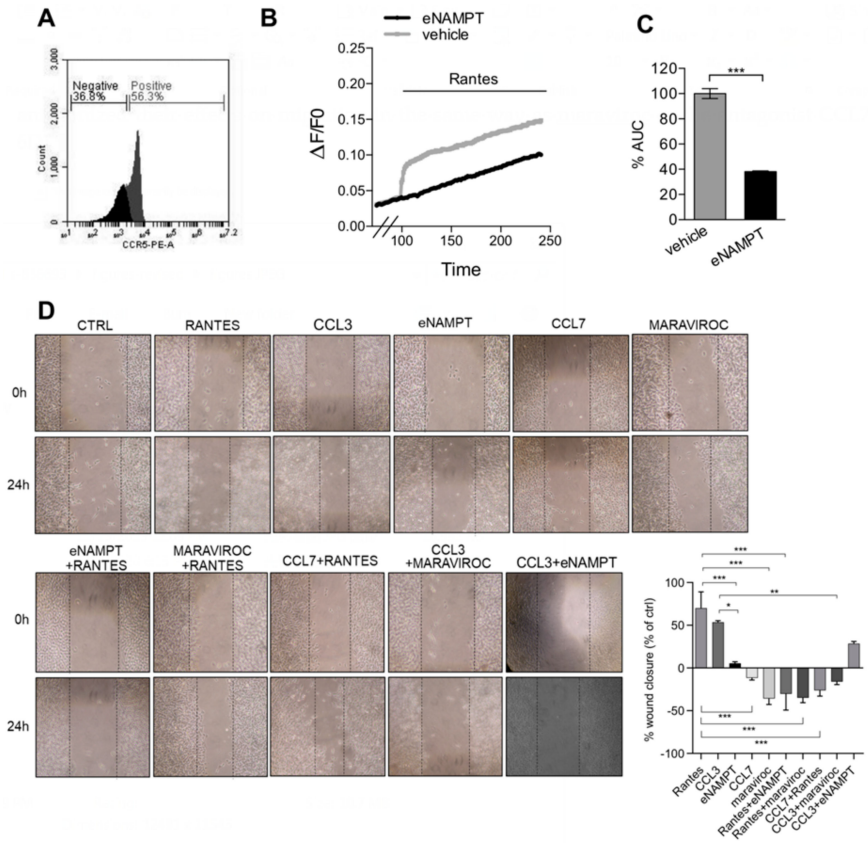

Figure 6. eNAMPT antagonizes the CCR5-mediated migration of B16 melanoma cells. (**A**) CCR5 expression in B16 cells stained with anti-mouse CCR5-PE and analyzed by flow cytometry. (**B**,**C**) AUC and percentage of responding cells of B16 cells loaded with FURA-2AM and pretreated with eNAMPT (500 ng/mL; 9 nM) for 100 s before the addition of RANTES (100 ng/mL; 12 nM) at 100 s. Mean ± S.E.M. of 180–210 cells from four independent experiments. (**D**) Left, representative wound healing images of B16 cells treated with vehicle, Rantes (100 ng/mL; 12 nM), eNAMPT (500 ng/mL; 9 nM) and/or maraviroc (10 μM), and/or CCL7 (250 ng/mL; 22 nM) and CCL3 (100 ng/mL; 9.9 nM) at time 0 and after 24 h of treatment. Right, percentage of wound closure (compared to % of the control) after 24 h of treatment. Mean ± S.E.M. of six determinations from two separate experiments. * $p < 0.05$, ** $p < 0.01$, *** $p < 0.001$.

4. Discussion

The aim of the present work was to characterize the biological significance of the interaction between eNAMPT and CCR5 in cancer cells. In the present contribution, we show that (i) eNAMPT competes with Rantes for fluorescent binding in CCR5 overexpressing cells; (ii) eNAMPT, unlike Rantes, is unable to activate either the ERK or Ca^{2+}-signaling pathways; (iii) pretreatment with eNAMPT results in the inhibition of CCR5 internalization and PKC activation, but not of ERK phosphorylation; (iv) eNAMPT antagonizes Rantes-dependent calcium signaling; (v) the effects of eNAMPT can be reproduced by eNAMPT H247E, the enzyme-dead mutant protein; and (vi) the effect on Ca^{2+}-signaling is observable also in a melanoma cell line (B16) expressing endogenous levels of CCR5 and this most likely is linked to an inhibition of Rantes-induced migration by eNAMPT. Overall, therefore, we take our results to demonstrate that eNAMPT is an antagonist of some of the signaling cascades of CCR5.

On the other hand, eNAMPT has been shown in cell cultures to elicit effects that cannot be reconducted to inhibition of CCR5. For example, it activates STAT3, NF-κB, Akt, and p38 in the absence

of CCR5 ligands [6,11]. It is therefore unlikely that CCR5 is the only plasma membrane receptor for eNAMPT. Indeed, two separate papers have now proven that eNAMPT is an agonist of the TLR4 receptor [10,11]. Furthermore, in the present manuscript, we solely looked at the interaction between eNAMPT and CCR5, as a binding K_D had already been ascertained [8], but we cannot exclude an involvement of other chemokine receptors in eNAMPT pathways.

To add to the complexity, it has been recently demonstrated that the effects on pancreatic beta cell functional mass of eNAMPT are bimodal and concentration and structure functionally dependent [23]. In our study, we used concentrations between 250 and 1000 ng/mL (corresponding to 4.5–18 nM), with the only exception of internalization and cell labelling experiments, in which higher concentrations were used to counteract the higher concentrations used of RANTES (in the second instance, RANTES induces rapid internalization only at high concentrations, while in the first instance RANTES-PE binding could be appreciated only at higher concentrations). It is possible, therefore that at lower concentrations or higher concentrations than those tested in the present study eNAMPT interacts and engages with other receptors. In the aforementioned study, part of the concentration-dependence was attributed to a different effect of the monomer (enzymatically inactive), compared to the dimer. Given that monomeric mutants exist, it is likely that wider concentration-response curves should be performed to disclose bimodal actions and that both wild-type and mutant monomers should be employed.

It is interesting that a natural antagonist of CCR5, CCL7 [26], like eNAMPT, also abolishes CCR5-dependent calcium signaling and cell migration. Surprisingly, *in silico* analysis using PyMol and Uniprot software reveals a common structure conformation and conserved sequence between eNAMPT and CCL7. As shown in Figure S4A, the Pymol analysis of the NAMPT (cyano) and CCL7 (orange) structures showed a high homology. Specifically, CCL7 random coil (highlighted by the red square), which is used by the protein to bind to CCR5, is superimposable with a portion of NAMPT structure (amino acids 420–430). Moreover, the chemical-physical features of the amino acids of this portion are comparable to the steric hindrance of CCL7 in the same region (Figure S4B). Given that CCL7 has been shown to be a promiscuous ligand, which alongside being a CCR5 antagonist is also an agonist of CCR1, CCR2, and CCR3, these receptors should be evaluated in the future to understand whether the effects of eNAMPT are the result of multiple interactions with a diverse array of receptors.

Supplementary Materials: The following are available online (Figures S1–S4) http://www.mdpi.com/2073-4409/9/2/496/s1. Figure S1. Immunofluorescence of CCR5 localization in Hela-CCR5: cells were treated with vehicle, Rantes (100 ng/mL = 9 nM) and/or eNAMPT (2.5 μg/mL = 45 nM) for 60 min at 37 or 4 °C. Then, cells were fixed in 4% formaldehyde and stained with an anti-mouse CCR5-PE and DRAQ5 (nuclear staining). Figure S2. (**A**) Representative Western blot and densitometry analysis of phosphorylated ERK after 2 h of starvation followed by cotreatment for 5 min with recombinant RANTES (25 ng/mL = 3 nM) in the presence of eNAMPT (500 ng/mL = 9 nM) or maraviroc (10 μM) or vehicle in serum-free conditions. Data from four separate experiments. (**B**) Representative Western blot and densitometry analysis of phosphorylated ERK after 2 h of starvation followed by pretreatment for 45 min with recombinant eNAMPT (500 ng/mL = 9 nM) or maraviroc (10 μM) or vehicle followed by treatment for 5 min with RANTES (25 ng/mL = 3 nM) in serum-free conditions. Data from three separate experiments. Figure S3. (**A**) Calcium release in HeLa-CCR5 loaded with FURA-2AM and treated with vehicle, eNAMPT (500 ng/mL) or ADH (500 ng/mL) or for 100 s before the addition of 25 ng/mL of Rantes. Histograms of responding cells. (**B**) Calcium release in HeLa-CCR5 loaded with FURA-2AM and treated with vehicle, eNAMPT (500 ng/mL), H247E eNAMPT (500 ng/mL), or NMNAT2 (500 ng/mL) for 100 s before the addition of 25 ng/mL of Rantes. Histograms of responding cells. Figure S4. (**A**) PyMol and Uniprot analysis of NAMPT (cyano) and CCL7 (orange). CCL7 random coil, which is used by the protein to bind to CCR5, is highlighted by the red square and is superimposable with a portion of NAMPT structure (amino acids 420–430). (**B**) Scheme of Rantes, CCL7, and eNAMPT signaling.

Author Contributions: S.T. and G.C. performed all experiments and contributed equally. C.T. and A.A.G. (Ambra A. Grolla) designed and supervised all biological experiments and wrote the manuscript. S.B. significantly contributed to the revision of the paper. D.L. supervised the calcium signaling experiments. A.A.G. (Armando A. Genazzani) co-supervised the project, provided funding, and wrote the manuscript. All authors have read and agreed to the published version of the manuscript.

Funding: This work was partly supported by grants from the Associazione Italiana per la Ricerca sul Cancro (AIRC: IG10509; IG2018 21842; 14832) to ArmAG and CT and from a grant from the Fondazione San Paolo to ArmAG. We thank Fondazione Umberto Veronesi (CT and AmbAG).

Acknowledgments: We wish to thank Silvia Garavaglia for technical help with protein production and purification, Locati and Benedetta Savino for advice on CCR5 biology, and Riccardo Miggiano for the *in silico* model presented in the supplementary material.

Conflicts of Interest: The authors declare no conflict of interest.

Abbreviations

eNAMPT	extracellular nicotinamide phosphoribosyltransferase
CCR5	C-C chemokine receptor type 5
Nam	nicotinamide
ATP	adenosine triphosphate
PRPP	phosphoribosyl pyrophosphate
NMN	nicotinamide mononucleotide
TLR4	Toll-like receptor 4
CCL5	Chemokine (C-C motif) ligand 5
CCL7	Chemokine (C-C motif) ligand 7
CCL3	Chemokine (C-C motif) ligand 3
GPCR	G-protein coupled receptor

References

1. Imai, S.-I. The NAD World 2.0: The importance of the inter-tissue communication mediated by NAMPT/NAD+/SIRT1 in mammalian aging and longevity control. *NPJ Syst. Biol. Appl.* **2016**, *2*, 16018. [CrossRef] [PubMed]
2. Carbone, F.; Liberale, L.; Bonaventura, A.; Vecchiè, A.; Casula, M.; Cea, M.; Monacelli, F.; Caffa, I.; Bruzzone, S.; Montecucco, F.; et al. Regulation and Function of Extracellular Nicotinamide Phosphoribosyltransferase/Visfatin. In *Comprehensive Physiology*; American Cancer Society: Atlanta, GA, USA, 2017; ISBN 978-0-470-65071-4.
3. Grolla, A.A.; Travelli, C.; Genazzani, A.A.; Sethi, J.K. Extracellular nicotinamide phosphoribosyltransferase, a new cancer metabokine. *Br. J. Pharmacol.* **2016**, *173*, 2182–2194. [CrossRef]
4. Maldi, E.; Travelli, C.; Caldarelli, A.; Agazzone, N.; Cintura, S.; Galli, U.; Scatolini, M.; Ostano, P.; Miglino, B.; Chiorino, G.; et al. Nicotinamide phosphoribosyltransferase (NAMPT) is over-expressed in melanoma lesions. *Pigment. Cell Melanoma Res.* **2013**, *26*, 144–146. [CrossRef] [PubMed]
5. Zhu, Y.; Guo, M.; Zhang, L.; Xu, T.; Wang, L.; Xu, G. Biomarker triplet NAMPT/VEGF/HER2 as a de novo detection panel for the diagnosis and prognosis of human breast cancer. *Oncol. Rep.* **2016**, *35*, 454–462. [CrossRef] [PubMed]
6. Grolla, A.A.; Torretta, S.; Gnemmi, I.; Amoruso, A.; Orsomando, G.; Gatti, M.; Caldarelli, A.; Lim, D.; Penengo, L.; Brunelleschi, S.; et al. Nicotinamide phosphoribosyltransferase (NAMPT/PBEF/visfatin) is a tumoural cytokine released from melanoma. *Pigment. Cell Melanoma Res.* **2015**, *28*, 718–729. [CrossRef] [PubMed]
7. Soncini, D.; Caffa, I.; Zoppoli, G.; Cea, M.; Cagnetta, A.; Passalacqua, M.; Mastracci, L.; Boero, S.; Montecucco, F.; Sociali, G.; et al. Nicotinamide phosphoribosyltransferase promotes epithelial-to-mesenchymal transition as a soluble factor independent of its enzymatic activity. *J. Biol. Chem.* **2014**, *289*, 34189–34204. [CrossRef]
8. Yoshida, M.; Satoh, A.; Lin, J.B.; Mills, K.F.; Sasaki, Y.; Rensing, N.; Wong, M.; Apte, R.S.; Imai, S.-I. Extracellular Vesicle-Contained eNAMPT Delays Aging and Extends Lifespan in Mice. *Cell Metab.* **2019**, *30*, 329–342. [CrossRef]
9. Fukuhara, A.; Matsuda, M.; Nishizawa, M.; Segawa, K.; Tanaka, M.; Kishimoto, K.; Matsuki, Y.; Murakami, M.; Ichisaka, T.; Murakami, H.; et al. Retraction. *Science* **2007**, *318*, 565. [CrossRef]
10. Camp, S.M.; Ceco, E.; Evenoski, C.L.; Danilov, S.M.; Zhou, T.; Chiang, E.T.; Moreno-Vinasco, L.; Mapes, B.; Zhao, J.; Gursoy, G.; et al. Unique Toll-Like Receptor 4 Activation by NAMPT/PBEF Induces NFκB Signaling and Inflammatory Lung Injury. *Sci. Rep.* **2015**, *5*. [CrossRef]

11. Managò, A.; Audrito, V.; Mazzola, F.; Sorci, L.; Gaudino, F.; Gizzi, K.; Vitale, N.; Incarnato, D.; Minazzato, G.; Ianniello, A.; et al. Extracellular nicotinate phosphoribosyltransferase binds Toll like receptor 4 and mediates inflammation. *Nat. Commun.* **2019**, *10*, 4116. [CrossRef]
12. Van den Bergh, R.; Morin, S.; Sass, H.J.; Grzesiek, S.; Vekemans, M.; Florence, E.; Thanh Thi Tran, H.; Imiru, R.G.; Heyndrickx, L.; Vanham, G.; et al. Monocytes Contribute to Differential Immune Pressure on R5 versus X4 HIV through the Adipocytokine Visfatin/NAMPT. *PLoS ONE* **2012**, *7*, e35074. [CrossRef] [PubMed]
13. Blanpain, C.; Libert, F.; Vassart, G.; Parmentier, M. CCR5 and HIV infection. *Recept. Channels* **2002**, *8*, 19–31. [CrossRef] [PubMed]
14. Zhang, W.; Canziani, G.; Plugariu, C.; Wyatt, R.; Sodroski, J.; Sweet, R.; Kwong, P.; Hendrickson, W.; Chaiken, I. Conformational changes of gp120 in epitopes near the CCR5 binding site are induced by CD4 and a CD4 miniprotein mimetic. *Biochemistry* **1999**, *38*, 9405–9416. [CrossRef] [PubMed]
15. Blanpain, C.; Migeotte, I.; Lee, B.; Vakili, J.; Doranz, B.J.; Govaerts, C.; Vassart, G.; Doms, R.W.; Parmentier, M. CCR5 binds multiple CC-chemokines: MCP-3 acts as a natural antagonist. *Blood* **1999**, *94*, 1899–1905. [CrossRef] [PubMed]
16. Haqqani, A.A.; Tilton, J.C. Entry inhibitors and their use in the treatment of HIV-1 infection. *Antivir. Res.* **2013**, *98*, 158–170. [CrossRef]
17. Weitzenfeld, P.; Ben-Baruch, A. The chemokine system, and its CCR5 and CXCR4 receptors, as potential targets for personalized therapy in cancer. *Cancer Lett.* **2014**, *352*, 36–53. [CrossRef]
18. Zhang, Y.; Lv, D.; Kim, H.-J.; Kurt, R.A.; Bu, W.; Li, Y.; Ma, X. A novel role of hematopoietic CCL5 in promoting triple-negative mammary tumor progression by regulating generation of myeloid-derived suppressor cells. *Cell Res.* **2013**, *23*, 394–408. [CrossRef]
19. van Deventer, H.W.; O'Connor, W.; Brickey, W.J.; Aris, R.M.; Ting, J.P.Y.; Serody, J.S. C-C chemokine receptor 5 on stromal cells promotes pulmonary metastasis. *Cancer Res.* **2005**, *65*, 3374–3379. [CrossRef]
20. Aldinucci, D.; Colombatti, A. The inflammatory chemokine CCL5 and cancer progression. *Mediators Inflamm.* **2014**, *2014*, 292376. [CrossRef]
21. Baek, J.M.; Ahn, S.-J.; Cheon, Y.-H.; Lee, M.S.; Oh, J.; Kim, J.-Y. Nicotinamide phosphoribosyltransferase inhibits receptor activator of nuclear factor-κB ligand-induced osteoclast differentiation in vitro. *Mol. Med. Rep.* **2017**, *15*, 784–792. [CrossRef] [PubMed]
22. Bannert, N.; Craig, S.; Farzan, M.; Sogah, D.; Santo, N.V.; Choe, H.; Sodroski, J. Sialylated O-glycans and sulfated tyrosines in the NH2-terminal domain of CC chemokine receptor 5 contribute to high affinity binding of chemokines. *J. Exp. Med.* **2001**, *194*, 1661–1673. [CrossRef] [PubMed]
23. Sayers, S.R.; Beavil, R.L.; Fine, N.H.F.; Huang, G.C.; Choudhary, P.; Pacholarz, K.J.; Barran, P.E.; Butterworth, S.; Mills, C.E.; Cruickshank, J.K.; et al. Structure-functional changes in eNAMPT at high concentrations mediate mouse and human beta cell dysfunction in type 2 diabetes. *Diabetologia* **2020**, *63*, 313–323. [CrossRef] [PubMed]
24. Burgos, E.S.; Ho, M.-C.; Almo, S.C.; Schramm, V.L. A phosphoenzyme mimic, overlapping catalytic sites and reaction coordinate motion for human NAMPT. *Proc. Natl. Acad. Sci. USA* **2009**, *106*, 13748–13753. [CrossRef] [PubMed]
25. Payne, A.S.; Cornelius, L.A. The role of chemokines in melanoma tumor growth and metastasis. *J. Invest. Dermatol.* **2002**, *118*, 915–922. [CrossRef]
26. Rollins, B.J. Chemokines. *Blood* **1997**, *90*, 909–928. [CrossRef]

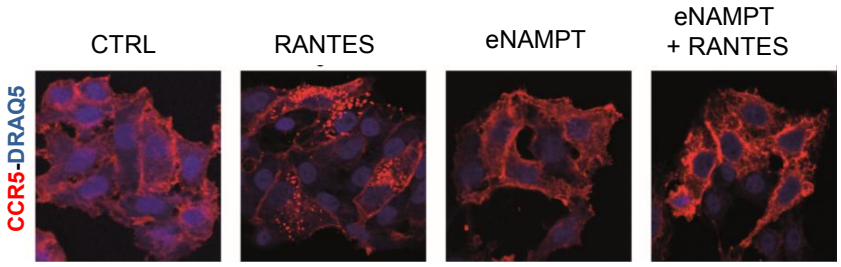

Supplementary Figure S1. Immunofluorescence of CCR5 localization in Hela-CCR5: cells were treated with vehicle, Rantes (100 ng/ml = 9 nM) and/or eNAMPT (2.5 µg/ml = 45 nM) for 60 minutes at 37°C or 4°C. Then, cells were fixed in 4% formaldehyde and stained with an anti-mouse CCR5-PE and DRAQ5 (nuclear staining).

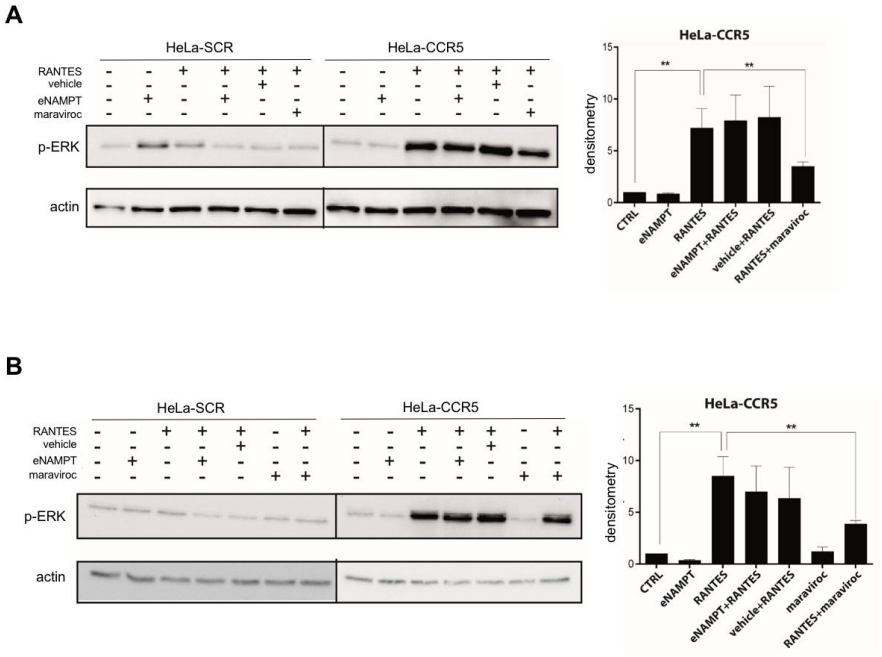

Supplementary Figure S2. (**A**) Representative Western blot and densitometry analysis of phosphorylated ERK after 2 hours of starvation followed by co-treatment for 5 minutes with recombinant RANTES (25 ng/mL = 3 nM) in the presence of eNAMPT (500 ng/mL = 9 nM) or maraviroc (10 μM) or vehicle in serum-free conditions. Data from 4 separate experiments. (**B**) Representative Western blot and densitometry analysis of phosphorylated ERK after 2 hours of starvation followed by pre-treatment for 45 minutes with recombinant eNAMPT (500 ng/mL = 9 nM) or maraviroc (10 μM) or vehicle followed by treatment for 5 minutes with RANTES (25 ng/mL = 3 nM) in serum-free conditions. Data from 3 separate experiments.

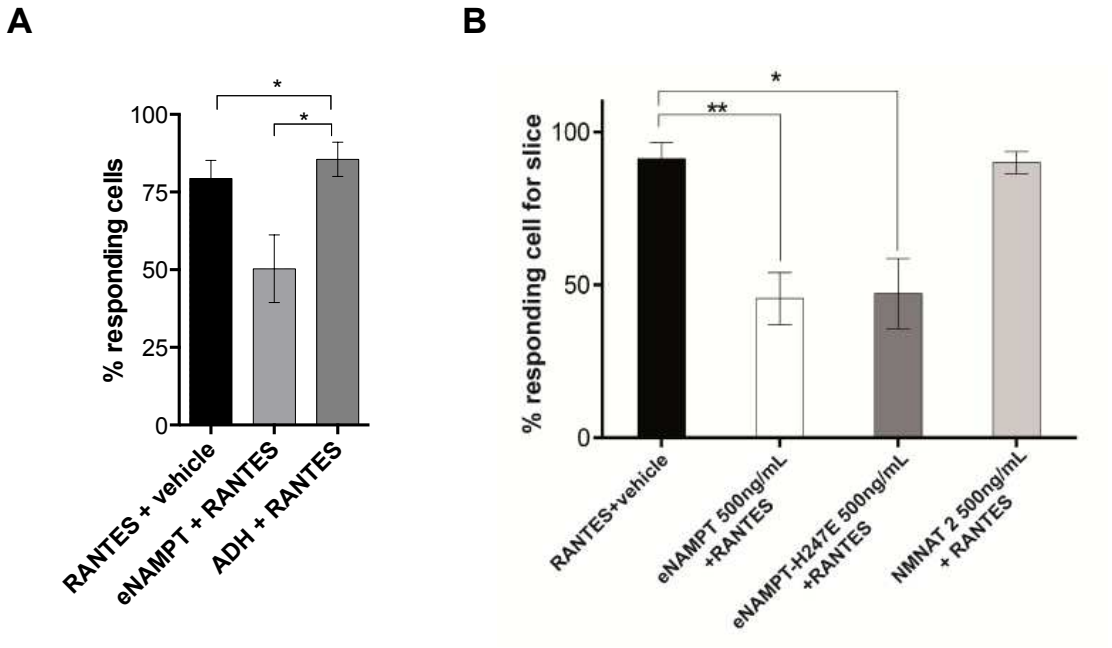

Supplementary Figure S3 (**A**) Calcium release in HeLa-CCR5 loaded with FURA-2AM and treated with vehicle, eNAMPT (500 ng/ml) or ADH (500 ng/mL) or for 100 sec before the addition of 25 ng/ml of Rantes. Histograms of responding cells. (**B**) Calcium release in HeLa-CCR5 loaded with FURA-2AM and treated with vehicle, eNAMPT (500 ng/ml), H247E eNAMPT (500 ng/mL) or NMNAT2 (500 ng/mL) for 100 sec before the addition of 25 ng/ml of Rantes. Histograms of responding cells.

A

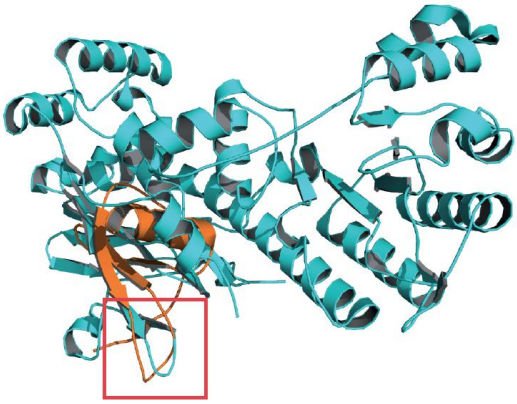

B

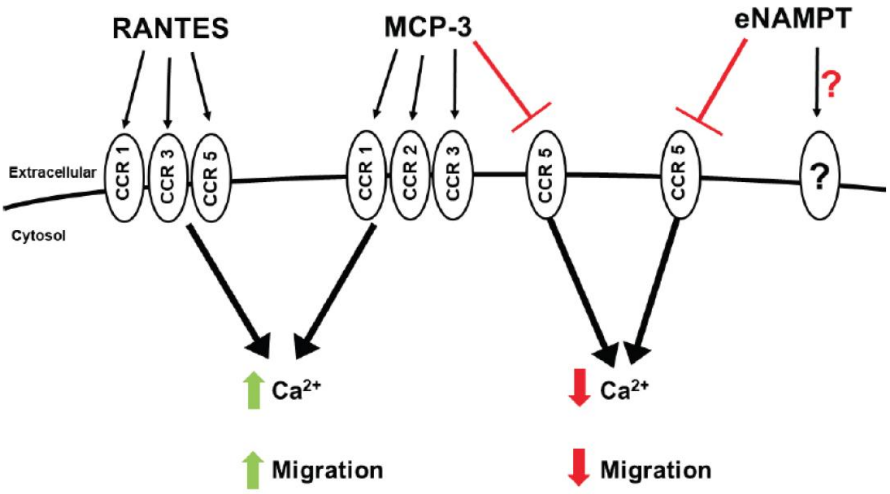

Supplementary Figure S4. (**A**) PyMol and Uniprot analysis of NAMPT (cyano) and CCL7 (orange). CCL7 random coil, which is used by the protein to bind to CCR5, is highlighted by the red square and is superimposable with a portion of NAMPT structure (amino acids 420-430). (**B**) Scheme of Rantes, CCL7 and eNAMPT signalling.

Chapter 5

Extracellular Nicotinamide Phosphoribosyltransferase (eNAMPT)-priming of murine peritoneal exudate cells (PECs) boosts interferon-γ (IFNγ)-induced proinflammatory response (UNPUBLISHED RESULTS)

Giorgia Colombo[1], Armando A. Genazzani[1], Chiara Porta[1], Cristina Travelli[2*]

[1] Department of Pharmaceutical Sciences, University of Eastern Piedmont, A. Avogadro, Novara, 28100, Italy.

[2] Department of Pharmaceutical Sciences, Università degli Studi di Pavia, Pavia, 27100, Italy.

*Corresponding author.

Author contributions: The study was designed by G.C., C.T. and C.P.
G.C. did the experiments and data analysis. C.T., C.P., G.C., and A.A.G. wrote the manuscript.

INTRODUCTION

Macrophages are the orchestrator of innate and adaptive immune response and are present in all the tissues, maintaining physiological homeostasis and defeating pathogens [1]. Plasticity is the typical characteristic of monocyte/macrophages, displaying plenty of biological process, determined by different physiologic and pathologic microenvironmental signals (*e.g.* microbial products, endogenous alarmins, metabolites, ROS). M1 and M2 dichotomy is used to better define macrophage polarized activation *in vitro* [2]. Classical or M1 activation occurs in front of inflammatory cytokines produced by Th-1 lymphocytes (*e.g*. IFN-γ, TNF-α) as well as by engagement of Pattern Recognition Receptors (PRRs) by microbial products (*e.g*. lipopolysaccharide, lipoteichoic acid) or endogenous alarmins (*e.g.* High Mobility Group Box 1, Heat Shock Proteins, adenosine triphosphate, Fetuin A) [3]. M1 macrophages can kill pathogens (bacteria, virus and protozoa) and tumour cells, but also induce tissue destructive reactions [4]. M1-activated macrophages produce several pro-inflammatory cytokines (*e.g.* TNFα, IL1β, IL-6) and cytotoxic molecules (ROS, NOS) to kill pathogens [5].

On the contrary, Th-2 cytokines (*e.g.* IL-4, IL-13), immune complexes and anti-inflammatory molecules (IL-10, glucocorticoids, adenosine monophosphate) prompt alternative M2 polarization, with immune-regulatory functions and resolutory ability [6].

Of note, IFN-γ is known to skew macrophages to a proinflammatory phenotype. IFN-γ is secreted by natural killer cells, T cells, and antigen presenting cells. In macrophages, IFN-γ role is to activate microbicidal functions through the induction of NADPH oxidase and inducible NO synthase, eliminating bacteria, viruses, parasites, and fungi [7].

Intracellular nicotinamide phosphoribosyltransferase (iNAMPT) has received significant attention over the years as it represents the cytosolic rate-limiting enzyme

of the NAD salvage-pathway in mammals and catalyses the synthesis of nicotinamide mononucleotide (NMN) from nicotinamide (NAM, vitamin B3 or PP) and 5-phosphoribosylpyrophosphate (PRPP) [8]. NAMPT has also been shown to be a secreted protein. Indeed, it is now well established that extracellular NAMPT (eNAMPT) is identical to Pre-B cell enhancing factor (PBEF), first described for its ability to synergize with IL-7 and stem cell factor, increasing the number of pre-B cell colonies, and to visfatin, a cytokine released from adipose tissue [9,10]. How eNAMPT exerts its extracellular functions has not been fully elucidated [11]. Van der Bergh et al. proposed a direct binding to CCR5 through which eNAMPT prevents HIV R5 strain infection in macrophages and PBMCs *in vitro* and we have confirmed that it may have an antagonistic role on this receptor [12], but data that shows TLR4 activation as the primary mechanism of action at present appears now more robust. In contrast, a second line of thought hypothesizes that the enzymatic activity is important [13], and it has been recently shown that a significant amount of eNAMPT is found in microvesicles [14]. What is known is that eNAMPT could be a mediator of some macrophage-related activity, as a pro-inflammatory stimulus [15]. Moreover, we have recently generated a monoclonal antibody against eNAMPT (C269) that has a neutralization potential against eNAMPT [16].

In the present manuscript, we deeper investigate eNAMPT role on peritoneal macrophages (PECs) and, in particular, its priming activity on IFNγ-stimulus.

MATERIALS and METHODS

Isolation of murine peritoneal macrophages. C57BL/6 male 8-weeks-old mice were injected in the peritoneal cavity with 1 ml of 3% Brewer thioglycolate medium. After 5 days, the mice were euthanized. After retracting the abdominal skin, exposing the peritoneal wall, 5 ml of sterile PBS was injected closed to abdominal adipose tissue. The liquid in the peritoneal cavity was shaking, aspirated with the syringe closed to sternum and collected for macrophages purification.
2 or 3x 10^6 cells peritoneal exudate cells (PEC) were plated in RPMI-FBS free Medium (RPMI, with 10 U/ml Penicillin, 100µg/ml streptomycin and 1% L-glutamine, Merck Life Science) within an hour. After 1h, the non-macrophages cells were washed away twice with PBS, compete RPMI-medium (RPMI with addition of 10% of FBS, Gibco, Thermo Fisher Scientific) was added, macrophages were laid at 37°C for at least 1 h and then treated (see below).

Treatments. Production, purification and characterization of control IgG1 (10 µg/ml), C269 (10 µg/ml) and recombinant NAMPT (rNAMPT, 500ng/ml) are described further on. PECs were also treated with LPS (100 ng/ml lipopolysaccharides from Escherichia coli O111:B4, Sigma, Cat. No. L2630) IFNγ (Peprotech, 200 U/ml) and IL-4 (Peprotech, 20 ng/ml).

Recombinant murine eNAMPT purification. Wild-type murine full-length NAMPT (ORF GenBank BC018358) was cloned in pET28a (NdeI/EcoRI) and expressed in ClearColi BL21(D3) (induction with IPTG 0.5 mM for 3 h at 21°C) and purified by His-tag affinity chromatography with NiNTA Superflow resin (Qiagen). Endotoxin levels were assessed with ToxinSensor Chromogenic LAL Endotoxin Assay kit (GeneScript). Only preparations with less than 0.1EU/ml endotoxin levels were utilized. NAMPT activity was tested accordingly [17].

Anti-eNAMPT antibody production and purification. All the procedures are described in [16]. 12 Hybridoma cell lines producing 12 different anti-eNAMPT antibodies were acquired by AbMart service.

Measurement of eNAMPT levels in cell medium. For eNAMPT measurement, 3x 10^6 cells were plated in 6-well plates. Cells were incubated in serum-free conditions, with or without treatments, until 48 hours, and the conditioned medium was collected. This was then concentrated with 30 kDa cut-off filters (VIVASPIN500 Sartorius, Germany) till 50µl and then analysed by Western blotting. Experiments were conducted in serum-free conditions because of the possible presence of eNAMPT in FBS or an artefact of immunoglobulins signal. In parallel, some no-concentrated samples were analysed for eNAMPT concentrations using a commercially available sandwich enzyme-linked immunosorbent assay for human or murine NAMPT (ELISA kit from AdipoGen Inc; Seoul Korea) with overlapping results.

Gene expression analysis. Cells were lysated with Trizol reagent (Life-technologies) using a scraper and extracted with chloroform. 1µg mRNA was reverse transcripted with SENSIFAST kit as manufacturer's protocol (Aurogene) and cDNA expression determined with qPCR using SYBR-green (Bio-Rad) and identified with CFX96 Real-Time System (Biorad). Expression data were normalized to actin expression. The sequences of gene-specific primers are reported in Supplementary Table I.

RNA sequencing and Data Analysis. Libraries were generated from total RNA of PECs treated (4 h) with, rNAMPT (500 ng/ml) or IFNγ (Peprotech, 200 U/ml). RNA was extracted using SPLIT RNA Extraction Kit (Lexogen, Vienna, Austria). Total RNA quality was evaluated using the Agilent 2100 Bioanalyzer System. Extracted

RNA samples were processed using the QuantSeq 3′ mRNA-Seq Library Prep Kit (Lexogen, Vienna, Austria) and sequenced on an Illumina NextSeq 500. Read counts were normalized for effective library size, and differentially expressed genes (DEGs) were analysed using DESeq2.21 DEGs were identified by a P value of <0.05 and an absolute fold change of >0.5.

The functional analysis of the identified differentially expressed genes was performed with DAVID v6.8 and Panther Classification System v12.0 by uploading all the genes highlighted. PPI networks were created using STRING v10.5 by uploading all the genes and excluding disconnected nodes from the resultant network. Venn diagrams were designed using Venny free on-line tools (http://bioinfogp.cnb.csic.es/tools/venny/) to picture intersections between class comparison results and to select the genes of interest.

Wound-Healing Assay. 3x 10^6 cells were plated in 6-well plates. We performed a cross-shaped scratch with tip. Then, the cells were washed twice with PBS to remove residual cell debris. Cells were then incubated with the treatments for 24 h and 48 h and pictures of a defined wound spot were made at different time points. The area of the wound in the microscopic pictures was measured and analysed using Image J software (National Institutes of Health, MD, USA).

Western Blot analysis. PECs were lysed in Lysis Buffer (20 mM HEPES, 100 mM NaCl, 5 mM EDTA, 1% Nonidet-P40+ Protease & Phosphatase Inhibitor Cocktail, Sigma). Proteins quantification was performed with Bradford Protein Assay (Sigma), and proteins were resolved on SDS–PAGE and transferred with TurboBlot system (BioRad, Hemel Hempstead, UK).

Statistics. Data are presented as mean ± SEM or Median and IQR. The normality of data distributions was evaluated using Shapiro–Wilk test. Parametric (unpaired t-test and One-way analysis of variance (ANOVA) followed by Tukey's post-hoc) or non-

parametric (Mann-Whitney U test and One-way Kruskal-Wallis H test followed by Dunn's post-hoc) statistical analysis were used for comparisons of data. All statistical assessments were two-sided and a value of $P < 0.05$ was considered statistically significant. Statistical analysis was performed using GraphPad Prism software (GraphPad Software, Inc., USA).

RESULTS

eNAMPT is increased during M1-polarization

Halvorsen et al. have highlighted that iNAMPT resulted to be up-regulated by a M1-stimulus (with LPS and IFNγ treatment) compared to M2-macrophages [18]. While it is already known that PMA-differentiated macrophages are able to secrete eNAMPT [19]; but nobody has determined the possible release of eNAMPT from this type of immune cells. To determine eNAMPT release on macrophages, we used peritoneal exudate cells (PECs), harvested from mice peritoneum after thioglycolate injection as *in vitro* model. As shown in Figure 1A, we observed a significant up-regulation of *Nampt* after 4h-treatment with IFNγ and LPS, which decreases after 18h-stimulus. Contrary, *Nampt* is not overexpressed after a typical M2-stimulus, as IL-4. Importantly, 4h-*Nampt* upregulation prompt an increase of iNAMPT abundance in PECs after 24h-stimulus with IFNγ and LPS (Figure 1B). This is translated as a consequent reduction of iNAMPT in lysates and oversecretion of eNAMPT in conditioned medium after 48 hours (Figure 1C). No changes or oversecretion were observed with IL-4 stimulus.

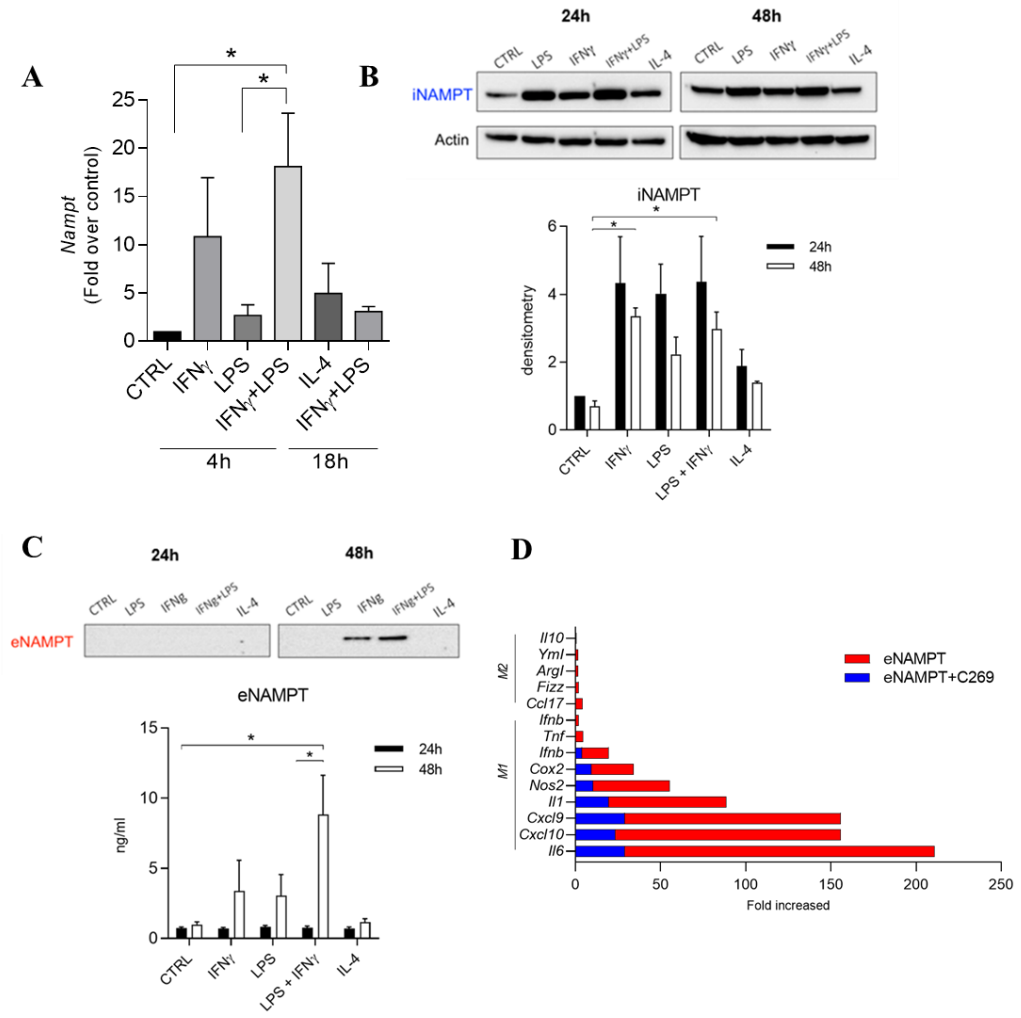

Figure 1. iNAMPT and eNAMPT are increased during M1 macrophage polarization. (**A**) *Nampt* mRNA levels after M1- or M2-stimuli; Mean + S.E.M. of 4 independent experiments. (**B**) Representative western blot of iNAMPT in total cell lysates of peritoneal macrophages treated or not with IFNγ and/or LPS or IL-4 at 24 and 48h and densitometry of iNAMPT fold increase. Mean + S.E.M. of 3 independent experiments. (**C**) Western blot analysis of eNAMPT released in the medium of peritoneal macrophages treated or not with IFNγ and/or LPS or IL-4 at 24 and 48h. Mean + S.E.M. of 3 independent experiments. eNAMPT determination by ELISA assay in the medium of macrophages under the indicated treatments used. (**D**) Fold changes values of M1 and M2 genes. Peritoneal macrophages were treated with eNAMPT (500 ng/ml) and C269 (10µg/ml) for 4/18 hours. Mean + S.E.M. of 7 independent experiments.

eNAMPT is a M1-enhancing stimulus

Being the expression (or secretion) of eNAMPT the result of M1-stimulation, we decided to determine if eNAMPT itself, present in the niche, may be a positive stimulus for macrophages. To do this, we used a recombinant form of eNAMPT, in endotoxin-free conditions (evaluated with LAL test and only preparations with less than 0.1EU/ml were used). We treated PECs with 500 ng/ml of eNAMPT and determined M1- and M2-associated genes with RT-PCR. Gene analysis revealed that eNAMPT treatment is able to induce plenty of M1-associated genes, including *Il6*, *Il1*, *Cxcl10*, *Cxcl9*, *Nos2*, *Cox2*, *Tnf* and *Il12b*, while no M2-associated genes were modulated (Figure 1E in red). Being conscious of having an important pharmacological tool able to counteract eNAMPT activity, we used C269, a monoclonal antibody against eNAMPT, generated by us [16]. As shown in Figure 1E in blue, C269 dramatically down-regulates eNAMPT-mediated overexpression, proving that eNAMPT is a possible target on macrophage polarization.

To better characterize eNAMPT role in skewing macrophage activity, we performed RNA sequencing on PECs treated or not with eNAMPT (500 ng/ml). eNAMPT is able to differentially upregulate 827 genes (Figure 2A). A straightforward analysis of bio-functions (Panther Classification System) was performed, showing a leading role for immune regulation and transcription activity in the genes regulated by eNAMPT (Figure 2B). GO analysis, using DAVID software, have evidenced the ability of eNAMPT to act on immune pathway, upregulating these genes, especially ERK and NF-κB cascade as seen by Managò et al. [20], but also able to upregulate the response to LPS or IL-6 production or chemotaxis (Figure 2C). Moreover, in Fig. 2D is highlighted the binding-activation mechanism, that sustains the model in which is described the possible interaction of eNAMPT with a putative receptor.

To better understand and explain the mechanism of eNAMPT-induced inflammatory response in PECs, a pathway enrichment analysis was conducted using the whole dataset of differentially expressed 827 genes. As evidenced by KEGG analysis dataset, eNAMPT is able to mediate different pathways, including Toll-Receptor

pathway, confirming the idea that TLR4 may be the putative receptor of eNAMPT (Figure 2E). Also, the 1229 downregulated genes were analysed, but no important significant pathways were evidenced, using both GO and KEGG datasets (Supplementary Figure 1).

More importantly, protein–protein interaction (PPI) network was created with all 827 differentially regulated genes and coupled with functional clustering using DAVID v6.8 (Figure 2F), revealing a number of highly interacting processes altered by PECs treated with eNAMPT. These include immune system responses, LPS response, chemotaxis and regulation of NF-κB.

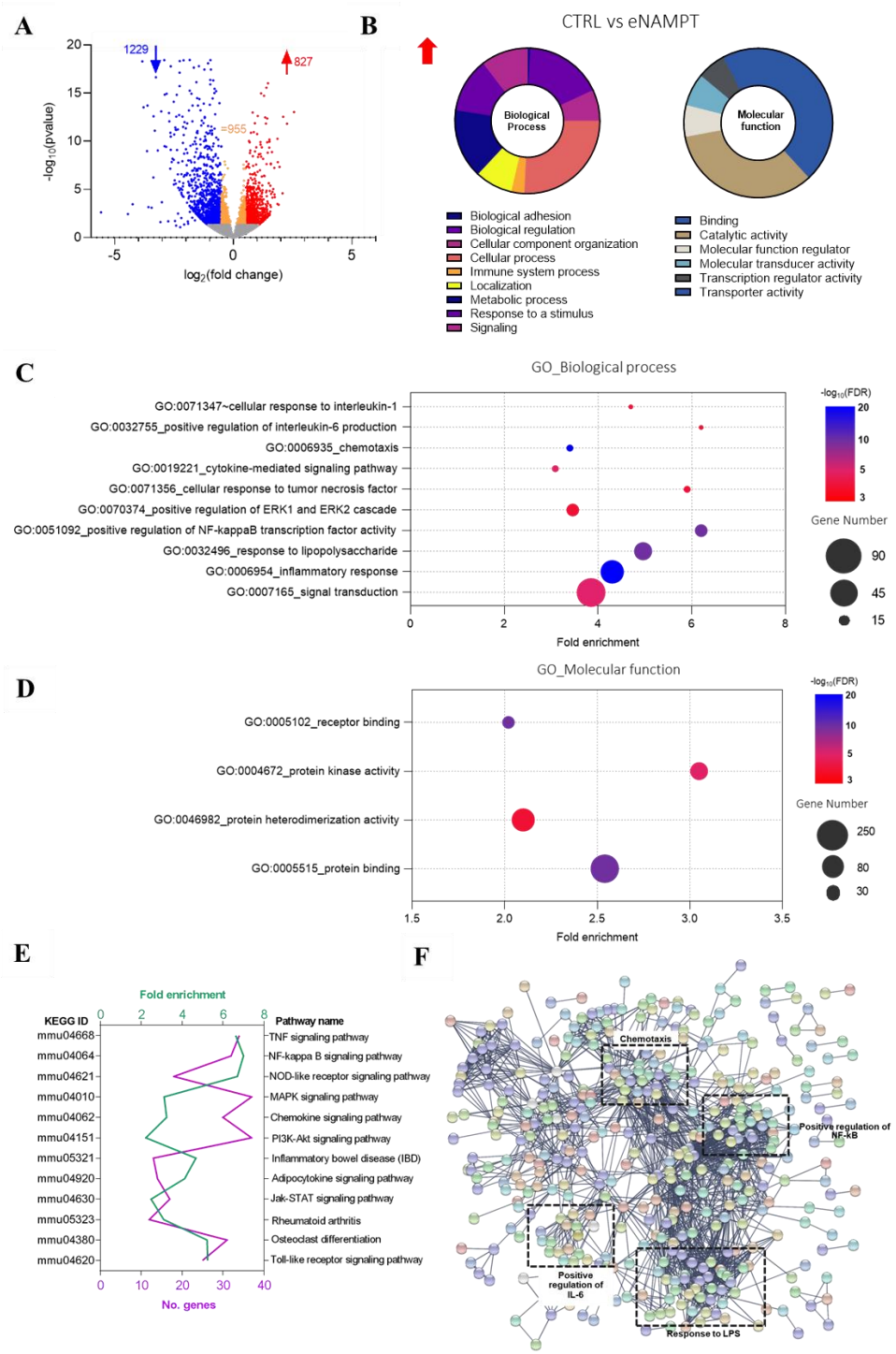
A
1229
827
=955
-log10(pvalue)
log2(fold change)
B
CTRL vs eNAMPT
Biological Process
Molecular function
Biological adhesion
Biological regulation
Cellular component organization
Cellular process
Immune system process
Localization
Metabolic process
Response to a stimulus
Signaling
Binding
Catalytic activity
Molecular function regulator
Molecular transducer activity
Transcription regulator activity
Transporter activity
C
GO_Biological process
GO:0071347~cellular response to interleukin-1
GO:0032755_positive regulation of interleukin-6 production
GO:0006935_chemotaxis
GO:0019221_cytokine-mediated signaling pathway
GO:0071356_cellular response to tumor necrosis factor
GO:0070374_positive regulation of ERK1 and ERK2 cascade
GO:0051092_positive regulation of NF-kappaB transcription factor activity
GO:0032496_response to lipopolysaccharide
GO:0006954_inflammatory response
GO:0007165_signal transduction
Fold enrichment
-log10(FDR)
Gene Number
D
GO_Molecular function
GO:0005102_receptor binding
GO:0004672_protein kinase activity
GO:0046982_protein heterodimerization activity
GO:0005515_protein binding
Fold enrichment
-log10(FDR)
Gene Number
E
Fold enrichment
KEGG ID
Pathway name
mmu04668 TNF signaling pathway
mmu04064 NF-kappa B signaling pathway
mmu04621 NOD-like receptor signaling pathway
mmu04010 MAPK signaling pathway
mmu04062 Chemokine signaling pathway
mmu04151 PI3K-Akt signaling pathway
mmu05321 Inflammatory bowel disease (IBD)
mmu04920 Adipocytokine signaling pathway
mmu04630 Jak-STAT signaling pathway
mmu05323 Rheumatoid arthritis
mmu04380 Osteoclast differentiation
mmu04620 Toll-like receptor signaling pathway
No. genes
F
Chemotaxis
Positive regulation of NF-kB
Positive regulation of IL-6
Response to LPS

Figure 2. Gene expression profile acquired during eNAMPT-mediated stimulus. (**A**) RNAseq analysis on PECs (n =5 replicates/condition) treated with 500 ng/ml eNAMPT, identified 2056 statistically significant ($p < 0.05$) differentially expressed genes which are presented as a volcano plot: fold change from eNAMPT *vs*. control, against p value. (**B**) Functional profiling of all 827 differentially expressed genes identified by RNAseq using Panther Classification System. (**C-D**) Upregulated genes with GO analysis. (**E**) Analysis of KEGG pathways of all 827 differentially expressed genes following treatment with eNAMPT. Number of genes annotated to each pathway (purple) and fold enrichment (green) are shown for the top 12 pathways. (**F**) Protein–protein interaction (PPI) network built with all 827 significantly altered genes using STRING. Further functional analysis was performed with DAVID and significantly enriched categories are highlighted.

eNAMPT promotes macrophage migration *in vitro*

RNA sequencing analysis highlighted eNAMPT effect on chemotaxis pathways. To prove this, we performed wound healing assay on PECs. After a scratch on confluent cells and treating them with 500 ng/ml eNAMPT and 100 ng/ml LPS, known to be a pro-migratory stimulus on macrophages [20], we monitored PECs migration at different times points. As shown in Figure 3, eNAMPT prompts PECs to move in the same way of LPS, confirming to be a chemotactic stimulus.

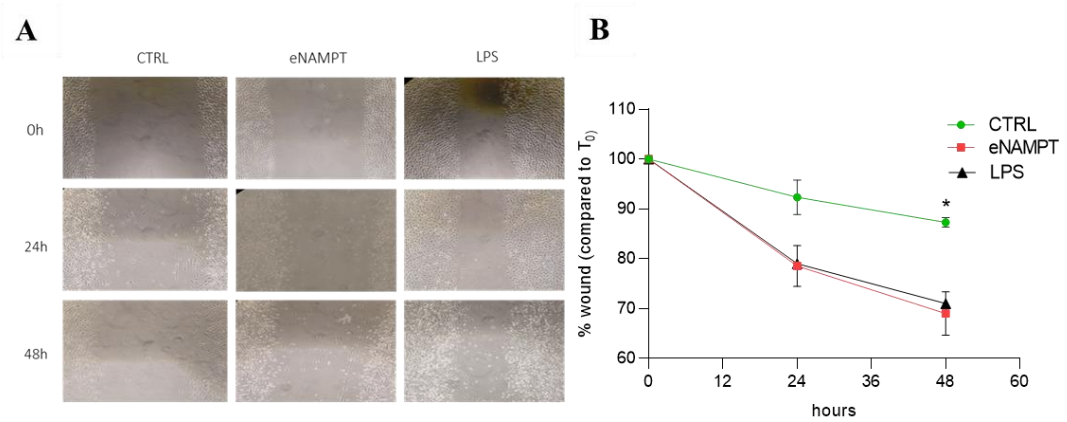

Figure 3. eNAMPT increases wound closure of peritoneal macrophages *in vitro*. (**A**) Representative wound healing images of peritoneal macrophages treated with vehicle, eNAMPT (500 ng/ml) and LPS (100 ng/ml) at time 0 and after 24 and 48 hours of treatment. (**B**) Percentage of wound (compared to % of each T0) after 24 and 48 hours of treatment. Mean ± S.E.M. of 3 determinations from 2 separate experiments.

eNAMPT priming of PECs boosts IFNγ-induced proinflammatory response

With the idea that eNAMPT may be present in the inflammatory niche, we decided to test if it may synergize with other cytokines involved in macrophage activation. As recapitulated in Figure 4A, there is no synergistic effect with IL-4, but also with IL-6, GM-CSF and IL-1β., while a mild effect has been detected with LPS. Notably, a very strong and significant effect has been determined in combination with IFNγ (100 ng/ml), indeed we observed a significant upregulation of the combination compared to IFNγ-treatment alone (Figure 4B). To deeper investigate the effect of the combination between eNAMPT and IFNγ, we performed RNA sequencing. As shown in Figure 4C, the co-stimulation of PECs with eNAMPT and IFNγ upregulates 1903 genes (*vs* 1800 in downregulation) compared to the control (Figure 4C). Of note, 1208 genes are significantly upregulated with eNAMPT and IFNγ co-treatment compared to IFNγ alone, while 521 genes are specifically activated with the co-treatment only (Figure 4C).

As depicted in Figure 4E, we highlighted the response to stimulus activity mediated by the combinatory treatment with the analysis of bio-functions (Panther Classification System) (Figure 4E). Protein–protein interaction (PPI) network was constructed with all 1208 differentially regulated genes evidencing the strict connection between the regulation of IFNγ and the response to LPS, prompting the idea of a priming effect of eNAMPT, binding TLR4, on IFNγ-dependent pathway (Figure 5A). Moreover, KEGG pathway analysis confirmed the involvement on Toll-like receptor pathway, that is not considered with IFNγ-treatment alone (Figure 5B), in addition of the activation of JAK/STAT pathways. Furthermore, in Figure 5C and 5D, GO analysis confirmed the effect on IFNγ-mediated pathway and LPS-mediated response.

Additionally, IFNγ in co-treatment with eNAMPT stimulates NAD^+-ADP ribosyltransferase activity, significantly upregulating *Nampt* (Figure 5D). The synergistic effect of this pathway occurs in presence of IFNγ and LPS, so eNAMPT may substitute LPS in TLR4 activation, increasing NAD^+-ADP ribosyltransferase

activity. The fold changes of the highlighted pathways are reported in the heat map in Figure 5E-G.

Likewise, we also analysed the 1800 IFNγ *plus* eNAMPT-mediated downregulated genes (Supplementary Figure 2), but they are correlated to the effect of IFNγ alone.

A

Cytokine	Synergic effect
IL-6	Absent
IL-4	Absent
GM-CSF	Absent
IL-1β	Absent
IFN	Present
LPS	Mild

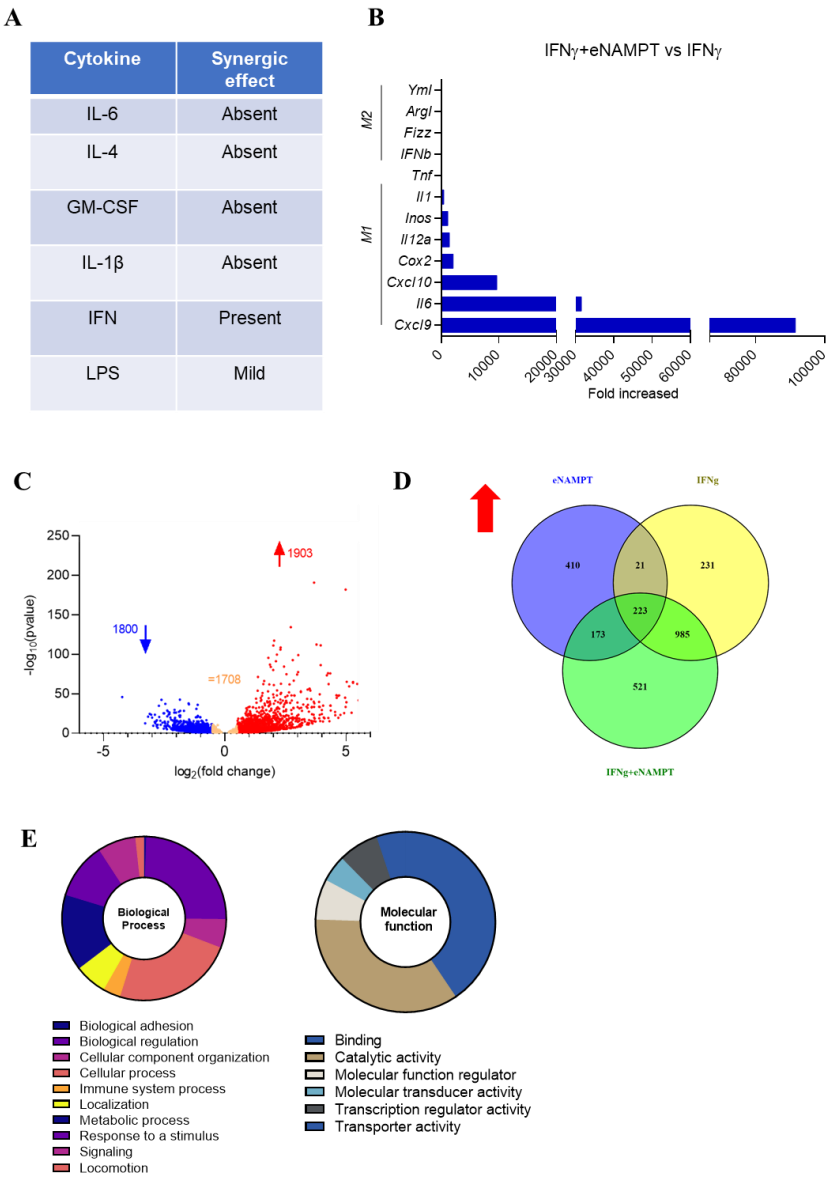

Figure 4. eNAMPT in combination with IFNγ prompts pro-inflammatory pathways. (**A**) Summary table of synergistic treatment with eNAMPT performed. (**B**) Fold changes values of M1 and M2 genes. Peritoneal macrophages were treated with IFNγ in combination with eNAMPT (500 ng/ml) for 4 hours. Data were compared to IFNγ fold changes (control values= 1). Mean + S.E.M. of

7 independent experiments. (**C**) RNAseq analysis on PECs (n =5 replicates/condition) treated with 500 ng/ml eNAMPT, identified 2056 statistically significant ($p < 0.05$) differentially expressed genes which are presented as a volcano plot: fold change from eNAMPT+IFNγ *vs.* control, against p value. (**D**) Venn diagram showing RNA-seq analysis results in PECs treated with eNAMPT, IFNγ or eNAMPT+IFNγ and compared to the control (n =5). (**E**) Functional profiling of all 1208 differentially expressed genes identified by RNAseq using Panther Classification System.

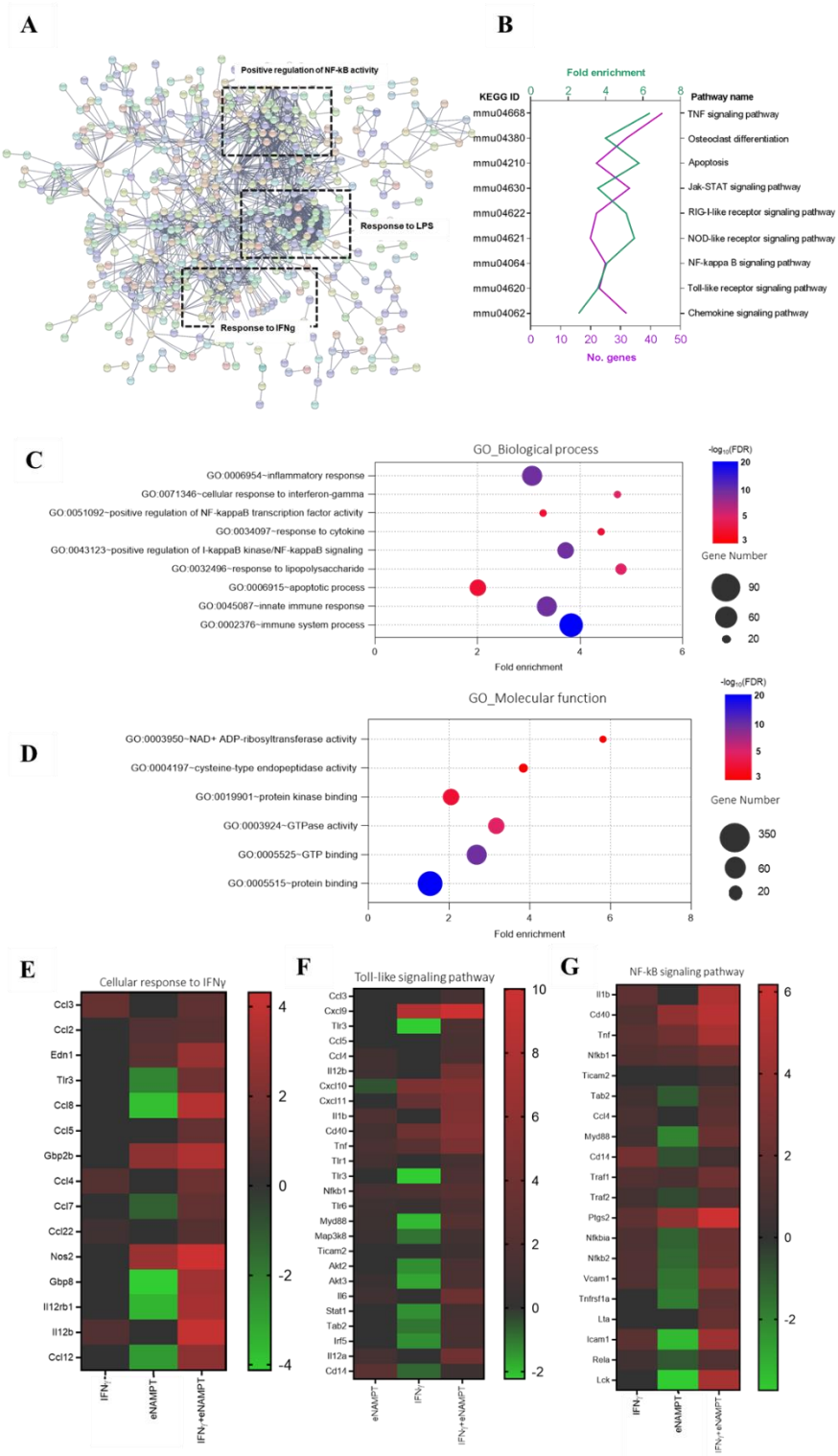
A
Positive regulation of NF-kB activity
Response to LPS
Response to IFNg
B
Fold enrichment
KEGG ID
Pathway name
mmu04668
TNF signaling pathway
mmu04380
Osteoclast differentiation
mmu04210
Apoptosis
mmu04630
Jak-STAT signaling pathway
mmu04622
RIG-I-like receptor signaling pathway
mmu04621
NOD-like receptor signaling pathway
mmu04064
NF-kappa B signaling pathway
mmu04620
Toll-like receptor signaling pathway
mmu04062
Chemokine signaling pathway
No. genes
C
GO_Biological process
GO:0006954~inflammatory response
GO:0071346~cellular response to interferon-gamma
GO:0051092~positive regulation of NF-kappaB transcription factor activity
GO:0034097~response to cytokine
GO:0043123~positive regulation of I-kappaB kinase/NF-kappaB signaling
GO:0032496~response to lipopolysaccharide
GO:0006915~apoptotic process
GO:0045087~innate immune response
GO:0002376~immune system process
Fold enrichment
-log10(FDR)
Gene Number
D
GO_Molecular function
GO:0003950~NAD+ ADP-ribosyltransferase activity
GO:0004197~cysteine-type endopeptidase activity
GO:0019901~protein kinase binding
GO:0003924~GTPase activity
GO:0005525~GTP binding
GO:0005515~protein binding
Fold enrichment
-log10(FDR)
Gene Number
E
Cellular response to IFNγ
Ccl3
Ccl2
Edn1
Tlr3
Ccl8
Ccl5
Gbp2b
Ccl4
Ccl7
Ccl22
Nos2
Gbp8
Il12rb1
Il12b
Ccl12
IFN-
eNAMPT
IFN-+eNAMPT
F
Toll-like signaling pathway
Ccl3
Cxcl9
Tlr3
Ccl5
Ccl4
Il12b
Cxcl10
Cxcl11
Il1b
Cd40
Tnf
Tlr1
Tlr3
Nfkb1
Tlr6
Myd88
Map3k8
Ticam2
Akt2
Akt3
Il6
Stat1
Tab2
Irf5
Il12a
Cd14
eNAMPT
IFN-
IFN-+eNAMPT
G
NF-kB signaling pathway
Il1b
Cd40
Tnf
Nfkb1
Ticam2
Tab2
Ccl4
Myd88
Cd14
Traf1
Traf2
Ptgs2
Nfkbia
Nfkb2
Vcam1
Tnfrsf1a
Lta
Icam1
Rela
Lck
IFN-
eNAMPT
IFN-+eNAMPT

Figure 5: eNAMPT priming of PECs boosts IFNγ-induced proinflammatory response. (**A**) Protein–protein interaction (PPI) network built with all 1208 significantly altered genes using STRING. Further functional analysis was performed with DAVID and significantly enriched categories are highlighted. (**B**) Analysis of KEGG pathways of all 1208 differentially upregulated genes following treatment with eNAMPT and IFNγ. Number of genes annotated to each pathway (purple) and fold enrichment (green) are shown for the top 12 pathways. (**C-D**) Upregulated genes with GO analysis. (**E-G**) Heatmaps of the most upregulated genes by eNAMPT, IFNγ and eNAMPT+IFNγ vs control, belonging to the cellular response to IFN, toll-like receptor signalling and NF-κB pathway.

CONCLUSION

The incredible plasticity of macrophages may be important to further target, indeed several inflammatory diseases, such as rheumatoid arthritis, IBD, asthma, atherosclerosis and diabetes see a direct involvement of macrophages in their pathogenesis [15,21]. Understanding their mechanism and the effect of "cytokine storm" during inflammation may be an important focus to investigate.

In the present manuscript, we showed up the effect of eNAMPT, as an extracellular cytokine, to mediate the inflammatory effect on macrophages. Of note, we have noticed different gaps into eNAMPT effect on macrophage knowledge. Firstly, we established that eNAMPT is predominantly released after a M1-stimulus (IFNγ and LPS). The data agree with what has been published by Halvorsen et al. and Svoboda et al. Moreover, eNAMPT itself may act as a M1-associated stimulus, able to upregulate M1-associated genes. The RNA sequencing analysis has evidenced the involvement of eNAMPT on different pathways, including Toll-like receptor pathway and the response to LPS, confirming the possible binding to TLR4. Importantly, the eNAMPT neutralizing antibody is able to rescue eNAMPT mediated M1 polarization.

We have proved for the first time that, eNAMPT is a priming to IFNγ response, indeed, eNAMPT is able to significantly increase gene associated to IFNγ response, correlated to the inflammatory process.

Using RNAseq analysis we have confirmed the priming effect of eNAMPT on IFNγ-mediated pathways. Moreover, this combination allows PECs to notably increase the inflammatory effect in the environment, for example promoting migration.

Likewise, targeting eNAMPT counteracts pro-inflammatory effects on macrophages, assuming its relevance in the inflammation establishment. We have recently underlined the importance of targeting eNAMPT in IBD, where the treatment with C269 is able to ameliorates inflammatory symptoms in DSS- and DNBS-induced colitis. This effect may be explicated by a direct intervention on activated macrophages that are mainly M1-skewed in IBD [22]. Besides, the primed effect with IFNγ may confirm the effect on TLR4 activation, mimicking LPS involvement.

In conclusion, we have demonstrated that eNAMPT alone has a moderate pro-inflammatory property, while eNAMPT acts as a priming to IFNγ, suggesting an important role of this cytokine in controlling the cytokine storm during inflammation.

References

1 Amit I, Winter DR, Jung S. The role of the local environment and epigenetics in shaping macrophage identity and their effect on tissue homeostasis. *Nat Immunol* 2016;**17**:18–25. doi:10.1038/ni.3325

2 Martinez FO, Gordon S. The M1 and M2 paradigm of macrophage activation: time for reassessment. *F1000Prime Rep* 2014;**6**:13. doi:10.12703/P6-13

3 Gordon S, Plüddemann A, Martinez Estrada F. Macrophage heterogeneity in tissues: phenotypic diversity and functions. *Immunol Rev* 2014;**262**:36–55. doi:10.1111/imr.12223

4 Sica A, Mantovani A. Macrophage plasticity and polarization: in vivo veritas. *J Clin Invest* 2012;**122**:787–95. doi:10.1172/JCI59643

5 Brundu S FA. Polarization and Repolarization of Macrophages. *J Clin Cell Immunol* 2015;**06**. doi:10.4172/2155-9899.1000319

6 Sica A, Schioppa T, Mantovani A, *et al.* Tumour-associated macrophages are a distinct M2 polarised population promoting tumour progression: potential targets of anti-cancer therapy. *Eur J Cancer* 2006;**42**:717–27. doi:10.1016/j.ejca.2006.01.003

7 Hayes MP, Freeman SL, Donnelly RP. IFN-gamma priming of monocytes enhances LPS-induced TNF production by augmenting both transcription and MRNA stability. *Cytokine* 1995;**7**:427–35. doi:10.1006/cyto.1995.0058

8 Garten A, Schuster S, Penke M, *et al.* Physiological and pathophysiological roles of NAMPT and NAD metabolism. *Nat Rev Endocrinol* 2015;**11**:535–46. doi:10.1038/nrendo.2015.117

9 Samal B, Sun Y, Stearns G, *et al.* Cloning and characterization of the cDNA encoding a novel human pre-B-cell colony-enhancing factor. *Mol Cell Biol* 1994;**14**:1431–7. doi:10.1128/mcb.14.2.1431

10 Fukuhara A, Matsuda M, Nishizawa M, *et al.* Retraction. *Science* 2007;**318**:565. doi:10.1126/science.318.5850.565b

11 Camp SM, Ceco E, Evenoski CL, *et al.* Unique Toll-Like Receptor 4 Activation by NAMPT/PBEF Induces NFκB Signaling and Inflammatory Lung Injury. *Sci Rep* 2015;**5**. doi:10.1038/srep13135

12 Van den Bergh R, Morin S, Sass HJ, *et al.* Monocytes Contribute to Differential Immune Pressure on R5 versus X4 HIV through the Adipocytokine Visfatin/NAMPT. *PLoS One* 2012;**7**. doi:10.1371/journal.pone.0035074

13 Revollo JR, Körner A, Mills KF, *et al.* Nampt/PBEF/Visfatin regulates insulin secretion in beta cells as a systemic NAD biosynthetic enzyme. *Cell Metab* 2007;**6**:363–75. doi:10.1016/j.cmet.2007.09.003

14 Yoshida M, Satoh A, Lin JB, *et al.* Extracellular Vesicle-Contained eNAMPT Delays Aging and Extends Lifespan in Mice. *Cell Metab* 2019;**30**:329-342.e5. doi:10.1016/j.cmet.2019.05.015

15 Travelli C, Colombo G, Mola S, *et al.* NAMPT: A pleiotropic modulator of monocytes and macrophages. *Pharmacological Research* 2018;**135**:25–36. doi:10.1016/j.phrs.2018.06.022

16 Colombo G, Clemente N, Zito A, *et al.* Neutralization of extracellular NAMPT (nicotinamide phosphoribosyltransferase) ameliorates experimental murine colitis. *J Mol Med* Published Online First: 27 April 2020. doi:10.1007/s00109-020-01892-0

17 Amici A, Grolla AA, Del Grosso E, *et al.* Synthesis and Degradation of Adenosine 5'-Tetraphosphate by Nicotinamide and Nicotinate Phosphoribosyltransferases. *Cell Chem Biol* 2017;**24**:553-564.e4. doi:10.1016/j.chembiol.2017.03.010

18 Halvorsen B, Espeland MZ, Andersen GØ, *et al.* Increased expression of NAMPT in PBMC from patients with acute coronary syndrome and in inflammatory M1 macrophages. *Atherosclerosis* 2015;**243**:204–10. doi:10.1016/j.atherosclerosis.2015.09.010

19 Svoboda P, KříŽová E, Čeňková K, *et al.* Visfatin is actively secreted in vitro from U-937 macrophages, but only passively released from 3T3-L1 adipocytes and HepG2 hepatocytes. *Physiol Res* 2017;**66**:709–14. doi:10.33549/physiolres.933370

20 Ortiz-Masiá D, Hernández C, Quintana E, *et al.* iNOS-derived nitric oxide mediates the increase in TFF2 expression associated with gastric damage: role of HIF-1. *FASEB J* 2010;**24**:136–45. doi:10.1096/fj.09-137489

21 Ponzoni M, Pastorino F, Di Paolo D, *et al.* Targeting Macrophages as a Potential Therapeutic Intervention: Impact on Inflammatory Diseases and Cancer. *Int J Mol Sci* 2018;**19**. doi:10.3390/ijms19071953

22 Moreira Lopes TC, Mosser DM, Gonçalves R. Macrophage polarization in intestinal inflammation and gut homeostasis. *Inflamm Res* 2020;**69**:1163–72. doi:10.1007/s00011-020-01398-y

SUPPLEMENTARY FIGURES

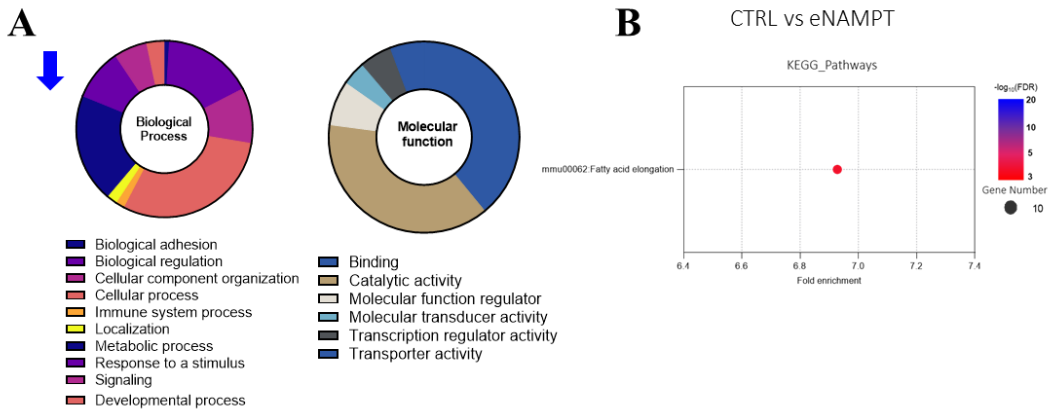

Supplementary Figure 1: (A) Functional profiling of all 1229 differentially expressed genes identified by RNAseq using Panther Classification System (**B**) Analysis of KEGG pathways of all 1229 differentially downregulated genes following treatment with eNAMPT.

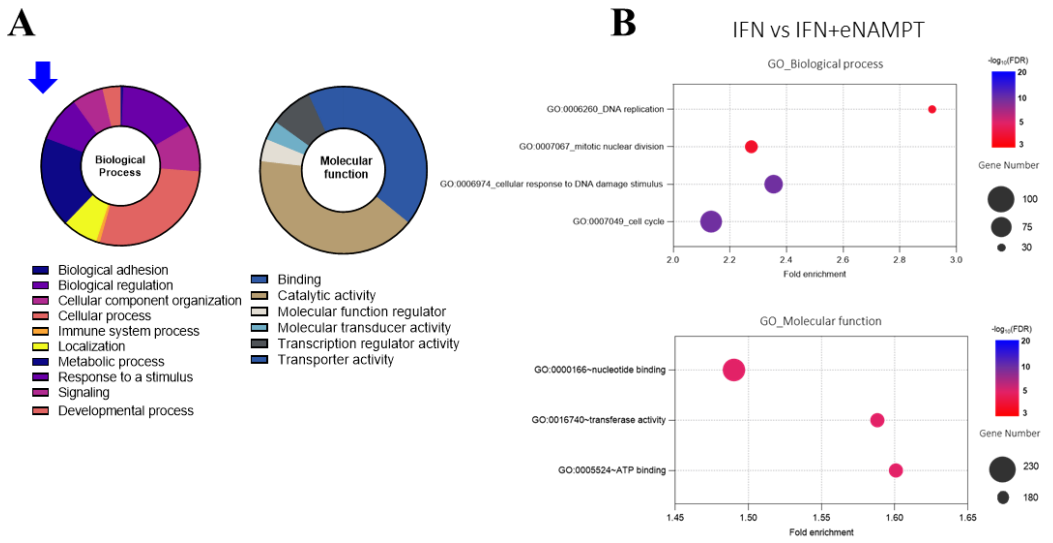

Supplementary Figure 2: (A) Functional profiling of all 1800 differentially expressed genes identified by RNAseq using Panther Classification System (**B**) Analysis of KEGG pathways of all 1800 differentially downregulated genes following treatment with eNAMPT.

Table I

Gene	Forward Primer (5'-> 3')	Reverse Primer (5'->3')

Mm_B-Actin	ATGACCCAAGCCGAGAAGG	CGGCCAAGTCTTAGAGTTGTTG
Mm_TNF-α	AGTTCTATGGCCCAGACCCTC	CAGGCTTGTCACTCGAATTTTG
Mm_NAMPT	GCAGAAGCCGAGTTCAACATC	TTTTCACGGCATTCAAAGTAGGA
Mm_IL-6	TGTTCTCTGGGAAATCGTGGA	AAGTGCATCATCGTTGTTCATACA
Mm_COX-2	GACCGCAATGAACTTCGGGA	TCCATTAGGTCTCTAAAGCCGAG
Mm_IL-1	GATGAGGACATGAGCACCTTCTT	GCAGGTTATCATCATCATCCCA
Mm_IL-18	GACTCTTGCGTCAACTTCAAGG	CAGGCTGTCTTTTGTCAACGA
Mm_IL-23p19	ATGCTGGATTGCAGAGCAGTA	ACGGGGCACATTATTTTTAGTCT
Mm_IL-12p40	TGGTTTGCCATCGTTTTGCTG	ACAGGTGAGGTTCACTGTTTCT
Mm_IFN-β	CAGCTCCAAGAAAGGACGAAC	GGCAGTGTAACTCTTCTGCAT
Mm_iNOS	CGAAACGCTTCACTTCCAA	TGAGCCTATATTGCTGTGGCT
Mm_CXCL9	GGAGTTCGAGGAACCCTAGTG	GGGATTTGTAGTGGATCGTGC
Mm_CXCL10	CCAAGTGCTGCCGTCATTTTC	GGCTCGCAGGGATGATTTCAA
Mm_CCL17	TACCATGAGGTCACTTCAGATGC	GCACTCTCGGCCTACATTGG
Mm_ArgI	AACACGGCAGTGGCTTTAACC	GGTTTTCATGTGGCGCATTC
Mm_Ym1	TCACAGGTCTGGCAATTCTTCTG	TTTGTCCTTAGGAGGGCTTCCTCG
Mm_Fizz1	GGTCCCAGTGCATATGGATGAGACCATAGA	CACCTCTTCACTCGAGGGACAGTTGGCAGC

Chapter 6

Identification of phosphorylation sites on Nicotinamide phosphoribosyltransferase (NAMPT) (UNDERGOING SUBMISSION)

Michele Bianchi[1*], Giorgia Colombo[1*], Melania Ronfani[2], Federica Losio[2], Laura Paganoni, Adarsh Mayank[3], William D. Barshop[3], Simone Torretta[1], Ambra Grolla[1], Erika del Grosso[1], James A. Wohlschlegel[3], Armando Genazzani[1§] and Cristina Travelli[2]

[1]Dipartimento di Scienze del Farmaco, via Bovio 6, Università del Piemonte Orientale, Novara, Italy, +39 0321375827
[2]Dipartimento di Scienze del Farmaco, Università degli studi di Pavia, Italy
[3] Department of Biological Chemistry, David Geffen School of Medicine, University of California, Los Angeles, Los Angeles, CA 90095, USA.

*these Authors contributed equally
§ corresponding Author

Author contributions.

The study was designed by C.T., M.B, G.C., E.D.G., A.A.Genazzani and J.A.W. M.B. did the major part of the LC-MS based proteomic experiments; G.C., C.T. M.B. did the majority of biological experiments; A.A.Grolla and S.T. helped in the generation of *B16-GFPNAMPT cells*; A.M., L.P., M.R. and F.L. helped us in the biological experiments, in setting up-the immunoprecipitation method; W.D.B. helped us in the bioinformatics analysis; M.B., C.T., G.C., A.A.Genazzani and J.A.W directed the work and wrote the manuscript. All of the authors have seen and approved the final version of the manuscript.

Abstract

Nicotinamide phosphoribosyltransferase (NAMPT) is the key enzyme involved in nicotinamide adenine dinucleotide (NAD^+) metabolism. NAMPT is a homodimer that catalyses the formation of nicotinamide mononucleotide (NMN), precursor of NAD^+, starting from phosphoribosyl pyrophosphate (PRPP) and nicotinamide (Nam) in the presence of ATP. NAMPT is present in cells in the cytosol and in the nucleus and it has been also found actively secreted in the extracellular space as eNAMPT, where it acts as a cytokine.

In the literature, few post-translational modifications on NAMPT have been described: the H247 autophosphorylation and the K53 deacetylation. Surprisingly, no data are available on other phosphorylation sites. Since it is well known that phosphorylation controls the switch-on or switch-off of several enzymes and their localization, the aim of our work was to identify, quantify and characterize possible NAMPT phosphorylated sites in melanoma cells, in which NAMPT is highly expressed. Interestingly, eight phosphorylated sites were identified and label-free quantified by LC-MS based proteomics. Based on quantitative data, S199, S200, Y240 and S241 NAMPT phosphorylated sites were the more abundant. We have focused our attention on the residues S199 and S200, which are located in the dimer interface and the recombinant mutated proteins (S199A and S200A) are enzymatically inactive. Moreover, the S199A mutation altered NAMPT localization. This work has identified for the first time several residues of NAMPT that are phosphorylated. Of note, the phosphorylation of S199 and S200 controls NAMPT activation while S200 may control NAMPT nuclear localization.

Introduction

Nicotinamide phosphoribosyltransferase (NAMPT) is a key enzyme controlling NAD^+ biosynthesis in mammalian cells. In detail, NAMPT is the rate-limiting enzyme in the so-called "NAD salvage pathway": starting from nicotinamide (Nam) and phosphoribosyl pyrophosphate (PRPP) it catalyses the synthesis of nicotinamide mononucleotide (NMN) [1], a substrate for NAD synthesis by NMNAT (REF). By maintaining NAD^+ pools in cells, NAMPT activity is crucial for cell proliferation and survival, for example controlling bioenergetics and PARP and sirtuin activity. For this reason it is not surprisingly that NAMPT expression and activity are increased in several disorders [2].

iNAMPT is an intracellular protein, detected in the cytosol and in the nucleus, while its presence in the mitochondria is still controversial [3,4]. Moreover, NAMPT is also secreted in the extracellular space, through an undefined mechanism, and it acts as a cytokine (eNAMPT, also referred to as visfatin or PBEF). At present, it is unclear whether eNAMPT, for all or some of its extracellular functions, requires the catalytic activity [3–6].

NAMPT is therefore a pleiotropic protein with multiple localizations (cytosolic, nuclear, extracellular space) and different functions (*e.g.* enzyme, cytokine). It has been shown that protein expression levels may vary in cells in different contexts, for example in cancer cells levels increase most likely to support ATP synthesis and to contrast PARP-induced NAD^+ depletion. Yet, for such a central protein, it would appear likely that post-translational modifications (PTM) may also control its function or localization, and this has not so far been investigated in detail.

The most important PTM so far described is an auto-phosphorylation on histidine 247, which significantly increases the catalytic efficiency of iNAMPT [1]. NAMPT, as a typical phosphoribosyltransferase, has an ATPase activity to shift the thermodynamic equilibrium toward mononucleotide formation. By coupling ATP

hydrolysis to NMN synthesis, the catalytic efficiency of the system is increased by a thousand-fold and the chemical equilibrium shifted toward NMN as long as ATP is being hydrolysed. The group of Burgos demonstrated that the phosphorylated histidine provides a new structural element that contributes to higher affinity between PRPP and the phosphorylated enzyme [7].

In a paper published by Imai et al. are described a series of NAMPT post-translational modifications, including acetylation and ADP-ribosylation, and revealed that iNAMPT is acetylated in brown and white adipose tissue [8]. They found that in cell extracts, relatively low levels of acetylated iNAMPT are detected and that its acetylation significantly increased when cells were treated with deacetylases inhibitors or were starved for 48 hours. The acetylation sites identified on iNAMPT are five (K53, K79, K107, K331, K369), all of them present in the intracellular protein, while only K369 is acetylated on eNAMPT. Of note, K53, which protrudes from each monomer, is aligned along the "cleft" of the dimer and remarkably close to the catalytic sites. However, the K53R mutant is still active, while displaying reduced acetylation levels and this in turn leads to a reduced NAMPT secretion in the extracellular space [8].

No other PTMs have so far been described. For this reason, we set to identify other possible phosphorylation sites in NAMPT *via* a phosphoproteomic approach. Briefly, we have analysed immunoprecipitated NAMPT from engineered melanoma cells under steady-state condition using LC/MS technology, try to understand their importance in the cellular settings.

2. MATERIALS AND METHODS

2.1 Generation of GFP-NAMPT over-expressing melanoma cells

Murine NAMPT (ORF GenBanK BC018358) was amplified by using the following primers: 5'CGAGATCTAATGCTGCGGCAGAAGCC (FW) and 5'CGGTCGACCTAATGAGGTGCCACGTCCTG (RV) and cloned (BglII/SalI) into pEGFP-C1 vector. Subsequently, GFP-NAMPT was sub-cloned (XbaI/SalI) into pLV-IRES-GFP bicistronic vector. Correct insertion and sequence were confirmed by sequencing. The lentiviral particles were produced as described elsewhere [9] in HEK293T cells transfected with pMDLg/pRRE, pMD2.VSVG, pRSV-Rev and pLV-GFP-NAMPT-IRES-GFP. Briefly, after 48 h, cell medium was collected, filtrated and centrifuged for 1 h 30 min at 100 000 × g. The viral particles, corresponding to the pellet fraction, were resuspended and used to infect B16 cells, after virus titration. A stable B16 GFP-NAMPT cell line was created, and the expression was monitored by Western blot.

B16 cells were cultured in DMEM supplemented with 10 % fetal bovine serum (FBS), 2 mg/mL glutamine, 10 U/mL penicillin and 100 lg/mL streptomycin.

2.2 Immunoprecipitation

2.2.1 Immunoprecipitation using agarose beads

Protein A/G PLUS-Agarose beads (30 µl, sc-2003, Santa Cruz Biotechnology) were balanced with RIPA buffer and centrifuged for 5 minutes at 4°C at 400 g. Subsequently, NAMPT antibody (5 µg of anti-visfatin rabbit Bethyl A300-779-A) was added to the beads in a final volume of 500 µl and incubated for 1 hour in agitation at 4 °C. Afterwards, 500 µg of lysate was added to the antibody-conjugated beads. The mix containing beads, lysate and antibody was centrifuged at 4°C at 400 g, and 20 µl of supernatant (pre-coupling) were collected. The beads were then incubated in agitation/rotation at 4°C overnight. The day after, beads were centrifuged for 5 minutes at 4°C in order to collect 20 µl of supernatant (post-coupling). Beads were washed twice with RIPA buffer and three times with HNGT

buffer (20 mM Hepes pH 7.5, 0.15 M NaCl, 10% glycerol, 0.1% Triton X-100) and 80 µl of glycine 100 mM pH 2.2 was added (5' at RT in agitation) and beads were centrifuged for a minute at 4°C at a speed of 400 g and the supernatant, containing NAMPT, was collected.

2.2.2 Immunoprecipitation using magnetic beads

Immunoprecipitation was done accordingly to Pierce™ Classic Magnetic IP/ Co-IP Kit instructions.

The anti-NAMPT antibody (visfatin rabbit, Bethyl, A300-779-A) was added to the lysate in Pierce IP Lysis/Wash buffer. Beads were then incubated at 4°C overnight in agitation. The day after, beads were washed twice with Pierce IP Lysis/Wash buffer. The supernatant was collected and eliminated using a magnetic support. Then, the lysate (500 µg) was added to 30 µl of magnetic beads and 20 µl of supernatant were collected (pre-coupling). Then beads were incubated in agitation at 4 °C overnight. Subsequently, supernatant (20 µl) was collected (post-coupling). Then, beads were washed three times with Pierce IP Lysis/Wash buffer and two times with milliQ water. Beads were eluted with Elution Buffer at room temperature for 10 minutes. After that, the supernatants were collected, neutralised with Neutralization Buffer and the Lane Marker Sample Buffer, Non-reducing (5X) has been added to each sample.

2.2.3 Immunoprecipitation using GFP-trap

B16 cells were engineered to stably express NAMPT as an N-terminal GFP fusion protein. For the identification of NAMPT phosphorylated sites, cells were harvested and lysed in lysis buffer (10 mM Tris-HCl pH 7.5, 150 mM NaCl, 0.5 mM EDTA, 0.5 % NP-40, 0.1mM PMSF, and Calbiochem Protease Inhibitor Cocktail Set V). After centrifuging at 13,000 g for 10 min at 4 °C, the supernatant was mixed with GFP-trap agarose beads (gta-100, Chromotek) and rotated at 4 °C O.N. Beads were pelleted, washed four times with ice-cold IP buffer, and then eluted with 0.2 M glycine pH 2.5.

2.3 Treatments

Cells were treated with: i) starvation: cells were grown in DMEM without FBS for 24h, (ii) starvation + FBS: cells were grown in DMEM without FBS for 24h followed by 2 hours of FBS; (iii) UV: cells were subjected to UV for 20'' followed by 3 hours of recovery; (iv) PMA + FSK: cells were treated with 20µM PMA and 200µM Forskolin (FSK) for 1 hour.

2.4 Cytosol/nucleus fractionation

Cells were lysed in 4x pellet volume of Buffer A (300mM Sucrose, 10 mM HEPES, 10 mM KCl, 2 mM $MgCl_2$, 1 mM EGTA) that included proteases and phosphatases inhibitors (Millipore) and with 0.1 % of NP-40 (lysis was controlled by trypan blue). Then, cells were centrifuged at 1300 rpm for 5 min at 4 °C. Supernatant (impure cytosol) was centrifuge at 13000 rpm for 15 min to remove the membranes. The pellet (nuclei) was washed five times with Buffer B (50 mM HEPES, 0.4 M NaCl, 1 mM EDTA) and then re-suspended in 3x pellet volume of Buffer B added with proteases and phosphatases inhibitors, sonicated and incubated on thermomixer for 45 min at 4 °C with 1300 rpm rotations every 5 minutes. Then nuclei were centrifuged for 15 min at 13000 rpm at 4 °C and the nuclear proteins resulted into the supernatant. Both cytosols and nuclei were quantified by Bradford reagent (Sigma-Aldrich).

2.5 Western blotting analysis

Total cell lysates were obtained by lysing whole cells in lysis buffer (20 mM HEPES, 100 mM NaCl, 5 mM EDTA, 1% Nonidet P-40) complemented with protease and phosphatase inhibitor cocktail (Millipore). Samples obtained by fractionation were resolved by western blot. Proteins quantification was performed with Bradford Reagent (Sigma-Aldrich), and proteins were resolved on home-made gradient 4-20% SDS–PAGE gels. Primary antibodies used are anti-NAMPT (Gene Tex), anti-NAMPT (Adipogen, OMNI379) and anti-GFP (Abcam).

When not transferred on nitrocellulose, proteins were resolved by Silver staining (Pierce kit) or Coomassie staining.

2.6 In solution digestion

Protein eluates were precipitated using trichloroacetic acid (TCA) and then washed with acetone. The dried protein was then dissolved in 8 M urea / 100 mM Tris-HCl, pH 8.5. Proteins were reduced with 5mM tris (2-carboxyethyl)phosphine hydrochloride (TCEP, Sigma-Aldrich) and alkylated with 10mM iodoacetamide (Sigma-Aldrich) [10,11]. Afterward, samples were sequentially digested with Lys-C and trypsin proteases as previously described [11]. Digestion was stopped with formic acid, 5% final concentration. Debris was removed by centrifugation. Digests were desalted with Thermo Scientific C18 pipette tips prior to injection in the LC-MS system.

2.7 LC-MS/MS analysis

Phosphorylated peptides were subjected to LC–MS/MS analysis using an Dionex Ultimate 3000 ultra-high pressure liquid chromatography system (Thermo Scientific) connected to an Orbitrap-Fusion-Tribrid mass spectrometer (Thermo Scientific) with a Phoenix Nimbus (Phoenix S&T) ion source. Data dependent acquisition (DDA) and parallel reaction monitoring (PRM) approaches were chosen for peptides identification and label free quantitation.

For DDA, peptides were eluted on a reverse phase C18 column (250 mm × 75 mm i.d., 3 μm p.d.) by a gradient mode constituted of solvent A (0.1% formic acid, 3% DMSO in water) and B (0.1% formic acid, 3% DMSO in ACN) at a flow rate of 200 nl min^{-1}: 1–5.5% solvent B in 5 min; 5.5–27.5% solvent B in 53 min; 27.5–35% solvent B in 7 min; 35–80% solvent B in 1 min and kept 2 min before the re-conditioning of the column. The total analysis time for each sample was 70 min.

In survey scans, full-scan MS spectra were acquired by the Orbitrap analyser at a resolution of 120,000, scanning from *m/z* 400 to *m/z* 1600. AGC target was 2e5 and maximum injection time was 100 ms. MS2 quadrupole selection isolation window was *m/z* 1.6. The top speed mode was selected. MS/MS spectra were detected using Orbitrap analyser at the resolution of 15,000. AGC target was 5.0e4 and the maximum injection time was 35 ms. The normalized HCD energy was set at 35%.

For PRM, the mass spectrometry system and the chromatography gradient was set as follow: peptides were eluted on a reversed phase C18 column (250 mm × 75 mm i.d., 3 μm p.d.) by a gradient mode constituted of solvent A (0.1% formic acid, 3% DMSO in water) and B (0.1% formic acid, 3% DMSO in ACN) at a flow rate of 200 nl min^{-1}: 1–5.5% solvent B in 5 min; 5.5–27.5% solvent B in 123 min; 27.5–35% solvent B in 7 min; 35–80% solvent B in 1 min and kept 2 min before the re-conditioning of the column. The total analysis time for each sample was 140 min.

The resolution of MS1 full scan was set to 50,000, scanning from *m/z* 100 to *m/z* 2000; AGC target was 5e4 and the maximum injection time is set to 100 ms. Precursors are selected by the quadrupole mass analyser using an isolation window set to 1.6 Da. The normalized HCD energy was set at 35%.

2.8 MS data processing

For the identification of phosphorylated peptides, Raw DDA MS files were processed using MS-GF+ search algorithm [12]. NAMPT phosphorylated peptides were identified using a target-decoy approach by searching all MS/MS spectra against a forward/reverse mouse database and filtered by using a percolator derived q value of 0.01 at peptide spectral level. Carbamidomethylation of cysteines was selected as the fixed modification and the phosphorylation (STY) as the variable modification. The database search was performed with an initial precursor ion tolerance of 15 p.p.m., MS/MS tolerance at 0.02 Da, and two missed cleavages are allowed. Phosphosite localization was assessed using PhosphoRS algorithm [13] and the phosphopeptide containing the residues with phosphor-probability greater than 0.95 were used for further quantification. Label free quantitation was performed with skyline (version 3.7). The quantification was performed using PRM data at the MS2 level [14], which is widely used for phosphopeptide quantification [15–17]. The intensity of phosphopeptide was derived from the peak area of specific daughter ion, and all Skyline integrated PRM data analysis were manually checked to validate peak Selection. The intensity of the phosphopeptide detected was normalized against the

daughter ion peak area of NAMPT unphosphorylated peptides, chosen as control to correct sample variations.

2.9 NAMPT Enzymatic activity.

The activity of recombinant NAMPT has been evaluated as previously described [29]. Briefly, the reaction mixtures containing 1mM ATP, 0.5 mM PRPP, 0.5 mM nicotinamide, 80 mM HEPES/NaOH buffer, pH=7.5, 12 mM MgCl2, 0.5 mg/ml bovine serum albumin, 75 mM ethanol, 30 mM semicarbazide, 4.5 mM NH_4Cl. All the assay mix was incubated at 37°C in the presence of 0.024 U/ml PncC, 0.192 U/ml NadD, 0.081 U/ml NadE, 12.5 U/ml ADH as the ancillary enzymes of NAD^+ pathway. The biosynthesis of NADH was continuously monitored by O.D. measurement at a fixed wavelength of 340 nm.

2.10 Cell viability assay

10 x 10^5 B16 GFP-NAMPT and mutated cell lines were plated in medium and viability of cells was measured using the 3-(4,5-dimethylthiazol-2-yl)-2,5-diphenyltetrazolium assay at different time points.

2.11 Immunofluorescence

5.0x10^4 cells were fixed in 4% paraformaldehyde (PFA) on glass cover slips in 24-well plates and then added with DAPI (Invitrogen), incubating them for 10 minutes at RT. Fluorescence images were developed using a Leica (Leica Microsystems, Wetzlar, Germany) epifluorescent microscope equipped with S Fluor 40x/1.3 objective using METAMORPH (Molecular Devices, Sunnyvale, CA, USA) software.

2.12 Statistics

All data represent the mean and SD of independent experiments. T-test analysis was carried out by PRISM program. A p value ≤ 0.05 was considered as significant and indicated in figures with asterisks (*). Lower p values were considered more statistically significant and were represented as follow: p value ≤ 0.01 (**), p value ≤ 0.001 (***) and p value ≤ 0.0001 (****).

3. Results and discussion

3.1 Cell generation and immunoprecipitation of NAMPT-GFP protein from melanoma cells

The aim of this work was to study the presence of phosphorylation sites on NAMPT as a possible means of fast regulation of metabolic activity or cell localization. We have optimized a protocol to enrich the matrix with cellular NAMPT that is amenable to high yield LC-MS analysis (Fig. 1).

Given the highly abundant presence of this protein in the B16 melanoma cell line, we opted to investigate it in this system. To define NAMPT phosphorylation, we first decided to immunoprecipitate endogenous NAMPT from B16 cell lysates. When immunoprecipitating NAMPT, though, we found that the Western blot analysis of this protein (55 KDa) superimposed with IgG heavy chains (Fig. 2A). This was an important limitation as it would not have allowed to monitor immunoprecipitation. To overcome this technical problem, we set up an immunoprecipitation assay using magnetic beads that allowed us to avoid contamination with IgG1. This technique prevent centrifugation, which can break weak antibody-antigen binding and causes loss of target protein, and it is therefore possible to increase the immunoprecipitation rate, alongside stopping IgG contamination.

As shown in Fig. 2B, we were able to pull-down a moderate level of endogenous NAMPT that was not contaminated with IgGs, that were detectable at 110 kDa (Fig. 2C).

We then decided to evaluate whether the immunoprecipitated NAMPT was reactive to a non-specific phosphor-Tyr antibody. Indeed, we found that immunoprecipitated NAMPT was most likely phosphorylated (Fig. 2C). However, the amount of immunoprecipitated NAMPT was limited, most likely due to a loss of material during the procedure and a moderate efficacy of the anti-NAMPT antibody to pull down the protein. We therefore felt that an enrichment was necessary to reliably perform high yield LC-MS analysis. To increase the amount of NAMPT, we then

generated a stable B16 cell line over-expressing GFP-NAMPT. The fusion protein, of 82 kDa, could be immunoprecipitated efficiently with anti-GFP beads, and was easily detectable by western blot and silver staining, without contamination of the IgG fragments (Fig. 2D left). Importantly, GFP-NAMPT was detected by the anti-Tyr antibody in steady-state conditions in B16 cells (Figure 2D right). GFP was located at the N-terminal, and it was acknowledged that this might have masked some phosphorylation sites close to the fluorescent protein.

3.2 Identification of NAMPT phosphorylation sites by LC-MS/MS analysis

To identify the phosphorylated sites on NAMPT, we pulled down GFP-NAMPT from 1 x 10^8 cells. Then, proteins were precipitated using the TCA method and digested with Lys-C and Trypsin. The trypsin digest was analysed by LC-MS/MS in the Data Dependent Acquisition mode. The method developed yielded a NAMPT sequence coverage of up to 78% (Fig. 3A). As expected, given the presence of the GFP, the N-terminal was the least covered. We identified eight phosphorylation sites by shot-gun LC-MS/MS proteomics. The NAMPT phosphorylated sites identified were: Y175, S199, S200, Y240, S241, S398, T406 and S472. The predicted localization of the sites is depicted in Fig. 3B. The MS/MS spectra are reported in Fig. 4. These spectra were manually interpreted to confirm the phosphorylation localization. Importantly, we also evaluated phosphorylation in murine recombinant NAMPT generated in various batches prepared from *E. Coli*. The S199 and S200 phosphosites were reproducibly found also in *E.Coli* recombinant protein, together with a T203 phosphosite, which instead is not found in the eukaryotic system. (Supplementary figure 1).

3.3 Label free semiquantitative data of phosphorylation sites in NAMPT

In order to have information about the relative abundance of each peptide, targeted analysis was performed. The phosphopeptides were analyzed by LC-MS/MS in Parallel Reaction Monitoring (PRM) mode, based on precursor ion, *m/z* and the charge of modified peptides obtained from the identification experiment. Semi-quantitative label free area at MS/MS level were determined and normalized against

the MS/MS area values of the unmodified peptides. As shown in Table 1, the most abundant phosphorylated sites were S199 and S200, followed by residues Y240 and S241. On the contrary, Y175 and S398 were present at low levels.

3.4 Phosphorylation sites in cytosolic and nuclear NAMPT

We then investigated if these eight residues were differentially phosphorylated in the cytosol and nucleus, given previous reports that NAMPT is present in both compartments in B16 cells (Fig. 5A). We performed fractionation of cytosol and nuclei (Fig. 5A) and then immune-precipitation of GFP-NAMPT was done as previously described. Semi-quantitative label free area at MS/MS level was measured and normalized against the MS/MS area values of NAMPT unmodified peptides. As shown in Fig. 5B, Y175 and S398, residues that were detectable al very low intensity in total cell lysate, were undetectable in these sets of experiments. Surprisingly, only S472 and T406 were present in both compartments, while S199, S200, Y240 and S241 were detected only in the cytosolic fraction.

3.5 Modification of phosphorylation in different conditions

While the aim of the present report was to define the phosphorylation sites under basal conditions in melanoma cells, we decided to investigate whether we could detect changes upon UV exposure or starvation, which should increase the energy demand of cells alone or starvation followed by the addition of FBS, and upon PMA and forskolin stimulation, which should increase Protein kinase A and protein kinase C activity. As shown in Table 2, under starvation T406 phosphorylation was increased, while no changes were found on other sites. Importantly, the addition of FBS reduced T406 phosphorylation, similar to basal level. Of note, FBS induced also a decrease in Y240 and S241 and an increase of S247 phosphorylation. Furthermore, the UV stimulation markedly reduced the phosphorylation level of S199, S200, Y240, S241 and T406. Finally, the stimulation with PMA/FSK induced a reduction in T406 and an increase in S398 phosphorylation. These data suggest that the modulation of energy demand or increasing DNA damage could be involved in

controlling NAMPT phosphorylation status and are the proof of principle that cells are able to modify the phosphorylation status of NAMPT.

3.6 Determination of the biological effect of the mutated variants of the phosphorylation sites

We next focused on the more abundant phosphorylation revealed, S199 and S200. Firstly, we generated a double mutated form of NAMPT, in which the serine residues 199 and 200, have been replaced with two alanine, therefore mimic the loss of phosphorylation sites. Importantly, we tested the enzymatic activity of this mutated variant (Figure 6), observing that NAMPT mutant (S199A-S200A) was completely inactive, compared to the *wild-type* protein. We then proceed with the expression ad purification of both the single mutated variants of NAMPT, namely S199A and S200A. Interestingly, both the recombinant enzymes appeared to be still inactive as the double mutated variant, in the same assay condition, suggesting that these two residues are essential for its activation.

To prove this finding in cells, we generated mutated cell lines (B16 GFP-NAMPT WT, GFP-S199-200A, GFP-S199A, GFP-S200A). As shown in Figure 6A, through a cell viability assay, we determined that the S199A, S200A and S199-S200A cell lines display a reduction in cellular growth compared to the wild-type cell line. Of note, since eNAMPT is fused with the GFP, we have monitored also the localization of this mutants.

First of all, GFP-NAMPT-S199-200A B16 cells NAMPT showed a marked nuclear localization compared to the GFP-NAMPT B16 (Figure 6B). In NAMPT-GFP-S199A B16 cells, NAMPT has a cytosolic localization, as the GFP-NAMPT B16, while GFP-NAMPT-S200A showed a characteristic nuclear localization. Conclusively, S200 phosphorylation site seems to be necessary to maintain NAMPT in the cytosol, maybe directly involving some transport mechanism, while S199 site is not necessary for this translocation.

Conclusions

Nicotinamide phosphoribosyltransferase (NAMPT) is a key enzyme involved in nicotinamide adenine dinucleotide (NAD^+) metabolism [18]. NAMPT is present in cells in the cytosol and in the nucleus and it has been also found actively secreted in the extracellular space as eNAMPT, where it acts as a cytokine [3,19]. Since it is well known that phosphorylation controls the switch-on or switch-off of several enzymes and their localization, the aim of our work was to identify, quantify and characterize possible NAMPT phosphorylated sites in melanoma cells, in which NAMPT is highly expressed. This is particularly important as it would be expected that NAD^+, and therefore energy demand, of cells, should have a fast switch on for replenishment.

Bioinformatic software predict a number of phosphorylation sites on NAMPT, which have never been confirmed experimentally. The only phosphorylation described to date on this enzyme is intrinsically linked to its catalytic activity and represents an auto-phosphorylation linked to the molecular mechanism of catalyses [1]. While many cell types increase NAMPT levels when a higher NAD^+ or bioenergetic supply is required (for example in cancer cells or in inflammation), we reasoned that PTMs might also participate in the control of this protein. This does not only pertain to the catalytic activity, but also to its localization.

To this aim, we used high-yield LC-MS to determine the phosphorylation sites present in basal conditions in a murine melanoma cell line. The performance of the analysis was of the highest quality, given that the *ms-gf*+ research algorithm coupled with a percolator q value of less than 0.01 and a Phosphorylation Probability calculated with PhosphoRS algorithm greater than 0.95 are index of robustness and reliability of the whole data presented.

This strategy identified 8 phosphorylation sites: 5 on serine (S199, S200, S241, S398 and S472), 2 on tyrosine (Y175 and Y240) and one on threonine (T406). This was supported by our ability to identify Tyr phosphorylation with a non-specific anti-Tyr antibody, while we did not investigate other non-specific anti-phospho antibodies.

The method developed does not allow to determine histidine phosphorylations, and this is the reason for which H247 was not identified.

The most abundant phosphorylations (S199 and S200) have been deeper investigated: both the mutated variants (double or single) are avoided of enzymatic activity. Moreover, the mutation in B16 cell line determined a significant lag of cellular growth, in particular with a different cellular localization. S200 phosphorylation site is determinant for maintaining NAMPT into the cytosol, while the mutated form is able to shuttle the protein into the nucleus.

Phosphosite (www.phosphosite.org) predicts 4 threonine, 10 serine and 13 tyrosine phosphorylation sites. Among the sites found in the present study, S398, S472, Y175 and S241 are sites are present on phosphosite, while S199, S200, T406 and Y240 have never been reported or postulated previously. It is interesting to note that S199 and S200 were the most abundant in B16 cells.

While we did not investigate deeply the role of each of these phosphorylations, we found that there is a differential phosphorylation of some of these proteins in the cytosol compared to the nucleus and between basal or stimulated conditions. It should also be noticed that B16 represent a highly proliferating and active cell, with a number of mutations, which might lead to constitutive activation of kinases. It might therefore be that what we refer to as basal phosphorylation might not be found in cells that have lower bioenergetics requirements. It has been recently shown, for example, that NAMPT can shuttle from the cytosol to the nucleus [20] and phosphorylation/dephosphorylation is a classical manner by which this occurs (for example for the transcription factor NFAT [21]. We therefore believe that phosphospecific antibodies should be developed to understand the role of the phosphorylations reported here.

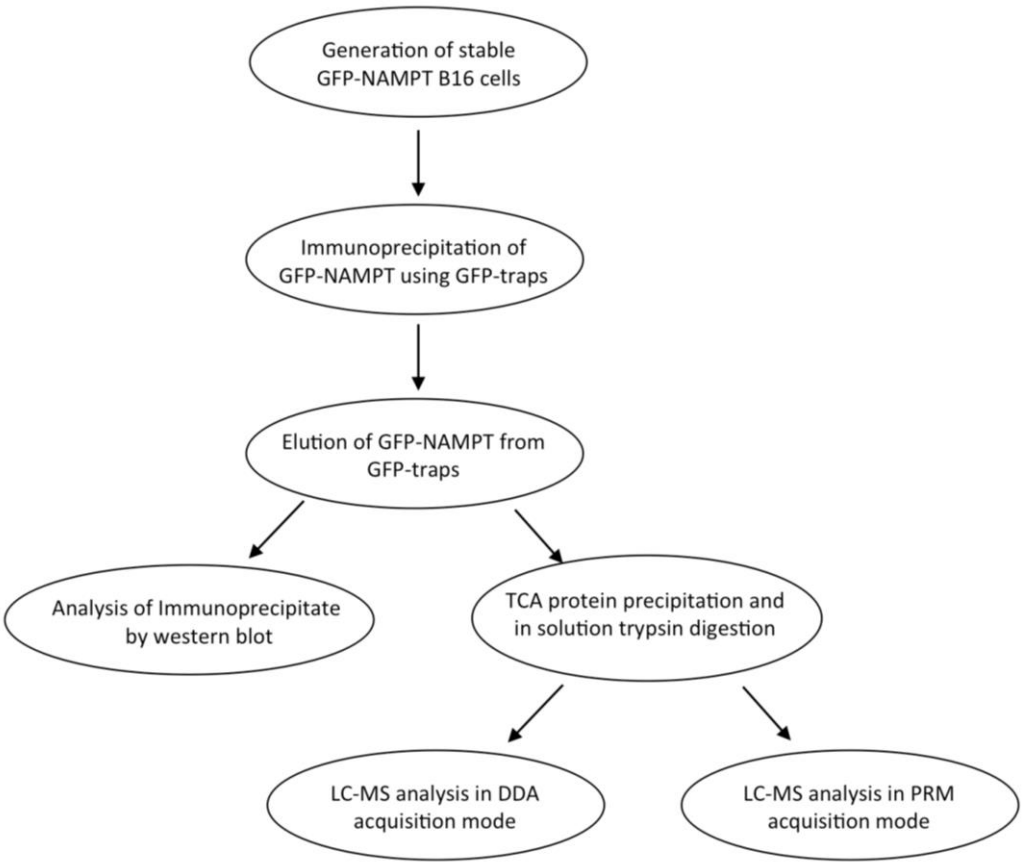

Fig. 1 Experimental design to identify NAMPT phosphorylations.

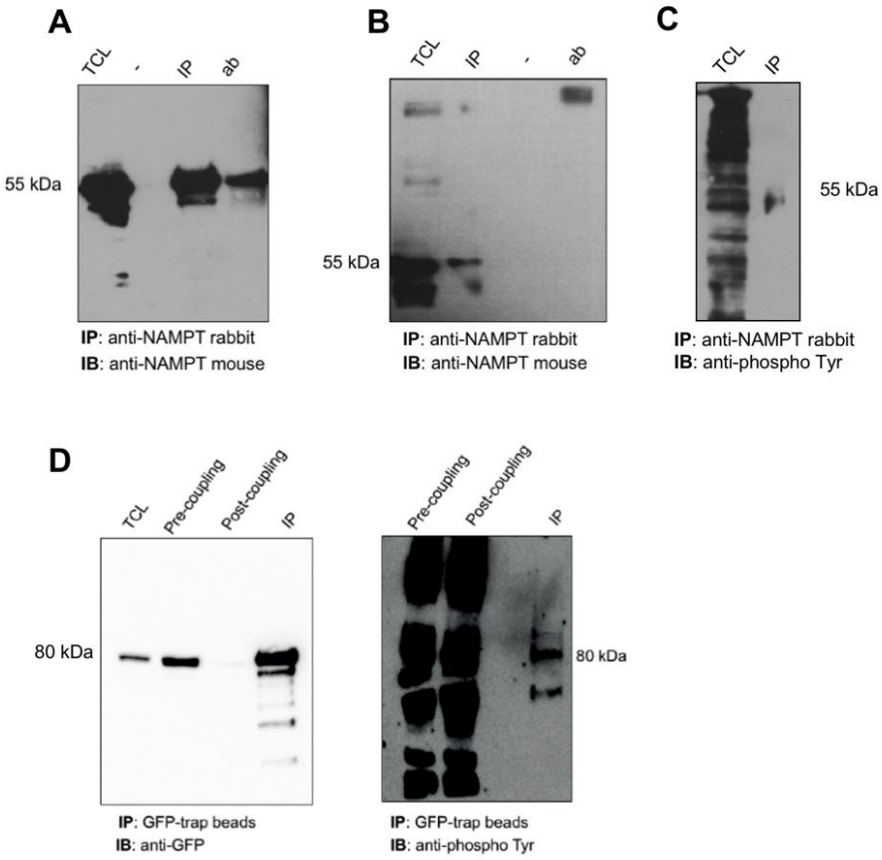

Fig. 2 (A) immunoprecipitation of endogenous NAMPT using agarose A/G beads, n=5; (**B**) immunoprecipitation of endogenous NAMPT and (**C**) detection of tyrosine phosphorylation using magnetic beads in not denaturing condition, n=3; (**D**) immunoprecipitation of GFP-NAMPT (left) and detection of tyrosine phosphorylation (right) using GFP-trap beads, n=6.

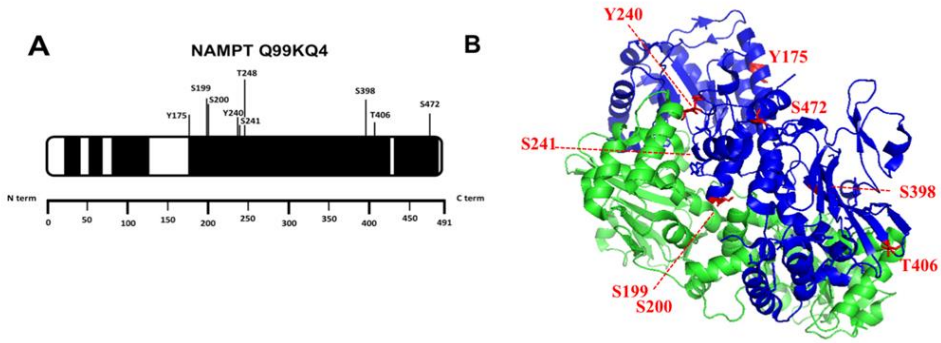

Fig. 3 (**A**) NAMPT sequence covered by LC-MS/MS experiment with NAMPT phosphorylated sites highlighted; (**B**) 3D structure of NAMPT dimer with phosphorylated sites indicated.

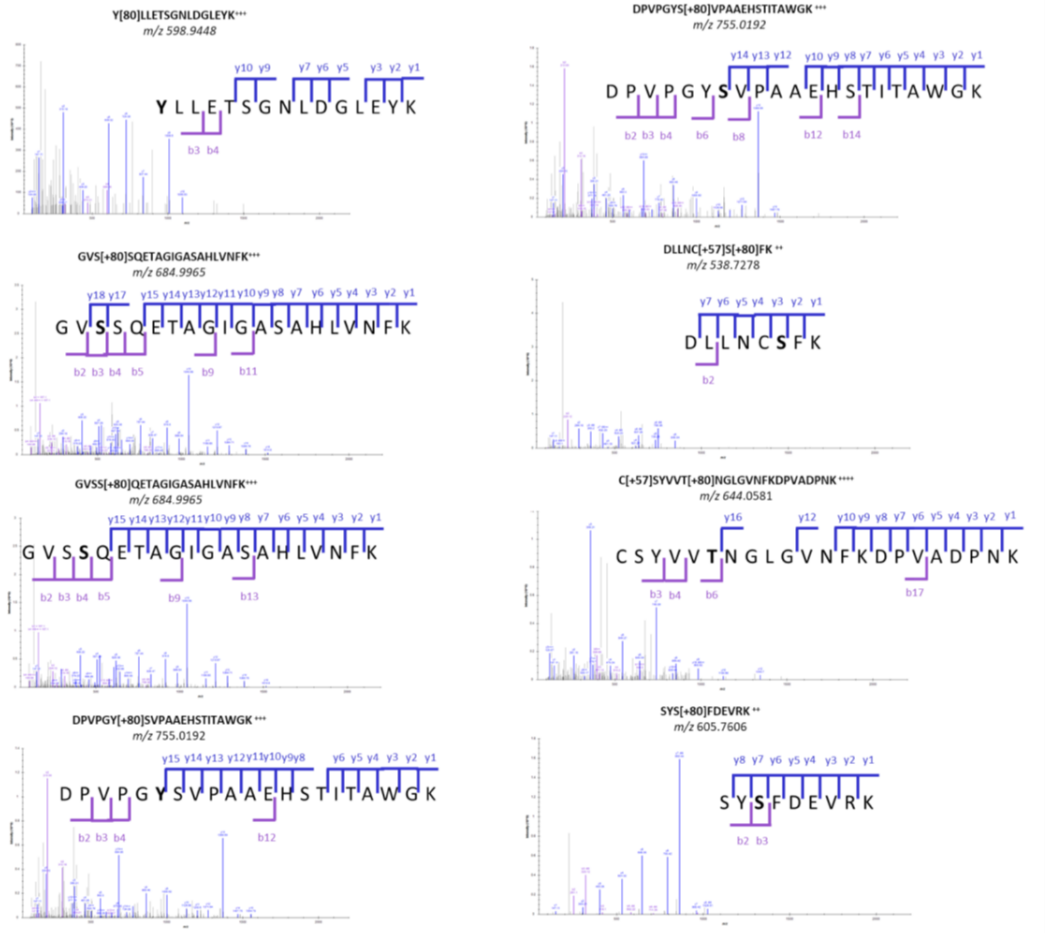

Fig. 4. MS/MS Higher-energy Collision Dissociation (HCD) spectra of NAMPT phosphorylated peptides identified by mass spectrometry, n=4 of n=2 independent experiments.

NAMPT Peptides modified	Amino acid phosphorylated	m/z	Charge	Normalized Area (Area average ± SD)
Y[+80]LLETSGNLDGLEYK	Y175	598.9448	3	0.32 ± 0.05
GVS[+80]SQETAGIGASAHLVNFK	S199	684.9965	3	7.66 ± 0.55
GVSS[+80]QETAGIGASAHLVNFK	S200	684.9965	3	6.05 ± 1.57
DPVPGY[+80]SVPAAEHSTITAWGK	Y240	755.0192	3	3.88 ± 0.39
DPVPGYS[+80]VPAAEHSTITAWGK	S241	755.0192	3	3.91 ± 0.46
DLLNC[+57]S[+80]FK	S398	538.7278	2	0.35 ± 0.06
C[+57]SYVVT[+80]NGLGVNVFKDPVADPNK	T406	644.0581	4	2.55 ± 0.15
SYS[+80]FDEVRK	S472	605.7606	2	1.03 ± 0.19

Table 1. NAMPT phosphorylated peptides with semiquantitative data of each modified site identified by mass spectrometry.

A

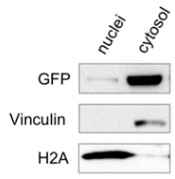

B

NAMPT Peptides modified	Amino acid phosphorylated	Normalized Area (Area average ± sd) cytosol	Normalized Area (Area average ± sd) nuclei
Y[+80]LLETSGNLDGLEYK	Y175	n.d.	n.d.
GVS[+80]SQETAGIGASAHLVNFK	S199	1.52 ± 0.71	-
GVSS[+80]QETAGIGASAHLVNFK	S200	1.45 ± 0.60	-
DPVPGY[+80]SVPAAEHSTITAWGK	Y240	0.13 ± 0.03	-
DPVPGYS[+80]VPAAEHSTITAWGK	S241	0.12 ± 0.03	-
DLLNC[+57]S[+80]FK	S398	n.d.	n.d.
C[+57]SYVVT[+80]NGLGVNVFKDPVADPNK	T406	5.66 ± 0.88	4.18 ± 0.67
SYS[+80]FDEVRK	S472	1.81 ± 0.35	2.85 ± 0.80

Fig. 5 (A) Representative western blot of nuclear and cytosolic fractions of B16-GFP NAMPT cells**. (B)** NAMPT phosphorylated peptides in cytosol and nuclei with semiquantitative data of each modified sites identified by mass spectrometry, n=4.

NAMPT Peptides modified	Amino acid phosphorylated	m/z	Charge	Normalized Area (Area average ± SD)
Y[+80]LLETSGNLDGLEYK	Y175	598.9448	3	0.32 ± 0.05
GVS[+80]SQETAGIGASAHLVNFK	S199	684.9965	3	7.66 ± 0.55
GVSS[+80]QETAGIGASAHLVNFK	S200	684.9965	3	6.05 ± 1.57
DPVPGY[+80]SVPAAEHSTITAWGK	Y240	755.0192	3	3.88 ± 0.39
DPVPGYS[+80]VPAAEHSTITAWGK	S241	755.0192	3	3.91 ± 0.46
DLLNC[+57]S[+80]FK	S398	538.7278	2	0.35 ± 0.06
C[+57]SYVVT[+80]NGLGVNVFKDPVADPNK	T406	644.0581	4	2.55 ± 0.15
SYS[+80]FDEVRK	S472	605.7606	2	1.03 ± 0.19

Table 2. NAMPT phosphorylated peptides with semiquantitative data of each modified site identified by mass spectrometry under basal condition or upon starvation, starvation + FBS (fetal bovine serum), UV stimulus or PMA/FSK stimulation, n=4.

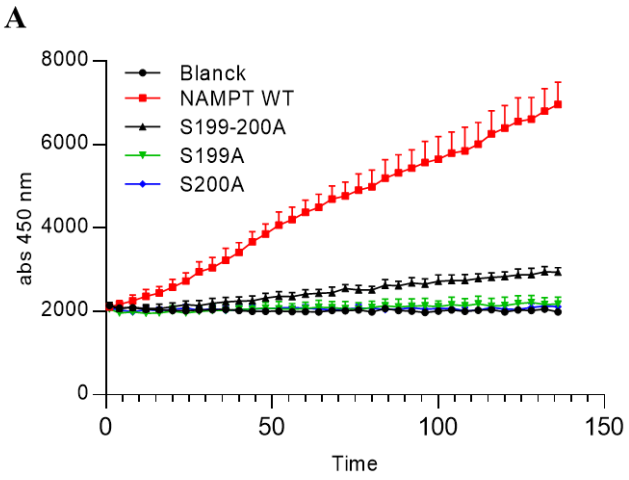

Figure 6. (**A**) In vitro NAMPT WT, NAMPT S199-200A, NAMPT S199A and NAMPT S200A enzymatic activity determination; n=4.

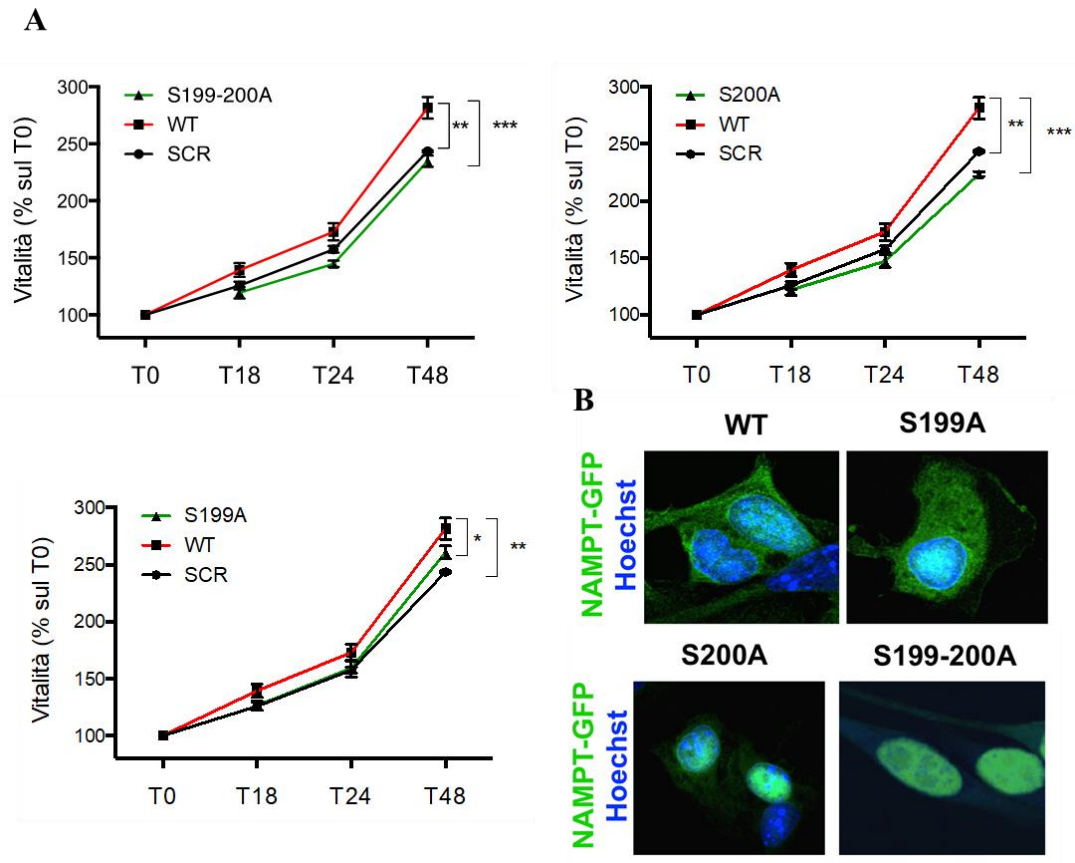

Figure 7. (**A**) Cell viability of GFP-NAMPT B16 cell line compared to SCR and B16 GFP-NAMPT S199-200A, B16 GFP-NAMPT S199A and B16 GFP-NAMPT S200A; n=3 of 4 determinations. (**B**) Confocal images of GFP-NAMPT B16 cell line, B16 GFP-NAMPT S199-200A, B16 GFP-NAMPT S199A and B16 GFP-NAMPT S200A.

Acknowledgments

This work was supported by grants from AIRC [grant number IG2018 21842] to AAG, from the Italian Ministry of Research [grant code PRIN 2017 CBNCYT] to AAG. CT acknowledges funding from the Fondazione Veronesi and AIRC [grant number14832].

Conflict of interest. The authors have declared that no conflict of interest exists.

References

1 Burgos ES, Ho M-C, Almo SC, *et al.* A phosphoenzyme mimic, overlapping catalytic sites and reaction coordinate motion for human NAMPT. *Proc Natl Acad Sci USA* 2009;**106**:13748–53. doi:10.1073/pnas.0903898106

2 Carbone F, Liberale L, Bonaventura A, *et al.* Regulation and Function of Extracellular Nicotinamide Phosphoribosyltransferase/Visfatin. In: *Comprehensive Physiology*. American Cancer Society 2017. 603–21. doi:10.1002/cphy.c160029

3 Grolla AA, Travelli C, Genazzani AA, *et al.* Extracellular nicotinamide phosphoribosyltransferase, a new cancer metabokine. *Br J Pharmacol* 2016;**173**:2182–94. doi:10.1111/bph.13505

4 Revollo JR, Körner A, Mills KF, *et al.* Nampt/PBEF/Visfatin regulates insulin secretion in beta cells as a systemic NAD biosynthetic enzyme. *Cell Metab* 2007;**6**:363–75. doi:10.1016/j.cmet.2007.09.003

5 Hara N, Yamada K, Shibata T, *et al.* Nicotinamide Phosphoribosyltransferase/Visfatin Does Not Catalyze Nicotinamide Mononucleotide Formation in Blood Plasma. *PLOS ONE* 2011;**6**:e22781. doi:10.1371/journal.pone.0022781

6 Pittelli M, Formentini L, Faraco G, *et al.* Inhibition of nicotinamide phosphoribosyltransferase: cellular bioenergetics reveals a mitochondrial insensitive NAD pool. *J Biol Chem* 2010;**285**:34106–14. doi:10.1074/jbc.M110.136739

7 Burgos ES, Vetticatt MJ, Schramm VL. Recycling Nicotinamide. The Transition-State Structure of Human Nicotinamide Phosphoribosyltransferase. *J Am Chem Soc* 2013;**135**:3485–93. doi:10.1021/ja310180c

8 Yoon MJ, Yoshida M, Johnson S, *et al.* SIRT1-Mediated eNAMPT Secretion from Adipose Tissue Regulates Hypothalamic NAD+ and Function in Mice. *Cell Metab* 2015;**21**:706–17. doi:10.1016/j.cmet.2015.04.002

9 Revell AD, Wang D, Boyd MA, *et al.* The development of an expert system to predict virological response to HIV therapy as part of an online treatment support tool. *AIDS* 2011;**25**:1855–63. doi:10.1097/QAD.0b013e328349a9c2

10 Kaiser P, Wohlschlegel J. Identification of ubiquitination sites and determination of ubiquitin-chain architectures by mass spectrometry. *Meth Enzymol* 2005;**399**:266–77. doi:10.1016/S0076-6879(05)99018-6

11 Wohlschlegel JA. Identification of SUMO-conjugated proteins and their SUMO attachment sites using proteomic mass spectrometry. *Methods Mol Biol* 2009;**497**:33–49. doi:10.1007/978-1-59745-566-4_3

12 Kim S, Pevzner PA. MS-GF+ makes progress towards a universal database search tool for proteomics. *Nat Commun* 2014;**5**:5277. doi:10.1038/ncomms6277

13 Taus T, Köcher T, Pichler P, *et al.* Universal and confident phosphorylation site localization using phosphoRS. *J Proteome Res* 2011;**10**:5354–62. doi:10.1021/pr200611n

14 MacLean B, Tomazela DM, Shulman N, *et al.* Skyline: an open source document editor for creating and analyzing targeted proteomics experiments. *Bioinformatics* 2010;**26**:966–8. doi:10.1093/bioinformatics/btq054

15 Guise AJ, Mathias RA, Rowland EA, *et al.* Probing phosphorylation-dependent protein interactions within functional domains of histone deacetylase 5 (HDAC5). *Proteomics* 2014;**14**:2156–66. doi:10.1002/pmic.201400092

16 Bauer M, Ahrné E, Baron AP, *et al.* Assessment of current mass spectrometric workflows for the quantification of low abundant proteins and phosphorylation sites. *Data Brief* 2015;**5**:297–304. doi:10.1016/j.dib.2015.08.015

17 Lawrence RT, Searle BC, Llovet A, *et al.* Plug-and-play analysis of the human phosphoproteome by targeted high-resolution mass spectrometry. *Nat Methods* 2016;**13**:431–4. doi:10.1038/nmeth.3811

18 Chiarugi A, Dölle C, Felici R, *et al.* The NAD metabolome--a key determinant of cancer cell biology. *Nat Rev Cancer* 2012;**12**:741–52. doi:10.1038/nrc3340

19 Travelli C, Colombo G, Mola S, *et al.* NAMPT: A pleiotropic modulator of monocytes and macrophages. *Pharmacological Research* 2018;**135**:25–36. doi:10.1016/j.phrs.2018.06.022

20 Svoboda P, Krizova E, Sestakova S, *et al.* Nuclear transport of nicotinamide phosphoribosyltransferase is cell cycle-dependent in mammalian cells, and its inhibition slows cell growth. *J Biol Chem* 2019;**294**:8676–89. doi:10.1074/jbc.RA118.003505

21 Li X. Phosphorylation, protein kinases and ADPKD. *Biochim Biophys Acta* 2011;**1812**:1219–24. doi:10.1016/j.bbadis.2011.03.001

Supplementary information

Identification of phosphorylation sites on Nicotinamide phosphoribosyltransferase (NAMPT)

1. NAMPT recombinant

1.1 In solution digestion

Performed as reported in paper starting from recombinant protein powder (approximately 1.5 μg for protein).

1.2 LC-MS/MS analysis

Digested peptides were subjected to LC–MS/MS analysis using an EASY-nLC 1000 ultra-high pressure liquid chromatography system (Thermo Scientific) coupled with a Q-Exactive mass spectrometer (Thermo Scientific) with a Nanaospray Flex ion source. NAMPT Peptides fractionated online using microscale C18 reverse-phase chromatography as previously described [1] and ms/ms spectra were acquired in Data dependent acquisition (DDA) mode.

1.3 MS data processing

For label free quantification, Raw DDA MS files were processed using MaxQuant (version 1.6.3.4). Database searching was performed using Andromeda which is integrated into the MaxQuant [2,3]. NAMPT and its phosphopeptides were identified using a target-decoy approach by searching all MS/MS spectra against a concatenated forward/reversed version of mouse sequence database and filtering using a false discovery rate (FDR) of 0.01 at both the peptide and protein level. Carbamidomethylatino of cysteines was selected as the fixed modification and phosphorylation (STY) were allowed for variable

modifications. Match between runs mode was enabled with a window of 1 min.
The database search was performed with an initial precursor ion tolerance of 20 p.p.m., MS/MS tolerance at 0.02 Da, and two missed cleavages are allowed. Phosphosite localization was assessed using Andromeda algorithm and the phosphopeptide containing the residues with phosphor-probability greater than 0.7. [4]

Bibliography:

[1] Wohlschlegel, J. A. Identification of SUMO-conjugated proteins and their SUMO attachment sites using proteomic mass spectrometry. *Methods Mol. Biol.* **497**, 33–49. (2009).
[2] Cox, J. et al. Andromeda: a peptide search engine integrated into the MaxQuant environment. *J. Proteome Res.* **10**, 1794–1805 (2011).
[3] Cox, J. & Mann, M. MaxQuant enables high peptide identification rates, individualized p.p.b.-range mass accuracies and proteome-wide protein quantification. *Nat. Biotechnol.* **26**, 1367–1372 (2008).
[4] Maclean, B. *et al.* Skyline : an open source document editor for creating and analyzing targeted proteomics experiments. *Bioinformatics*. **26,** 966–968 (2010).

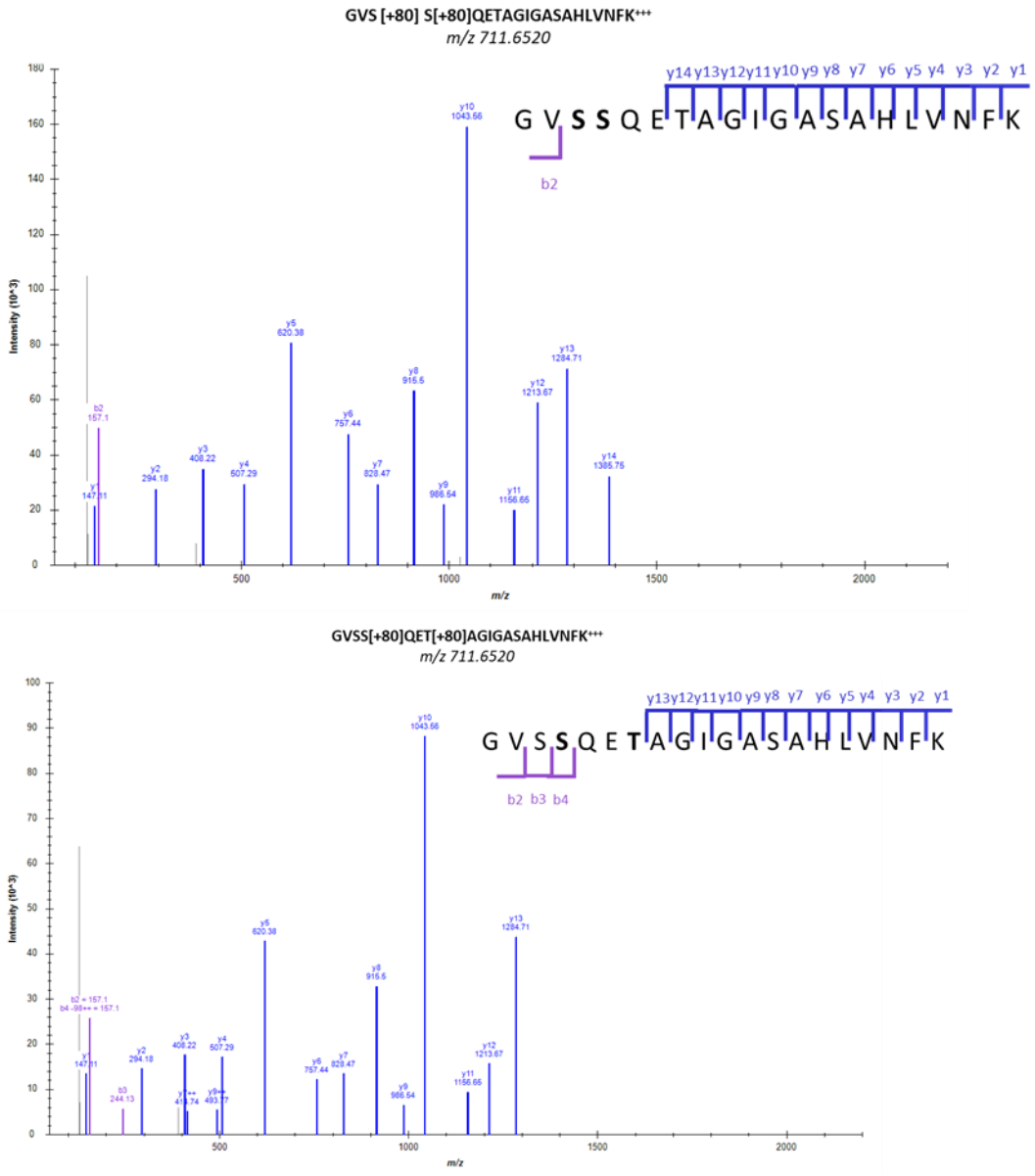

Supplementary Figure 1. MS/MS Higher-energy Collision Dissociation (HCD) spectra of recombinant NAMPT phosphorylated peptides identified by mass spectrometry, n=4 independent experiments.

Chapter 7

CONCLUSIONS AND DISCUSSION

Crohn's disease (CD) and ulcerative colitis (UC) are the two major forms of **inflammatory bowel disease (IBD), a chronic inflammatory disease of the gastrointestinal tract** associated with a genetic predisposition, compromised epithelial barrier permeability, an abnormal gut microbiota and exacerbated intestinal immune responses [1]. Although, the pathogenesis of IBD is still poorly understood, the insights in the molecular networks driving intestinal homeostasis and its breakdown have led to the development of different biological drugs (e.g. anti-TNF, anti-IL12\23, anti-integrins) that are effective in many IBD patients [2]. Furthermore, a large proportion of **patients with severe disease fail to achieve long-term remission** due to the lack of drug feedback, loss of response, drug intolerance, or severe side effects that require therapy interruption. In case of biological agents, when immunogenicity develops, response can be regained by introduction of an alternative biological of the same or different class. Efficacy is reduced with second-line agents either within or across classes compared with naïve patients. The different therapeutic options available would significantly benefit from biomarkers predictive of response to tailor therapies and care for patients, improving the general clinical outcome.

There is therefore still an urgent and pressing clinical need for new therapeutic strategies. These urgent clinical requirements warrant studying and characterizing novel factors that may control the pathogenesis or progression of this pathology.

Interestingly, the main topic of my Ph.D. thesis is the extracellular form of an **interesting pleiotropic protein called nicotinamide phosphoribosyltransferase (NAMPT)**, that was found elevated in serum of three different cohorts of IBD patients (both adults and paediatric) and its levels dropped upon anti-TNF treatment in responsive, but not in non-responsive patients. This evidence may be translated into **a non-responsiveness to anti-TNF biologic when NAMPT serum levels were high**. Therefore, eNAMPT might represent a novel serum biomarker of disease

activity and predictor of response to therapy. Moreover, eNAMPT has also shown to be correlated with unfavourable disease outcomes, as in the Crohn's Disease Activity Index and Mayo score [3–5]. Importantly, in a phase 2 open-label study of 103 golimumab-treated UC-patients, NAMPT emerged as one of the 13 genes in the gene expression signature predictive of poor response [6]. Further high serum levels of eNAMPT have been reported in different cohorts of IBD patients [4,7,8]. Recently, the analysis in a large cohort has highlighted a high degree of variability and a correlation between high eNAMPT levels in serum and lack of response to corticosteroids and azathioprine [8].

NAMPT exists in two distinct forms: (i) an intracellular form (iNAMPT) and (ii) an extracellular form (eNAMPT) [9,10].

In sharp contrast to our understanding of iNAMPT, the role of the extracellular NAMPT is poorly understood, despite the number of articles published, that are mostly descriptive. In the extracellular space, eNAMPT is a cytokine (also referred to pre-B enhancing factor, PBEF, or visfatin) with pro-inflammatory properties [7,9,11].

Importantly, both iNAMPT and eNAMPT have been found deregulated in pathological conditions, including IBD. Indeed, iNAMPT is upregulated in inflammatory myeloid cells [12,13], which are recognized as the crucial drivers of chronic intestinal inflammation leading to disruption of the epithelial barrier and activation of pathogenic T cell responses.

Likewise, both our group and Moschen's group have shown that they are highly effective in two different models of IBD (DSS and DNBS models [13,14]). Unfortunately, enzymatic inhibitors of iNAMPT have been found associated with severe off-target side effects, such as retinopathy and cardiotoxicity [15,16], due to the importance of this ubiquitous protein to produce NAD.

For this reason, **my strategy has turned to the extracellular cytokine eNAMPT as new therapeutical target in IBD**.

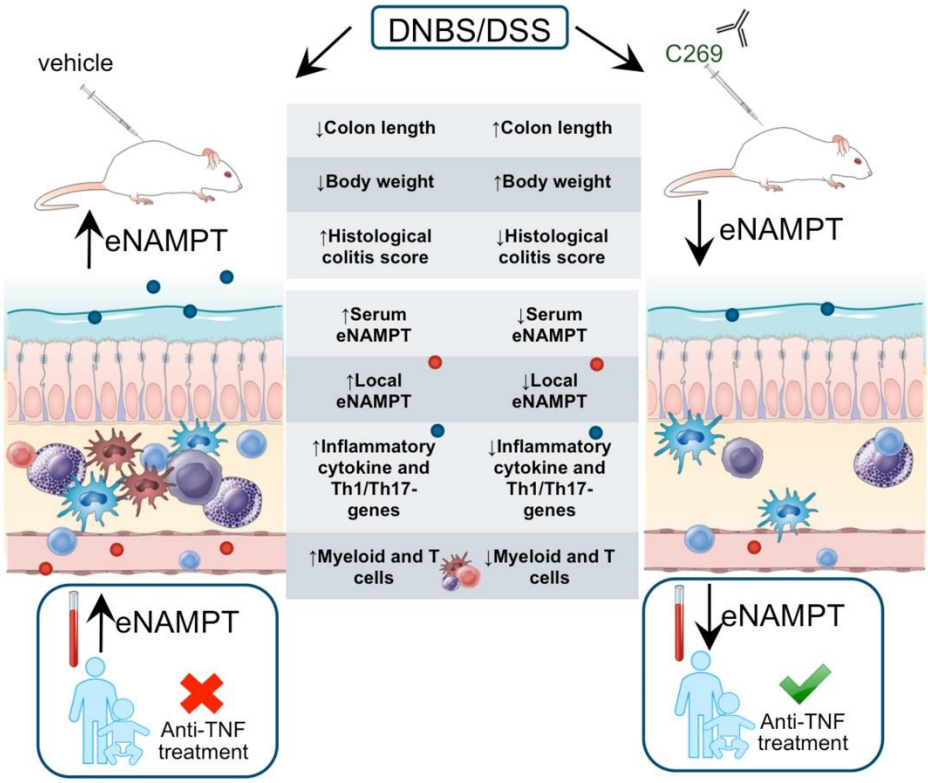

Figure 1: Graphical abstract of eNAMPT role in IBD

To understand the role of eNAMPT in IBD, we have evaluated whether increasing eNAMPT could exacerbate intestinal inflammation. For this, we administered recombinant murine NAMPT to mice treated with low doses of DNBS, which *per se* induces only a modest colitis. In this instance, **daily injection of recombinant NAMPT heightened mucosal inflammation** (as demonstrated by body weight loss, colon shortening and histological damage score). Consistent with this finding, immunohistochemical analysis (IHC) showed an enhanced expression of ICAM1, TNFα, IL-1β and degradation of IκBα in eNAMPT-treated colons, as a down-regulation of several pro-inflammatory genes.

On these bases, **we have generated a murine IgG1k antibody against eNAMPT (called C269) that neutralizes the cytokine activity** of this protein but does not interfere with its enzymatic properties. Indeed, C269 specifically recognizes and

neutralizes eNAMPT, abolishing phosphorylation of STAT-3 induced by eNAMPT in 4T1 cells, without affecting its enzymatic activity.

C269 administration reverted the main features of DSS- and DNBS-induced IBD, and similar effects were obtained in a chronic setting, in which the neutralization of eNAMPT was able to rescue intestinal inflammation and to reduce mortality.

Overall, these results indicate that targeting eNAMPT by the neutralizing antibody C269 ameliorates acute and chronic inflammatory bowel disease. We evaluated the *ex vivo* production of eNAMPT in colon explants, evaluating the local production of this cytokine. In comparison to sham mice, **colonic explants from colitic IgG1-treated mice released a higher amount of eNAMPT, whereas C269 treatment was able to drop down eNAMPT levels to the steady state level**. Importantly, in preclinical models of IBD we have observed that eNAMPT is firstly increased in the colon (estimated by colonic explants, as a local production of the cytokine) and in mice blood.

Taken together, the results demonstrate that eNAMPT-targeting by C269 leads to a consistent reduction of intestinal inflammation that is paralleled by a decrease of eNAMPT present in serum or produced by the inflamed colon.

We also analysed the expression of inflammatory and immune-related genes by RT-PCR and IHC. eNAMPT neutralization by C269 was able to hamper the expression of genes encoding for inflammatory cytokines (*Tnf*, *Il6*, *Il1*), enzymes involved in the production of crucial inflammatory molecules (*Nos2*, *Cox2*, *Nox2*), genes involved in cytotoxic type 1 immune responses (*Il12b*, *Tbx21* and *Ifn*) and involved in typical type 17-immune response (*Il17a*, *Il17f*, *Rorc2*, *Il23a*, *Il21* and *Il22*).

On the contrary, the expression of the anti-inflammatory cytokine *Il4* and *Il10*, as well as the Treg-specific transcription factor Foxp3 was not altered by DNBS or C269 treatments suggesting that eNAMPT does not impair differentiation/activity of gut associated immunoregulatory cells.

Importantly, we also found that C269 administration significantly hampered the expression of ICAM-1 and P-selectin in vessels of the *lamina propria* (LP), both markers indicating a lower capacity to recruit inflammatory cells.

Last, **C269 reduced the frequency of monocytes, neutrophils, CD4, and CD8 cells in *lamina propria*** and also the TNFα expression in monocytes/neutrophils. We observed also an impairment of expansion and activation of pathogenic Th1 ($CD3^+CD4^+IFN\gamma^+$) and cytotoxic effector cells ($CD3^+CD8^+IFN\gamma^+$).

These findings suggest that C269 can dampen DNBS-induced intestinal inflammation by limiting the recruitment and the activation of monocytes, neutrophils and T-cells in the colon, leading to the hypothesis that **eNAMPT controls inflammatory circuits during colitis.**

All these data suggest that the cytokine eNAMPT may represent a crucial player in IBD pathogenesis and progression and a novel pharmacological target.

My Ph.D. thesis aims to characterize eNAMPT as a new biomarker and putative target in IBD, but at the same time it intends to deeply investigate many aspects of this interest protein that still remain unclear, which might help to define also its physiological role as cytokine, including (*i*) its role in macrophage activities, (*ii*) the possible involvement of CCR5 as putative receptor and (*iii*) PTMs able to determine conformational/localization changes that may affect NAMPT activity.

It is known that in response to inflammatory triggers, **many cell types, including monocytes/macrophages, actively secrete eNAMPT** that acts as a positive contributor to inflammation in the extracellular space [14]. For example, eNAMPT secretion appears to be increased in response to LPS, LPS/IFNγ and PPARγ in macrophages [12,17,18].

When present in the extracellular space, eNAMPT plays an important role in acting on innate and adaptive immunity. First, it has been demonstrated that eNAMPT impairs the differentiation of bone macrophages by promoting bone deposition and stimulating the differentiation of bone marrow-derived mesenchymal stem cells into osteoblasts [19]. Moreover, eNAMPT promotes cell survival, increases activated

morphology, and controls polarization in macrophages [20]. We have now demonstrated that **eNAMPT is a priming to IFNγ response**.

Moreover, it has already found that the myeloid-specific ablation of NAMPT prevented MDSCs mobilization from the bone marrow, reactivated specific antitumor immunity and enhanced the antitumor activity of immune checkpoint inhibitors, indicating a role of NAMPT in controlling myeloid cells migration and activation form the bone marrow [21].

To go insight into the cellular mechanism by which eNAMPT exacerbate IBD, we have evaluated the effect of eNAMPT directly on macrophages. **eNAMPT is predominantly released by M1-macrophages** (treated with IFNγ and LPS), while no release is observed during M2-polarization. Moreover, **eNAMPT is able to sustain M1-polarization itself, increasing M1-associated genes** as *Il6*, *Cxcl9*, *Cxcl10*, *Il1*, *Tnf* and *Nos2*, upregulation reverted by our anti-NAMPT antibody, C269. To deeper investigate the role of eNAMPT on macrophage activation, we have validated, **through RNAseq analysis**, the different pathways activated by eNAMPT. From KEGG and Gene Ontology analysis, we have highlighted eNAMPT promotion of different signalling pathways, including TNF, NF-κB and TLR pathways, associated to pro-inflammatory response, moreover, eNAMPT acts as a priming to IFNγ modulation.

eNAMPT emerges as an important modulator of immune responses, however, the mechanism of action of eNAMPT has yet to be elucidated.

To date there is still an open debate if eNAMPT in the extracellular space acts as a "metabokine", therefore an active enzyme producing NMN, or as a common cytokine by acting to a receptor. Nevertheless, it is likely that eNAMPT represents a secreted form of iNAMPT, but this theory has not been formally demonstrated. Although there are accounts that the enzymatic activity is important extracellularly [22], the low levels of the substrates in the extracellular space [23] suggest that a receptor binding mode may be a more plausible mechanism. In support of this, the treatment with exogenous eNAMPT is sufficient to activate specific intracellular

signalling pathways (e.g. STAT-3, NF-κB, Akt) within minutes [24], indicating that eNAMPT has cytokine-like properties and may act through a cell surface receptor. Several receptors have been postulated (e.g. insulin receptor, CCR5, TLR4). We have proven that **eNAMPT is a natural antagonist of C-C chemokine receptor type 5 (CCR5)**, suggesting that it is not the main receptor by which eNAMPT exerts some of its effects.

Currently, the most plausible receptor is Toll-like receptor 4 (TLR4), indeed it has been demonstrated that it is able to promote NF-κB activation in macrophages. Of course, further confirmations are needed before TLR4 can be considered *bona fide* mediator of the biologic effects of eNAMPT.

Lastly, few NAMPT PTMs have been highlighted through years as autophosphorylation on His247 that strengthens the interactions between the two monomers that form the catalytic site, K53, K79, K107, K331, K369 acetylation sites, but their role is not fully understood. Between all the PTMs, protein phosphorylation has a role in the regulation of a broad spectrum of cellular reactions. The phosphate conjugation to peptides normally alters protein function by inducing conformational changes or by affecting protein-protein/enzyme-substrate interactions. We tried to identify phosphorylation sites that may be present on NAMPT. **Through high-yield LC-MS we identified 8 phosphorylation sites**: 5 on serine (S199, S200, S241, S398 and S472), 2 on tyrosine (Y175 and Y240) and one on threonine (T406). We focused on **S199-200 residues, that seem to be implicated in the positive regulation of the enzymatic activity**, expressing and purifying the single and double mutated variants of NAMPT (S199A, S200A and S199-200A). Interestingly, the mutant S200A is able to maintain NAMPT in the nucleus rather than the cytosol, and this data suggest the importance in the study of this mutant, according to the ability of NAMPT to shuttle in different cellular compartments due to the different phosphorylation of specific sites.

Concluding, all these evidences helped to better characterized NAMPT physiology, with the aim to determine its role as a possible target for inflammatory bowel disease.

References

1 Park JH, Peyrin-Biroulet L, Eisenhut M, *et al.* IBD immunopathogenesis: A comprehensive review of inflammatory molecules. *Autoimmunity Reviews* 2017;**16**:416–26. doi:10.1016/j.autrev.2017.02.013

2 Friedrich M, Pohin M, Powrie F. Cytokine Networks in the Pathophysiology of Inflammatory Bowel Disease. *Immunity* 2019;**50**:992–1006. doi:10.1016/j.immuni.2019.03.017

3 Starr AE, Deeke SA, Ning Z, *et al.* Proteomic analysis of ascending colon biopsies from a paediatric inflammatory bowel disease inception cohort identifies protein biomarkers that differentiate Crohn's disease from UC. *Gut* 2017;**66**:1573–83. doi:10.1136/gutjnl-2015-310705

4 Dogan S, Guven K, Celikbilek M, *et al.* Serum Visfatin Levels in Ulcerative Colitis. *Journal of Clinical Laboratory Analysis* 2016;**30**:552–6. doi:10.1002/jcla.21901

5 Waluga M, Hartleb M, Boryczka G, *et al.* Serum adipokines in inflammatory bowel disease. *World J Gastroenterol* 2014;**20**:6912–7. doi:10.3748/wjg.v20.i22.6912

6 Telesco SE, Brodmerkel C, Zhang H, *et al.* Gene Expression Signature for Prediction of Golimumab Response in a Phase 2a Open-Label Trial of Patients With Ulcerative Colitis. *Gastroenterology* 2018;**155**:1008-1011.e8. doi:10.1053/j.gastro.2018.06.077

7 Moschen AR, Kaser A, Enrich B, *et al.* Visfatin, an Adipocytokine with Proinflammatory and Immunomodulating Properties. *The Journal of Immunology* 2007;**178**:1748–58. doi:10.4049/jimmunol.178.3.1748

8 Neubauer K, Bednarz-Misa I, Walecka-Zacharska E, *et al.* Oversecretion and Overexpression of Nicotinamide Phosphoribosyltransferase/Pre-B Colony-Enhancing Factor/Visfatin in Inflammatory Bowel Disease Reflects the Disease

Activity, Severity of Inflammatory Response and Hypoxia. *Int J Mol Sci* 2019;**20**. doi:10.3390/ijms20010166

9 Carbone F, Liberale L, Bonaventura A, *et al.* Regulation and Function of Extracellular Nicotinamide Phosphoribosyltransferase/Visfatin. In: *Comprehensive Physiology*. American Cancer Society 2017. 603–21. doi:10.1002/cphy.c160029

10 Burgos ES, Vetticatt MJ, Schramm VL. Recycling Nicotinamide. The Transition-State Structure of Human Nicotinamide Phosphoribosyltransferase. *J Am Chem Soc* 2013;**135**:3485–93. doi:10.1021/ja310180c

11 Samal B, Sun Y, Stearns G, *et al.* Cloning and characterization of the cDNA encoding a novel human pre-B-cell colony-enhancing factor. *Mol Cell Biol* 1994;**14**:1431–7. doi:10.1128/mcb.14.2.1431

12 Bermudez B, Dahl TB, Medina I, *et al.* Leukocyte Overexpression of Intracellular NAMPT Attenuates Atherosclerosis by Regulating PPARγ-Dependent Monocyte Differentiation and Function. *Arterioscler Thromb Vasc Biol* 2017;**37**:1157–67. doi:10.1161/ATVBAHA.116.308187

13 Gerner RR, Klepsch V, Macheiner S, *et al.* NAD metabolism fuels human and mouse intestinal inflammation. *Gut* 2018;**67**:1813–23. doi:10.1136/gutjnl-2017-314241

14 Colombo G, Clemente N, Zito A, *et al.* Neutralization of extracellular NAMPT (nicotinamide phosphoribosyltransferase) ameliorates experimental murine colitis. *J Mol Med* Published Online First: 27 April 2020. doi:10.1007/s00109-020-01892-0

15 Misner DL, Kauss MA, Singh J, *et al.* Cardiotoxicity Associated with Nicotinamide Phosphoribosyltransferase Inhibitors in Rodents and in Rat and Human-Derived Cells Lines. *Cardiovasc Toxicol* 2017;**17**:307–18. doi:10.1007/s12012-016-9387-6

16 Zabka TS, Singh J, Dhawan P, *et al.* Retinal toxicity, in vivo and in vitro, associated with inhibition of nicotinamide phosphoribosyltransferase. *Toxicol Sci* 2015;**144**:163–72. doi:10.1093/toxsci/kfu268

17 Halvorsen B, Espeland MZ, Andersen GØ, *et al.* Increased expression of NAMPT in PBMC from patients with acute coronary syndrome and in inflammatory M1 macrophages. *Atherosclerosis* 2015;**243**:204–10. doi:10.1016/j.atherosclerosis.2015.09.010

18 Mayi TH, Rigamonti E, Pattou F, *et al.* Liver X Receptor (LXR) activation negatively regulates visfatin expression in macrophages. *Biochem Biophys Res Commun* 2011;**404**:458–62. doi:10.1016/j.bbrc.2010.12.002

19 Tsiklauri L, Werner J, Kampschulte M, *et al.* Visfatin alters the cytokine and matrix-degrading enzyme profile during osteogenic and adipogenic MSC differentiation. *Osteoarthr Cartil* 2018;**26**:1225–35. doi:10.1016/j.joca.2018.06.001

20 Travelli C, Colombo G, Mola S, *et al.* NAMPT: A pleiotropic modulator of monocytes and macrophages. *Pharmacological Research* 2018;**135**:25–36. doi:10.1016/j.phrs.2018.06.022

21 Travelli C, Consonni FM, Sangaletti S, *et al.* Nicotinamide Phosphoribosyltransferase Acts as a Metabolic Gate for Mobilization of Myeloid-Derived Suppressor Cells. *Cancer Res* Published Online First: 18 February 2019. doi:10.1158/0008-5472.CAN-18-1544

22 Revollo JR, Körner A, Mills KF, *et al.* Nampt/PBEF/Visfatin regulates insulin secretion in beta cells as a systemic NAD biosynthetic enzyme. *Cell Metab* 2007;**6**:363–75. doi:10.1016/j.cmet.2007.09.003

23 Hara N, Yamada K, Shibata T, *et al.* Nicotinamide Phosphoribosyltransferase/Visfatin Does Not Catalyze Nicotinamide Mononucleotide Formation in Blood Plasma. *PLOS ONE* 2011;**6**:e22781. doi:10.1371/journal.pone.0022781

24 Grolla AA, Travelli C, Genazzani AA, *et al.* Extracellular nicotinamide phosphoribosyltransferase, a new cancer metabokine. *Br J Pharmacol* 2016;**173**:2182–94. doi:10.1111/bph.13505

Chapter 8

List publications

1. Travelli C, **Colombo G**, Mola S, Genazzani AA, Porta C. **NAMPT: a pleiotropic modulator of monocytes and macrophages.** Pharmacol Res. 2018 Jul 18;135:25-36. doi: 10.1016/j.phrs.2018.06.022
2. Cristina Travelli, Silvio Aprile, Daiana Mattoteia, **Giorgia Colombo**, Nausicaa Clemente, Eugenio Scanziani, Salvatore Terrazzino, Maria Alessandra Alisi, Lorenzo Polenzani, Giorgio Grosa, Armando A. Genazzani, Gian Cesare Tron, and Ubaldina Galli. **Identification of Potent Triazolylpyridine Nicotinamide Phosphoribosyltransferase (NAMPT) Inhibitors Bearing a 1,2,3-Triazole Tail Group**. Eur J Med Chem, 181, 111576. DOI: 10.1016/j.ejmech.2019.111576
3. **Giorgia Colombo**, Nausicaa Clemente, Andrea Zito, Cristiano Bracci, Federico Simone Colombo, Davide Giuseppe Ribaldone, Gian Paolo Caviglia, Luca Pastorelli, Marco De Andrea, Samuele Naviglio, Marianna Lucafò, Gabriele Stocco, Ambra A. Grolla, Michela Campolo, Giovanna Casili, Salvatore Cuzzocrea, Emanuela Esposito, Fabio Malavasi, Armando A. Genazzani, Chiara Porta and Cristina Travelli. **Neutralization of extracellular NAMPT (nicotinamide phosphoribosyltransferase) ameliorates experimental murine colitis.** Journal of Molecular Medicine, 2020. Doi: 10.1007/s00109-020-01892-0
4. Ambra A Grolla, Riccardo Miggiano, Daniele Di Marino, Michele Bianchi, Alessandro Gori, Giuseppe Orsomando, Federica Gaudino, Ubaldina Galli, Erika Del Grosso, Francesca Mazzola, Carlo Angeletti, Martina Guarneri, Simone Torretta, Marta Calabrò, Sara Boumya, Xiaorui Fan, **Giorgia Colombo**, Cristina Travelli, Francesca Rocchio, Eleonora Aronica, James A Wohlschlegel, Silvia Deaglio, Menico Rizzi, Armando A Genazzani, Silvia Garavaglia. **A Nicotinamide phosphoribosyltransferase-GAPDH Interaction Sustains the Stress-Induced NMN/NAD + Salvage Pathway in the Nucleus**. J Biol Chem, 2020. DOI: 10.1074/jbc.RA119.010571
5. Simone Torretta †, **Giorgia Colombo** †, Cristina Travelli, Sara Boumya, Dmitry Lim, Armando A. Genazzani and Ambra A. Grolla. **The Cytokine Nicotinamide Phosphoribosyltransferase (eNAMPT; PBEF; Visfatin) Acts as a Natural Antagonist of C-C Chemokine Receptor Type 5 (CCR5).** Cells, 2020. Doi: 10.3390/cells9020496 (**co-first**)
6. Marta Serafini, Enza Torre, Silvio Aprile, Erika Del Grosso, Alessandro Gesù, Alessia Griglio, **Giorgia Colombo**, Cristina Travelli, Salvatore Paiella, Annalisa Adamo, Elena Orecchini, Alice Coletti, Maria Teresa Pallotta, Stefano Ugel,

Alberto Massarotti, Tracey Pirali, Silvia Fallarini. **Discovery of Highly Potent Benzimidazole Derivatives as Indoleamine 2,3-Dioxygenase-1 (IDO1) Inhibitors: From Structure-Based Virtual Screening to in Vivo Pharmacodynamic Activity.** J Med Chem. 2020 Mar 26;63(6):3047-3065. doi: 10.1021/acs.jmedchem.9b01809.

7. Luca Quattrini, Edoardo Luigi Maria Gelardi, Giovanni Petrarolo, **Giorgia Colombo**, Davide Maria Ferraris, Francesca Picarazzi, Menico Rizzi, Silvia Garavaglia, Concettina La Motta. **Progress in the Field of Aldehyde Dehydrogenase Inhibitors: Novel Imidazo[1,2-a]pyridines against the 1A Family.** ACS Med. Chem. Lett. 2020. Doi: 10.1021/acsmedchemlett.9b00686
8. Ubaldina Galli, **Giorgia Colombo**, Cristina Travelli, Gian Cesare Tron, Armando A. Genazzani, Ambra Grolla. **Recent Advances in NAMPT Inhibitors: A Novel Immunotherapic Strategy.** Front. Pharmcol. 11:656 doi: 10.3389/fpharm.2020.00656
9. Finetti, F., Travelli, C., Ercoli, J., **Colombo, G.**, Buoso, E., and Trabalzini, L. (2020). Prostaglandin E2 and Cancer: Insight into Tumor Progression and Immunity. Biology (Basel) 9. doi:10.3390/biology9120434.
10. Gelardi, E. L. M. †, **Colombo, G**. †, Picarazzi, F., Ferraris, D. M., Mangione, A., Petrarolo, G., et al. (2021). A Selective Competitive Inhibitor of Aldehyde Dehydrogenase 1A3 Hinders Cancer Cell Growth, Invasiveness and Stemness In Vitro. Cancers (Basel) 13. doi:10.3390/cancers13020356 (**co-first**)

ACKNOWLEDGEMENTS

"La strada per la nostra destinazione non è sempre diritta. Prendiamo il percorso sbagliato, ci perdiamo, ci voltiamo indietro. Forse non importa su quale strada ci imbarchiamo. Forse quello che conta è che ci si imbarchi." (B. Hall)

Grazie a Cristina, per essere il mio mentore, ma anche una sorella. Grazie per avermi trasmesso l'entusiasmo e la capacità di andare oltre in questi tre anni. La tua assenza a Novara per me è e rimarrà uno scoglio invalicabile. Grazie ad Ambra, per essere una sorella, per avermi spronato nei momenti più bui ed esserci stata sempre, nonostante le avversità. Avervi trovato è stata la mia fortuna più grande. Questa tesi è anche un po' vostra.

Grazie alla Dott.ssa Chiara Porta, per le interessanti discussioni, per aver trovato sempre tempo da dedicarmi e per le belle parole spese per me. Lo apprezzo e non lo dimenticherò mai.

Grazie al Prof. Armando Genazzani, per avermi permesso di vivere questa avventura nel suo laboratorio e per aver creduto nelle mie idee.

Grazie ai miei genitori, per aver capito che questa era l'unico percorso che volevo intraprendere e che, nonostante le difficoltà, hanno supportato, mentalmente ed economicamente questi tre anni.

Grazie a Edoardo, per esserci sempre, per capire, per sedarmi e non avermi abbandonato nei momenti difficili. Aver condiviso con te questo percorso lo ha reso ancora più ricco.

Grazie a tutto il Genazzani Lab, a chi c'è ancora e chi ci è stato in questi anni. Ho imparato qualcosa da ognuno di voi e siete stati per me una famiglia.

Grazie a chi, anche se in piccola parte, ha dato un piccolo sostegno nella realizzazione sperimentale di questo progetto e alla mia formazione personale nel mondo della scienza, in particolare grazie a Nausicaa, grazie alla Prof.ssa Garavaglia e al Lab di Biochimica, alla Prof.ssa Galli, al Prof. Malavasi e ai Dott.ri Ribaldone e Caviglia.

Un sentito ringraziamento al Professor Corrado Blandizzi, custodirò il suo ricordo in questa tesi.